DECODING MICROGLIAL RESPONSE TO EARLY ALPHA-SYNUCLEIN INCLUSION FORMATION

By

Jacob W. Howe

A DISSERTATION

Submitted to
Michigan State University
in partial fulfillment of the requirements
for the degree of

Neuroscience – Doctor of Philosophy

2025

ABSTRACT

Parkinson's disease (PD) is the second most common neurodegenerative disorder and is poised to increase in prevalence as the population ages. Hallmark pathologies of the disease include aggregation of alpha-synuclein (α-Syn) into Lewy bodies accompanied by the loss of dopamine neurons in the nigrostriatal system. A potential third pathological hallmark of PD is the presence of reactive microglia within the substantia nigra (SN), surrounding inclusion-bearing neurons. The contribution of early inclusion-associated microglial activation to nigrostriatal degeneration is not well understood.

The rat α-Syn preformed fibril (PFF) model of synucleinopathy demonstrates two distinct phases of pathology progression in the SN. The first phase is the aggregation phase, characterized by the accumulation of α-Syn into phosphorylated alpha-synuclein (pSyn) inclusions, followed by the degeneration phase, characterized by the loss of tyrosine hydroxylase (TH) phenotype and overt degeneration of nigral neurons. By leveraging the distinct aggregation phase of the PFF model, we are able to specifically investigate the transcriptomic response within the SN to pSyn inclusion formation prior to neurodegeneration.

In the present dissertation we used a laser capture microdissection (LCM) technique and RNA sequencing to investigate differential gene expression within the inclusion-bearing nigra at one- and two-months post PFF injection, prior to phenotype loss and subsequent neurodegeneration. Our results suggest that genes and pathways associated with inflammation and the immune response are increased at both timepoints, and that genes and pathways associated with synaptic transmission and

synaptic signaling are decreased at both timepoints. In addition, we found that upregulation of genes and pathways implicating defense responses to virus are uniquely upregulated at the two-month time point. Furthermore, we identified a family of proteases, called cathepsins, that are upregulated in the inclusion-bearing SN at both timepoints. Subsequent follow up analysis using droplet digital PCR (ddPCR), fluorescent *in situ* hybridization (FISH), and immunofluorescence (IF) revealed increases in multiple cathepsins within the inclusion-bearing SN. Specifically, cathepsin H (*Ctsh*), S (*Ctss*), and X (*Ctsx*) were all found to be enriched within microglia in the inclusion-bearing SN at either one, two, or both timepoints following PFF injection. Collectively, these results suggest that the impact of microglia to pSyn inclusions in the SNpc is temporally dynamic. These results suggest a role for reactive microglia in early alpha-synuclein pathology and may provide therapeutic targets for disease intervention.

ACKNOWLEDGEMENTS

This dissertation would not have been possible without the efforts of Drs. Caryl Sortwell and Joseph Patterson. Throughout my research journey, you have provided invaluable guidance, unwavering support, and steadfast patience along this winding path. Your mentorship transformed me from a bull in a China shop into a refined and intentional scientist. Thank you for taking a chance on me, and I hope I have made you proud.

The opportunity to complete this dissertation stems from the foundational support and guidance I received during my upbringing. To Chris & Susan, Bill & Marie, and Dave & Mary – thank you for teaching me curiosity, instilling a strong work ethic, and showing me how to love deeply. Whatever my hand finds to do, I will do it with all my might. Thank you for the opportunities you've given me; I hope I have made you all proud.

To my wife, Ashley – thank you for loving me unconditionally, and letting me love you in return. We would not be here today if it weren't for the sacrifices you made long ago. I am forever grateful for your unwavering support and look forward to raising our children together. Thank you for being the fiercely loving woman that you are; I hope I have made you proud and will continue to do so.

To my coaches, teachers, mentors, teammates, family, and friends – although there are too many of you to list individually, that fact alone speaks volumes about the strength and depth of my support network. If you are reading this, know that you played a role in this dissertation and in shaping who I am today. You are valued and loved. I hope I have made you proud.

PREFACE

We intend to combine chapters 2 and 3 and submit for publication upon completion of this dissertation.

TABLE OF CONTENTS

LIST OF ABBREVIATIONS vii

CHAPTER 1: INTRODUCTION 1
INTRODUCTION TO PARKINSON'S DISEASE 2
NEUROINFLAMMATION IN PD 18
MICROGLIA IN HEALTH AND DISEASE 23
INSIGHTS INTO THE ROLE OF NEUROINFLAMMATION IN PD USING PRECLINICAL MODELS 38
SUMMARY AND DISSERTATION FOCUS 52
BIBLIOGRAPHY 56

CHAPTER 2: TRANSCRIPTOMIC ALTERATIONS IN THE SUBSTANTIA NIGRA ASSOCIATED WITH EARLY AND MATURE LEWY BODY-LIKE INCLUSIONS – FOCUS ON NEUROINFLAMMATORY SIGNALING 85
INTRODUCTION 86
METHODS 87
RESULTS 99
DISCUSSION 120
BIBLIOGRAPHY 129

CHAPTER 3: VALIDATION AND LOCALIZATION OF THE MICROGLIAL TRANSCRIPTIONAL RESPONSE TO A-SYN INCLUSIONS 135
INTRODUCTION 136
METHODS 139
RESULTS 152
DISCUSSION 175
BIBLIOGRAPHY 187

CHAPTER 4: CONCLUSION AND FUTURE DIRECTIONS 193
OVERVIEW 194
TECHNICAL LIMITATIONS OF THE CURRENT METHODS 196
BIOLOGICAL LIMITATIONS OF THE CURRENT METHODS 200
FUTURE DIRECTIONS WITH THE PFF MODEL 201
FUTURE RESEARCH DIRECTIONS 202
BIBLIOGRAPHY 208

LIST OF ABBREVIATIONS

PD	Parkinson’s Disease
NMS	Non motor symptoms
CNS	Central nervous system
PNS	Peripheral nervous system
ANS	Autonomic nervous system
DATscan	Dopamine transporter scan
GPi	Globus pallidus pars interna
STR	Striatum
STN	Subthalamic nucleus
GPe	Globus pallidus pars externa
SN	Substantia nigra
SNpc	Substantia nigra pars compacta
SNpr	Substantia nigra pars reticulata
DA	Dopamine
α-Syn	Alpha-synuclein
LBs	Lewy bodies
LNs	Lewy neurites
VTA	Ventral tegmental area
AGTR1	Angiotensin II receptor type 1
BBB	Blood brain barrier
CSF	Cerebrospinal fluid
IL-1ß	interleukin 1-beta

TNF-α	Tumor necrosis factor alpha
PET	Positron emission tomography
GWAS	Genome wide association study
GPNMB	Glycoprotein NMB
GRN	Progranulin
BST1	Bone marrow stromal cell antigen 1
SYT11	Synaptotagmin 11
NSAID	Non-steroidal anti-inflammatory drug
TLR	Toll-like receptor
PRR	Pattern recognizing receptors
PAMP	Pathogen associated molecular patterns
DAMP	Damage associated molecular patterns
MHC	Major histocompatibility complex
HLA-DR	Human leukocyte antigen DR isotype
6-OHDA	6-hydroxydopamine
AAV	Adeno-associated virus
pSyn	Phosphorylated alpha synuclein
BDNF	Brain derived neurotrophic factor
HIV	Human immunodeficiency virus
ALS	Amyotrophic lateral sclerosis
MS	Multiple sclerosis
AD	Alzheimer's disease
LPS	Lipopolysaccharide

Iba-1	Ionized calcium-binding adaptor molecule 1
NPCs	Neural progenitor cells
IL-4	Interleukin-4
IFN-γ	Interferon gamma
C1q	Complement component 1q
TNF	Tumor necrosis factor
Aβ	Amyloid beta
MAC	Membrane attack complex
TGF-ß1	Transforming growth factor-beta 1
CD-68	Cluster of differentiation 68
CD4	Cluster of differentiation 4
CD8	Cluster of differentiation 8
IGF-1	Insulin-like growth factor-1
ROS	Reactive oxygen species
cGAS	Cyclic GMP-AMP synthase
PRR	Pattern recognition receptor
STING	Stimulator of interferon genes
CCL5	C-C motif chemokine ligand 5
CCL10	C-C motif chemokine ligand 10
RNAseq	RNA sequencing
BAMs	Border associated macrophages
DAT	Dopamine transporter
FISH	Fluorescent in-situ hybridization

IF	Immunofluorescence
NO	Nitric oxide
Ctsa	Cathepsin A
Ctsb	Cathepsin B
Ctsc	Cathepsin C
Ctsd	Cathepsin D
Ctse	Cathepsin E
Ctsf	Cathepsin F
Ctsh	Cathepsin H
Ctsk	Cathepsin K
Ctsl	Cathepsin L
Ctss	Cathepsin S
Ctsw	Cathepsin W
Ctsx	Cathepsin X

CHAPTER 1: INTRODUCTION

INTRODUCTION TO PARKINSON'S DISEASE

Discovery

Parkinson's disease (PD) was first described by James Parkinson in his *Essay on the Shaking Palsy* in 1817. As Dr. Parkinson put it "*So slight and nearly imperceptible are the first inroads of this malady, and so extremely slow its progress, that it rarely happens, that the patient can form any recollection of the precise period of its commencement*" (Parkinson, 2002). The symptoms of the disease slowly infiltrate the body, where a slight quiver in the hand can crescendo over years into an ensemble of debilitating symptoms. Dr. Parkinson coined the term *paralysis agitans* for what he observed, a name that would later be replaced with Parkinson's disease in 1872 by Dr. Jean-Martin Charcot. Dr. Charcot refined the symptoms of Parkinson's Disease, and differentiated the disease from other similar disorders such as multiple sclerosis and alcoholism (Charcot and Sigerson, 1879). Since these descriptions 200 years ago, much has been learned about the potential causes of PD, primary risk factors for developing the disease, symptom management therapies, and more recently we have begun to understand the genetic factors that influence disease onset and progression. Still today, however, there are no cures, disease modifying therapies, or interventions that slow or halt disease progression. It is the second most common neurological disorder, only behind Alzheimer's Disease, and is the fastest growing neurological disorder as of 2018 (Dorsey *et al.*, 2018). Diagnosis rates are expected to double over the coming decades, and the economic burden is expected to reach $79.1 billion in the United States alone by 2040 (Yang *et al.*, 2020). One of the biggest challenges with the disease is how difficult it can be for clinicians to diagnose the disease. PD has a

variable symptom presentation in patients, as some patients have clearly defined symptoms, with others presenting only a subtle tremor. Patients can live with the disease for decades, while others only a few years after diagnosis. The variability in disease presentation presents challenges for patients, clinicians, and caretakers alike - as no uniform disease management plan exists. With that, there are disease hallmarks used to predict diagnosis and initiate a treatment plan.

Motor-Symptoms

The most observable signs for Parkinson's Disease are the motor deficits. There are four hallmark motor symptoms that can be broken down with the acronym TRAP; tremor at rest, rigidity, akinesia (or bradykinesia), and postural instability (Frank, Pari and Rossiter, 2006; Jankovic, 2008). Although there is a heterogeneity of symptoms, to clinically diagnose PD bradykinesia in addition to one or more of the motor symptoms must be present (Jankovic, 2008). Furthermore, these symptoms can be present in other clinical disorders, and thus, additional clinical evaluation is required for PD diagnosis, such as responsiveness to dopamine (DA) replacement therapies or a DA transporter scan (DATscan) (Seifert and Wiener, 2013). Diagnosis can take years, require traveling to specialists, and is longitudinally monitored using the Unified Parkinson's Disease Rating Scale (UPDRS) (Postuma *et al.*, 2015). The UPDRS includes tracking of patient mood and memory, daily living activities, and motor symptom examination.

Non-motor Symptoms

Sometimes less observable, yet often more debilitating, are the non-motor symptoms (NMS) of PD, which can be present 5-10 years prior to motor symptom

presentation (Pont-Sunyer *et al.*, 2015). The range of NMS in PD is vast, with 31 recognized symptoms ranging from mood disturbances, constipation, unexplained pain, fatigue, sleep disturbances, to loss of smell and taste. Broadly, the NMS can be broken into four categories: neuropsychiatric, cognitive, autonomic, and sleep; and on average, an individual with PD will experience 11 non-motor symptoms (Lyons and Pahwa, 2011). Up to 80% of individuals will experience some form of depression, and cognitive decline impacts 83% of individuals with PD 20 years after diagnosis (Biundo, Weis and Antonini, 2016; Aarsland *et al.*, 2021). Many complain that the non-motor symptoms have a strong impact on quality of life and daily activity, yet there are limited treatments or cures targeting this aspect of disease.

The underlying cause of PD has yet to be discovered. However, there are many observations from postmortem analyses that have revealed clues and hallmark pathologies that can help us elucidate some of the causes for the symptoms discussed above.

Neuropathology and Neuroanatomy

Parkinson's disease is a multi-circuit, multi-system disease that affects both the central nervous system (CNS) and autonomic nervous system (ANS). Within the CNS, the primary brain regions that are affected in PD are within the basal ganglia (Figure 1.1). The basal ganglia is composed of the caudate and putamen (the dorsal striatum; STR), the globus pallidus pars interna (GPi) and pars externa (GPe), subthalamic nucleus (STN), and substantia nigra pars compacta (SNpc) and pars reticulata (SNpr) (Bolam *et al.*, 2000). In healthy individuals, these highly interconnected brain regions are responsible for voluntary movement, procedural learning, emotion, and executive

function (Redgrave *et al.*, 2010). In individuals with PD, dysfunction of these brain regions is responsible for the motor and non-motor symptoms.

Direct and Indirect Pathway

The primary input to the basal ganglia is from the cortex to the striatum, while the primary output is from the globus pallidus interna (GPi) and substantia nigra pars reticulata (SNpr) to the thalamus, which projects to the motor cortex (Lanciego, Luquin and Obeso, 2012) (Figure 1.1). Within the basal ganglia, there are direct and indirect pathways that facilitate or inhibit action selection, regulating the flow of information through and out of the system, coordinating voluntary motor behavior.

Broadly speaking, movement initiation begins in the cortex, which sends excitatory signals to the striatum. Activity in striatal neurons is regulated by the SNpc via DA, and signals are sent to the globus pallidus and subthalamic nucleus, ending in the thalamus. The thalamus then sends excitatory signals to the entire frontal cortex which allow for the execution of the initial movement request. This simplified process is much more complex (DeLong and Wichmann, 2009), but it is important to have a basic framework of the basal ganglia-movement facilitation process before diving deeper into how the pathway is impacted in PD.

The SNpc has dopaminergic projections to the caudate and putamen (dorsal striatum; STR) that act on medium spiny neurons expressing either dopamine receptor 1 (D1; direct pathway) or dopamine receptor 2 (D2; indirect pathway) (Calabresi *et al.*, 2014). In the direct pathway, DA released from the SNpc bind to D1 receptors in the dorsal striatum (caudate and putamen) which leads to enhanced GABAergic inhibitory input in the GPi, resulting in inhibition of the inhibitory output from the thalamus (i.e.,

disinhibition) and excitation of the cortex, thereby, facilitating a particular motor behavior. In the indirect pathway, DA released from the SNpc binds to D2 receptors in the caudate and putamen, which sends inhibitory signals to the GPe, and then to the subthalamic nucleus (STN), finally to the GPi. The indirect pathway, “inactivated” by D2 receptor binding in the STR, results in eventual inhibition of the thalamus, which results in inactivation of the frontal cortex, and thus suppressing unwanted movements. In the PD brain, loss of DA neurons in the SN result in decreased activity of the direct pathway, and a relative overactivity of the indirect pathway, which impairs goal directed movement (Figure 1.1). The overactivation of the indirect pathway results in greater inhibition of GPe, resulting in a decrease of inhibitory signals to the STN, resulting in overactivity (decrease in inhibition = overactivity). Overactivity of the STN results in increased activity of the GPi, which sends excess inhibitory signals to the thalamus. Overactivity of inhibitory signals to the thalamus results in the thalamus sending fewer excitatory signals to the cortex, thus decreasing activity in the cortex.

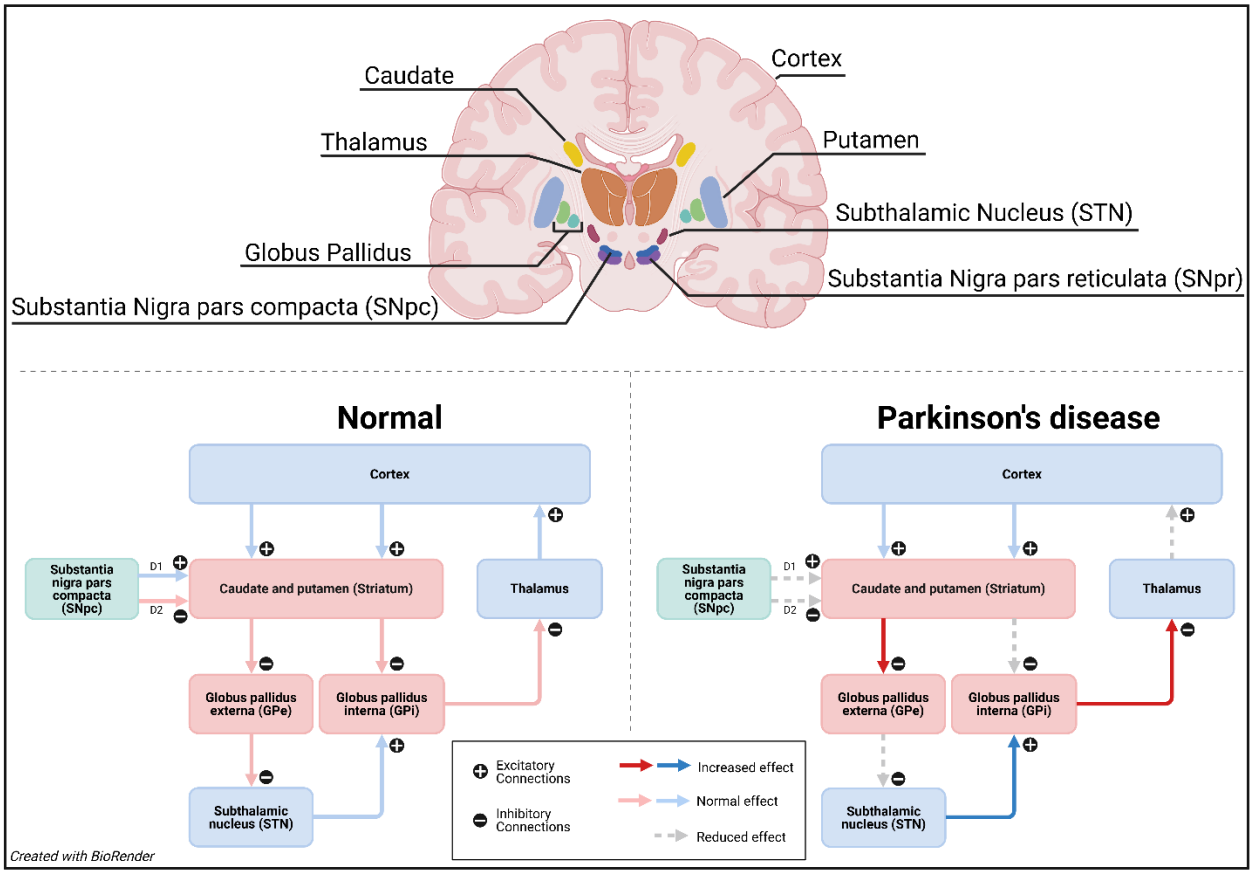

Figure 1.1 Basal ganglia circuitry and parkinsonian impact

Anatomical and pathway illustration comparing normal functioning direct-indirect pathways and changes in Parkinson's disease impacted direct-indirect pathway. *(Top)* Neuroanatomical illustration of relevant brain regions in the basal ganglia direct-indirect pathway including caudate and putamen, thalamus, globus pallidus (externa & interna; GPe & GPi), cortex, subthalamic nucleus (STN), substantia nigra pars compacta (SNpc), and substantia nigra pars reticulata (SNpr). *(Bottom)* Specific circuit diagrams for normally functioning direct-indirect pathways *(left)* and Parkinson's Disease impact *(right)*.

Lewy Body Composition and Pathology

Post-mortem analysis of individuals with PD reveals loss of DA neurons in the SN and dopaminergic terminals in the STR, in addition to the presence of Lewy bodies (LBs) and/or Lewy neurites (LNs). However, the specific mechanisms contributing to the death of nigrostriatal circuitry is incompletely understood. LBs are cellular inclusions which were first observed and described by Dr. Frederic Lewy in 1912 (Goedert *et al.*, 2013). LNs, on the other hand, are located in axons and dendrites of diseased neurons (Spillantini *et al.*, 1998). It wasn't until 1997 that the primary component of LBs and LNs were identified as the protein alpha-synuclein (α-Syn) by Dr. Maria Spillantini and colleagues (Spillantini *et al.*, 1997). α-Syn is a small protein, 140 amino acids long, and is one of the most abundant proteins in the brain, including in the neocortex, hippocampus, substantia nigra, and thalamus (Stefanis, 2012). α-Syn is generally found in the synapse and nucleus of cells, and is an intrinsically disordered protein that can alter its shape based on the environment and interactions with other molecules to form secondary and tertiary structures (Stefanis, 2012). The process of α-Syn aggregation can be triggered by either binding to a protein complex such as Tau or β-amyloid, or by misfolding into an oligomeric or fibrillar forms that seed, or corrupt, monomeric α-Syn (Cremades *et al.*, 2012; Bernal-Conde *et al.*, 2019). Once formed, LBs are composed of a heterogeneous mixture of up to 90 molecules that can accumulate into a mature inclusion, composed of mitochondrial proteins, structural proteins, ubiquitin-proteasome complex proteins, lipid membrane fragments, and vesicles, to name a few of the potentially contained components of cellular debris (Shults, 2006; Wakabayashi *et al.*, 2013; Shahmoradian *et al.*, 2019).

The initial discovery of LBs were localized to the dorsal motor nucleus of the vagus nerve, however, it is now understood that LBs are present throughout the central and peripheral nervous system in PD patients (Engelhardt and Gomes, 2017). In the peripheral nervous system (PNS), LBs can be found in the enteric nervous system, sympathetic ganglia, and the gastrointestinal system (Barrenschee *et al.*, 2017). In the CNS, LBs can be observed in regions ranging from the olfactory bulb, spinal cord, SN, STR, and brainstem (Wakabayashi *et al.*, 2013). Within the brain, some regions with LB development are accompanied by demonstrable neurodegeneration (namely, the SN and locus coeruleus), whereas other brain regions develop LBs but do not degenerate to the same magnitude (amygdala, cerebral cortex, hypothalamus, posterior pituitary, dorsal raphe nucleus, dorsal vagal nucleus, cerebellum, and spinal cord (Wakabayashi *et al.*, 2013)).

Braak Staging of Lewy Pathology

Braak staging was first described in 2003 by Braak and colleagues as a framework for understanding PD progression and emphasizing the location and distribution of LBs and LNs based on varying times after PD diagnosis (Braak *et al.*, 2003). Six stages were proposed based on observations of LB and LN pathology within different brain regions (Braak and Del Tredici, 2009).

Stage 1: Dorsal motor nucleus, intermediate reticular zone, and olfactory bulbs.

Stage 2: Pathologies of Stage 1 as well as the pontine tegmentum (raphe, locus coeruleus.

Stage 3: Pathologies of Stages 1-2 as well as the midbrain (SNpc, amygdala, basal forebrain).

Stage 4: Pathologies of Stages 1-3 as well as the temporal mesocortex; and

Stage 5/6: Pathologies of Stages 1-4 as well as the neocortex and premotor cortex.

Braak staging of PD has become the gold standard of post-mortem evaluation of PD brain. The Braak staging system provides a neuroanatomical explanation for development of symptoms in PD patients. In addition, the Braak staging system has driven the field to consider whether or not LBs can spread between cells in a prion-like fashion, known as the Braak Prion Hypothesis (Steiner, Angot and Brundin, 2011).

Nigrostriatal Degeneration

LB formation is one of two pathological hallmarks of PD, where neurodegeneration of DA neurons in the nigrostriatal pathway is the second. Loss of these neurons is responsible for the constellation of motor symptoms of PD, via a lack of DA being released in the STR, disrupting basal ganglia circuitry (Figure 1.1) (Blandini *et al.*, 2000). At the time of clinical diagnosis, it is estimated that there is a ~60% loss of striatal DA, and a 50% loss of SN DA neurons (Kordower *et al.*, 2013; Kurowska *et al.*, 2016). Interestingly, not all SN DA neurons are equally affected in PD. DA neurons in the ventral portion of the SNpc, which project to the putamen, demonstrate a higher proportion of DA neurodegeneration than in the dorsal SNpc, which project to the caudate (Gibb and Lees, 1991; Hornykiewicz, 2001). Furthermore, brain regions directly neighboring the SNpc, such as the ventral tegmental area (VTA), contain DA neurons that remain mostly unaffected in early PD (Agid, 1991). The reason for DA neuron selective vulnerability remains unclear. There is evidence to suggest it is related to high metabolic demand, reactive oxygen species, iron and neuromelanin content, and/or proximity to dense microglial cell populations (Hirsch, Graybiel and Agid, 1988; Chan,

Gertler and Surmeier, 2010; González-Hernández *et al.*, 2010). Most recently, transcriptional profiling of DA neurons within the SNpc have revealed that the gene AGTR1 (angiotensin II receptor type 1) is primarily expressed in the ventral region of the SNpc, which may play a role in selective vulnerability of these DA neurons (Kamath *et al.*, 2022).

Current Treatment Strategies

Disease modifying therapies aim to slow, or halt, disease progression by impacting one, or both, of the PD pathological hallmarks (LB formation and nigrostriatal degeneration). To date, there are no treatments or therapies that can accomplish either. By the time motor symptoms are detectable there is already a substantial loss of SNpc neurons, thus, there are 2 unmet needs in the PD research field. The first is an ability to detect disease prior to emergence of clinical symptoms, and the second is to identify targets that participate in disease causation and progression. The current treatments available to PD patients are restricted to symptom management, which I discuss in the following sections.

Pharmacotherapies

Current pharmacotherapies focus on increasing dopamine levels in the brain which are relatively effective at restoring balance to basal ganglia circuitry and alleviating motor symptoms (DeMaagd and Philip, 2015). The most common DA pharmacotherapy is levodopa (L-dihydroxyphenylalanine, L-DOPA), which crosses the blood brain barrier (BBB) and, once in the brain, is converted into dopamine. L-DOPA is a product of the rate-limiting step in DA synthesis, which, when supplemented, boosts DA levels that effectively restore signaling in the basal ganglia. However, there are

caveats to this drug. Due to the short half-life of L-DOPA (~1.5 hours), frequent dosing is required to achieve therapeutic benefit, and the symptom relief is temporary. Patients also develop tolerance to L-DOPA via increases in peripheral metabolism in addition to nigrostriatal system restructuring (Khor and Hsu, 2007). Peripheral metabolism in the gut occurs from bacteria that express tyrosine decarboxylase, which converts L-DOPA to DA in the small intestine. DA, unlike L-DOPA, does not readily cross the BBB, reducing the amount of bioavailable DA in the CNS following L-DOPA metabolism. To combat this, carbidopa was developed, a decarboxylase inhibitor, that prevents the immature metabolism of L-DOPA prior to CNS delivery. Carbidopa is now co-administered with L-DOPA which is the gold standard therapy for care for PD patients (carbidopa-levodopa co-administration). However, increasing the amount of bioavailable DA does not completely prevent development of tolerance. Once in the CNS, L-DOPA is converted into DA that will supplement DA transmission in the nigrostriatal system, specifically within the striatum. In early PD, there are sufficient DA terminals to buffer L-DOPA derived DA packaged into synaptic vesicles for release. However, as the disease progresses and DA terminals are depleted, there is less DA to buffer L-DOPA delivery, resulting in DA “surges” that promote pulsatile receptor stimulation (Bandopadhyay et al., 2022). This pulsatile receptor stimulation results in DA receptor restructuring and internalization, requiring more L-DOPA to achieve therapeutic effects, further exacerbating DA surges, pulsatile receptor stimulation, and receptor internalization. In some patients, this duality of needing more drug, while building tolerance, can result in hyperkinetic side effects following L-DOPA doses, called levodopa induced dyskinesias (Ahlskog and Muenter, 2001; Hauser *et al.*, 2017). There are limited options for treating

L-DOPA induced dyskinesias, with a highly variable treatment response between patients. There is an unmet need to identify a uniformly effective and well tolerated treatment, however, there have been promising results from recent preclinical investigations (Steece-Collier *et al.*, 2019).

Other pharmacotherapies alone may not be as effective as L-DOPA-carbidopa, but can be taken in tandem to enhance the efficacy of L-DOPA/carbidopa or alone as monotherapies (Borovac, 2016). DA agonists mimic the structure of DA and bind to DA receptors (bromocriptine, pramipexole, ropinirole, apomorphine, and cabergoline) to enhance DA signaling in the striatum. DA metabolism can also be manipulated by inhibiting the enzymes that breakdown DA, specifically, catechol-o-methyltransferase (COMT) and monoamine oxidase (MAO), to enhance DA signaling.

Surgical Intervention

Pharmacological treatments are considered a first line treatment for PD, however, when these treatments are no longer effective for symptom management, surgical intervention is an alternative option for patients (Pahwa *et al.*, 2006; Graat, Figee and Denys, 2017). Approved by the FDA in 2002, deep brain stimulation (DBS) involves surgical insertion of an electrode into the basal ganglia, usually the GPi or subthalamic nucleus. The electrode restores balance to the basal ganglia system with intermittent pulses of electricity, like a pacemaker of the heart. DBS does provide symptom relief, as well as improve daily living activities for patients, however, it is not a permanent solution. Although a majority of patients (~90%) have a positive review of the surgery and would recommend it to other patients, patient quality of life scores generally

return to pre-surgery levels 5-years after surgical implantation (Limousin and Foltynie, 2019; Hitti *et al.*, 2020).

Etiology and Pathogenic Mechanisms

Several genetic and environmental factors have been associated with increased PD risk. Around 10% of PD cases are associated with an inherited monogenic mutation or gene multiplication that leads to development of PD (Ohnmacht *et al.*, 2020). The remaining ~90% of PD cases are sporadic, or non-familial, and have no known direct cause of the disease. The development of PD has multiple contributors that ultimately converge on common pathogenic mechanisms. These contributing factors will be explored in the following section.

Contributing Factors: Age, Sex, Ethnicity & Race

The largest risk factor when it comes to developing PD is age (Collier, Kanaan and Kordower, 2011). Aging in and of itself is not necessarily associated with developing PD, but it is the natural aging process that may contribute to compromised cellular mechanisms that increase DA neuron susceptibility to PD. For example, mitochondria turnover and ubiquitin protease degradation are cellular processes that become less efficient with aging (Hindle, 2010; Collier, Kanaan and Kordower, 2011). These changes may not contribute to disease risk alone but may leave DA neurons more susceptible to additional risk factors.

Sex is another contributing risk factor for development of PD, where biologically born males have a nearly 2X higher risk of developing the disease in their lifetime (Baldereschi *et al.*, 2000). Interestingly, although biologically born women are less susceptible to developing PD, the disease progresses more rapidly and has a higher

mortality rate than in men (Cerri, Mus and Blandini, 2019). While the reason for this disparity between the sexes is unknown, it is thought that estrogen may play a role, as estrogen has potent antioxidant properties that play an important role in neuronal homeostasis (Zárate, Stevnsner and Gredilla, 2017). To further support this idea, studies have shown that the number of children and length of a woman's fertility cycle can delay PD onset, and that postmenopausal hormone therapy can improve motor function in women diagnosed with PD (although, hormone therapy has mixed results, where not every patient will see the same benefit) (Saunders-Pullman *et al.*, 1999; Strijks, Kremer and Horstink, 1999; Frentzel *et al.*, 2017).

Population studies have also revealed influences by ethnicity and race that may contribute to developing PD. For example, within the Ashkenazi Jewish population, there is a higher prevalence of genetic mutations associated with PD (specifically, Leucine rich repeat kinase 2 (LRRK2) G2019S mutation) (Marder *et al.*, 2015). Multiple studies have looked at race as a contributing factor and found that white and Hispanic populations have a higher incidence of PD compared to Asian and Black populations (Wright Willis *et al.*, 2010; Ben-Joseph *et al.*, 2020). That being said, geographical location may have a more contributory role, as Black-Africans residing in sub-Saharan Africa have a lower incidence rate compared to people of African descent living in the USA (Dotchin *et al.*, 2008; Ben-Joseph *et al.*, 2020). Additionally, there is an overall lower incidence rate of PD in Asia compared to Europe, North America, and Australia (Pringsheim *et al.*, 2014). Many factors can contribute to this disparity, such as socio-economic factors, access to healthcare, diet, and environmental exposures (Yang *et al.*, 2016; Solch *et al.*, 2022).

α-Synuclein, Genetics & Environmental Exposures

α-Syn is implicated in both sporadic and inherited forms of PD, and thus, plays a critical role in our understanding of PD. α-Syn is a 140 amino acid long, natively unfolded, and highly abundant protein; comprising 1% of all cytosolic proteins (Maroteaux, Campanelli and Scheller, 1988). The protein is enriched in presynaptic terminals and is thought to play a role in synaptic transmission (Iwai *et al.*, 1995; Benskey, Perez and Manfredsson, 2016). An intrinsically disordered protein, α-Syn has a dynamic structure with a tertiary structure which can alter its conformation depending on the environment, allowing for a wide array of physiological functions (Weinreb *et al.*, 1996; Benskey, Perez and Manfredsson, 2016). Because of this, α-Syn is prone to aggregation and can self-assemble into insoluble aggregates (Conway, Harper and Lansbury, 1998).

The gene that encodes α-Syn, *SNCA*, was the first definitive genetic-mutation linked to PD risk. In 1997, a point mutation (A30P) on the *SNCA* gene was identified as an autosomal dominant cause of PD (Polymeropoulos *et al.*, 1997). Since then, there have been additional discoveries of point mutations (A53T, G51D, E46K) as well as duplications and triplications of the *SNCA* gene that are associated with familial PD (Krüger *et al.*, 1998; Singleton *et al.*, 2003; Chartier-Harlin *et al.*, 2004; Ibáñez *et al.*, 2004; Zarranz *et al.*, 2004). The underlying reason for these mutations to cause PD is not fully understood, however, there is evidence to suggest that point mutations increase the kinetics of α-Syn, and multiplications increase endogenous protein levels, thereby increasing the risk of aggregation (Conway, Harper and Lansbury, 1998; Oliveira *et al.*, 2015; Flagmeier *et al.*, 2016). Other genetic mutations associated with autosomal

dominant inheritance of PD are leucine-rich repeat kinase 2 (*LRRK2*), vacuolar protein sorting associated protein 35 (*VPS35),* and many more (Funayama *et al.*, 2002; Vilariño-Güell *et al.*, 2011). Mutations to the *LRRK2* gene are the most common monogenic cause in familial PD, which results in a toxic gain-of-function phenotype, whereas mutations to *VPS35* result in a toxic loss-of-function phenotype (Zimprich *et al.*, 2004; Rahman and Morrison, 2019). There are some identified autosomal recessive genes associated with PD, namely: parkin (*PRKN,* an E3 ubiquitin ligase)*,* PTEN induced kinase 1 *(PINK1,* a mitochondrial serine/threonine kinase*) and* DJ-1 (PARK7, a cysteine protease) which result in a toxic loss-of-function phenotype that results in early onset PD (Kitada *et al.*, 1998; Lücking *et al.*, 2000; Giasson *et al.*, 2006; Ross *et al.*, 2006; Lees, Hardy and Revesz, 2009; Gasser, Hardy and Mizuno, 2011; Trempe and Fon, 2013).

Individual genotypes and environmental exposures to toxicants have a complex interplay that can lead to the development of PD. Not every individual exposed to an environmental toxin will end up developing PD, but there are observed and understood environmental toxins that have been shown to increase the risk of developing PD. Certain occupations, such as farmers working with herbicides and pesticides or miners exposed to heavy metals, have been shown to increase the risk of developing PD (Castillo *et al.*, 2017; Pouchieu *et al.*, 2018; Ball *et al.*, 2019). Air pollution has also been investigated as increasing the risk of developing PD, and it has been shown that ambient air pollution from traffic is correlated with developing PD (Finkelstein and Jerrett, 2007; Ritz *et al.*, 2016). Certain herbicides and pesticides, such as paraquat, rotenone, and dieldrin to name a few, have been investigated for increasing the risk of

PD, and results consistently demonstrate a correlation between exposure to these compounds and development of PD (Kanthasamy *et al.*, 2005; Tanner *et al.*, 2009). Paraquat in particular is one of the most commonly used herbicides in U.S, as well as one of the most toxic, and is strongly linked to PD development (Spivey, 2011; Paul *et al.*, 2024). The compound is banned in more than 50 countries, including the U.K, E.U, China, and Brazil, and studies have shown that banning the compound does result in significant decreases in pesticide-associated mortalities (Kim *et al.*, 2017).

With any cause of PD, monogenic mutation, sporadic or environmental exposure, the consequences of disease progression remain the same - loss of DA neurons within the nigrostriatal pathway, and in most cases, development of LB pathology. However, there is a potential third hallmark of disease, neuroinflammation, which will be discussed in the following sections.

NEUROINFLAMMATION IN PD

Evidence for Inflammation in PD

Clinical findings have revealed consistent upregulation of inflammatory markers in the biofluids sampled from PD subjects. Cytokines, molecules associated with inflammatory signaling, are increased in the cerebrospinal fluid (CSF) of PD subjects (Mogi *et al.*, 1996; Nagatsu *et al.*, 2000; Lindqvist *et al.*, 2013; Qin *et al.*, 2016; Chen *et al.*, 2018). Mutations in multiple proinflammatory cytokine genes (*TNF, IL1ß, and IL6*) are associated with an increased risk of developing PD (Chu, Zhou and Luo, 2012). Cytokines can also be anti-inflammatory, and it has been shown that PD subjects have decreased anti-inflammatory cytokines in brain regions affected by PD (Garcia-Esparcia *et al.*, 2014). Cytokines such as interleukin 1-beta (IL-1ß), interleukin 18 (IL-18), tumor

necrosis factor (TNF), among many others, are examples of molecules released by, as well as activated by, microglia within the PD brain.

Microglia are the resident immune cells of the brain; they are the first line of defense against insults induced by infections, cell death, neurotransmitter imbalance, or other stressors. Making up 10% of the cellular population in the CNS, microglia play a key role in orchestrating the immune response (Augusto-Oliveira *et al.*, 2019). When microglia receive damage or pathogen signals, they become 'activated' and recruit additional immune cells to the area via cytokine release. Positron emission tomography (PET) imaging, as well as post mortem studies, have revealed a consistent upregulation of activated microglia in the brains of PD subjects (Ouchi *et al.*, 2005; Gerhard *et al.*, 2006). Collectively, there is accumulating evidence for inflammation playing a role in PD. The following sections delve into greater detail about the topics described above, and expand into additional topics that support the role of inflammation in PD.

GWAS Studies, Autoimmune Diseases, and Anti-Inflammatory Medication

GWAS, or genome-wide association studies, are studies that explore the genomes of a large group of individuals to understand if there are underlying genetic associations with disease outcomes. More than 90 genetic loci have been identified to be associated with sporadic PD, including loci associated with microglia (human leukocyte antigen; HLA) (Nalls *et al.*, 2014; Tan *et al.*, 2020). Other loci associated with immune functions and an increased risk for PD include glycoprotein NMB (*GPNMB*), synaptotagmin 11 (*SYT11*), progranulin (*GRN*), bone marrow stromal cell antigen 1 (*BST1* or *CD157*), among others (Tansey *et al.*, 2022).

GWAS studies have revealed overlapping genetic loci with autoimmune diseases, as well. In autoimmune diseases, the body mistakenly recognizes healthy cells as foreign and launches a periphery-wide, consistent, and robust immune response. A chronically activated immune system producing inflammatory mediators such as cytokines leaves the body susceptible to additional complications, such as PD (Tansey *et al.*, 2022). A 2017 GWAS study revealed 17 genetic loci overlapping with PD and either type-1 diabetes, Crohn's disease, ulcerative colitis, rheumatoid arthritis, psoriasis, multiple sclerosis, or celiac disease (Witoelar *et al.*, 2017). Similarly, studies have shown that autoimmune diseases can increase the risk of developing PD. Patients with multiple sclerosis, Hashimoto's, Graves', or polymyalgia rheumatica have up to a 33% increased risk of PD (Li, Sundquist and Sundquist, 2012).

Conversely, autoimmune treatments that focus on anti-inflammatory outcome measures have shown to decrease PD risk. Chloroquine or hydroxychloroquine, used to decrease inflammation in Rheumatoid arthritis, has been shown to decrease risk for developing PD (Paakinaho *et al.*, 2022). The use of anti-inflammatory drugs (non-steroidal anti-inflammatory drugs (NSAID), aspirin) has also shown to decrease the risk of developing PD (Chen *et al.*, 2003, 2005; Wahner *et al.*, 2007). The mechanism by which anti-inflammatory medication is thought to be neuroprotective is through inhibition of cyclooxygenase 1 and 2 (COX1 & COX2), by which COX inhibition results in increased nitric oxide radical scavenging, reducing oxidative stress levels (Asanuma *et al.*, 2001). It is also worth mentioning that there are conflicting studies which have shown that anti-inflammatory medication does not reduce the risk of developing PD, and

thus, more studies are needed to clarify this relationship (Ren *et al.*, 2018; Poly *et al.*, 2019).

Innate Immune System

There are two parts of the immune system: innate and adaptive immune systems. The two systems are intimately linked, where the innate immune system, primarily composed of microglia in the CNS, recruit peripheral immune cells of the adaptive immune system to the area of insult and launch their own immune response. Specifically in PD, microglia activation is associated with pathological α-Syn (LBs and LNs) as well as neurodegeneration, and evidence suggests that T-lymphocytes (T-cells) of the adaptive immune system are recruited to the area.

Microglia express receptors (i.e., Toll-like receptors (TLRs)) on their cell surface that are crucial to recognizing insults and initiating the innate immune response. TLRs are in the family of pattern recognition receptors (PRR's) which respond to exogenous, foreign structures such as viruses and bacteria (pathogen associated molecular patterns; PAMPs) or endogenous molecules released when a cell is damaged (damage associated molecular patterns; DAMPs) (Arroyo *et al.*, 2011). Activation of TLRs triggers a series of cellular processes within microglia that result in production and release of cytokines, such as IL-1ß and tumor necrosis factor alpha (TNF-α), which create a chemokine gradient to guide additional immune cells to the area.

Cytokine release and chemokine gradients are responsible for recruiting additional immune cells to the location of insult, additionally, microglia will go one step further and 'present' antigens, or portions of molecules, proteins, or other pathogen debris, on the microglial cell surface to immune cells recruited from the adaptive

immune system. This is the process by which the innate immune system (microglia) activates and communicates with the adaptive immune system (cluster of differentiation 4 positive T-cells; CD4+ T-cells). To “show” adaptive immune cells what initiated the recruitment signals, microglia express major-histocompatibility complexes (MHC) on their cell surfaces.

Major Histocompatibility Complexes and the Adaptive Immune System

Major histocompatibility complexes (encoded by the human leukocyte antigen complex gene - *HLA* in humans, *RT1* in rats (Günther and Walter, 2001)) are a family of cell surface proteins that are responsible for presenting antigens to immune cells. There are two MHC complex types: MHC-I and MHC-II. Expressed on neurons, MHC-I is responsible for presenting peptides from within the neuron to cluster of differentiation 8 positive t-cells (CD8+ T-cells), which functions as a distress signal that can induce cell death via delivery of proteases (called granzymes) through pore forming proteins called perforins (Corriveau, Huh and Shatz, 1998; Thiery and Lieberman, 2014; Peng *et al.*, 2017). On the other hand, MHC-II is expressed on microglia, as well as astrocytes, and is responsible for presenting antigens scavenged from the extracellular space. These antigens are recognized by CD4+ T-cells, which secrete proinflammatory cytokines, or by B cells, which produce antibodies against the presented antigen.

Clinical, as well as preclinical, evidence for MHCs and infiltrating CD4+/CD8+ T cells have implicated the innate and adaptive immune system in PD. Post mortem PD studies have revealed an increased level of MHC-II in the vicinity of PD pathology, specifically LBs, in the SNpc and STR (McGeer *et al.*, 1988; McGeer, Itagaki and McGeer, 1988). In the healthy brain, MHC-II expression is nearly undetectable, thus,

observations of MHC-II immunoreactive (MHC-IIir) microglia in the SNpc, and later the cortex, putamen, and hippocampus of PD subjects indicate either aggregated α-Syn and/or neurodegeneration can induce an inflammatory response (Imamura *et al.*, 2003; Harms *et al.*, 2013). Additionally, MHC-II expression is tightly correlated with α-Syn deposition in the SNpc of PD subjects as well as some preclinical PD models (Croisier *et al.*, 2005; Duffy, Collier, Patterson, Kemp, Luk, *et al.*, 2018). GWAS studies have shown several variants associated with HLA-DR (human leukocyte antigen DR isotype; MHC-II) encoding regions to be associated with an increased risk for PD (Kannarkat *et al.*, 2015). As it relates to T cells, CD4+ and CD8+ T cells are increased in the midbrain of PD subjects, and interestingly, it has been shown that peripherally circulating T cells can be decreased in PD subjects (Brochard *et al.*, 2009; Jiang *et al.*, 2017). Lastly, T cells from PD subjects, but not healthy controls, are able to recognize different peptides within the α-Syn protein (Lindestam Arlehamn *et al.*, 2020). Collectively, the evidence above supports a role for the innate and adaptive immune system in PD progression, which heavily relies on the initial response and coordination of microglia. In the following sections, we will dive deeper into the homeostatic, as well as disease responding, role that microglia play in Parkinson's Disease.

MICROGLIA IN HEALTH AND DISEASE

Discovery

Microglia have a unique history of discovery based on the observations of a group of pioneering Spanish scientists in the fields of microscopy and histology in the early 1900's. Scientist and Nobel Prize laureate, Santiago Ramón y Cajal, was investigating the different types of cells in the brain, and up to this point, had only

characterized two of the four known cells in the brain: Neurons and astrocytes. The third cell and fourth cell type would later be discovered by two of his students; Nicolás Achúcarro and Pío del Río-Hortega. Achúcarro was piloting a novel staining technique using ammoniacal silver carbonate solution, and Río-Hortega observed that altering the incubation times would stain different cell types. This allowed Río-Hortega to distinguish between cell populations and led to the discovery of the two unknown cell types: microglia and oligodendrocytes. In 1919 he published *El “Tercer Elemento" de los Centros Nerviosos* in which he laid out his characterization of microglia, or the third element of the CNS (Río Hortega, 1919a; Sierra, Paolicelli and Kettenmann, 2019).

Initial Description of Microglia and Origin

Describing these cells without computers or camera-mounted microscopes posed quite a challenge for scientists. To share their observations, they had to create hand illustrations of what they were observing under the microscope on paper with pencil. Some of the drawings, like the ones from Río-Hortega, were quite beautiful and incredibly detailed, however, not all researchers had the gift of the artist's touch. Microglia were described many years prior to Río-Hortega’s 1919 papers, seen by different scientists, given different names, drawn in a unique style. Franz Nissle, Alois Alzheimer, and Ludwig Merzbacher all described cells that would later to be revealed to be microglia: rod cells, clearing cells, and scavenger cells were all previous names of microglia (Nissl, 1904; Alzheimer, 1910; Peiffer and Gehrmann, 1995). The name assigned by Río-Hortega comes from the Latin word ‘micro’, meaning small, and ‘glia’, meaning glue. The term “glia” was used early as a term used to describe cells in the brain that were not neurons. Today we know there are three types of glial cells in the

brain: microglia, astrocytes, and oligodendrocytes. It was initially hypothesized that these cells, which did not have a name when they were first discovered, functioned like a glue to hold neurons in place. We now understand that not to be the case, but the name has since “stuck”.

The origin of microglia was initially hypothesized to derive from the mesoderm during embryonic development, and over time, was thought to derive from the ectoderm. It wasn’t until 1999 that it was proposed that microglia originate in the yolk sac and derive from progenitor cells (Alliot, Godin and Pessac, 1999). Since then, it has been confirmed that microglia are derived from a pool of macrophages that differentiate into microglia in the yolk sac that will reside in the CNS throughout life (Paolicelli et al., 2022). This is contrary to other types of immune cells found in the brain, such as bone marrow derived macrophages, that infiltrate various tissue types in response to injury, including the CNS. Another feature that makes microglia unique is their replication and population management. Microglia can self-replicate to maintain their populations, and can expand their population in response to stimuli, injury, or inflammation. This is contrary to peripheral immune cells that are derived from hematopoietic stem cells in bone marrow and circulate throughout the blood before reaching their target.

Microglial Morphology

The morphology of microglia, their shape, structure and size, is dependent on their environment, which makes them a very dynamic and responsive cell (Nimmerjahn, Kirchhoff and Helmchen, 2005). Río-Hortega, in addition to the other scientists that observed these cells, noted how many microglia had a resting morphology, where the microglial arms or projections were long and thin, constantly reaching out and surveying

the environment. However, in the presence of pathogen infiltration, or lesion to the brain, microglia take on an 'activated' shape, shrinking their projections, and increasing the size of their soma to engulf cellular debris, pathogens, and dead or dying neurons (Nissl, 1904; Alzheimer, 1910; Río Hortega, 1919b; Sierra *et al.*, 2016; Colonna and Butovsky, 2017). Additionally, microglia are observed throughout the brain, with higher cell populations in some brain regions and less dense in other regions (Río Hortega, 1919a; Sierra, Paolicelli and Kettenmann, 2019). Another key feature of microglia is their ability and tendency to migrate within the brain, either in surveillance mode, or response mode. In the initial, rather crude, experiments on microglia, Río-Hortega observed that upon stabbing, or lesioning, the brain, microglia would migrate to the site of lesion and become ramified in their morphology (Río Hortega, 1919b). Additionally, Río-Hortega looked at the response of microglia to neurodegeneration - an excerpt from his 1919 paper, "*The nomadic nature of microglia is best observed in neurodegenerative processes, during which the apparent rest they enjoyed in the normal state turns into migratory and phagocytic activity*" (Río Hortega, 1919a; Sierra, Paolicelli and Kettenmann, 2019).

Phagocytosis and Debris Clearance

Phagocytosis is the process by which particles, proteins, cellular debris, or even whole cells are engulfed by a cell, digested, and recycled (Flannagan, Jaumouillé and Grinstein, 2012; Galloway *et al.*, 2019). Microglia are the resident macrophages of the brain and primary phagocytes, although, phagocytosis is not exclusive to microglia, as many cell types can phagocytose (astrocytes, neutrophils, and dendritic cells to name a few). Phagocytosis plays a key role in homeostatic functions, for example, through

synaptic pruning, and as a first line of defense against pathogens, such as removal of bacteria or fungi that have made their way into the CNS. The mechanism of phagocytosis is a receptor-mediated process - in that, receptors on the cell surface will interact with foreign bodies, or endogenous cells to detect if engulfment will occur (Flannagan, Jaumouillé and Grinstein, 2012). Phagocytosis is essential during neurodevelopment and is responsible for maintaining neural synapses throughout life. Through a process called synaptic pruning, microglia interact with neurons and will phagocytose individual synapses that are either damaged or unnecessary to optimize energy consumption within neurons (Schafer *et al.*, 2012).

Neurodevelopment

During neurodevelopment, and into young adulthood, the brain is constantly developing and optimizing neural pathways. More cells are produced than needed, and thus cells need to be pruned, or removed, to avoid excess neurons that require energy to maintain, but do not serve a function. Microglia, which originate in the yolk sac, play a key role in the process of removing neurons during development (Alliot, Godin and Pessac, 1999). For example, it has been shown that in the developing mouse cerebellum, a majority of developing Purkinje cells are tagged and removed by microglia (up to 60%) through the process of apoptosis, or programmed cell death via phagocytosis (Marín-Teva *et al.*, 2004). When microglia were selectively depleted in this study, apoptosis and Purkinje cell removal were significantly impaired. Of note, a specialized form of apoptosis, called efferocytosis, is used to engulf or remove an entire

neuron or cell that is undergoing apoptosis, a process that is anti-inflammatory (Zhao *et al.*, 2021).

It has been shown that microglia play a role in cortical development, as well, by regulating the number of neuronal precursor cells in the precursor cell pool during cortical development (Cunningham, Martínez-Cerdeño and Noctor, 2013). In addition to removal, microglia have been shown to play a role in neuronal survival during development. Microglia have the ability to release trophic factors, such as insulin-like growth factor-1 (IGF-1), that directly support neuronal growth during development (Ueno *et al.*, 2013). Neuronal wiring can also be impacted by microglia. For example, during dopaminergic forebrain development, microglia are crucial for outgrowth of dopaminergic neurons and positioning of neocortical interneurons (Squarzoni *et al.*, 2014). In other words, microglia can control outgrowth of neurons, and the positioning of where neurons are located, directly impacting the neural wiring process during development.

Adult Neurogenesis

After neurodevelopment is complete, there is still a constant process of birth, growth, and death from neurons in specific regions of the adult brain. This process, called neurogenesis, is highly dependent on microglia interaction. For example, in the adult hippocampus, neural progenitor cells (NPCs) give rise to neuroblasts, which can be differentiated into multiple cell types. However, only a small subset of these neuroblasts become mature neurons, and a majority of newborn cells will undergo apoptosis-associated death via microglia phagocytosis (Sierra *et al.*, 2010). Interestingly, there is evidence to suggest that microglia not only play a role in removing

NPCs but can alter the differentiation of these cells as well. Microglia activated by interleukin-4 (IL-4) or interferon gamma (IFN-γ) co-cultured with NPCs, or grown together in a cell culture system, will induce neurogenesis, however, microglia activated with an inflammatory stimulus (such as lipopolysaccharide; LPS), will impair neurogenesis when co-cultured with NPCs (Butovsky *et al.*, 2006). Further, it has been shown that activated microglia, either by lesion or pathogenic disease, will impair neurogenesis, and that by blocking activated microglia, neurogenesis function is restored (Ekdahl *et al.*, 2003; Kempermann and Neumann, 2003; Monje, Toda and Palmer, 2003). Collectively, this indicates that microglia play a key role in maintaining homeostasis of brain regions that undergo adult neurogenesis. Specifically, within the hippocampal region, which is imperative for memory formation.

Neuronal Plasticity and Rewiring

Another role that microglia play in maintaining brain environment homeostasis is via contributing to neuronal plasticity and rewiring. It has been shown that microglia are constantly surveying neuronal environments, extending their processes and making physical contact with neuronal synapses for brief periods (5 minutes) as often as every hour (Wake *et al.*, 2009; Tremblay, Lowery and Majewska, 2010). Microglia also increase or decreases their interaction with neurons in an activity dependent manner - if a neuron has increased activity, microglia will interact more frequently. However, in pathogenic or injury conditions, microglia will make prolonged contact with synapses which can result in synapse removal, indicating that microglia may be diagnosing the problem and attempting to restore neuronal functionality following injury. Microglia, however, are not alone in the synaptic pruning process; it has been shown that

astrocytes work together with microglia to optimize adult synapses and neuronal connectivity. Astrocytes have the ability to contribute to synaptic pruning by tagging synapses using complement proteins (specifically C1q, one of three proteins used in the classical complement cascade) that are recognized by microglia (Stevens *et al.*, 2007). Upon recognition of C1q, microglia activate a protease cascade by depositing downstream complement protein C3, or C3 protein fragments, which lead to synapse removal either by phagocytosis or cell lysis. This process, complement associated synaptic pruning, is an activity dependent process, whereby neuronal synapses with decreased activity, or “weaker” connections, are more likely to be pruned than more active, “stronger”, connections (Schafer *et al.*, 2012). The involvement of the adaptive immune system in maintaining homeostasis is not strictly a pruning process but can also be an active contributor to growth of neurons and neuronal pathways. BDNF, or brain derived neurotrophic factor, is a neurotrophin secreted by neurons, microglia, astrocytes, and oligodendrocytes and is critical for neuron survival, differentiation, and plasticity (Dougherty, Dreyfus and Black, 2000; Chao, 2003). It has been shown that microglial-derived BDNF plays an important role in synaptic plasticity, learning and memory, whereby lack of microglia-derived BDNF results in weakened synapses, as well as memory and learning impairments (Parkhurst *et al.*, 2013).

Collectively, microglia have been shown to play active and imperative roles in removal, as well as strengthening of neuronal synapses involved in adult plasticity and rewiring. As we will discuss in the subsequent sections, microglia activity, or lack thereof, is key to understanding disease pathologies and disease progressions.

Microglial Response to Disease and Proteinopathies

Before diving into microglia's response to disease, it is worth emphasizing the complexity of microglial research. For example, impaired microglia function and decreased microglia activity can increase the risk of developing Alzheimer's Disease, concurrently, activated microglia can directly contribute to neurodegeneration and cytotoxicity (Hansen, Hanson and Sheng, 2018). Herein lies the crux of the matter, activation of microglia is an essential function of maintaining brain homeostasis, and at the same time, the microglial response can contribute to disease progression if the response is not tightly regulated and controlled. Additionally, microglia become more reactive with the natural aging process (Costa et al., 2021). Termed "inflammaging", it is understood that microglia are at the center of aging induced changes that occur in the brain: reduced neurogenesis, oxidative stress, and mitochondria dysfunction. With age, microglia express a "weakened" phenotype, characterized by an altered transcriptomic profile, altered morphology, and decreased activity levels. "Aged" microglia display less motility, decrease phagocytosis activity, and increase their production of pro-inflammatory cytokines, resulting in a comprised response to injury, insult, or inflammation.

With that, microglia have been shown to play key roles in almost any brain pathology or disease - from prion diseases such as bovine spongiform encephalopathy, scrapie, and Creutzfeldt-Jakob disease (Brown, Schmidt and Kretzschmar, 1996), to human immunodeficiency virus (HIV) (He *et al.*, 1997), Amyotrophic lateral sclerosis (ALS) (Boillée *et al.*, 2006), stroke (Savitz and Cox, 2016; Wolf, Boddeke and Kettenmann, 2017), Multiple sclerosis (MS) (Bogie, Stinissen and Hendriks, 2014; Wolf,

Boddeke and Kettenmann, 2017), Alzheimer's disease (AD) (El Khoury *et al.*, 1996), and the focus of this dissertation, PD (McGeer *et al.*, 1988). In the following section, mechanisms used by microglia in response to pathologies will be discussed.

Cytokines, Chemokines, and Neuroinflammation

Microglial phenotype is tightly regulated in the CNS, where minor changes to the brain microenvironment can impact the coordinated response of microglia. Cytokines and chemokines are small molecules produced and released by microglia that are used to survive, communicate, and orchestrate the coordinated response to changes (Wang *et al.*, 2012). These molecules are like a double-edged sword: on one hand, they are required for survival, to clear toxins, and combat pathogens. However, prolonged release of cytokines and chemokines can promote neurodegeneration and induce cytotoxicity (Badanjak *et al.*, 2021). During injury conditions, either acute or chronic, microglial cell surface receptors such as TLRs or NOD like receptors (nucleotide-binding oligomerization domain) detect PAMPs (pathogen associated molecular patterns) or DAMPs (damage associated molecular patterns) (Perry, Nicoll and Holmes, 2010). Examples of these molecular patterns include heat shock proteins, oxidized lipids, damaged DNA, ATP, misfolded proteins, and many more. Binding of PAMPs or DAMPs induce a cascade of intracellular processes that result in the synthesis of cytokines such as interleukin-1-beta (IL-1β), interleukin-18, interleukin-6, interleukin-23, and TNF (Prinz, Jung and Priller, 2019). Cytokine synthesis will lead to chemokine release, which creates a chemokine gradient that recruits infiltrating peripheral immune cells from the adaptive immune system, such as neutrophils and monocytes (Zhang *et al.*, 2022). An example of this process is the cGAS-STING pathway. Cyclic GMP-AMP synthase

(cGAS) is a cytosolic pattern recognition receptor (PRR) that recognizes DNA that is either a PAMP (foreign DNA, either from a virus or bacteria) or DAMP (self-DNA released from damaged cells or organelles) (Gulen *et al.*, 2023). Activation of cGAS results in the activation of STING (stimulator of interferon genes) which interacts with transcription factors to drive the transcription and synthesis of proinflammatory cytokines (TNF- α, IL-6, IL-1β), interferons (IFN- β), and chemokines (C-C motif chemokine ligand 5, and 10; CCL5, CCL10) (Govindarajulu *et al.*, 2023). Chronic activation of these pathways within microglia will result in the release of concentrated cytokines (IL-1α, TNF-α, and C1q; complement component 1q) that transform neighboring astrocytes into a reactive, neurotoxic phenotype observed in PD, AD, and MS conditions (Liddelow *et al.*, 2017). Under normal conditions, these processes are required and essential for maintaining homeostasis. In the case of chronic diseases, such as neurodegenerative disease, the prolonged release of cytokines and chemokines can be detrimental to neuronal health and further exacerbate disease progression (Akiyama *et al.*, 2000). Microglia's response to proteinopathies, or pathologies caused by protein aggregation, will be discussed in the following section.

Microglial Response to Proteinopathies

Proteinopathies, such as AD and PD among others, are diseases where misfolded proteins will accumulate within cells or in the extracellular space to create inclusions. In AD, amyloid beta (Aβ) plaques and hyperphosphorylated tau proteins (neurofibrillary tangles) are the two primary proteinopathies. In PD, α-Syn is the primary component of LBs and LNs. In either case, inclusion formation can lead to a toxic gain-of-function phenotype, where the inclusions themselves create a toxic environment, or a

toxic loss-of-function phenotype, where the proteins are unable to perform their normal duties and lack of function creates a toxic environment. Whether inclusions are gain-of-function or loss-of-function is actively debated (Benskey, Perez and Manfredsson, 2016).

As it relates to AD, research in the early 1990's focused on microglia's ability to phagocytose Aβ plaques from the extracellular space (Frackowiak *et al.*, 1992). These early studies demonstrated that microglia, although able to engulf plaques, were unable to degrade the plaques 20 days after initial engulfment, demonstrating either plaque resistance to phagocytosis, or slow lysosomal degradation. Similar research demonstrated that microglia with ramified morphology congregate around Aβ plaques and release cytokines as well as ROS upon interacting with plaques, which may contribute to disease progression (Ishii and Haga, 1992; El Khoury *et al.*, 1996). More recent research has focused on how the complement pathway is implicated in AD progression. Broadly speaking, the complement pathway is composed of more than 20 components, starting with C1q and CR3 expressed on unhealthy synaptic surfaces, which is recognized by microglia and results in the formation of membrane attack complex (MAC) pore formation (Akiyama *et al.*, 2000; Carpanini *et al.*, 2022). MAC pores allow for free flow of ions across a cell membrane that disrupt cellular homeostasis and result in cell lysis, and, interestingly, can induce lysis of neighboring, healthy cells (Akiyama *et al.*, 2000). GWAS have implicated multiple single nucleotide polymorphisms (SNPs) in complement components and risk of developing AD, and post mortem immunohistological studies have shown increases and colocalization of complement components around Aβ plaques and tau tangles (Hong *et al.*, 2016;

Carpanini *et al.*, 2022). Complement pathways are essential for maintaining homeostasis, but it is the constant and chronic activation that leads to the exaggerated disruption that results in neurodegeneration. Single cell RNA sequencing (RNAseq) has revealed two molecularly distinct microglial phenotypes in response to amyloid-β induced neurodegeneration (Mathys *et al.*, 2017). The first category of microglia are early response microglia, prior to degeneration, that primarily express upregulation of genes related to cell proliferation, cell cycle, and DNA replication or repair. The second subtype of microglia are called the late response group, and these microglia express an upregulation of genes related to immune responses, such as MHC-II, cytokines (specifically, interferon related genes), and other genes related to host-defense innate immune response. This study was the first to recognize a temporally distinct, heterogeneous response by microglia to neurodegeneration that followed proteinopathy. In the following section, microglial response specifically to PD will be discussed.

Challenges with Microglial Research in PD

Neuroinflammation and neurodegenerative disease research poses unique challenges. From a clinical tissue standpoint, tissue collected post-mortem represents a single snapshot in time, after years of complex cellular interactions that led to disease progression, and it is difficult to understand what led to neuronal dysfunction and death. This scenario is analogous to looking at a photo of a murder scene and trying to identify the murderer. Who was in the room first? What caused the death? What murder weapon was involved? Were there multiple assailants? An understanding of the full sequence of events is essential to determining how the crime occurred. This is the

conundrum of using post-mortem PD tissue to understand pathogenic mechanisms and the role of inflammation.

Like other neurodegenerative diseases, there is a particular threshold of cellular loss that needs to occur before symptoms appear and a preliminary diagnosis can be made. Thus, post-mortem PD tissue is comprised of ongoing degeneration and LB pathology, making it difficult to understand the distinct role of either component in contributing to inflammation. Post-mortem studies using Incidental Lewy Body Disease (ILBD) tissue can be particularly informative. In ILBD, LBs and LNs are present but neuronal loss is either nonappreciable or relatively minor, and has been inadequate to reach a threshold to observe clinical PD symptoms (Spillantini *et al.*, 1997; Iacono *et al.*, 2015). While still a snapshot in time, post-mortem ILBD tissue decreases the likelihood of degeneration associated inflammation and may enhance our understanding of specific LB immunogenicity. Ultimately, our understanding of the triggers and consequences of inflammation in the PD brain have been informed by longitudinal imaging and analysis of CSF, blood, and post-mortem tissue across PD disease stages. In this section, I will briefly summarize the evidence connecting microglial activation to PD.

Microglial Activation in PD

In 1988, scientists studying PD post-mortem tissue observed enriched microglial expression of human leukocyte antigen related-D (HLA-DR; human analog for major histocompatibility complex II; MHC-II) in the PD SNpc compared to age-matched controls (McGeer *et al.*, 1988). HLA-DR or MHC-II is a protein on microglia presents phagocytosed antigens to CD4+ and CD8+ T cells, triggering an immune response

(Rock, Reits and Neefjes, 2016). In PD, these T cells have been observed invading the brain from the periphery (Alberts *et al.*, 2007; Brochard *et al.*, 2009). Still to this day it is unclear if HLA-DR positive microglia adjacent to LBs present antigens, and if so, what they are presenting. Subsequent studies have explored the correlation between LB load, degeneration, and microglial HLA-DR (or MHC-II) expression. Quantitatively, it has been shown that as greater nigral degeneration is positively associated with greater MHC-II expression (Imamura *et al.*, 2003). It has also been shown that the amount of MHC-II positive microglia is correlated with the amount of α-Syn inclusions, or Lewy bodies, in PD brains (Croisier *et al.*, 2005). In ILBD, a similar association between *HLA-DRA* (MHC-II) and pathological α-Syn deposition has been observed, suggesting a neuroinflammatory role in early disease pathogenesis (Dijkstra *et al.*, 2015). PET studies have revealed increases in activated microglia within the midbrain of early-stage PD subjects which correlated with motor symptom severity (Ouchi *et al.*, 2005). Longitudinal PET studies reveal increases in activated microglia within the brainstem, basal ganglia, and cortical regions over a 2-year period (Gerhard *et al.*, 2006). Interestingly, microglial activation remained stable over the 2-years, despite symptom severity increasing and DA function decreasing.

In addition to antigen presentation expression, microglia morphologically respond to PD by retracting their projections and increasing soma size, indicating an inflamed state of activation in response to LBs/α-Syn (Imamura *et al.*, 2003; Croisier *et al.*, 2005; Smajić *et al.*, 2022). Cluster of differentiation 68 (CD68), a microglial transmembrane protein associated with phagocytosis, has been shown to correlate with PD duration (Croisier *et al.*, 2005). Toll-like receptor 2 (*TLR2*) also has been demonstrated to

correlate with Lewy-pathology in the PD brain (Doorn et al., 2014; Drouin-Ouellet et al., 2014). In post-mortem PD brain tissue, elevated levels of proinflammatory cytokines associated with microglial activation have been reported, including TNF-α, interleukins 2, 4, 6, and beta (IL-2, IL-4, IL-6, IL-1ß) (Mogi *et al.*, 1996; Nagatsu *et al.*, 2000). Cerebrospinal fluid taken from PD subjects also reveals increased cytokines such as IL-1ß, IL-6, TGFß-1 (transforming growth factor beta-1) (Chen *et al.*, 2018). Blood samples from PD subjects have also shown increased cytokines such as IL-2, IL-6, IL-10, TNF-α, and IL-1ß (Qin *et al.*, 2016).

While these clinical and post-mortem analyses have provided substantial evidence for microglial activation in PD, we are still limited in our ability to elucidate the early phases of disease progression and associate any causal relationships between microglia activation and neurodegeneration. To address this limitation and investigate the mechanisms underlying microglia activation and contributions to PD pathogenesis, preclinical models have been developed to study PD.

INSIGHTS INTO THE ROLE OF NEUROINFLAMMATION IN PD USING PRECLINICAL MODELS

Cell Culture Models

Given the complexities associated with using clinical samples to delineate the role of neuroinflammation in PD, investigations using preclinical cell culture and rodent models of PD have been undertaken. *In vitro*, oligomeric α-Syn released from neurons has been shown to activate microglial TLR2, initiating a downstream cascade that results in the release of proinflammatory cytokines (Kim *et al.*, 2013). Additionally, genetically knock out of TLR2 from microglia and exposing them to oligomeric α-Syn

results in no cytokine release or chemokine gradient. Collectively, this indicates a key role of TLR2 in recognizing pathological α-Syn as pathogenic, thereby initiating an immune response. However, there are limitations associated with studying the response of microglia in cell culture systems because neuroinflammatory responses involve crosstalk between and contributions from multiple innate and adaptive inflammatory cell types. Based on this, many rodent models of PD have been utilized.

Modeling Parkinson's Disease in Rodents

To study PD in rodents, models have been developed to recapitulate the two main pathological hallmarks of PD, loss of nigral DA neurons and α-Syn pathology. The ideal rodent model would reproducibly feature progression of both of these pathologies in which the formation of α-Syn inclusions precedes degeneration, as well as relevant behavioral abnormalities (Martinez and Greenamyre, 2012). Three types of rodent PD models have been developed over the last 50 years: neurotoxicant models, α-Syn overexpression models and the α-Syn preformed fibril (α-Syn PFF) model. In the following section neurotoxicant models, α-Syn transgenic models and viral vector mediated α-Syn overexpression models will be discussed, including the pros and cons of each model and results of neuroinflammatory investigations in these models. This will be followed by a deeper dive into the α-Syn PFF model.

Neurotoxicant Models

The first models of PD relied on chemical ablation of DA neurons, that is, there are chemical compounds that will selectively kill DA neurons within the midbrain. The first model, developed in 1968, uses 6-hydroxydopamine (6-OHDA) to ablate DA neurons within the SNpc via mitochondrial dysfunction and oxidative stress caused by

reactive oxygen species (Ungerstedt, 1968). This model shows toxicity very quickly, only taking 1-3 weeks for nigrostriatal neurons to die in rats or mice following intracranial injection, and can lead to varying loss of DA neurons within the SNpc (Sauer and Oertel, 1994; Spieles-Engemann, Collier and Sortwell, 2010; Jagmag *et al.*, 2015). Injection of 6-OHDA into the SNpc, STR, or medial forebrain bundle results in DA neuron death in the SNpc as well as the adjacent ventral tegmental area (VTA). 6-OHDA is a widely used preclinical model that recapitulates SN DA neuron death features but lacks LB-like pathology or alterations to α-Syn levels.

The next neurotoxicant model, MPTP (1-methyl-4-phenyl-1,2,3,6-tetrahydropyridine) has the most unique history of any model. During the 1980's, a new synthetic heroin was released into the drug scene in California and resulted in patients being hospitalized for acute onset, severe parkinsonian-like symptoms. Ultimately, it was discovered that this synthetic heroin was contaminated with a chemical called MPTP, which, when ingested, is metabolized into a toxic metabolite called MPP+ (1-methyl-4-phenylpyridinium) (Langston, 2017). MPP+ has a very similar structure to DA, and is taken up via DA transporters on the neuron presynaptic terminals, resulting in mitochondrial dysfunction and cell death (Forno *et al.*, 1993; Kim-Han, Antenor-Dorsey and O'Malley, 2011). The MPTP model is more common than the 6-OHDA model, as MPTP and MPP+ are selective to DA neurons due to the means of cellular uptake (DA transporter). Whereas most acute MPTP administration paradigms do not result in LB-like pathology, some sub-acute chronic MPTP administration paradigms have demonstrated the formation of α-Syn inclusions (Gibrat *et al.*, 2009). However, subacute MPTP parameters that result in α-Syn inclusions do not result in loss of striatal

terminals. In addition, MPTP, not pathological inclusions, drives microglial activation in the subacute chronic MPTP model (Ou *et al.*, 2021). Overall, the MPTP model of PD lacks a demonstrable relationship between the formation of LB-like inclusions and nigrostriatal degeneration and, as such, does not allow investigations into synucleinopathy-induced degeneration or inclusion-associated neuroinflammation.

Rotenone is a naturally occurring compound that is extracted from the roots of some tropical plants, namely from the *Lonchocarpus* and *Darris* genera (Soloway, 1976). It has been used in the past as an agricultural insecticide and pesticide, and more recently is used as a tool to control certain fish populations, as it is extremely toxic to fish (Robertson and Smith-Vaniz, 2008). One of the unique features of rotenone is that it is extremely lipophilic and easily crosses biological membranes, including the blood brain barrier, making it efficient at entering most cells within the body upon exposure (Martinez and Greenamyre, 2012). Once inside the body, the mechanism of action of rotenone is within the electron transport chain, acting as a complex I inhibitor. This leads to reduced ATP levels, electron leakage, oxidative stress and cell death (Martinez and Greenamyre, 2012; Johnson and Bobrovskaya, 2015). Rotenone exposure (in addition to commonly used herbicides, such as Paraquat) have been linked to increased PD risk (Tanner *et al.*, 2011). When systemically injected into rodents, rotenone recapitulates features of PD, such that damage occurs to DA terminals in the striatum and DA cell bodies in the SNpc. Interestingly, DA neurons within the VTA are relatively spared, similar to PD. Additionally, rotenone administration can result in cytoplasmic LB-like inclusions in the SN and other regions, inclusions that are associated with microglial activation that precedes degeneration (Zhang *et al.*,

2021). However, major limitations of the rotenone model include dose-dependent systemic toxicity and mortality, and lack of reproducibility in the magnitude of damage to the nigrostriatal system.

Collectively, neurotoxicant models can provide a model of rapid nigrostriatal degeneration. Under some experimental parameters both MPTP and rotenone administration can result in LB-like pathology. However, none of these neurotoxicant models provide a dependable model in which the formation of α-Syn inclusions consistently drives nigrostriatal degeneration and thus these models have limited utility for advancing our understanding of the distinct roles each pathological feature may plays in neuroinflammation in PD. Instead, the nigrostriatal degeneration and robust behavioral deficits observed make neurotoxicant models ideal for studying the consequences of nigrostriatal degeneration and the development of novel therapies to mitigate these consequences.

α-Syn Overexpression Models

To replicate α-Syn and LB pathology more consistently, transgenic and viral vector-mediated preclinical models were developed to overexpress α-Syn in rodents. With the viral vector approach, direct stereotaxic injection of a viral capsid, such as a lentivirus or adeno-associated virus (AAV), is used to drive α-Syn overexpression in the nigrostriatal system specifically. Numerous transgenic models of widespread or nigrostriatal-targeted α-Syn overexpression driven by various promoters also have been developed. With both approaches, overexpression of human wildtype or mutated forms of α-Syn has been pursued (Koprich *et al.*, 2008; Wang *et al.*, 2008; Gao *et al.*, 2011; Gombash *et al.*, 2013). In α-Syn overexpression models, α-Syn protein is expressed at

supraphysiological levels, most strikingly in viral-vector mediated models in which levels of α-Syn as high as 18-fold above normal can be achieved (Volpicelli-Daley *et al.*, 2016). Of note, most α-Syn overexpression models result in α-Syn levels that far exceed levels observed even in α-Syn triplication PD cases (Farrer *et al.*, 2004). Multiple transgenic α-Syn overexpression models result in abundant LB-like inclusions, although rarely is this followed by significant neurodegeneration (Fernagut and Chesselet, 2004). In contrast, viral-vector mediated α-Syn overexpression models can results in significant titer-dependent, rapid nigrostriatal degeneration (Gombash *et al.*, 2013), however, the α-Syn perturbations that result do not share some important features of true LBs (Kirik *et al.*, 2002). Both viral vector-mediated and transgenic α-Syn models demonstrate a robust neuroinflammatory response driven by reactive microglia, characterized by a pro-inflammatory cytokine response and infiltrating immune cells (Theodore *et al.*, 2008; Sanchez-Guajardo *et al.*, 2010; Harms *et al.*, 2013). These models reveal that α-Syn overexpression can trigger neuroinflammation prior to overt neurodegeneration, with key mechanisms involving MHC-II upregulation, TLR2 activation, border associated macrophages (BAMs) regulation, and infiltrating T cell involvement (Schonhoff *et al.*, 2023). That being said, the supraphysiological levels of α-Syn can generate an exaggerated inflammatory response which can make it difficult to interpret the subtle inflammatory processes that may be occurring in the disease (Duffy, Collier, Patterson, Kemp, Fischer, *et al.*, 2018). Additionally, the α-Syn inclusions observed in α-Syn overexpression and transgenic models are dissimilar to clinical LBs and LNs. The neuronal location, spreading pattern, cellular morphology, and molecular composition lack the key features of clinical LBs and LNs, suggesting the inclusions may not be as

complex as observed in the disease (Kuusisto, Parkkinen and Alafuzoff, 2003; Duffy, Collier, Patterson, Kemp, Fischer, *et al.*, 2018; Gómez-Benito *et al.*, 2020).

Collectively, while an advance over their neurotoxicant model predecessors, vectored α-Syn overexpression models still have limitations regarding advancing our understanding of the distinct contributions of LBs/α-Syn versus degeneration to neuroinflammation in PD. The reliance on supraphysiological α-Syn levels may drive pathogenic mechanisms (neuroinflammation, toxicity) unrelated to idiopathic PD (Duffy, Collier, Patterson, Kemp, Fischer, *et al.*, 2018). Most transgenic α-Syn models do not result in nigrostriatal degeneration, whereas viral vector-mediated α-Syn overexpression generally do not result in LB-like inclusions. Lastly, there are downstream effects of genetic manipulation where insertions of genes can impact neighboring genes on a genome that can result in off-target effects (Li and Yang, 2023). The final PD model to be discussed below, the α-Syn PFF model, was developed to address the limitations of previous PD models. It is the optimal preclinical platform to leverage for my dissertation experiments.

α-Syn Preformed Fibril Model

Developed in 2011 by Dr. Virginia Lee and colleagues, the α-Syn preformed fibril (PFF) model recapitulates both of the pathological hallmarks of PD, as well as shares many of the neuroinflammation features seen in clinical PD (Volpicelli-Daley *et al.*, 2011; Luk, V. M. Kehm, *et al.*, 2012). This is one of the most recently developed models of PD, which leverages exogenous, oligomerized, and fibrilized α-Syn injected directly into the striatum of wild type rodents to induce templating of endogenous α-Syn. Templating with endogenous α-Syn results in LB-like aggregate formation in regions directly innervated

by the striatum (SNpc, cortical regions, amygdala). Dependence upon endogenous α-Syn for inclusion formation has been validated by the fact that PFFs do not lead to inclusion formation in α-Syn knockouts (Volpicelli-Daley *et al.*, 2011). Following intrastriatal PFF injection in rats, the observed inclusions colocalize with markers commonly observed in LBs (pSyn, p62 and ubiquitin), consist of α-Syn oligomers and fibrils, and are also thioflavin-S positive and proteinase-K resistant (Paumier *et al.*, 2015; Polinski *et al.*, 2018; Patterson *et al.*, 2019; Howe *et al.*, 2021). In vitro studies examining the process and properties of PFF-seeded inclusion formation reveal that initial inclusions are comprised solely of phosphorylated α-Syn (pSyn) fibrils (Mahul-Mellier *et al.*, 2020) (Figure 1.3A). Over time however, the pSyn inclusions consist of an increasing percentage of additional proteins, membranous structures and organelles like mitochondria and vesicles proteins (Mahul-Mellier *et al.*, 2020), with 22% maturing to become LB-like in nature within 3 weeks (Gai *et al.*, 2000; Shahmoradian *et al.*, 2019) (Figure 1.3A). Importantly, these mature LB-like structures, and not earlier aggregate forms, are associated with upregulation of cell death signaling pathways (Mahul-Mellier *et al.*, 2020).This suggests that the transition from soluble α-Syn to pSyn fibrils to LB-like inclusions requires time, post-translational modifications and interaction with organelles and that mature LBs are associated with neuronal toxicity.

The impact of PFF injections has been studied in multiple species, including mice, rats, marmosets, & monkeys (Luk, V. Kehm, *et al.*, 2012; Luk, V. M. Kehm, *et al.*, 2012; Paumier *et al.*, 2015; Abdelmotilib *et al.*, 2017; Shimozawa *et al.*, 2017; Thakur *et al.*, 2017; Duffy, Collier, Patterson, Kemp, Luk, *et al.*, 2018; Chu *et al.*, 2019; Henderson *et al.*, 2019; Patterson *et al.*, 2019; Creed and Goldberg, 2020; Stoyka *et al.*, 2020;

Negrini *et al.*, 2022). One of the most useful features of the PFF model is the relatively protracted timeline of two distinct stages: accumulation of pSyn pathology followed by neurodegeneration, with LB-like inclusions containing neurons ultimately degenerating (Osterberg *et al.*, 2015). Specifically, following intrastriatal PFF injection to rat, the accumulation of pSyn immunoreactive inclusions in the SNpc peaks at 1-2 months (Duffy, Collier, Patterson, Kemp, Luk, *et al.*, 2018; Patterson *et al.*, 2019; Howe *et al.*, 2021; Miller *et al.*, 2021; Stoll, Kemp, Patterson, Howe, *et al.*, 2024) (Figure 1.3B). Following this peak, the number of pSyn neurons in the SNpc gradual declines over the next 4 months as inclusion bearing neurons degenerate (Osterberg *et al.*, 2015; Duffy, Collier, Patterson, Kemp, Luk, *et al.*, 2018; Patterson *et al.*, 2019; Stoll, Kemp, Patterson, Howe, *et al.*, 2024).

The PFF model demonstrates a progressive loss of tyrosine hydroxylase (TH) immunoreactivity and overt neurodegeneration in both the striatum and SNpc as well as behavioral DA dysfunction. Starting at 2-months post PFF injection, TH immunoreactivity within the striatum significantly decreases compared to phosphate buffered saline (PBS) controls, with further progressive loss occurring at the 4-, 6-, and 8-month timepoints (Paumier *et al.*, 2015; Patterson *et al.*, 2019; Centner *et al.*, 2024). Similarly, PET imaging of the rat striatum shows significant decreases in DAT starting at 2-months and progressing significantly out to 6-months (Sossi *et al.*, 2022). High-performance liquid chromatography (HPLC) investigations of the striatum in the mouse PFF model reveal decreases in DA at the 6-month timepoint (Cole *et al.*, 2021). Within the SNpc, TH immunoreactivity decreases start at 2-months post PFF injection and progresses through the 4-, 6-, and 9-month timepoints (Patterson *et al.*, 2019; Centner

et al., 2024). DA neuron loss begins at 4-months post PFF injection, and continues to progress at the 6- and 9-month timepoint (Patterson *et al.*, 2019; Centner *et al.*, 2024). As it relates to DA-loss behavioral deficits in the PFF model, it has been shown that there are subtle motor perturbations at the 6-month timepoint as measured by gait analysis (Patterson *et al.*, 2019).

Whereas the magnitude of nigrostriatal dysfunction and degeneration in the PFF model is somewhat lower than neurotoxin or viral vector-mediated α-Syn overexpression models, this characteristic of the model overall does not limit the model's utility for understanding the neuroinflammatory response specific to LBs and neurodegeneration, discussed in the following section.

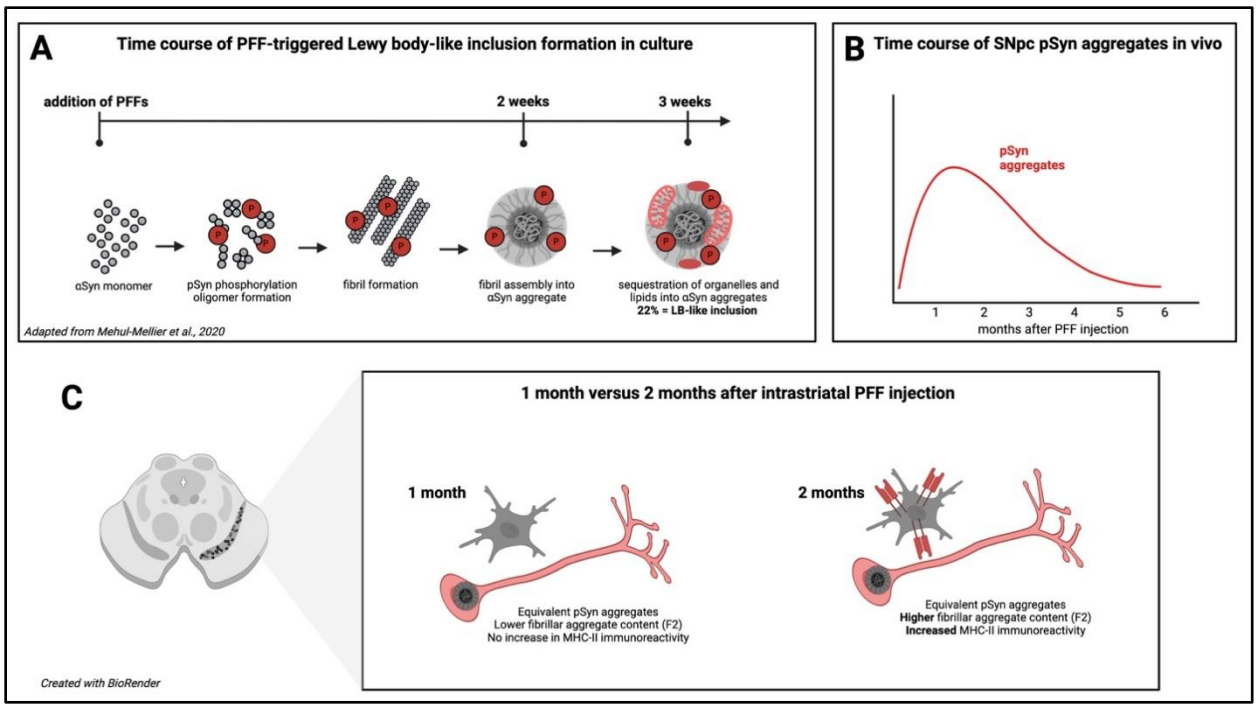

Figure 1.3. Temporal progression of α-Synuclein inclusion pathology in the PFF model

(A) Schematic representation of PFF triggered α-Syn inclusion formation *in-vitro*, adopted from (Mahul-Mellier *et al.*, 2020). Sequential formation from α-Syn monomer through phosphorylation, fibril formation, and sequestration of organelles into a LB-like structure over the course of 3-weeks. **(B)** Time course and magnitude of pSyn aggregate accumulation in the SNpc following intrastriatal PFF injection. **(C)** Comparison of neuronal pathology at the one- and two-months post intrastriatal PFF injection timepoint, showing an increased fibrillar aggregate content and MHC-II immunoreactivity at the two-month timepoint.

Neuroinflammation Observed in the α-Syn Preformed Fibril Model

The distinct aggregation and degeneration phases of the rat PFF model provide the opportunity to delineate and compare neuroinflammatory responses to LB-like inclusions versus neuroinflammatory responses to neurodegeneration (Stoll and Sortwell, 2022). We have previously observed that during the peak of nigral pSyn inclusion accumulation (2-months following intrastriatal PFF injection), microglia increase in size and number, however, during the later degenerative phase of the model (5-6 months) this is no longer observed (Duffy, Collier, Patterson, Kemp, Luk, *et al.*, 2018; Stoll, Kemp, Patterson, Howe, *et al.*, 2024). Similarly, the number of MHC-II immunoreactive microglia significantly increase 2-months post PFF injection, tightly correlating with the magnitude of pSyn immunoreactive nigral neurons at that same time point (Harms *et al.*, 2017; Duffy, Collier, Patterson, Kemp, Luk, *et al.*, 2018; Miller *et al.*, 2021; Thomsen *et al.*, 2021; Stoll, Kemp, Patterson, Howe, *et al.*, 2024). Interestingly, despite similar abundance of pSyn inclusions in the SNpc at 1 month, no impact on MHC-II immunoreactivity is observed (Duffy, Collier, Patterson, Kemp, Luk, *et al.*, 2018). During the later neurodegenerative phase, the number of MHC-II immunoreactive microglia declines relative to 2 months, although numbers remain elevated relative to controls (Duffy, Collier, Patterson, Kemp, Luk, *et al.*, 2018). Importantly, this pattern of MHC-II response is not observed following intrastriatal injections of vehicle, rat serum albumin or α-Syn monomer (Duffy, Collier, Patterson, Kemp, Luk, *et al.*, 2018; Miller *et al.*, 2021; Stoll, Kemp, Patterson, Howe, *et al.*, 2024; Stoll, Kemp, Patterson, Kubik, *et al.*, 2024), parameters in which LB-like inclusions do not form, indicating an aggregate-specific microglial response. Having identified the peak of MHC-II immunoreactivity at 2

months after PFF injection, we previously performed additional experiments to investigate the functional phenotype of reactive microglia in proximity to α-Syn inclusions (Stoll, Kemp, Patterson, Howe, *et al.*, 2024). We observed that microglia upregulate a suite of inflammatory genes including *Cd74, Cxcl10, Rt-1a2, Grn, Csf1r, Tyrobp, C3, C1qa, Serping1* and *Fcer1g,* associated with cytokine regulation, antigen presentation, the complement system, ROS production, and phagocytosis/endocytosis (Stoll, Kemp, Patterson, Howe, *et al.*, 2024; Stoll, Kemp, Patterson, Kubik, *et al.*, 2024). In addition, microglia responding to nigral pSyn inclusions no longer are dependent upon colony stimulating factor-1 receptor (CSF1R) activation for survival (Stoll, Kemp, Patterson, Kubik, *et al.*, 2024), a functional phenotype associated with efferocytosis, or clearance, of apoptotic neurons (Anderson *et al.*, 2019). Collectively, abundant evidence has amassed to demonstrate a diverse reaction of microglia to LB-like inclusions 2 months after PFF injection, prior to nigrostriatal degeneration.

In addition to microglial reactivity, astrocytes surrounding pSyn inclusions have been shown to increase expression of glial fibrillary acidic protein (GFAP) 2 months following PFF injection, as well as increased branching (Earls *et al.*, 2019; Izco *et al.*, 2021; Miller *et al.*, 2021; Miller, Mercado and Sortwell, 2021; Garcia *et al.*, 2022; Stoll, Kemp, Patterson, Howe, *et al.*, 2024). Nigral pSyn is also associated with increased expression of mRNA for the proinflammatory cytokines TNF-α and IL-1ß, which could be derived from either astrocytes or microglia (Izco *et al.*, 2021). Lastly, the adaptive immune system is also implicated in the response to pSyn pathology in the PFF model, as there is evidence of infiltrating peripheral immune cells into the CNS: B lymphocytes,

CD4+ and CD8+ T cells, in addition to natural killer cells (NK cells) (Harms *et al.*, 2017; Earls *et al.*, 2020; Garcia *et al.*, 2022).

Collectively, the PFF model is an ideal platform to leverage for investigating neuroinflammatory response to LB-like inclusions. Control procedures aimed at producing quality PFFs have resulted in improved consistency and reproducibility of the model. The PFF model recapitulates both the LB-like pathology and nigrostriatal degeneration hallmarks of PD while retaining endogenous α-Syn levels, with pSyn inclusions specifically associated with ultimate neuronal degeneration. The temporal separation between the aggregation phase and the neurodegeneration phase enables identification of LB-like inclusion specific, versus neurodegeneration specific neuroinflammatory responses. Microglial reactivity to pSyn inclusions after PFF injection is exceptionally localized, with proinflammatory morphology and phenotypes (MHC-II, *C3, Cd74, Cxcl10, C1qa*) restricted to the immediate vicinity whereas microglia only a short distance away, not near pSyn inclusions, appearing homeostatic, or at rest (Duffy, Collier, Patterson, Kemp, Luk, *et al.*, 2018; Miller *et al.*, 2021; Stoll, Kemp, Patterson, Howe, *et al.*, 2024; Stoll, Kemp, Patterson, Kubik, *et al.*, 2024). Whether these local reactive microglia contribute to the dysfunction and/or degeneration of their neighboring pSyn inclusion-bearing neurons remains to be determined. Identification of LB-triggered microglial signature can guide studies to determine the role of microglial activation in degeneration. Further, microglia may play an additional role in contributing to LB formation, as microglia in preclinical studies can release pSyn containing exosomes that induce LB-like inclusions (Guo *et al.*, 2020). Combined with novel biomarkers for detection of LBs prior to the emergence of clinical symptoms (Siderowf *et al.*, 2023),

understanding of the microglial response to LBs may inform the development of neuroprotective therapeutics to slow or prevent PD progression.

SUMMARY AND DISSERTATION FOCUS

Parkinson's Disease is a complex disease that has a multidimensional immune response associated with LB pathology and neurodegeneration. Critical to identifying targets for therapeutic intervention is the ability to understand the initial inflammatory processes triggered by the deposition of α-Syn inclusions. Microglia are the brain's first innate immune responders, with their activation associated with both α-Syn deposition and neuronal loss. The rat PFF model provides a platform with which to deconvolute the specific triggers of microglial associated with distinct PD pathologies. Informed by the initial observation that microglial MHC-II expression is not detectable until two months following PFF injection (Figure 1.3C), my laboratory's previous work has solely focused on the 2-month time point to investigate the functional phenotype of reactive microglia responding to pSyn inclusions (Duffy, Collier, Patterson, Kemp, Luk, *et al.*, 2018; Miller *et al.*, 2021; Patterson *et al.*, 2023; Stoll, Kemp, Patterson, Howe, *et al.*, 2024; Stoll, Kemp, Patterson, Kubik, *et al.*, 2024). However, pSyn inclusions in the SNpc are present earlier in the PFF model, with the initial peak starting at 1 month and remaining constant until 2 months (Duffy, Collier, Patterson, Kemp, Luk, *et al.*, 2018; Howe *et al.*, 2021). In vitro studies suggest that 1 month after PFF exposure a percentage of pSyn aggregates will mature into LB-like aggregates, and it is likely that this process continues (Mahul-Mellier *et al.*, 2020). Indeed, we have observed that two months following intrastriatal PFF injection, nigral pSyn aggregates contain a greater percentage of fibrillar α-Syn compared to the percentage of fibrillar α-Syn observed at one month defined by F2

(fibrillar-predominant α-Syn) staining (1 month ~55%, 2 months ~84%) (Duffy, Collier, Patterson, Kemp, Luk, *et al.*, 2018; Patterson *et al.*, 2019). This suggests that studying both the 1- and 2-month time point may provide an opportunity to understand the earliest microglial response to the formation of LB-like inclusions as well as to understand dynamic temporal responses to protein aggregation. Previous work has demonstrated that microglial response genes can be categorized into early and late-stage response genes, albeit in the context of a mouse AD model of amyloid beta (Aß) deposition (Mathys *et al.*, 2017). In the experiments undertaken in this dissertation I investigated and compared the transcriptomic alterations in the inclusion-bearing SNpc at one and two months following intrastriatal PFF injection to rats using ribonucleic acid sequencing (RNA-Seq, **Aim 1**). I then validated my RNA-Seq findings for a family of genes, the cathepsins, implicated in my RNA-Seq results across both time points using immunofluorescence (IF), droplet digital polymerase chain reaction (ddPCR), fluorescence in situ hybridization (FISH) (**Aim 2**).

Specific Aims

Specific Aim 1: Investigate and compare the transcriptomic alterations in the inclusion-bearing SNpc at one month (early inclusion) and two months (mature inclusions) following intrastriatal PFF injection to rats using ribonucleic acid sequencing with a focus on neuroinflammatory signaling.

To enrich inclusion-bearing nigral samples for immediately adjacent microglia, I used a laser capture microdissection (LCM) approach in male, TH-enhanced green fluorescent protein (TH-EGFP) Sprague Dawley rats, leveraging the endogenous GFP to visualize the SNpc during microdissection. Comparisons in differentially expressed

genes at each time point was made following intrastriatal PFF and PBS injection, as well as across both time points.

My results suggest that cytokine production and microglial activation are upregulated in association with both early and more mature pSyn inclusion stages. The earlier one-month time point is specifically associated with upregulation of differentially expressed genes (DEGs) associated with ribosomal biogenesis, RNA processing and protein degradation whereas the later, two-month, time point is specifically associated with the upregulation of DEGs implicating microglial activation of defense responses to viruses to protect the host. Downregulation of DEGs associated with cell signaling, neurotransmitter synthesis, and synaptic transmission are also common across both time points. Collectively, these results suggest that the response to pSyn inclusions in the SNpc is temporally dynamic. Further, the results support a role for multiple cathepsins over the course of both early and more mature pSyn inclusions.

Specific Aim 2: Validation and localization of the microglial transcriptional response to α-syn inclusions

In a separate cohort of non-transgenic male Fischer 344 rats receiving intrastriatal PBS or PFF injections I will validate and localize mRNA and/or protein expression of a cathepsins 1 and 2 months after surgery. Validation of cathepsin mRNA expression will be performed using ddPCR (*Ctsa, Ctsb, Ctsc, Ctsd, Ctse, Ctsf, Ctsh, Ctsk, Ctsl, Ctss, Ctsw, Ctsz/x/p*). mRNA localization and quantification of a subset of cathepsins (*Ctsh, Ctsl, Ctss, Ctsz/x/p*) within microglia will be conducted using fluorescent in-situ hybridization (FISH) or immunofluorescence (IF).

My results suggest that the one-month timepoint featured decreased expression of *Th, Ctsa, Ctsb, Ctsd* and *Ctsf* and increased expression of *Ctsw* and *Ctsx* compared to control PBS-injected rats. At two months, decreased *Th* expression in the SN was again observed in PFF-injected rats, along with increased *Ctse, Ctsh*, and *Ctsx*. I next investigated the cellular source of specific cathepsins (*Ctsh, Ctsl, Ctss*, Ctsx) by leveraging various combinations of FISH combined with IF. I observed that microglia in the pSyn inclusion-bearing SNpc increased expression of *Ctsh, Ctss* and Ctsx at both timepoints after PFF injection suggesting that these specific cathepsins play a role in the microglial response to α-syn inclusions.

BIBLIOGRAPHY

Aarsland, D., Batzu, L., Halliday, G. M., Geurtsen, G. J., Ballard, C., Ray Chaudhuri, K., & Weintraub, D. (2021). Parkinson disease-associated cognitive impairment. *Nature Reviews. Disease Primers*, *7*(1), 47. https://doi.org/10.1038/s41572-021-00280-3

Abdelmotilib, H., Maltbie, T., Delic, V., Liu, Z., Hu, X., Fraser, K. B., Moehle, M. S., Stoyka, L., Anabtawi, N., Krendelchtchikova, V., Volpicelli-Daley, L. A., & West, A. (2017). α-Synuclein fibril-induced inclusion spread in rats and mice correlates with dopaminergic Neurodegeneration. *Neurobiology of Disease*, *105*, 84–98. https://doi.org/10.1016/j.nbd.2017.05.014

Agid, Y. (1991). Parkinson's disease: pathophysiology. *The Lancet*, *337*(8753), 1321–1324. https://doi.org/10.1016/0140-6736(91)92989-f

Ahlskog, J. E., & Muenter, M. D. (2001). Frequency of levodopa-related dyskinesias and motor fluctuations as estimated from the cumulative literature. *Movement Disorders*, *16*(3), 448–458. https://doi.org/10.1002/mds.1090

Akiyama, H., Barger, S., Barnum, S., Bradt, B., Bauer, J., Cole, G. M., Cooper, N. R., Eikelenboom, P., Emmerling, M., Fiebich, B. L., Finch, C. E., Frautschy, S., Griffin, W. S., Hampel, H., Hull, M., Landreth, G., Lue, L., Mrak, R., Mackenzie, I. R., … Wyss-Coray, T. (2000). Inflammation and Alzheimer's disease. *Neurobiology of Aging*, *21*(3), 383–421. https://doi.org/10.1016/s0197-4580(00)00124-x

Alberts, B., Johnson, A., Lewis, J., Raff, M., Roberts, K., & Walter, P. (2007). The adaptive immune system. In *Molecular biology of the cell* (pp. 1539–1602). Garland Science. https://doi.org/10.1201/9780203833445-25

Alliot, F., Godin, I. and Pessac, B. (1999) "Microglia derive from progenitors, originating from the yolk sac, and which proliferate in the brain.," Brain research. Developmental brain research, 117(2), pp. 145–152. doi:10.1016/S0165-3806(99)00113-3.

Alzheimer, A. (1910). Beiträge zur Kenntnis der pathologischen Neuroglia und ihrer Beziehungen zu den Abbauvorgängen im Nervengewebe. *Beiträge Zur Kenntnis Der Pathologischen Neuroglia Und Ihrer Beziehungen Zu Den Abbauvorgängen Im Nervengewebe*.

Anderson, S. R., Roberts, J. M., Zhang, J., Steele, M. R., Romero, C. O., Bosco, A., & Vetter, M. L. (2019). Developmental Apoptosis Promotes a Disease-Related Gene Signature and Independence from CSF1R Signaling in Retinal Microglia. *Cell Reports*, *27*(7), 2002-2013.e5. https://doi.org/10.1016/j.celrep.2019.04.062

Arroyo, D. S., Soria, J. A., Gaviglio, E. A., Rodriguez-Galan, M. C., & Iribarren, P. (2011). Toll-like receptors are key players in neurodegeneration. *International*

Immunopharmacology, *11*(10), 1415–1421. https://doi.org/10.1016/j.intimp.2011.05.006

Asanuma, M., Nishibayashi-Asanuma, S., Miyazaki, I., Kohno, M., & Ogawa, N. (2001). Neuroprotective effects of non-steroidal anti-inflammatory drugs by direct scavenging of nitric oxide radicals. *Journal of Neurochemistry*, *76*(6), 1895–1904. https://doi.org/10.1046/j.1471-4159.2001.00205.x

Augusto-Oliveira, M., Arrifano, G. P., Lopes-Araújo, A., Santos-Sacramento, L., Takeda, P. Y., Anthony, D. C., Malva, J. O., & Crespo-Lopez, M. E. (2019). What do microglia really do in healthy adult brain? *Cells*, *8*(10). https://doi.org/10.3390/cells8101293

Badanjak, K., Fixemer, S., Smajić, S., Skupin, A., & Grünewald, A. (2021). The contribution of microglia to neuroinflammation in parkinson's disease. *International Journal of Molecular Sciences*, *22*(9). https://doi.org/10.3390/ijms22094676

Baldereschi, M., Di Carlo, A., Rocca, W. A., Vanni, P., Maggi, S., Perissinotto, E., Grigoletto, F., Amaducci, L., & Inzitari, D. (2000). Parkinson's disease and parkinsonism in a longitudinal study: two-fold higher incidence in men. ILSA Working Group. Italian Longitudinal Study on Aging. *Neurology*, *55*(9), 1358–1363. https://doi.org/10.1212/wnl.55.9.1358

Ball, N., Teo, W.-P., Chandra, S., & Chapman, J. (2019). Parkinson's disease and the environment. *Frontiers in Neurology*, *10*, 218. https://doi.org/10.3389/fneur.2019.00218

Bandopadhyay, R., Mishra, N., Rana, R., Kaur, G., Ghoneim, M. M., Alshehri, S., Mustafa, G., Ahmad, J., Alhakamy, N. A., & Mishra, A. (2022). Molecular Mechanisms and Therapeutic Strategies for Levodopa-Induced Dyskinesia in Parkinson's Disease: A Perspective Through Preclinical and Clinical Evidence. *Frontiers in Pharmacology*, *13*, 805388. https://doi.org/10.3389/fphar.2022.805388

Barrenschee, M., Zorenkov, D., Böttner, M., Lange, C., Cossais, F., Scharf, A. B., Deuschl, G., Schneider, S. A., Ellrichmann, M., Fritscher-Ravens, A., & Wedel, T. (2017). Distinct pattern of enteric phospho-alpha-synuclein aggregates and gene expression profiles in patients with Parkinson's disease. *Acta Neuropathologica Communications*, *5*(1), 1. https://doi.org/10.1186/s40478-016-0408-2

Ben-Joseph, A., Marshall, C. R., Lees, A. J., & Noyce, A. J. (2020). Ethnic variation in the manifestation of parkinson's disease: A narrative review. *Journal of Parkinson's Disease*, *10*(1), 31–45. https://doi.org/10.3233/JPD-191763

Benskey, M. J., Perez, R. G., & Manfredsson, F. P. (2016). The contribution of alpha synuclein to neuronal survival and function - Implications for Parkinson's disease. *Journal of Neurochemistry*, *137*(3), 331–359. https://doi.org/10.1111/jnc.13570

Bernal-Conde, L. D., Ramos-Acevedo, R., Reyes-Hernández, M. A., Balbuena-Olvera, A. J., Morales-Moreno, I. D., Argüero-Sánchez, R., Schüle, B., & Guerra-Crespo, M. (2019). Alpha-Synuclein Physiology and Pathology: A Perspective on Cellular Structures and Organelles. *Frontiers in Neuroscience*, *13*, 1399. https://doi.org/10.3389/fnins.2019.01399

Biundo, R., Weis, L., & Antonini, A. (2016). Cognitive decline in Parkinson's disease: the complex picture. *Npj Parkinson's Disease*, *2*, 16018. https://doi.org/10.1038/npjparkd.2016.18

Blandini, F., Nappi, G., Tassorelli, C., & Martignoni, E. (2000). Functional changes of the basal ganglia circuitry in Parkinson's disease. *Progress in Neurobiology*, *62*(1), 63–88. https://doi.org/10.1016/S0301-0082(99)00067-2

Bogie, J. F. J., Stinissen, P., & Hendriks, J. J. A. (2014). Macrophage subsets and microglia in multiple sclerosis. *Acta Neuropathologica*, *128*(2), 191–213. https://doi.org/10.1007/s00401-014-1310-2

Boillée, S., Yamanaka, K., Lobsiger, C. S., Copeland, N. G., Jenkins, N. A., Kassiotis, G., Kollias, G., & Cleveland, D. W. (2006). Onset and progression in inherited ALS determined by motor neurons and microglia. *Science*, *312*(5778), 1389–1392. https://doi.org/10.1126/science.1123511

Bolam, J. P., Hanley, J. J., Booth, P. A., & Bevan, M. D. (2000). Synaptic organisation of the basal ganglia. *Journal of Anatomy*, *196 (Pt 4)*(Pt 4), 527–542. https://doi.org/10.1046/j.1469-7580.2000.19640527.x

Borovac, J. A. (2016). Side effects of a dopamine agonist therapy for Parkinson's disease: a mini-review of clinical pharmacology. *The Yale Journal of Biology and Medicine*, *89*(1), 37–47.

Braak, H., Del Tredici, K., Rüb, U., de Vos, R. A. I., Jansen Steur, E. N. H., & Braak, E. (2003). Staging of brain pathology related to sporadic Parkinson's disease. *Neurobiology of Aging*, *24*(2), 197–211. https://doi.org/10.1016/s0197-4580(02)00065-9

Braak, H., & Del Tredici, K. (2009). Neuroanatomy and pathology of sporadic Parkinson's disease. *Advances in Anatomy, Embryology, and Cell Biology*, *201*, 1–119. https://doi.org/10.1007/978-3-540-79850-7

Brochard, V., Combadière, B., Prigent, A., Laouar, Y., Perrin, A., Beray-Berthat, V., Bonduelle, O., Alvarez-Fischer, D., Callebert, J., Launay, J.-M., Duyckaerts, C., Flavell, R. A., Hirsch, E. C., & Hunot, S. (2009). Infiltration of CD4+ lymphocytes into the brain contributes to neurodegeneration in a mouse model of Parkinson disease. *The Journal of Clinical Investigation*, *119*(1), 182–192. https://doi.org/10.1172/JCI36470

Brown, D. R., Schmidt, B., & Kretzschmar, H. A. (1996). Role of microglia and host prion protein in neurotoxicity of a prion protein fragment. *Nature*, *380*(6572), 345–347. https://doi.org/10.1038/380345a0

Butovsky, O., Ziv, Y., Schwartz, A., Landa, G., Talpalar, A. E., Pluchino, S., Martino, G., & Schwartz, M. (2006). Microglia activated by IL-4 or IFN-gamma differentially induce neurogenesis and oligodendrogenesis from adult stem/progenitor cells. *Molecular and Cellular Neurosciences*, *31*(1), 149–160. https://doi.org/10.1016/j.mcn.2005.10.006

Calabresi, P., Picconi, B., Tozzi, A., Ghiglieri, V., & Di Filippo, M. (2014). Direct and indirect pathways of basal ganglia: a critical reappraisal. *Nature Neuroscience*, *17*(8), 1022–1030. https://doi.org/10.1038/nn.3743

Carpanini, S. M., Torvell, M., Bevan, R. J., Byrne, R. A. J., Daskoulidou, N., Saito, T., Saido, T. C., Taylor, P. R., Hughes, T. R., Zelek, W. M., & Morgan, B. P. (2022). Terminal complement pathway activation drives synaptic loss in Alzheimer's disease models. *Acta Neuropathologica Communications*, *10*(1), 99. https://doi.org/10.1186/s40478-022-01404-w

Castillo, S., Muñoz, P., Behrens, M. I., Diaz-Grez, F., & Segura-Aguilar, J. (2017). On the role of mining exposure in epigenetic effects in parkinson's disease. *Neurotoxicity Research*, *32*(2), 172–174. https://doi.org/10.1007/s12640-017-9736-7

Centner, A., Del Priore, I., Chambers, N., Cohen, S. R., Terry, M. L., Coyle, M., Glinski, J., Stoll, A. C., Patterson, J. R., Kemp, C. J., Miller, K. M., Kubik, M., Kuhn, N., Luk, K. C., Sortwell, C. E., & Bishop, C. (2024). Deficits in basal and evoked striatal dopamine release following alpha-synuclein preformed fibril injection: An in vivo microdialysis study. *The European Journal of Neuroscience*, *59*(7), 1585–1603. https://doi.org/10.1111/ejn.16275

Cerri, S., Mus, L., & Blandini, F. (2019). Parkinson's disease in women and men: what's the difference? *Journal of Parkinson's Disease*, *9*(3), 501–515. https://doi.org/10.3233/JPD-191683

Chan, C. S., Gertler, T. S., & Surmeier, D. J. (2010). A molecular basis for the increased vulnerability of substantia nigra dopamine neurons in aging and Parkinson's disease. *Movement Disorders*, *25 Suppl 1*, S63-70. https://doi.org/10.1002/mds.22801

Chao, M. V. (2003). Neurotrophins and their receptors: a convergence point for many signalling pathways. *Nature Reviews. Neuroscience*, *4*(4), 299–309. https://doi.org/10.1038/nrn1078

Charcot, J. M., & Sigerson, George. (1879). *Lectures on the diseases of the nervous system delivered at La Salpêtrière* (pp. xii, 271 pages). H.C. Lea.

Chartier-Harlin, M.-C., Kachergus, J., Roumier, C., Mouroux, V., Douay, X., Lincoln, S., Levecque, C., Larvor, L., Andrieux, J., Hulihan, M., Waucquier, N., Defebvre, L., Amouyel, P., Farrer, M., & Destée, A. (2004). Alpha-synuclein locus duplication as a cause of familial Parkinson's disease. *The Lancet*, *364*(9440), 1167–1169. https://doi.org/10.1016/S0140-6736(04)17103-1

Chen, H., Jacobs, E., Schwarzschild, M. A., McCullough, M. L., Calle, E. E., Thun, M. J., & Ascherio, A. (2005). Nonsteroidal antiinflammatory drug use and the risk for Parkinson's disease. *Annals of Neurology*, *58*(6), 963–967. https://doi.org/10.1002/ana.20682

Chen, H., Zhang, S. M., Hernán, M. A., Schwarzschild, M. A., Willett, W. C., Colditz, G. A., Speizer, F. E., & Ascherio, A. (2003). Nonsteroidal anti-inflammatory drugs and the risk of Parkinson disease. *Archives of Neurology*, *60*(8), 1059–1064. https://doi.org/10.1001/archneur.60.8.1059

Cheng, H.-C., Ulane, C. M., & Burke, R. E. (2010). Clinical progression in Parkinson disease and the neurobiology of axons. *Annals of Neurology*, *67*(6), 715–725. https://doi.org/10.1002/ana.21995

Chen, X., Hu, Y., Cao, Z., Liu, Q., & Cheng, Y. (2018). Cerebrospinal Fluid Inflammatory Cytokine Aberrations in Alzheimer's Disease, Parkinson's Disease and Amyotrophic Lateral Sclerosis: A Systematic Review and Meta-Analysis. *Frontiers in Immunology*, *9*, 2122. https://doi.org/10.3389/fimmu.2018.02122

Chu, K., Zhou, X., & Luo, B. (2012). Cytokine gene polymorphisms and Parkinson's disease: a meta-analysis. *The Canadian Journal of Neurological Sciences. Le Journal Canadien Des Sciences Neurologiques*, *39*(1), 58–64. https://doi.org/10.1017/s0317167100012695

Chu, Y., Muller, S., Tavares, A., Barret, O., Alagille, D., Seibyl, J., Tamagnan, G., Marek, K., Luk, K. C., Trojanowski, J. Q., Lee, V. M. Y., & Kordower, J. H. (2019). Intrastriatal alpha-synuclein fibrils in monkeys: spreading, imaging and neuropathological changes. *Brain: A Journal of Neurology*, *142*(11), 3565–3579. https://doi.org/10.1093/brain/awz296

Cole, T. A., Zhao, H., Collier, T. J., Sandoval, I., Sortwell, C. E., Steece-Collier, K., Daley, B. F., Booms, A., Lipton, J., Welch, M., Berman, M., Jandreski, L., Graham, D., Weihofen, A., Celano, S., Schulz, E., Cole-Strauss, A., Luna, E., Quach, D., … Paumier, K. L. (2021). α-Synuclein antisense oligonucleotides as a disease-modifying therapy for Parkinson's disease. *Journal of Clinical Investigation Insight*, *6*(5). https://doi.org/10.1172/jci.insight.135633

Collier, T. J., Kanaan, N. M., & Kordower, J. H. (2011). Ageing as a primary risk factor for Parkinson's disease: evidence from studies of non-human primates. *Nature Reviews. Neuroscience*, *12*(6), 359–366. https://doi.org/10.1038/nrn3039

Colonna, M., & Butovsky, O. (2017). Microglia function in the central nervous system during health and neurodegeneration. *Annual Review of Immunology*, *35*, 441–468. https://doi.org/10.1146/annurev-immunol-051116-052358

Conway, K. A., Harper, J. D., & Lansbury, P. T. (1998). Accelerated in vitro fibril formation by a mutant alpha-synuclein linked to early-onset Parkinson disease. *Nature Medicine*, *4*(11), 1318–1320. https://doi.org/10.1038/3311

Corriveau, R. A., Huh, G. S., & Shatz, C. J. (1998). Regulation of class I MHC gene expression in the developing and mature CNS by neural activity. *Neuron*, *21*(3), 505–520. https://doi.org/10.1016/s0896-6273(00)80562-0

Costa, J., Martins, S., Ferreira, P., Cardoso, A. M. S., Guedes, J. R., Peça, J. M., & Cardoso, A. L. (2021). The old guard: age-related changes in microglia and their consequences. *Mechanisms of Ageing and Development*, 111512. https://doi.org/10.1016/j.mad.2021.111512

Creed, R. B., & Goldberg, M. S. (2020). Enhanced Susceptibility of PINK1 Knockout Rats to α-Synuclein Fibrils. *Neuroscience*, *437*, 64–75. https://doi.org/10.1016/j.neuroscience.2020.04.032

Cremades, N., Cohen, S. I. A., Deas, E., Abramov, A. Y., Chen, A. Y., Orte, A., Sandal, M., Clarke, R. W., Dunne, P., Aprile, F. A., Bertoncini, C. W., Wood, N. W., Knowles, T. P. J., Dobson, C. M., & Klenerman, D. (2012). Direct observation of the interconversion of normal and toxic forms of α-synuclein. *Cell*, *149*(5), 1048–1059. https://doi.org/10.1016/j.cell.2012.03.037

Croisier, E., Moran, L. B., Dexter, D. T., Pearce, R. K. B., & Graeber, M. B. (2005). Microglial inflammation in the parkinsonian substantia nigra: relationship to alpha-synuclein deposition. *Journal of Neuroinflammation*, *2*, 14. https://doi.org/10.1186/1742-2094-2-14

Cunningham, C. L., Martínez-Cerdeño, V., & Noctor, S. C. (2013). Microglia regulate the number of neural precursor cells in the developing cerebral cortex. *The Journal of Neuroscience*, *33*(10), 4216–4233. https://doi.org/10.1523/JNEUROSCI.3441-12.2013

DeLong, M., & Wichmann, T. (2009). Update on models of basal ganglia function and dysfunction. *Parkinsonism & Related Disorders*, *15 Suppl 3*(0 3), S237-40. https://doi.org/10.1016/S1353-8020(09)70822-3

DeMaagd, G., & Philip, A. (2015). Part 2: introduction to the pharmacotherapy of Parkinson's disease, with a focus on the use of dopaminergic agents. *P & T : A Peer-Reviewed Journal for Formulary Management*, *40*(9), 590–600.

Dijkstra, A. A., Ingrassia, A., de Menezes, R. X., van Kesteren, R. E., Rozemuller, A. J. M., Heutink, P., & van de Berg, W. D. J. (2015). Evidence for immune response, axonal dysfunction and reduced endocytosis in the substantia nigra in early stage parkinson's disease. *Plos One*, *10*(6), e0128651. https://doi.org/10.1371/journal.pone.0128651

Dorsey, E. R., Sherer, T., Okun, M. S., & Bloem, B. R. (2018). The emerging evidence of the parkinson pandemic. *Journal of Parkinson's Disease*, *8*(s1), S3–S8. https://doi.org/10.3233/JPD-181474

Dotchin, C., Msuya, O., Kissima, J., Massawe, J., Mhina, A., Moshy, A., Aris, E., Jusabani, A., Whiting, D., Masuki, G., & Walker, R. (2008). The prevalence of Parkinson's disease in rural Tanzania. *Movement Disorders*, *23*(11), 1567–1672. https://doi.org/10.1002/mds.21898

Dougherty, K. D., Dreyfus, C. F., & Black, I. B. (2000). Brain-derived neurotrophic factor in astrocytes, oligodendrocytes, and microglia/macrophages after spinal cord injury. *Neurobiology of Disease*, *7*(6 Pt B), 574–585. https://doi.org/10.1006/nbdi.2000.0318

Duffy, M. F., Collier, T. J., Patterson, J. R., Kemp, C. J., Fischer, D. L., Stoll, A. C., & Sortwell, C. E. (2018). Quality Over Quantity: Advantages of Using Alpha-Synuclein Preformed Fibril Triggered Synucleinopathy to Model Idiopathic Parkinson's Disease. *Frontiers in Neuroscience*, *12*, 621. https://doi.org/10.3389/fnins.2018.00621

Duffy, M. F., Collier, T. J., Patterson, J. R., Kemp, C. J., Luk, K. C., Tansey, M. G., Paumier, K. L., Kanaan, N. M., Fischer, D. L., Polinski, N. K., Barth, O. L., Howe, J. W., Vaikath, N. N., Majbour, N. K., El-Agnaf, O. M. A., & Sortwell, C. E. (2018). Lewy body-like alpha-synuclein inclusions trigger reactive microgliosis prior to nigral degeneration. *Journal of Neuroinflammation*, *15*(1), 129. https://doi.org/10.1186/s12974-018-1171-z

Earls, R. H., Menees, K. B., Chung, J., Barber, J., Gutekunst, C.-A., Hazim, M. G., & Lee, J.-K. (2019). Intrastriatal injection of preformed alpha-synuclein fibrils alters central and peripheral immune cell profiles in non-transgenic mice. *Journal of Neuroinflammation*, *16*(1), 250. https://doi.org/10.1186/s12974-019-1636-8

Earls, R. H., Menees, K. B., Chung, J., Gutekunst, C.-A., Lee, H. J., Hazim, M. G., Rada, B., Wood, L. B., & Lee, J.-K. (2020). NK cells clear α-synuclein and the depletion of NK cells exacerbates synuclein pathology in a mouse model of α-synucleinopathy. *Proceedings of the National Academy of Sciences of the United States of America*, *117*(3), 1762–1771. https://doi.org/10.1073/pnas.1909110117

Ekdahl, C. T., Claasen, J.-H., Bonde, S., Kokaia, Z., & Lindvall, O. (2003). Inflammation is detrimental for neurogenesis in adult brain. *Proceedings of the National Academy of Sciences of the United States of America*, *100*(23), 13632–13637. https://doi.org/10.1073/pnas.2234031100

El Khoury, J., Hickman, S. E., Thomas, C. A., Cao, L., Silverstein, S. C., & Loike, J. D. (1996). Scavenger receptor-mediated adhesion of microglia to beta-amyloid fibrils. *Nature*, *382*(6593), 716–719. https://doi.org/10.1038/382716a0

Engelhardt, E., & Gomes, M. da M. (2017). Lewy and his inclusion bodies: Discovery and rejection. *Dementia & Neuropsychologia*, *11*(2), 198–201. https://doi.org/10.1590/1980-57642016dn11-020012

Farrer, M., Kachergus, J., Forno, L., Lincoln, S., Wang, D.-S., Hulihan, M., Maraganore, D., Gwinn-Hardy, K., Wszolek, Z., Dickson, D., & Langston, J. W. (2004). Comparison of kindreds with parkinsonism and alpha-synuclein genomic multiplications. *Annals of Neurology*, *55*(2), 174–179. https://doi.org/10.1002/ana.10846

Fernagut, P.-O., & Chesselet, M.-F. (2004). Alpha-synuclein and transgenic mouse models. *Neurobiology of Disease*, *17*(2), 123–130. https://doi.org/10.1016/j.nbd.2004.07.001

Finkelstein, M. M., & Jerrett, M. (2007). A study of the relationships between Parkinson's disease and markers of traffic-derived and environmental manganese air pollution in two Canadian cities. *Environmental Research*, *104*(3), 420–432. https://doi.org/10.1016/j.envres.2007.03.002

Flagmeier, P., Meisl, G., Vendruscolo, M., Knowles, T. P. J., Dobson, C. M., Buell, A. K., & Galvagnion, C. (2016). Mutations associated with familial Parkinson's disease alter the initiation and amplification steps of α-synuclein aggregation. *Proceedings of the National Academy of Sciences of the United States of America*, *113*(37), 10328–10333. https://doi.org/10.1073/pnas.1604645113

Flannagan, R. S., Jaumouillé, V., & Grinstein, S. (2012). The cell biology of phagocytosis. *Annual Review of Pathology*, *7*, 61–98. https://doi.org/10.1146/annurev-pathol-011811-132445

Forno, L. S., DeLanney, L. E., Irwin, I., & Langston, J. W. (1993). Similarities and differences between MPTP-induced parkinsonsim and Parkinson's disease. Neuropathologic considerations. *Advances in Neurology*, *60*, 600–608.

Frackowiak, J., Wisniewski, H. M., Wegiel, J., Merz, G. S., Iqbal, K., & Wang, K. C. (1992). Ultrastructure of the microglia that phagocytose amyloid and the microglia that produce beta-amyloid fibrils. *Acta Neuropathologica*, *84*(3), 225–233. https://doi.org/10.1007/BF00227813

Frank, C., Pari, G., & Rossiter, J. P. (2006). Approach to diagnosis of Parkinson disease. *Canadian Family Physician*, *52*, 862–868.

Frentzel, D., Judanin, G., Borozdina, O., Klucken, J., Winkler, J., & Schlachetzki, J. C. M. (2017). Increase of reproductive life span delays age of onset of parkinson's disease. *Frontiers in Neurology*, *8*, 397. https://doi.org/10.3389/fneur.2017.00397

Funayama, M., Hasegawa, K., Kowa, H., Saito, M., Tsuji, S., & Obata, F. (2002). A new locus for Parkinson's disease (PARK8) maps to chromosome 12p11.2-q13.1. *Annals of Neurology*, *51*(3), 296–301. https://doi.org/10.1002/ana.10113

Gai, W. P., Yuan, H. X., Li, X. Q., Power, J. T., Blumbergs, P. C., & Jensen, P. H. (2000). In situ and in vitro study of colocalization and segregation of alpha-synuclein, ubiquitin, and lipids in Lewy bodies. *Experimental Neurology*, *166*(2), 324–333. https://doi.org/10.1006/exnr.2000.7527

Galloway, D. A., Phillips, A. E. M., Owen, D. R. J., & Moore, C. S. (2019). Phagocytosis in the brain: homeostasis and disease. *Frontiers in Immunology*, *10*, 790. https://doi.org/10.3389/fimmu.2019.00790

Gao, H.-M., Zhang, F., Zhou, H., Kam, W., Wilson, B., & Hong, J.-S. (2011). Neuroinflammation and α-synuclein dysfunction potentiate each other, driving chronic progression of neurodegeneration in a mouse model of Parkinson's disease. *Environmental Health Perspectives*, *119*(6), 807–814. https://doi.org/10.1289/ehp.1003013

Garcia-Esparcia, P., Llorens, F., Carmona, M., & Ferrer, I. (2014). Complex deregulation and expression of cytokines and mediators of the immune response in Parkinson's disease brain is region dependent. *Brain Pathology*, *24*(6), 584–598. https://doi.org/10.1111/bpa.12137

Garcia, P., Jürgens-Wemheuer, W., Uriarte Huarte, O., Michelucci, A., Masuch, A., Brioschi, S., Weihofen, A., Koncina, E., Coowar, D., Heurtaux, T., Glaab, E., Balling, R., Sousa, C., Kaoma, T., Nicot, N., Pfander, T., Schulz-Schaeffer, W., Allouche, A., Fischer, N., … Buttini, M. (2022). Neurodegeneration and neuroinflammation are linked, but independent of alpha-synuclein inclusions, in a seeding/spreading mouse model of Parkinson's disease. *Glia*, *70*(5), 935–960. https://doi.org/10.1002/glia.24149

Gasser, T., Hardy, J., & Mizuno, Y. (2011). Milestones in PD genetics. *Movement Disorders*, *26*(6), 1042–1048. https://doi.org/10.1002/mds.23637

Gerhard, A., Pavese, N., Hotton, G., Turkheimer, F., Es, M., Hammers, A., Eggert, K., Oertel, W., Banati, R. B., & Brooks, D. J. (2006). In vivo imaging of microglial activation with [11C](R)-PK11195 PET in idiopathic Parkinson's disease. *Neurobiology of Disease*, *21*(2), 404–412. https://doi.org/10.1016/j.nbd.2005.08.002

Giasson, B. I., Covy, J. P., Bonini, N. M., Hurtig, H. I., Farrer, M. J., Trojanowski, J. Q., & Van Deerlin, V. M. (2006). Biochemical and pathological characterization of Lrrk2. *Annals of Neurology*, *59*(2), 315–322. https://doi.org/10.1002/ana.20791

Gibb, W. R., & Lees, A. J. (1991). Anatomy, pigmentation, ventral and dorsal subpopulations of the substantia nigra, and differential cell death in Parkinson's disease. *Journal of Neurology, Neurosurgery, and Psychiatry*, *54*(5), 388–396. https://doi.org/10.1136/jnnp.54.5.388

Gibrat, C., Saint-Pierre, M., Bousquet, M., Lévesque, D., Rouillard, C., & Cicchetti, F. (2009). Differences between subacute and chronic MPTP mice models: investigation of dopaminergic neuronal degeneration and alpha-synuclein inclusions. *Journal of Neurochemistry*, *109*(5), 1469–1482. https://doi.org/10.1111/j.1471-4159.2009.06072.x

Goedert, M., Spillantini, M. G., Del Tredici, K., & Braak, H. (2013). 100 years of Lewy pathology. *Nature Reviews. Neurology*, *9*(1), 13–24. https://doi.org/10.1038/nrneurol.2012.242

Gombash, S. E., Manfredsson, F. P., Kemp, C. J., Kuhn, N. C., Fleming, S. M., Egan, A. E., Grant, L. M., Ciucci, M. R., MacKeigan, J. P., & Sortwell, C. E. (2013). Morphological and behavioral impact of AAV2/5-mediated overexpression of human wildtype alpha-synuclein in the rat nigrostriatal system. *Plos One*, *8*(11), e81426. https://doi.org/10.1371/journal.pone.0081426

Gómez-Benito, M., Granado, N., García-Sanz, P., Michel, A., Dumoulin, M., & Moratalla, R. (2020). Modeling Parkinson's Disease With the Alpha-Synuclein Protein. *Frontiers in Pharmacology*, *11*, 356. https://doi.org/10.3389/fphar.2020.00356

González-Hernández, T., Cruz-Muros, I., Afonso-Oramas, D., Salas-Hernandez, J., & Castro-Hernandez, J. (2010). Vulnerability of mesostriatal dopaminergic neurons in Parkinson's disease. *Frontiers in Neuroanatomy*, *4*, 140. https://doi.org/10.3389/fnana.2010.00140

Govindarajulu, M., Ramesh, S., Beasley, M., Lynn, G., Wallace, C., Labeau, S., Pathak, S., Nadar, R., Moore, T., & Dhanasekaran, M. (2023). Role of cGAS-Sting Signaling in Alzheimer's Disease. *International Journal of Molecular Sciences*, *24*(9). https://doi.org/10.3390/ijms24098151

Graat, I., Figee, M., & Denys, D. (2017). The application of deep brain stimulation in the treatment of psychiatric disorders. *International Review of Psychiatry*, *29*(2), 178–190. https://doi.org/10.1080/09540261.2017.1282439

Gulen, M. F., Samson, N., Keller, A., Schwabenland, M., Liu, C., Glück, S., Thacker, V. V., Favre, L., Mangeat, B., Kroese, L. J., Krimpenfort, P., Prinz, M., & Ablasser, A. (2023). cGAS-STING drives ageing-related inflammation and neurodegeneration. *Nature*, *620*(7973), 374–380. https://doi.org/10.1038/s41586-023-06373-1

Günther, E., & Walter, L. (2001). The major histocompatibility complex of the rat (Rattus norvegicus). *Immunogenetics*, *53*(7), 520–542. https://doi.org/10.1007/s002510100361

Guo, M., Wang, J., Zhao, Y., Feng, Y., Han, S., Dong, Q., Cui, M., & Tieu, K. (2020). Microglial exosomes facilitate α-synuclein transmission in Parkinson's disease. *Brain: A Journal of Neurology*, *143*(5), 1476–1497. https://doi.org/10.1093/brain/awaa090

Hansen, D. V., Hanson, J. E., & Sheng, M. (2018). Microglia in Alzheimer's disease. *The Journal of Cell Biology*, *217*(2), 459–472. https://doi.org/10.1083/jcb.201709069

Harms, A. S., Cao, S., Rowse, A. L., Thome, A. D., Li, X., Mangieri, L. R., Cron, R. Q., Shacka, J. J., Raman, C., & Standaert, D. G. (2013). MHCII is required for α-synuclein-induced activation of microglia, CD4 T cell proliferation, and dopaminergic neurodegeneration. *The Journal of Neuroscience*, *33*(23), 9592–9600. https://doi.org/10.1523/JNEUROSCI.5610-12.2013

Harms, A. S., Delic, V., Thome, A. D., Bryant, N., Liu, Z., Chandra, S., Jurkuvenaite, A., & West, A. B. (2017). α-Synuclein fibrils recruit peripheral immune cells in the rat brain prior to neurodegeneration. *Acta Neuropathologica Communications*, *5*(1), 85. https://doi.org/10.1186/s40478-017-0494-9

Hauser, R. A., Pahwa, R., Tanner, C. M., Oertel, W., Isaacson, S. H., Johnson, R., Felt, L., & Stempien, M. J. (2017). ADS-5102 (Amantadine) Extended-Release Capsules for Levodopa-Induced Dyskinesia in Parkinson's Disease (EASE LID 2 Study): Interim Results of an Open-Label Safety Study. *Journal of Parkinson's Disease*, *7*(3), 511–522. https://doi.org/10.3233/JPD-171134

Henderson, M. X., Cornblath, E. J., Darwich, A., Zhang, B., Brown, H., Gathagan, R. J., Sandler, R. M., Bassett, D. S., Trojanowski, J. Q., & Lee, V. M. Y. (2019). Spread of α-synuclein pathology through the brain connectome is modulated by selective vulnerability and predicted by network analysis. *Nature Neuroscience*, *22*(8), 1248–1257. https://doi.org/10.1038/s41593-019-0457-5

He, J., Chen, Y., Farzan, M., Choe, H., Ohagen, A., Gartner, S., Busciglio, J., Yang, X., Hofmann, W., Newman, W., Mackay, C. R., Sodroski, J., & Gabuzda, D. (1997). CCR3 and CCR5 are co-receptors for HIV-1 infection of microglia. *Nature*, *385*(6617), 645–649. https://doi.org/10.1038/385645a0

Hindle, J. V. (2010). Ageing, neurodegeneration and Parkinson's disease. *Age and Ageing*, *39*(2), 156–161. https://doi.org/10.1093/ageing/afp223

Hirsch, E., Graybiel, A. M., & Agid, Y. A. (1988). Melanized dopaminergic neurons are differentially susceptible to degeneration in Parkinson's disease. *Nature*, *334*(6180), 345–348. https://doi.org/10.1038/334345a0

Hitti, F. L., Ramayya, A. G., McShane, B. J., Yang, A. I., Vaughan, K. A., & Baltuch, G. H. (2020). Long-term outcomes following deep brain stimulation for Parkinson's disease. *Journal of Neurosurgery*, *132*(1), 205–210. https://doi.org/10.3171/2018.8.JNS182081

Hong, S., Beja-Glasser, V. F., Nfonoyim, B. M., Frouin, A., Li, S., Ramakrishnan, S., Merry, K. M., Shi, Q., Rosenthal, A., Barres, B. A., Lemere, C. A., Selkoe, D. J., & Stevens, B. (2016). Complement and microglia mediate early synapse loss in Alzheimer mouse models. *Science*, *352*(6286), 712–716. https://doi.org/10.1126/science.aad8373

Hornykiewicz, O. (2001). Chemical neuroanatomy of the basal ganglia--normal and in Parkinson's disease. *Journal of Chemical Neuroanatomy*, *22*(1–2), 3–12. https://doi.org/10.1016/s0891-0618(01)00100-4

Howe, J. W., Sortwell, C. E., Duffy, M. F., Kemp, C. J., Russell, C. P., Kubik, M., Patel, P., Luk, K. C., El-Agnaf, O. M. A., & Patterson, J. R. (2021). Preformed fibrils generated from mouse alpha-synuclein produce more inclusion pathology in rats than fibrils generated from rat alpha-synuclein. *Parkinsonism & Related Disorders*, *89*, 41–47. https://doi.org/10.1016/j.parkreldis.2021.06.010

Iacono, D., Geraci-Erck, M., Rabin, M. L., Adler, C. H., Serrano, G., Beach, T. G., & Kurlan, R. (2015). Parkinson disease and incidental Lewy body disease: Just a question of time? *Neurology*, *85*(19), 1670–1679. https://doi.org/10.1212/WNL.0000000000002102

Ibáñez, P., Bonnet, A. M., Débarges, B., Lohmann, E., Tison, F., Pollak, P., Agid, Y., Dürr, A., & Brice, A. (2004). Causal relation between alpha-synuclein gene duplication and familial Parkinson's disease. *The Lancet*, *364*(9440), 1169–1171. https://doi.org/10.1016/S0140-6736(04)17104-3

Imamura, K., Hishikawa, N., Sawada, M., Nagatsu, T., Yoshida, M., & Hashizume, Y. (2003). Distribution of major histocompatibility complex class II-positive microglia and cytokine profile of Parkinson's disease brains. *Acta Neuropathologica*, *106*(6), 518–526. https://doi.org/10.1007/s00401-003-0766-2

Ishii, T., & Haga, S. (1992). Complements, microglial cells and amyloid fibril formation. *Research in Immunology*, *143*(6), 614–616. https://doi.org/10.1016/0923-2494(92)80043-k

Iwai, A., Masliah, E., Yoshimoto, M., Ge, N., Flanagan, L., de Silva, H. A., Kittel, A., & Saitoh, T. (1995). The precursor protein of non-A beta component of Alzheimer's disease amyloid is a presynaptic protein of the central nervous system. *Neuron*, *14*(2), 467–475. https://doi.org/10.1016/0896-6273(95)90302-x

Izco, M., Blesa, J., Verona, G., Cooper, J. M., & Alvarez-Erviti, L. (2021). Glial activation precedes alpha-synuclein pathology in a mouse model of Parkinson's disease. *Neuroscience Research*, *170*, 330–340. https://doi.org/10.1016/j.neures.2020.11.004

Jagmag, S. A., Tripathi, N., Shukla, S. D., Maiti, S., & Khurana, S. (2015). Evaluation of Models of Parkinson's Disease. *Frontiers in Neuroscience*, *9*, 503. https://doi.org/10.3389/fnins.2015.00503

Jankovic, J. (2008). Parkinson's disease: clinical features and diagnosis. *Journal of Neurology, Neurosurgery, and Psychiatry*, *79*(4), 368–376. https://doi.org/10.1136/jnnp.2007.131045

Jiang, S., Gao, H., Luo, Q., Wang, P., & Yang, X. (2017). The correlation of lymphocyte subsets, natural killer cell, and Parkinson's disease: a meta-analysis. *Neurological Sciences*, *38*(8), 1373–1380. https://doi.org/10.1007/s10072-017-2988-4

Johnson, M. E., & Bobrovskaya, L. (2015). An update on the rotenone models of Parkinson's disease: their ability to reproduce the features of clinical disease and model gene-environment interactions. *Neurotoxicology*, *46*, 101–116. https://doi.org/10.1016/j.neuro.2014.12.002

Kamath, T., Abdulraouf, A., Burris, S. J., Langlieb, J., Gazestani, V., Nadaf, N. M., Balderrama, K., Vanderburg, C., & Macosko, E. Z. (2022). Single-cell genomic profiling of human dopamine neurons identifies a population that selectively degenerates in Parkinson's disease. *Nature Neuroscience*, *25*(5), 588–595. https://doi.org/10.1038/s41593-022-01061-1

Kannarkat, G. T., Cook, D. A., Lee, J. K., Chang, J., Chung, J., Sandy, E., Paul, K. C., Ritz, B., Bronstein, J., Factor, S. A., Boss, J. M., & Tansey, M. G. (2015). Common Genetic Variant Association with Altered HLA Expression, Synergy with Pyrethroid Exposure, and Risk for Parkinson's Disease: An Observational and Case-Control Study. *Npj Parkinson's Disease*, *1*, 15002. https://doi.org/10.1038/npjparkd.2015.2

Kanthasamy, A. G., Kitazawa, M., Kanthasamy, A., & Anantharam, V. (2005). Dieldrin-induced neurotoxicity: relevance to Parkinson's disease pathogenesis. *Neurotoxicology*, *26*(4), 701–719. https://doi.org/10.1016/j.neuro.2004.07.010

Kempermann, G., & Neumann, H. (2003). Neuroscience. Microglia: the enemy within? *Science*, *302*(5651), 1689–1690. https://doi.org/10.1126/science.1092864

Khor, S.-P., & Hsu, A. (2007). The pharmacokinetics and pharmacodynamics of levodopa in the treatment of Parkinson's disease. *Current Clinical Pharmacology*, *2*(3), 234–243.

Kim-Han, J. S., Antenor-Dorsey, J. A., & O'Malley, K. L. (2011). The parkinsonian mimetic, MPP+, specifically impairs mitochondrial transport in dopamine axons. *The*

Journal of Neuroscience, *31*(19), 7212–7221. https://doi.org/10.1523/JNEUROSCI.0711-11.2011

Kim, C., Ho, D.-H., Suk, J.-E., You, S., Michael, S., Kang, J., Joong Lee, S., Masliah, E., Hwang, D., Lee, H.-J., & Lee, S.-J. (2013). Neuron-released oligomeric α-synuclein is an endogenous agonist of TLR2 for paracrine activation of microglia. *Nature Communications*, *4*, 1562. https://doi.org/10.1038/ncomms2534

Kim, J., Shin, S. D., Jeong, S., Suh, G. J., & Kwak, Y. H. (2017). Effect of prohibiting the use of Paraquat on pesticide-associated mortality. *BMC Public Health*, *17*(1), 858. https://doi.org/10.1186/s12889-017-4832-4

Kirik, D., Rosenblad, C., Burger, C., Lundberg, C., Johansen, T. E., Muzyczka, N., Mandel, R. J., & Björklund, A. (2002). Parkinson-like neurodegeneration induced by targeted overexpression of alpha-synuclein in the nigrostriatal system. *The Journal of Neuroscience*, *22*(7), 2780–2791. https://doi.org/10.1523/JNEUROSCI.22-07-02780.2002

Kitada, T., Asakawa, S., Hattori, N., Matsumine, H., Yamamura, Y., Minoshima, S., Yokochi, M., Mizuno, Y., & Shimizu, N. (1998). Mutations in the parkin gene cause autosomal recessive juvenile parkinsonism. *Nature*, *392*(6676), 605–608. https://doi.org/10.1038/33416

Koprich, J. B., Reske-Nielsen, C., Mithal, P., & Isacson, O. (2008). Neuroinflammation mediated by IL-1beta increases susceptibility of dopamine neurons to degeneration in an animal model of Parkinson's disease. *Journal of Neuroinflammation*, *5*, 8. https://doi.org/10.1186/1742-2094-5-8

Kordower, J. H., Olanow, C. W., Dodiya, H. B., Chu, Y., Beach, T. G., Adler, C. H., Halliday, G. M., & Bartus, R. T. (2013). Disease duration and the integrity of the nigrostriatal system in Parkinson's disease. *Brain: A Journal of Neurology*, *136*(Pt 8), 2419–2431. https://doi.org/10.1093/brain/awt192

Krüger, R., Kuhn, W., Müller, T., Woitalla, D., Graeber, M., Kösel, S., Przuntek, H., Epplen, J. T., Schöls, L., & Riess, O. (1998). Ala30Pro mutation in the gene encoding alpha-synuclein in Parkinson's disease. *Nature Genetics*, *18*(2), 106–108. https://doi.org/10.1038/ng0298-106

Kurowska, Z., Kordower, J. H., Stoessl, A. J., Burke, R. E., Brundin, P., Yue, Z., Brady, S. T., Milbrandt, J., Trapp, B. D., Sherer, T. B., & Medicetty, S. (2016). Is axonal degeneration a key early event in parkinson's disease? *Journal of Parkinson's Disease*, *6*(4), 703–707. https://doi.org/10.3233/JPD-160881

Kuusisto, E., Parkkinen, L., & Alafuzoff, I. (2003). Morphogenesis of Lewy bodies: dissimilar incorporation of alpha-synuclein, ubiquitin, and p62. *Journal of*

Neuropathology and Experimental Neurology, *62*(12), 1241–1253. https://doi.org/10.1093/jnen/62.12.1241

Lanciego, J. L., Luquin, N., & Obeso, J. A. (2012). Functional neuroanatomy of the basal ganglia. *Cold Spring Harbor Perspectives in Medicine*, *2*(12), a009621. https://doi.org/10.1101/cshperspect.a009621

Langston, J. W. (2017). The MPTP Story. *Journal of Parkinson's Disease*, *7*(s1), S11–S19. https://doi.org/10.3233/JPD-179006

Lees, A. J., Hardy, J., & Revesz, T. (2009). Parkinson's disease. *The Lancet*, *373*(9680), 2055–2066. https://doi.org/10.1016/S0140-6736(09)60492-X

Liddelow, S. A., Guttenplan, K. A., Clarke, L. E., Bennett, F. C., Bohlen, C. J., Schirmer, L., Bennett, M. L., Münch, A. E., Chung, W.-S., Peterson, T. C., Wilton, D. K., Frouin, A., Napier, B. A., Panicker, N., Kumar, M., Buckwalter, M. S., Rowitch, D. H., Dawson, V. L., Dawson, T. M., … Barres, B. A. (2017). Neurotoxic reactive astrocytes are induced by activated microglia. *Nature*, *541*(7638), 481–487. https://doi.org/10.1038/nature21029

Limousin, P., & Foltynie, T. (2019). Long-term outcomes of deep brain stimulation in Parkinson disease. *Nature Reviews. Neurology*, *15*(4), 234–242. https://doi.org/10.1038/s41582-019-0145-9

Lindestam Arlehamn, C. S., Dhanwani, R., Pham, J., Kuan, R., Frazier, A., Rezende Dutra, J., Phillips, E., Mallal, S., Roederer, M., Marder, K. S., Amara, A. W., Standaert, D. G., Goldman, J. G., Litvan, I., Peters, B., Sulzer, D., & Sette, A. (2020). α-Synuclein-specific T cell reactivity is associated with preclinical and early Parkinson's disease. *Nature Communications*, *11*(1), 1875. https://doi.org/10.1038/s41467-020-15626-w

Lindqvist, D., Hall, S., Surova, Y., Nielsen, H. M., Janelidze, S., Brundin, L., & Hansson, O. (2013). Cerebrospinal fluid inflammatory markers in Parkinson's disease--associations with depression, fatigue, and cognitive impairment. *Brain, Behavior, and Immunity*, *33*, 183–189. https://doi.org/10.1016/j.bbi.2013.07.007

Li, A. H., & Yang, S.-B. (2023). The caveats and setbacks of mouse genome editing tools in biomedical studies. *Gene Reports*, *33*, 101834. https://doi.org/10.1016/j.genrep.2023.101834

Li, X., Sundquist, J., & Sundquist, K. (2012). Subsequent risks of Parkinson disease in patients with autoimmune and related disorders: a nationwide epidemiological study from Sweden. *Neuro-Degenerative Diseases*, *10*(1–4), 277–284. https://doi.org/10.1159/000333222

Lücking, C. B., Dürr, A., Bonifati, V., Vaughan, J., De Michele, G., Gasser, T., Harhangi, B. S., Meco, G., Denèfle, P., Wood, N. W., Agid, Y., Brice, A., French Parkinson's Disease Genetics Study Group, & European Consortium on Genetic Susceptibility in Parkinson's Disease. (2000). Association between early-onset Parkinson's disease and mutations in the parkin gene. *The New England Journal of Medicine*, *342*(21), 1560–1567. https://doi.org/10.1056/NEJM200005253422103

Luk, K. C., Kehm, V., Carroll, J., Zhang, B., O'Brien, P., Trojanowski, J. Q., & Lee, V. M.-Y. (2012). Pathological α-synuclein transmission initiates Parkinson-like neurodegeneration in nontransgenic mice. *Science*, *338*(6109), 949–953. https://doi.org/10.1126/science.1227157

Luk, K. C., Kehm, V. M., Zhang, B., O'Brien, P., Trojanowski, J. Q., & Lee, V. M. Y. (2012). Intracerebral inoculation of pathological α-synuclein initiates a rapidly progressive neurodegenerative α-synucleinopathy in mice. *The Journal of Experimental Medicine*, *209*(5), 975–986. https://doi.org/10.1084/jem.20112457

Lyons, K. E., & Pahwa, R. (2011). The impact and management of nonmotor symptoms of Parkinson's disease. *The American Journal of Managed Care*, *17 Suppl 12*, S308-14.

Mahul-Mellier, A.-L., Burtscher, J., Maharjan, N., Weerens, L., Croisier, M., Kuttler, F., Leleu, M., Knott, G. W., & Lashuel, H. A. (2020). The process of Lewy body formation, rather than simply α-synuclein fibrillization, is one of the major drivers of neurodegeneration. *Proceedings of the National Academy of Sciences of the United States of America*, *117*(9), 4971–4982. https://doi.org/10.1073/pnas.1913904117

Marder, K., Wang, Y., Alcalay, R. N., Mejia-Santana, H., Tang, M.-X., Lee, A., Raymond, D., Mirelman, A., Saunders-Pullman, R., Clark, L., Ozelius, L., Orr-Urtreger, A., Giladi, N., Bressman, S., & LRRK2 Ashkenazi Jewish Consortium. (2015). Age-specific penetrance of LRRK2 G2019S in the Michael J. Fox Ashkenazi Jewish LRRK2 Consortium. *Neurology*, *85*(1), 89–95. https://doi.org/10.1212/WNL.0000000000001708

Marín-Teva, J. L., Dusart, I., Colin, C., Gervais, A., van Rooijen, N., & Mallat, M. (2004). Microglia promote the death of developing Purkinje cells. *Neuron*, *41*(4), 535–547. https://doi.org/10.1016/s0896-6273(04)00069-8

Maroteaux, L., Campanelli, J. T., & Scheller, R. H. (1988). Synuclein: a neuron-specific protein localized to the nucleus and presynaptic nerve terminal. *The Journal of Neuroscience*, *8*(8), 2804–2815. https://doi.org/10.1523/JNEUROSCI.08-08-02804.1988

Martinez, T. N., & Greenamyre, J. T. (2012). Toxin models of mitochondrial dysfunction in Parkinson's disease. *Antioxidants & Redox Signaling*, *16*(9), 920–934. https://doi.org/10.1089/ars.2011.4033

Mathys, H., Adaikkan, C., Gao, F., Young, J. Z., Manet, E., Hemberg, M., De Jager, P. L., Ransohoff, R. M., Regev, A., & Tsai, L.-H. (2017). Temporal Tracking of Microglia Activation in Neurodegeneration at Single-Cell Resolution. *Cell Reports*, *21*(2), 366–380. https://doi.org/10.1016/j.celrep.2017.09.039

McGeer, P. L., Itagaki, S., Boyes, B. E., & McGeer, E. G. (1988). Reactive microglia are positive for HLA-DR in the substantia nigra of Parkinson's and Alzheimer's disease brains. *Neurology*, *38*(8), 1285–1291. https://doi.org/10.1212/wnl.38.8.1285

McGeer, P. L., Itagaki, S., & McGeer, E. G. (1988). Expression of the histocompatibility glycoprotein HLA-DR in neurological disease. *Acta Neuropathologica*, *76*(6), 550–557. https://doi.org/10.1007/BF00689592

Miller, K. M., Mercado, N. M., & Sortwell, C. E. (2021). Synucleinopathy-associated pathogenesis in Parkinson's disease and the potential for brain-derived neurotrophic factor. *Npj Parkinson's Disease*, *7*(1), 35. https://doi.org/10.1038/s41531-021-00179-6

Miller, K. M., Patterson, J. R., Kochmanski, J., Kemp, C. J., Stoll, A. C., Onyekpe, C. U., Cole-Strauss, A., Steece-Collier, K., Howe, J. W., Luk, K. C., & Sortwell, C. E. (2021). Striatal afferent BDNF is disrupted by synucleinopathy and partially restored by STN DBS. *The Journal of Neuroscience*, *41*(9), 2039–2052. https://doi.org/10.1523/JNEUROSCI.1952-20.2020

Mogi, M., Harada, M., Narabayashi, H., Inagaki, H., Minami, M., & Nagatsu, T. (1996). Interleukin (IL)-1 beta, IL-2, IL-4, IL-6 and transforming growth factor-alpha levels are elevated in ventricular cerebrospinal fluid in juvenile parkinsonism and Parkinson's disease. *Neuroscience Letters*, *211*(1), 13–16. https://doi.org/10.1016/0304-3940(96)12706-3

Monje, M. L., Toda, H., & Palmer, T. D. (2003). Inflammatory blockade restores adult hippocampal neurogenesis. *Science*, *302*(5651), 1760–1765. https://doi.org/10.1126/science.1088417

Nagatsu, T., Mogi, M., Ichinose, H., & Togari, A. (2000). Changes in cytokines and neurotrophins in Parkinson's disease. *Journal of Neural Transmission. Supplementum*, *60*, 277–290. https://doi.org/10.1007/978-3-7091-6301-6_19

Nalls, M. A., Pankratz, N., Lill, C. M., Do, C. B., Hernandez, D. G., Saad, M., DeStefano, A. L., Kara, E., Bras, J., Sharma, M., Schulte, C., Keller, M. F., Arepalli, S., Letson, C., Edsall, C., Stefansson, H., Liu, X., Pliner, H., Lee, J. H., … Singleton, A. B. (2014). Large-scale meta-analysis of genome-wide association data identifies six new risk loci for Parkinson's disease. *Nature Genetics*, *46*(9), 989–993. https://doi.org/10.1038/ng.3043

Negrini, M., Tomasello, G., Davidsson, M., Fenyi, A., Adant, C., Hauser, S., Espa, E., Gubinelli, F., Manfredsson, F. P., Melki, R., & Heuer, A. (2022). Sequential or

Simultaneous Injection of Preformed Fibrils and AAV Overexpression of Alpha-Synuclein Are Equipotent in Producing Relevant Pathology and Behavioral Deficits. *Journal of Parkinson's Disease*, *12*(4), 1133–1153. https://doi.org/10.3233/JPD-212555

Nimmerjahn, A., Kirchhoff, F., & Helmchen, F. (2005). Resting microglial cells are highly dynamic surveillants of brain parenchyma in vivo. *Science*, *308*(5726), 1314–1318. https://doi.org/10.1126/science.1110647

Nissl, F. (1904). Zur histopathologie der paralytischen rindenerkrankung. *Histol Histopathol Arb Grosshirn*, *1*.

Ohnmacht, J., May, P., Sinkkonen, L., & Krüger, R. (2020). Missing heritability in Parkinson's disease: the emerging role of non-coding genetic variation. *Journal of Neural Transmission*, *127*(5), 729–748. https://doi.org/10.1007/s00702-020-02184-0

Oliveira, L. M. A., Falomir-Lockhart, L. J., Botelho, M. G., Lin, K. H., Wales, P., Koch, J. C., Gerhardt, E., Taschenberger, H., Outeiro, T. F., Lingor, P., Schüle, B., Arndt-Jovin, D. J., & Jovin, T. M. (2015). Elevated α-synuclein caused by SNCA gene triplication impairs neuronal differentiation and maturation in Parkinson's patient-derived induced pluripotent stem cells. *Cell Death & Disease*, *6*(11), e1994. https://doi.org/10.1038/cddis.2015.318

Osterberg, V. R., Spinelli, K. J., Weston, L. J., Luk, K. C., Woltjer, R. L., & Unni, V. K. (2015). Progressive aggregation of alpha-synuclein and selective degeneration of lewy inclusion-bearing neurons in a mouse model of parkinsonism. *Cell Reports*, *10*(8), 1252–1260. https://doi.org/10.1016/j.celrep.2015.01.060

Ouchi, Y., Yoshikawa, E., Sekine, Y., Futatsubashi, M., Kanno, T., Ogusu, T., & Torizuka, T. (2005). Microglial activation and dopamine terminal loss in early Parkinson's disease. *Annals of Neurology*, *57*(2), 168–175. https://doi.org/10.1002/ana.20338

Ou, Z., Zhou, Y., Wang, L., Xue, L., Zheng, J., Chen, L., & Tong, Q. (2021). NLRP3 Inflammasome Inhibition Prevents α-Synuclein Pathology by Relieving Autophagy Dysfunction in Chronic MPTP-Treated NLRP3 Knockout Mice. *Molecular Neurobiology*, *58*(4), 1303–1311. https://doi.org/10.1007/s12035-020-02198-5

Paakinaho, A., Koponen, M., Tiihonen, M., Kauppi, M., Hartikainen, S., & Tolppanen, A.-M. (2022). Disease-Modifying Antirheumatic Drugs and Risk of Parkinson Disease: Nested Case-Control Study of People With Rheumatoid Arthritis. *Neurology*, *98*(12), e1273–e1281. https://doi.org/10.1212/WNL.0000000000013303

Pahwa, R., Factor, S. A., Lyons, K. E., Ondo, W. G., Gronseth, G., Bronte-Stewart, H., Hallett, M., Miyasaki, J., Stevens, J., Weiner, W. J., & Quality Standards Subcommittee of the American Academy of Neurology. (2006). Practice Parameter:

treatment of Parkinson disease with motor fluctuations and dyskinesia (an evidence-based review): report of the Quality Standards Subcommittee of the American Academy of Neurology. *Neurology*, *66*(7), 983–995. https://doi.org/10.1212/01.wnl.0000215250.82576.87

Parkhurst, C. N., Yang, G., Ninan, I., Savas, J. N., Yates, J. R., Lafaille, J. J., Hempstead, B. L., Littman, D. R., & Gan, W.-B. (2013). Microglia promote learning-dependent synapse formation through brain-derived neurotrophic factor. *Cell*, *155*(7), 1596–1609. https://doi.org/10.1016/j.cell.2013.11.030

Parkinson, J. (2002). An essay on the shaking palsy. 1817. *The Journal of Neuropsychiatry and Clinical Neurosciences*, *14*(2), 223–236; discussion 222. https://doi.org/10.1176/jnp.14.2.223

Patterson, J., Kochmanski, J., Stoll, A., Kubik, M., Kemp, C., Duffy, M., Thompson, K., Howe, J., Cole-Strauss, A., Kuhn, N., Miller, K., Nelson, S., Onyekpe, C., Beck, J., Counts, S., Bernstein, A., Steece-Collier, K., Luk, K., & Sortwell, C. (2024). Transcriptomic Profiling of Early Synucleinopathy in Rats Induced with Preformed Fibrils. *Research Square*. https://doi.org/10.21203/rs.3.rs-3253289/v1

Patterson, J. R., Duffy, M. F., Kemp, C. J., Howe, J. W., Collier, T. J., Stoll, A. C., Miller, K. M., Patel, P., Levine, N., Moore, D. J., Luk, K. C., Fleming, S. M., Kanaan, N. M., Paumier, K. L., El-Agnaf, O. M. A., & Sortwell, C. E. (2019). Time course and magnitude of alpha-synuclein inclusion formation and nigrostriatal degeneration in the rat model of synucleinopathy triggered by intrastriatal α-synuclein preformed fibrils. *Neurobiology of Disease*, *130*, 104525. https://doi.org/10.1016/j.nbd.2019.104525

Paul, K. C., Cockburn, M., Gong, Y., Bronstein, J., & Ritz, B. (2024). Agricultural paraquat dichloride use and Parkinson's disease in California's Central Valley. *International Journal of Epidemiology*, *53*(1). https://doi.org/10.1093/ije/dyae004

Paumier, K. L., Luk, K. C., Manfredsson, F. P., Kanaan, N. M., Lipton, J. W., Collier, T. J., Steece-Collier, K., Kemp, C. J., Celano, S., Schulz, E., Sandoval, I. M., Fleming, S., Dirr, E., Polinski, N. K., Trojanowski, J. Q., Lee, V. M., & Sortwell, C. E. (2015). Intrastriatal injection of pre-formed mouse α-synuclein fibrils into rats triggers α-synuclein pathology and bilateral nigrostriatal degeneration. *Neurobiology of Disease*, *82*, 185–199. https://doi.org/10.1016/j.nbd.2015.06.003

Peiffer, J., & Gehrmann, J. (1995). Ludwig Merzbacher (1875-1942): the man behind the disease. *Brain Pathology*, *5*(3), 311–318. https://doi.org/10.1111/j.1750-3639.1995.tb00608.x

Peng, S.-P., Zhang, Y., Copray, S., Schachner, M., & Shen, Y.-Q. (2017). Participation of perforin in mediating dopaminergic neuron loss in MPTP-induced Parkinson's disease in mice. *Biochemical and Biophysical Research Communications*, *484*(3), 618–622. https://doi.org/10.1016/j.bbrc.2017.01.150

Perry, V. H., Nicoll, J. A. R., & Holmes, C. (2010). Microglia in neurodegenerative disease. *Nature Reviews. Neurology*, *6*(4), 193–201. https://doi.org/10.1038/nrneurol.2010.17

Polinski, N. K., Volpicelli-Daley, L. A., Sortwell, C. E., Luk, K. C., Cremades, N., Gottler, L. M., Froula, J., Duffy, M. F., Lee, V. M. Y., Martinez, T. N., & Dave, K. D. (2018). Best Practices for Generating and Using Alpha-Synuclein Pre-Formed Fibrils to Model Parkinson's Disease in Rodents. *Journal of Parkinson's Disease*, *8*(2), 303–322. https://doi.org/10.3233/JPD-171248

Polymeropoulos, M. H., Lavedan, C., Leroy, E., Ide, S. E., Dehejia, A., Dutra, A., Pike, B., Root, H., Rubenstein, J., Boyer, R., Stenroos, E. S., Chandrasekharappa, S., Athanassiadou, A., Papapetropoulos, T., Johnson, W. G., Lazzarini, A. M., Duvoisin, R. C., Di Iorio, G., Golbe, L. I., & Nussbaum, R. L. (1997). Mutation in the alpha-synuclein gene identified in families with Parkinson's disease. *Science*, *276*(5321), 2045–2047. https://doi.org/10.1126/science.276.5321.2045

Poly, T. N., Islam, M. M. R., Yang, H.-C., & Li, Y.-C. J. (2019). Non-steroidal anti-inflammatory drugs and risk of Parkinson's disease in the elderly population: a meta-analysis. *European Journal of Clinical Pharmacology*, *75*(1), 99–108. https://doi.org/10.1007/s00228-018-2561-y

Pont-Sunyer, C., Hotter, A., Gaig, C., Seppi, K., Compta, Y., Katzenschlager, R., Mas, N., Hofeneder, D., Brücke, T., Bayés, A., Wenzel, K., Infante, J., Zach, H., Pirker, W., Posada, I. J., Álvarez, R., Ispierto, L., De Fàbregues, O., Callén, A., … Tolosa, E. (2015). The onset of nonmotor symptoms in Parkinson's disease (the ONSET PD study). *Movement Disorders*, *30*(2), 229–237. https://doi.org/10.1002/mds.26077

Postuma, R. B., Berg, D., Stern, M., Poewe, W., Olanow, C. W., Oertel, W., Obeso, J., Marek, K., Litvan, I., Lang, A. E., Halliday, G., Goetz, C. G., Gasser, T., Dubois, B., Chan, P., Bloem, B. R., Adler, C. H., & Deuschl, G. (2015). MDS clinical diagnostic criteria for Parkinson's disease. *Movement Disorders*, *30*(12), 1591–1601. https://doi.org/10.1002/mds.26424

Pouchieu, C., Piel, C., Carles, C., Gruber, A., Helmer, C., Tual, S., Marcotullio, E., Lebailly, P., & Baldi, I. (2018). Pesticide use in agriculture and Parkinson's disease in the AGRICAN cohort study. *International Journal of Epidemiology*, *47*(1), 299–310. https://doi.org/10.1093/ije/dyx225

Pringsheim, T., Jette, N., Frolkis, A., & Steeves, T. D. L. (2014). The prevalence of Parkinson's disease: a systematic review and meta-analysis. *Movement Disorders*, *29*(13), 1583–1590. https://doi.org/10.1002/mds.25945

Prinz, M., Jung, S., & Priller, J. (2019). Microglia biology: one century of evolving concepts. *Cell*, *179*(2), 292–311. https://doi.org/10.1016/j.cell.2019.08.053

Qin, X.-Y., Zhang, S.-P., Cao, C., Loh, Y. P., & Cheng, Y. (2016). Aberrations in Peripheral Inflammatory Cytokine Levels in Parkinson Disease: A Systematic Review and Meta-analysis. *JAMA Neurology*, *73*(11), 1316–1324. https://doi.org/10.1001/jamaneurol.2016.2742

Rahman, A. A., & Morrison, B. E. (2019). Contributions of VPS35 mutations to parkinson's disease. *Neuroscience*, *401*, 1–10. https://doi.org/10.1016/j.neuroscience.2019.01.006

Redgrave, P., Rodriguez, M., Smith, Y., Rodriguez-Oroz, M. C., Lehericy, S., Bergman, H., Agid, Y., DeLong, M. R., & Obeso, J. A. (2010). Goal-directed and habitual control in the basal ganglia: implications for Parkinson's disease. *Nature Reviews. Neuroscience*, *11*(11), 760–772. https://doi.org/10.1038/nrn2915

Ren, L., Yi, J., Yang, J., Li, P., Cheng, X., & Mao, P. (2018). Nonsteroidal anti-inflammatory drugs use and risk of Parkinson disease: A dose-response meta-analysis. *Medicine*, *97*(37), e12172. https://doi.org/10.1097/MD.0000000000012172

Río Hortega, P. (1919a). El "Tercer Elemento" de los centros nerviosos I. La microglia en estado normal. *Boletín de La Sociedad Española de Biología*, *III*, 67–82.

Río Hortega, P. (1919b). El "Tercer Elemento" de los centros nerviosos IV. Poder fagocitario y movilidad de la microglia. *Boletín de La Sociedad Española de Biología*, *III*, 154–166.

Ritz, B., Lee, P.-C., Hansen, J., Lassen, C. F., Ketzel, M., Sørensen, M., & Raaschou-Nielsen, O. (2016). Traffic-Related Air Pollution and Parkinson's Disease in Denmark: A Case-Control Study. *Environmental Health Perspectives*, *124*(3), 351–356. https://doi.org/10.1289/ehp.1409313

Robertson, D. R., & Smith-Vaniz, W. F. (2008). Rotenone: an essential but demonized tool for assessing marine fish diversity. *Bioscience*, *58*(2), 165–170. https://doi.org/10.1641/B580211

Rock, K. L., Reits, E., & Neefjes, J. (2016). Present yourself! by MHC class I and MHC class II molecules. *Trends in Immunology*, *37*(11), 724–737. https://doi.org/10.1016/j.it.2016.08.010

Ross, O. A., Toft, M., Whittle, A. J., Johnson, J. L., Papapetropoulos, S., Mash, D. C., Litvan, I., Gordon, M. F., Wszolek, Z. K., Farrer, M. J., & Dickson, D. W. (2006). Lrrk2 and Lewy body disease. *Annals of Neurology*, *59*(2), 388–393. https://doi.org/10.1002/ana.20731

Sanchez-Guajardo, V., Febbraro, F., Kirik, D., & Romero-Ramos, M. (2010). Microglia acquire distinct activation profiles depending on the degree of alpha-synuclein

neuropathology in a rAAV based model of Parkinson's disease. *Plos One*, *5*(1), e8784. https://doi.org/10.1371/journal.pone.0008784

Sauer, H., & Oertel, W. H. (1994). Progressive degeneration of nigrostriatal dopamine neurons following intrastriatal terminal lesions with 6-hydroxydopamine: a combined retrograde tracing and immunocytochemical study in the rat. *Neuroscience*, *59*(2), 401–415. https://doi.org/10.1016/0306-4522(94)90605-x

Saunders-Pullman, R., Gordon-Elliott, J., Parides, M., Fahn, S., Saunders, H. R., & Bressman, S. (1999). The effect of estrogen replacement on early Parkinson's disease. *Neurology*, *52*(7), 1417–1421. https://doi.org/10.1212/wnl.52.7.1417

Savitz, S. I., & Cox, C. S. (2016). Concise review: cell therapies for stroke and traumatic brain injury: targeting microglia. *Stem Cells*, *34*(3), 537–542. https://doi.org/10.1002/stem.2253

Schafer, D. P., Lehrman, E. K., Kautzman, A. G., Koyama, R., Mardinly, A. R., Yamasaki, R., Ransohoff, R. M., Greenberg, M. E., Barres, B. A., & Stevens, B. (2012). Microglia sculpt postnatal neural circuits in an activity and complement-dependent manner. *Neuron*, *74*(4), 691–705. https://doi.org/10.1016/j.neuron.2012.03.026

Schonhoff, A. M., Figge, D. A., Williams, G. P., Jurkuvenaite, A., Gallups, N. J., Childers, G. M., Webster, J. M., Standaert, D. G., Goldman, J. E., & Harms, A. S. (2023). Border-associated macrophages mediate the neuroinflammatory response in an alpha-synuclein model of Parkinson disease. *Nature Communications*, *14*(1), 3754. https://doi.org/10.1038/s41467-023-39060-w

Seifert, K. D., & Wiener, J. I. (2013). The impact of DaTscan on the diagnosis and management of movement disorders: A retrospective study. *American Journal of Neurodegenerative Disease*, *2*(1), 29–34.

Shahmoradian, S. H., Lewis, A. J., Genoud, C., Hench, J., Moors, T. E., Navarro, P. P., Castaño-Díez, D., Schweighauser, G., Graff-Meyer, A., Goldie, K. N., Sütterlin, R., Huisman, E., Ingrassia, A., Gier, Y. de, Rozemuller, A. J. M., Wang, J., Paepe, A. D., Erny, J., Staempfli, A., … Lauer, M. E. (2019). Lewy pathology in Parkinson's disease consists of crowded organelles and lipid membranes. *Nature Neuroscience*, *22*(7), 1099–1109. https://doi.org/10.1038/s41593-019-0423-2

Shimozawa, A., Ono, M., Takahara, D., Tarutani, A., Imura, S., Masuda-Suzukake, M., Higuchi, M., Yanai, K., Hisanaga, S.-I., & Hasegawa, M. (2017). Propagation of pathological α-synuclein in marmoset brain. *Acta Neuropathologica Communications*, *5*(1), 12. https://doi.org/10.1186/s40478-017-0413-0

Shults, C. W. (2006). Lewy bodies. *Proceedings of the National Academy of Sciences of the United States of America*, *103*(6), 1661–1668. https://doi.org/10.1073/pnas.0509567103

Siderowf, A., Concha-Marambio, L., Lafontant, D.-E., Farris, C. M., Ma, Y., Urenia, P. A., Nguyen, H., Alcalay, R. N., Chahine, L. M., Foroud, T., Galasko, D., Kieburtz, K., Merchant, K., Mollenhauer, B., Poston, K. L., Seibyl, J., Simuni, T., Tanner, C. M., Weintraub, D., … Parkinson's Progression Markers Initiative. (2023). Assessment of heterogeneity among participants in the Parkinson's Progression Markers Initiative cohort using α-synuclein seed amplification: a cross-sectional study. *Lancet Neurology*, *22*(5), 407–417. https://doi.org/10.1016/S1474-4422(23)00109-6

Sierra, A., de Castro, F., Del Río-Hortega, J., Rafael Iglesias-Rozas, J., Garrosa, M., & Kettenmann, H. (2016). The "Big-Bang" for modern glial biology: Translation and comments on Pío del Río-Hortega 1919 series of papers on microglia. *Glia*, *64*(11), 1801–1840. https://doi.org/10.1002/glia.23046

Sierra, A., Encinas, J. M., Deudero, J. J. P., Chancey, J. H., Enikolopov, G., Overstreet-Wadiche, L. S., Tsirka, S. E., & Maletic-Savatic, M. (2010). Microglia shape adult hippocampal neurogenesis through apoptosis-coupled phagocytosis. *Cell Stem Cell*, *7*(4), 483–495. https://doi.org/10.1016/j.stem.2010.08.014

Sierra, A., Paolicelli, R. C., & Kettenmann, H. (2019). Cien años de microglía: milestones in a century of microglial research. *Trends in Neurosciences*, *42*(11), 778–792. https://doi.org/10.1016/j.tins.2019.09.004

Singleton, A. B., Farrer, M., Johnson, J., Singleton, A., Hague, S., Kachergus, J., Hulihan, M., Peuralinna, T., Dutra, A., Nussbaum, R., Lincoln, S., Crawley, A., Hanson, M., Maraganore, D., Adler, C., Cookson, M. R., Muenter, M., Baptista, M., Miller, D., … Gwinn-Hardy, K. (2003). alpha-Synuclein locus triplication causes Parkinson's disease. *Science*, *302*(5646), 841. https://doi.org/10.1126/science.1090278

Smajić, S., Prada-Medina, C. A., Landoulsi, Z., Ghelfi, J., Delcambre, S., Dietrich, C., Jarazo, J., Henck, J., Balachandran, S., Pachchek, S., Morris, C. M., Antony, P., Timmermann, B., Sauer, S., Pereira, S. L., Schwamborn, J. C., May, P., Grünewald, A., & Spielmann, M. (2022). Single-cell sequencing of human midbrain reveals glial activation and a Parkinson-specific neuronal state. *Brain: A Journal of Neurology*, *145*(3), 964–978. https://doi.org/10.1093/brain/awab446

Solch, R. J., Aigbogun, J. O., Voyiadjis, A. G., Talkington, G. M., Darensbourg, R. M., O'Connell, S., Pickett, K. M., Perez, S. R., & Maraganore, D. M. (2022). Mediterranean diet adherence, gut microbiota, and Alzheimer's or Parkinson's disease risk: A systematic review. *Journal of the Neurological Sciences*, *434*, 120166. https://doi.org/10.1016/j.jns.2022.120166

Soloway, S. B. (1976). Naturally occurring insecticides. *Environmental Health Perspectives*, *14*, 109–117. https://doi.org/10.1289/ehp.7614109

Sossi, V., Patterson, J. R., McCormick, S., Kemp, C. J., Miller, K. M., Stoll, A. C., Kuhn, N., Kubik, M., Kochmanski, J., Luk, K. C., & Sortwell, C. E. (2022). Dopaminergic Positron Emission Tomography Imaging in the Alpha-Synuclein Preformed Fibril Model Reveals Similarities to Early Parkinson's Disease. *Movement Disorders*, *37*(8), 1739–1748. https://doi.org/10.1002/mds.29051

Spieles-Engemann, A. L., Collier, T. J., & Sortwell, C. E. (2010). A functionally relevant and long-term model of deep brain stimulation of the rat subthalamic nucleus: advantages and considerations. *The European Journal of Neuroscience*, *32*(7), 1092–1099. https://doi.org/10.1111/j.1460-9568.2010.07416.x

Spillantini, M. G., Crowther, R. A., Jakes, R., Hasegawa, M., & Goedert, M. (1998). alpha-Synuclein in filamentous inclusions of Lewy bodies from Parkinson's disease and dementia with lewy bodies. *Proceedings of the National Academy of Sciences of the United States of America*, *95*(11), 6469–6473. https://doi.org/10.1073/pnas.95.11.6469

Spillantini, M. G., Schmidt, M. L., Lee, V. M., Trojanowski, J. Q., Jakes, R., & Goedert, M. (1997). Alpha-synuclein in Lewy bodies. *Nature*, *388*(6645), 839–840. https://doi.org/10.1038/42166

Spivey, A. (2011). Rotenone and paraquat linked to Parkinson's disease: human exposure study supports years of animal studies. *Environmental Health Perspectives*, *119*(6), A259. https://doi.org/10.1289/ehp.119-a259a

Squarzoni, P., Oller, G., Hoeffel, G., Pont-Lezica, L., Rostaing, P., Low, D., Bessis, A., Ginhoux, F., & Garel, S. (2014). Microglia modulate wiring of the embryonic forebrain. *Cell Reports*, *8*(5), 1271–1279. https://doi.org/10.1016/j.celrep.2014.07.042

Steece-Collier, K., Stancati, J. A., Collier, N. J., Sandoval, I. M., Mercado, N. M., Sortwell, C. E., Collier, T. J., & Manfredsson, F. P. (2019). Genetic silencing of striatal CaV1.3 prevents and ameliorates levodopa dyskinesia. *Movement Disorders*, *34*(5), 697–707. https://doi.org/10.1002/mds.27695

Stefanis, L. (2012). α-Synuclein in Parkinson's disease. *Cold Spring Harbor Perspectives in Medicine*, *2*(2), a009399. https://doi.org/10.1101/cshperspect.a009399

Steiner, J. A., Angot, E., & Brundin, P. (2011). A deadly spread: cellular mechanisms of α-synuclein transfer. *Cell Death and Differentiation*, *18*(9), 1425–1433. https://doi.org/10.1038/cdd.2011.53

Stevens, B., Allen, N. J., Vazquez, L. E., Howell, G. R., Christopherson, K. S., Nouri, N., Micheva, K. D., Mehalow, A. K., Huberman, A. D., Stafford, B., Sher, A., Litke, A. M., Lambris, J. D., Smith, S. J., John, S. W. M., & Barres, B. A. (2007). The classical complement cascade mediates CNS synapse elimination. *Cell*, *131*(6), 1164–1178. https://doi.org/10.1016/j.cell.2007.10.036

Stoll, A. C., Kemp, C. J., Patterson, J. R., Howe, J. W., Steece-Collier, K., Luk, K. C., Sortwell, C. E., & Benskey, M. J. (2024). Neuroinflammatory gene expression profiles of reactive glia in the substantia nigra suggest a multidimensional immune response to alpha synuclein inclusions. *Neurobiology of Disease*, *191*, 106411. https://doi.org/10.1016/j.nbd.2024.106411

Stoll, A. C., Kemp, C. J., Patterson, J. R., Kubik, M., Kuhn, N., Benskey, M., Duffy, M. F., Luk, K. C., & Sortwell, C. E. (2024). Alpha-synuclein inclusion responsive microglia are resistant to CSF1R inhibition. *Journal of Neuroinflammation*, *21*(1), 108. https://doi.org/10.1186/s12974-024-03108-5

Stoll, A. C., & Sortwell, C. E. (2022). Leveraging the preformed fibril model to distinguish between alpha-synuclein inclusion- and nigrostriatal degeneration-associated immunogenicity. *Neurobiology of Disease*, *171*, 105804. https://doi.org/10.1016/j.nbd.2022.105804

Stoyka, L. E., Arrant, A. E., Thrasher, D. R., Russell, D. L., Freire, J., Mahoney, C. L., Narayanan, A., Dib, A. G., Standaert, D. G., & Volpicelli-Daley, L. A. (2020). Behavioral defects associated with amygdala and cortical dysfunction in mice with seeded α-synuclein inclusions. *Neurobiology of Disease*, *134*, 104708. https://doi.org/10.1016/j.nbd.2019.104708

Strijks, E., Kremer, J. A., & Horstink, M. W. (1999). Effects of female sex steroids on Parkinson's disease in postmenopausal women. *Clinical Neuropharmacology*, *22*(2), 93–97. https://doi.org/10.1097/00002826-199903000-00005

Tanner, C. M., Kamel, F., Ross, G. W., Hoppin, J. A., Goldman, S. M., Korell, M., Marras, C., Bhudhikanok, G. S., Kasten, M., Chade, A. R., Comyns, K., Richards, M. B., Meng, C., Priestley, B., Fernandez, H. H., Cambi, F., Umbach, D. M., Blair, A., Sandler, D. P., & Langston, J. W. (2011). Rotenone, paraquat, and Parkinson's disease. *Environmental Health Perspectives*, *119*(6), 866–872. https://doi.org/10.1289/ehp.1002839

Tanner, C. M., Ross, G. W., Jewell, S. A., Hauser, R. A., Jankovic, J., Factor, S. A., Bressman, S., Deligtisch, A., Marras, C., Lyons, K. E., Bhudhikanok, G. S., Roucoux, D. F., Meng, C., Abbott, R. D., & Langston, J. W. (2009). Occupation and risk of parkinsonism: a multicenter case-control study. *Archives of Neurology*, *66*(9), 1106–1113. https://doi.org/10.1001/archneurol.2009.195

Tansey, M. G., Wallings, R. L., Houser, M. C., Herrick, M. K., Keating, C. E., & Joers, V. (2022). Inflammation and immune dysfunction in Parkinson disease. *Nature Reviews. Immunology*, *22*(11), 657–673. https://doi.org/10.1038/s41577-022-00684-6

Tan, E.-K., Chao, Y.-X., West, A., Chan, L.-L., Poewe, W., & Jankovic, J. (2020). Parkinson disease and the immune system - associations, mechanisms and therapeutics. *Nature Reviews. Neurology*, *16*(6), 303–318. https://doi.org/10.1038/s41582-020-0344-4

Thakur, P., Breger, L. S., Lundblad, M., Wan, O. W., Mattsson, B., Luk, K. C., Lee, V. M. Y., Trojanowski, J. Q., & Björklund, A. (2017). Modeling Parkinson's disease pathology by combination of fibril seeds and α-synuclein overexpression in the rat brain. *Proceedings of the National Academy of Sciences of the United States of America*, *114*(39), E8284–E8293. https://doi.org/10.1073/pnas.1710442114

Theodore, S., Cao, S., McLean, P. J., & Standaert, D. G. (2008). Targeted overexpression of human alpha-synuclein triggers microglial activation and an adaptive immune response in a mouse model of Parkinson disease. *Journal of Neuropathology and Experimental Neurology*, *67*(12), 1149–1158. https://doi.org/10.1097/NEN.0b013e31818e5e99

Thiery, J., & Lieberman, J. (2014). Perforin: a key pore-forming protein for immune control of viruses and cancer. *Sub-Cellular Biochemistry*, *80*, 197–220. https://doi.org/10.1007/978-94-017-8881-6_10

Thomsen, M. B., Ferreira, S. A., Schacht, A. C., Jacobsen, J., Simonsen, M., Betzer, C., Jensen, P. H., Brooks, D. J., Landau, A. M., & Romero-Ramos, M. (2021). PET imaging reveals early and progressive dopaminergic deficits after intra-striatal injection of preformed alpha-synuclein fibrils in rats. *Neurobiology of Disease*, *149*, 105229. https://doi.org/10.1016/j.nbd.2020.105229

Tremblay, M.-È., Lowery, R. L., & Majewska, A. K. (2010). Microglial interactions with synapses are modulated by visual experience. *PLoS Biology*, *8*(11), e1000527. https://doi.org/10.1371/journal.pbio.1000527

Trempe, J.-F., & Fon, E. A. (2013). Structure and Function of Parkin, PINK1, and DJ-1, the Three Musketeers of Neuroprotection. *Frontiers in Neurology*, *4*, 38. https://doi.org/10.3389/fneur.2013.00038

Ueno, M., Fujita, Y., Tanaka, T., Nakamura, Y., Kikuta, J., Ishii, M., & Yamashita, T. (2013). Layer V cortical neurons require microglial support for survival during postnatal development. *Nature Neuroscience*, *16*(5), 543–551. https://doi.org/10.1038/nn.3358

Ungerstedt, U. (1968). 6-Hydroxy-dopamine induced degeneration of central monoamine neurons. *European Journal of Pharmacology*, *5*(1), 107–110. https://doi.org/10.1016/0014-2999(68)90164-7

Vilariño-Güell, C., Wider, C., Ross, O. A., Dachsel, J. C., Kachergus, J. M., Lincoln, S. J., Soto-Ortolaza, A. I., Cobb, S. A., Wilhoite, G. J., Bacon, J. A., Behrouz, B., Melrose, H. L., Hentati, E., Puschmann, A., Evans, D. M., Conibear, E., Wasserman, W. W., Aasly, J. O., Burkhard, P. R., … Farrer, M. J. (2011). VPS35 mutations in Parkinson disease. *American Journal of Human Genetics*, *89*(1), 162–167. https://doi.org/10.1016/j.ajhg.2011.06.001

Volpicelli-Daley, L. A., Kirik, D., Stoyka, L. E., Standaert, D. G., & Harms, A. S. (2016). How can rAAV-α-synuclein and the fibril α-synuclein models advance our understanding of Parkinson's disease? *Journal of Neurochemistry*, *139 Suppl 1*(Suppl 1), 131–155. https://doi.org/10.1111/jnc.13627

Volpicelli-Daley, L. A., Luk, K. C., Patel, T. P., Tanik, S. A., Riddle, D. M., Stieber, A., Meaney, D. F., Trojanowski, J. Q., & Lee, V. M.-Y. (2011). Exogenous α-synuclein fibrils induce Lewy body pathology leading to synaptic dysfunction and neuron death. *Neuron*, *72*(1), 57–71. https://doi.org/10.1016/j.neuron.2011.08.033

Wahner, A. D., Bronstein, J. M., Bordelon, Y. M., & Ritz, B. (2007). Nonsteroidal anti-inflammatory drugs may protect against Parkinson disease. *Neurology*, *69*(19), 1836–1842. https://doi.org/10.1212/01.wnl.0000279519.99344.ad

Wakabayashi, K., Tanji, K., Odagiri, S., Miki, Y., Mori, F., & Takahashi, H. (2013). The Lewy body in Parkinson's disease and related neurodegenerative disorders. *Molecular Neurobiology*, *47*(2), 495–508. https://doi.org/10.1007/s12035-012-8280-y

Wake, H., Moorhouse, A. J., Jinno, S., Kohsaka, S., & Nabekura, J. (2009). Resting microglia directly monitor the functional state of synapses in vivo and determine the fate of ischemic terminals. *The Journal of Neuroscience*, *29*(13), 3974–3980. https://doi.org/10.1523/JNEUROSCI.4363-08.2009

Wang, Yaming, Szretter, K. J., Vermi, W., Gilfillan, S., Rossini, C., Cella, M., Barrow, A. D., Diamond, M. S., & Colonna, M. (2012). IL-34 is a tissue-restricted ligand of CSF1R required for the development of Langerhans cells and microglia. *Nature Immunology*, *13*(8), 753–760. https://doi.org/10.1038/ni.2360

Wang, Yijun, Gao, X., Hong, B., Jia, C., & Gao, S. (2008). Brain-computer interfaces based on visual evoked potentials. *IEEE Engineering in Medicine and Biology Magazine*, *27*(5), 64–71. https://doi.org/10.1109/MEMB.2008.923958

Weinreb, P. H., Zhen, W., Poon, A. W., Conway, K. A., & Lansbury, P. T. (1996). NACP, a protein implicated in Alzheimer's disease and learning, is natively unfolded. *Biochemistry*, *35*(43), 13709–13715. https://doi.org/10.1021/bi961799n

Witoelar, A., Jansen, I. E., Wang, Y., Desikan, R. S., Gibbs, J. R., Blauwendraat, C., Thompson, W. K., Hernandez, D. G., Djurovic, S., Schork, A. J., Bettella, F., Ellinghaus, D., Franke, A., Lie, B. A., McEvoy, L. K., Karlsen, T. H., Lesage, S., Morris, H. R., Brice, A., … International Parkinson's Disease Genomics Consortium (IPDGC), North American Brain Expression Consortium (NABEC), and United Kingdom Brain Expression Consortium (UKBEC) Investigators. (2017). Genome-wide Pleiotropy Between Parkinson Disease and Autoimmune Diseases. *JAMA Neurology*, *74*(7), 780–792. https://doi.org/10.1001/jamaneurol.2017.0469

Wolf, S. A., Boddeke, H. W. G. M., & Kettenmann, H. (2017). Microglia in physiology and disease. *Annual Review of Physiology*, *79*, 619–643. https://doi.org/10.1146/annurev-physiol-022516-034406

Wright Willis, A., Evanoff, B. A., Lian, M., Criswell, S. R., & Racette, B. A. (2010). Geographic and ethnic variation in Parkinson disease: a population-based study of US Medicare beneficiaries. *Neuroepidemiology*, *34*(3), 143–151. https://doi.org/10.1159/000275491

Yang, F., Johansson, A. L. V., Pedersen, N. L., Fang, F., Gatz, M., & Wirdefeldt, K. (2016). Socioeconomic status in relation to Parkinson's disease risk and mortality: A population-based prospective study. *Medicine*, *95*(30), e4337. https://doi.org/10.1097/MD.0000000000004337

Yang, W., Hamilton, J. L., Kopil, C., Beck, J. C., Tanner, C. M., Albin, R. L., Ray Dorsey, E., Dahodwala, N., Cintina, I., Hogan, P., & Thompson, T. (2020). Current and projected future economic burden of Parkinson's disease in the U.S. *Npj Parkinson's Disease*, *6*, 15. https://doi.org/10.1038/s41531-020-0117-1

Zárate, S., Stevnsner, T., & Gredilla, R. (2017). Role of estrogen and other sex hormones in brain aging. neuroprotection and DNA repair. *Frontiers in Aging Neuroscience*, *9*, 430. https://doi.org/10.3389/fnagi.2017.00430

Zarranz, J. J., Alegre, J., Gómez-Esteban, J. C., Lezcano, E., Ros, R., Ampuero, I., Vidal, L., Hoenicka, J., Rodriguez, O., Atarés, B., Llorens, V., Gomez Tortosa, E., del Ser, T., Muñoz, D. G., & de Yebenes, J. G. (2004). The new mutation, E46K, of alpha-synuclein causes Parkinson and Lewy body dementia. *Annals of Neurology*, *55*(2), 164–173. https://doi.org/10.1002/ana.10795

Zhang, D., Li, S., Hou, L., Jing, L., Ruan, Z., Peng, B., Zhang, X., Hong, J.-S., Zhao, J., & Wang, Q. (2021). Microglial activation contributes to cognitive impairments in rotenone-induced mouse Parkinson's disease model. *Journal of Neuroinflammation*, *18*(1), 4. https://doi.org/10.1186/s12974-020-02065-z

Zhang, Y., Lian, L., Fu, R., Liu, J., Shan, X., Jin, Y., & Xu, S. (2022). Microglia: the hub of intercellular communication in ischemic stroke. *Frontiers in Cellular Neuroscience*, *16*, 889442. https://doi.org/10.3389/fncel.2022.889442

Zhao, J., Zhang, W., Wu, T., Wang, H., Mao, J., Liu, J., Zhou, Z., Lin, X., Yan, H., & Wang, Q. (2021). Efferocytosis in the central nervous system. *Frontiers in Cell and Developmental Biology*, *9*, 773344. https://doi.org/10.3389/fcell.2021.773344

Zimprich, A., Biskup, S., Leitner, P., Lichtner, P., Farrer, M., Lincoln, S., Kachergus, J., Hulihan, M., Uitti, R. J., Calne, D. B., Stoessl, A. J., Pfeiffer, R. F., Patenge, N., Carbajal, I. C., Vieregge, P., Asmus, F., Müller-Myhsok, B., Dickson, D. W., Meitinger, T., … Gasser, T. (2004). Mutations in LRRK2 cause autosomal-dominant parkinsonism with pleomorphic pathology. *Neuron*, *44*(4), 601–607. https://doi.org/10.1016/j.neuron.2004.11.005

CHAPTER 2: TRANSCRIPTOMIC ALTERATIONS IN THE SUBSTANTIA NIGRA ASSOCIATED WITH EARLY AND MATURE LEWY BODY-LIKE INCLUSIONS – FOCUS ON NEUROINFLAMMATORY SIGNALING

INTRODUCTION

Insights into the inflammatory processes triggered by the formation of Lewy bodies (LBs) may provide targets for therapeutic intervention. The rat alpha-synuclein preformed fibril (α-Syn PFF) model allows for examination of inflammatory responses to LB-like inclusions separate from responses associated with degeneration. In the rat α-Syn PFF model a peak of phosphorylated α-Syn (pSyn) accumulation is observed in the substantia nigra pars compacta (SNpc) between one to two months after surgery. Previous studies in my lab have focused on the two-month time point to investigate the response of SNpc neurons to inclusions and the functional phenotype of pSyn inclusion responsive microglia (J. Patterson et al., 2024; Stoll & Sortwell, 2022; Stoll, Kemp, Patterson, Howe, et al., 2024; Stoll, Kemp, Patterson, Kubik, et al., 2024). The two-month time point was chosen due to our initial observation that microglial major histocompatibility complex class-II (MHC-II) expression is not detectable via immunohistochemistry until this time (Duffy et al., 2018). However, an equivalent pSyn inclusion load is observed one month prior, and MHC-II expression represents only one facet of microglial reactivity. Previous work conducted in a mouse model of Alzheimer's disease (AD) featuring amyloid beta (Aß) deposition demonstrates distinct early versus late-stage microglial response genes (Mathys et al., 2017). Interestingly, the upregulation of *Cd74*, a protein associated with the formation of the MHC-II complex, was categorized as a late-stage response gene. What remains unknown is whether the inflammatory response to pSyn inclusions is similarly dynamic.

In vitro studies suggest pSyn aggregates mature over weeks to become more LB-like, with maturation of inclusions associated with increasing percentages of other

proteins, membranous structures and organelles, and that mature LB-like inclusions are associated with cell death signaling pathways (Mahul-Mellier et al., 2020). The concept that pSyn inclusions continue to mature in the SNpc between one and two months in the rat PFF model is supported by our observation that a greater percentage of fibrillar α-Syn is present at two months compared to one month (Duffy et al., 2018; J. R. Patterson, Duffy, et al., 2019). This suggests that comparisons between the one-month and two-month time point may provide insights into inflammatory responses specifically associated with LB formation, inflammatory responses that may contribute to degeneration.

In the experiments undertaken in this chapter I will use ribonucleic acid sequencing (RNA-Seq) to compare and contrast the transcriptomic profile of the pSyn inclusion bearing SNpc at one and two months following intrastriatal PFF injection to rats. Direct comparisons in total differentially expressed genes (DEGs), as well as Kyoto Encyclopedia of Genes and Genomes (KEGG) and Gene Ontology (GO) enrichment analyses were made to understand functional pathways and biological processes associated with both time points or unique to one or two months.

METHODS

Experimental Subjects

All rats used were housed 2-3 to a cage in a room with a 12-H light/dark cycle and were provided food ad libitum. All animal work was performed inside the Michigan State Research Center vivarium in Grand Rapids, MI, a facility accredited by the Association for Assessment and Accreditation of Laboratory Animal Care (AAALAC). All procedures were conducted in accordance with the Institute for Animal Care and Use

Committee (IACUC) at Michigan State University. Male 5-month-old Sprague hTH-EGFP rats were purchased from Taconic Biosciences (Taconic #12141; NTac:SD-TG) (TH-EGFP) 24Xen). hTH-EGFP rats express an enhanced green fluorescent protein (EGFP) transgene driven by a human tyrosine hydroxylase (TH) promoter inserted onto the X chromosome, allowing for the identification of TH expressing cells. Breeding colonies were established to produce hemizygous transgene expressing males to be used for laser capture microdissection. A total of 37 five month old hemizygous males were used (J. Patterson et al., 2024).

α-Syn Preformed Fibrils (PFFs) preparation and size validation

PFFs were generated from wild-type, full length, recombinant mouse α-syn monomers as previously described (Luk et al., 2012; J. R. Patterson, Duffy, et al., 2019; Polinski et al., 2018; Volpicelli-Daley et al., 2011). Prior to use, quality control assessments were performed *in-vitro* to assess amyloid structure (Thioflavin T assay), pelletability (sedimentation assay), structure (electron microscopy), and endotoxin levels (Limulus amebocyte lysate assay; <0.5 endotoxin units/mg of total protein); and *in vivo* to confirm seeding efficiency. For surgery, monomers were diluted to 4 µg/µL with sterile Delbucco's Phosphate-Buffered Saline (dPBS) and centrifuged at 15,000 x g for 30 min. at 4°C. During surgery monomers were kept on wet ice. Centrifugation and storage on ice limits the presence/formation of oligomers. To prepare PFFs for surgeries, PFFs were diluted to 4 µg/µL in sterile Delbecco's PBS (PBS) and sonicated at room temperature using an ultrasonic homogenizer (Q125 Sonicator; Qsonica, newtown, CT); amplitude 30%, 60, 1s pulses with 1s between pulses (J. R. Patterson, Polinski, et al., 2019). Aliquots of sonicated PFFs were imaged via transmission electron microscopy,

and fibril lengths were measured using ImageJ (Schneider et al., 2012). Fibril length distribution ranged from 14.1 to 78.2 nm, with an average size of 39.1 ± 0.5 nm and 95.9% of sonicated PFFs measured were ≤60 nm (Figure 2.1B). Notably, the average size is ≤50 nm, which has been determined to be the optimal size for fibril uptake (Abdelmotilib et al., 2017; Tarutani et al., 2016).

Stereotaxic Surgeries

hTH-EGFP rats received 16μg of PFFs or α-Syn monomer (4 μg/μl, 2x2 μl injections), or an equal volume Dulbecco's Phosphate-Buffered Saline (dPBS) vehicle as previously described (J. Patterson et al., 2024; J. R. Patterson, Duffy, et al., 2019). Rats were anesthetized with isoflurane and received unilateral intrastriatal injections of preformed fibrils (AP + 1.0, ML + 2.0, DV - 4.0; AP + 0.1, ML + 4.2, DV - 5.0). AP and ML coordinates were measured from bregma, and DV coordinates were measured from dura. These PFF coordinates result in > 90% of α-syn inclusions forming in the SNpc, with minimal inclusions forming in the VTA (Polinski et al., 2018). Injections were delivered using a pulled glass needle attached to a 10 μl Hamilton syringe with a flow rate of 0.5 μl min^{-1}. Needles remained in place for 1 minute following injection, retracted 0.5 μl and remained in place for an additional 2 minutes to prevent possible backflow. Following surgeries, rats received an injection of buprenorphine (1.2 mg / k^{-1}) and monitored until day 30 (1 month post injection) or day 60 (2 months post injection). Surgeries for each treatment group were completed within three hours. Final surgical groups for the one-month time point: PBS n=6, monomer n=10, PFF n=10. Final surgical groups for the two-month time point: PBS n=6, PFF n=10 (J. Patterson et al., 2024).

Tissue Collection

Rats were euthanized with an overdose of pentobarbital (Beuthanasia-D Special, Merck Animal Health; 30 mg/kg) and perfused intracardially with ~150mL of cold heparinized saline (0.9%, 10,000 units per liter). Brains were removed and transferred to a chilled brain matrix, the frontal cortex rostral to the corpus callosum was collected, immersed in 4% paraformaldehyde in 0.1 M phosphate buffer (pH 7.3) for 48 h at 4°C, and transferred to a 30% sucrose solution. The remaining brain was flash frozen in 2-methylbutane on dry ice and stored at -80°C.

Immunohistochemistry

As previously shown in this model, intrastriatal injection of PFFs results in accumulation of pSyn pathology within the cortex and SNpc, and thus, can be used as a surrogate-marker for PFF injection accuracy and seeding efficiency outside of the SNpc (Duffy et al., 2018; Howe et al., 2021; J. R. Patterson, Duffy, et al., 2019; Polinski et al., 2018). The presence of pSyn pathology in the cortex was used as an inclusion criterion for PFF injected rats, as well as to confirm lack of pSyn pathology following monomer or PBS injection (Figure 2.1D). Brain cortex was sectioned at 40 µm on a freezing microtome and transferred into cryoprotectant solution. Free-floating sections (1:6 series) were transferred to 0.1M tris-buffered saline containing 0.5% triton-X100 (TBS-Tx) and washed 4 times for 5 minutes each. Tissue was then quenched in 0.3% hydrogen peroxide for 1h followed by TBS-Tx washes. Tissue was blocked with 10% normal goat serum (NGS) for 1h and washed with TBS-Tx before being transferred to primary antibody solution overnight at 4°C (TBS-Tx, 1% NGS, 1:10,000 mouse anti-phosphorylated α-Syn at serine 129; Abcam, AB184674). Sections were washed in

TBS-Tx and transferred to secondary antibody solution for 2.5h at RT (TBS-Tx, 1% NGS, 1:500 goat anti-mouse; Millipore, AP124B). Sections were washed in TBS-Tx and incubated for 2h at RT in standard avidin-biotin complex detection kit (Vector Laboratories, PK-6100). Following TBS-Tx washes, tissue was developed using nickel ammonium enhanced DAB solution (2.5mg mL^{-1} nickel ammonium sulfate hexahydrate (Fisher, N48-500) / 0.5 mg/mL^{-1} diaminobenzidine (DAB, Sigma-Aldrich, D5637) and 0.03% hydrogen peroxide in TBS-Tx). Sections were mounted onto subbed microscope slides and dehydrated with series graded ethanol solutions before bathing in (2) 100% xylene solutions and cover slipped with Cytoseal (Thermo-Fisher, 22-050-262). Two of ten PFF-injected rats at the one-month time point (Figure 2.1E) and none of the PFF-injected rats at the two-month time point (J. Patterson et al., 2024) were excluded due to lack of cortical pSyn pathology.

Laser Capture Microdissection

Laser capture microdissection (LCM) was used to collect SNpc samples to enrich for pSyn inclusion containing nigral neurons as well as immediately adjacent activated microglia (Figure 2.1F). The frozen hemispheres containing the ipsilateral SNpc were mounted on pre-chilled cryostat chucks with Tissue-Tek O.C.T (Sakura, 4583) and frozen on dry ice. Brains were transferred to the cryostat chamber set at -19°C and allowed to equilibrate for 5 minutes. The entire SN was sectioned at a 20 µm thickness and mounted on a chilled membrane frame slide (nuclease and human nucleic acid free polyethylene terephthalate (PET) membrane frame slide; Leica, 11505190). Slides were transferred to a 50 ml conical tube and covered with dry ice before being stored at -80°C. Conical tubes containing the membrane frame slides were removed from storage

and held on dry ice until the slides were locked into the stage of a Leica 6500 Laser Capture Microdissection System (Leica, Wetzlar, Germany). GFP expression was used to demarcate the boundary of the SNpc at 10X magnification. A UV laser (Power = 60, aperture = 15, speed = 5) was used to microdissect the SNpc, dropping the tissue into a sample tube cap filled with 50 µl of TRIzol reagent (Invitrogen, 26696026) to prevent RNA degradation. To ensure RNA integrity, all microdissection was limited to 60 minutes per slide. Two of ten monomer-injected rats and one of eight PFF-injected rats in the one-month study were excluded due to lack of or poor EGFP expression (Figure 2.1E). None of the PFF-injected rats in the two-month study were excluded due to lack of or poor EGFP expression (J. Patterson et al., 2024). Collected samples were placed on dry ice before returning to -80°C storage until RNA isolation was performed.

RNA Isolation

Phasemaker tubes (Invitrogen, A33248) were labeled and centrifuged for 30s at 16,000gs. Samples in TRIzol were thawed on ice and briefly centrifuged to dislodge tissue in the bottom of the tube. Samples from the same brain were pooled together into one tube and the total volume was brought up to 1mL with TRIzol. Samples were transferred to a phasemaker tube and incubated at RT for 5mins. 200 µL of 100% chloroform was added to each sample and shaken by hand in the phasemaker tube before incubating at RT for 10 mins. Tubes were centrifuged at 4°C at 16,000 x g for 5 min. Following, the aqueous phase (clear liquid) was removed and transferred to an RNase-free 1.5mL tube and an equal volume of 100% ethanol was added. Samples were vortexed for 3s and ran through a column-based nucleic acid purification kit using a method modified from manufacturer’s instructions (Zymo Research, R1016). Samples

were transferred to the column 600 µL at a time and centrifuged for 1m at 12,000 x g until the entire sample was transferred. All RNA wash & prep buffers were added to the column and centrifuged for 1m at 4°C at 12,000 x g. First, samples were washed with 400 µL of RNA wash buffer, then incubated in a 1X concentration of a DNase I cocktail (DNase I from Thermo Scientific, FEREN0521, with a reaction buffer containing $MgCl_2$ from Thermo Scientific, FERB43) for 15m at RT. After incubation, DNase I cocktail was centrifuged through the column, then 400 µL of RNA prep buffer was washed through the column, followed by 700 µL of RNA wash buffer, and lastly 400 µL of RNA wash buffer. Columns were then dried by centrifuging for 2m at 12,000 x g. 15 µL of DNase/RNase free molecular grade water was added to the column, incubated for 1m at RT, and then centrifuged for 1m at 10,0000 x g. 10 µL of the flow-through (containing the RNA) was re-run through the column to increase RNA yield. Quality and quantity of RNA was assessed with an Agilent RNA 6000 Pico (5067-1513) on an Agilent 2100 Bioanalyzer. None of the samples in the one-month study were excluded due to low RIN (RNA integrity number). One of the six PFF-injected rats and two of the five PBS-injected rats in the two-month study were excluded due to low RIN (J. Patterson et al., 2024). Samples were stored at -80°C prior to library preparation and sequencing.

Construction and Sequencing of Directional total RNA-seq Libraries

Libraries were prepared by the Van Andel Genomics Core from 150 ng of total RNA using the KAPA RNA HyperPrep Kit (Kapa Biosystems, Wilmington, MA USA). Ribosomal RNA material was reduced using the QIAseq FastSelect –rRNA HMR Kit (Qiagen, Germantown, MD, USA). RNA was sheared to 300-400 bp. Prior to PCR amplification, cDNA fragments were ligated to IDT for Illumina TruSeq UD Indexed

adapters (Illumina Inc, San Diego CA, USA)). Quality and quantity of the finished libraries were assessed using a combination of Agilent DNA High Sensitivity chip (Agilent Technologies, Inc.), QuantiFluor® dsDNA System (Promega Corp., Madison, WI, USA), and Kapa Illumina Library Quantification qPCR assays (Kapa Biosystems). Individually indexed libraries were pooled and 50 bp, paired end sequencing was performed on an Illumina NovaSeq6000 sequencer to an average depth of 50M raw paired-reads per transcriptome. Base calling was done by Illumina RTA3 and output of NCS was demultiplexed and converted to FastQ format with Illumina Bcl2fastq v1.9.0.

Data Processing and Differential Gene Expression Analysis

Adapter sequences and low-quality bases were trimmed using TrimGalore v0.6.10 (https://github.com/FelixKrueger/TrimGalore) using the parameters, '--paired -q 20'. The rnor6 genome and gene annotations were downloaded from ENSEMBL release 104 (Harrison et al., 2024). Trimmed reads were aligned to the rnor6 reference genome to obtain gene counts using STAR v2.7.10a (Dobin et al., 2013), with the parameters, '--twopassMode Basic --quantMode GeneCounts.' Transcript-level TPMs were calculated using the 'quant' function from Salmon v1.10.0 (Patro et al., 2017), with the parameters, "-l A --validateMappings", and summarized into gene-level TPMs using tximport v1.30.0 (Soneson et al., 2015). Raw gene counts from STAR were processed and analyzed using DESeq2 v1.40.2 (Love et al., 2014). Variance stabilizing transformation (VST) counts were calculated using the vst() with 'blind=FALSE', and the top 10,000 genes with the highest variance were used for principal component analysis (PCA). Differential

expression analysis was performed using DESeq2 also, fitting the design, '~ Group,' and testing pairwise contrasts using the default adjusted pvalue cutoff of 0.1.

In our published 2-month study (J. Patterson et al., 2024), reads were aligned to the rat transcriptome (Ji et al., 2020) using Salmon and differential transcript expression assed with Kallisto-Slueth (Patro et al., 2017). This study identified 57,623 total transcripts, of which the reference transcriptome only linked ~27% to known rat genes without manual annotation using the UCSC genome browser (Ji et al., 2020; Tyner et al., 2017). To address this issue in the current study, we used the splice aware aligner STAR paired with DESeq2 for differential expression analysis to align the reads to rat genome (Dobin et al., 2013; Love et al., 2014). Although Salmon-Sleuth is less recourse intensive, we opted to use the STAR-DESeq2 method due to the superior handling of splice variants and capability to map directly to the rat genome, rather than depending on the poorly-annotated rat transcriptome (Liu et al., 2022; Schaarschmidt et al., 2020). To appropriately compare transcriptional effects observed at 1 and 2 months, the reads from the 2-month study were downloaded from the Gene Expression Omnibus (GEO) data repository (accession number GSE246112) and processed using the STAR-DESeq2 workflow.

Data analysis and visualization were performed using RStudio version 2024.12.0+467 ("Kousa Dogwood" release). The tidyverse package was used for data transformation and ggplot2 package was used for generating heatmaps, volcano plots, and dot plots. Heatmap hierarchical clustering was performed separately for genes and samples using the hclust function with complete linkage method. Pathway enrichment analyses were generated using ShinyGo0.81 (Ge et al., 2020). We limited GO

enrichment terms to a minimum of 15 genes and a maximum of 500 genes in the pathway, as previously described (Reimand et al., 2019).

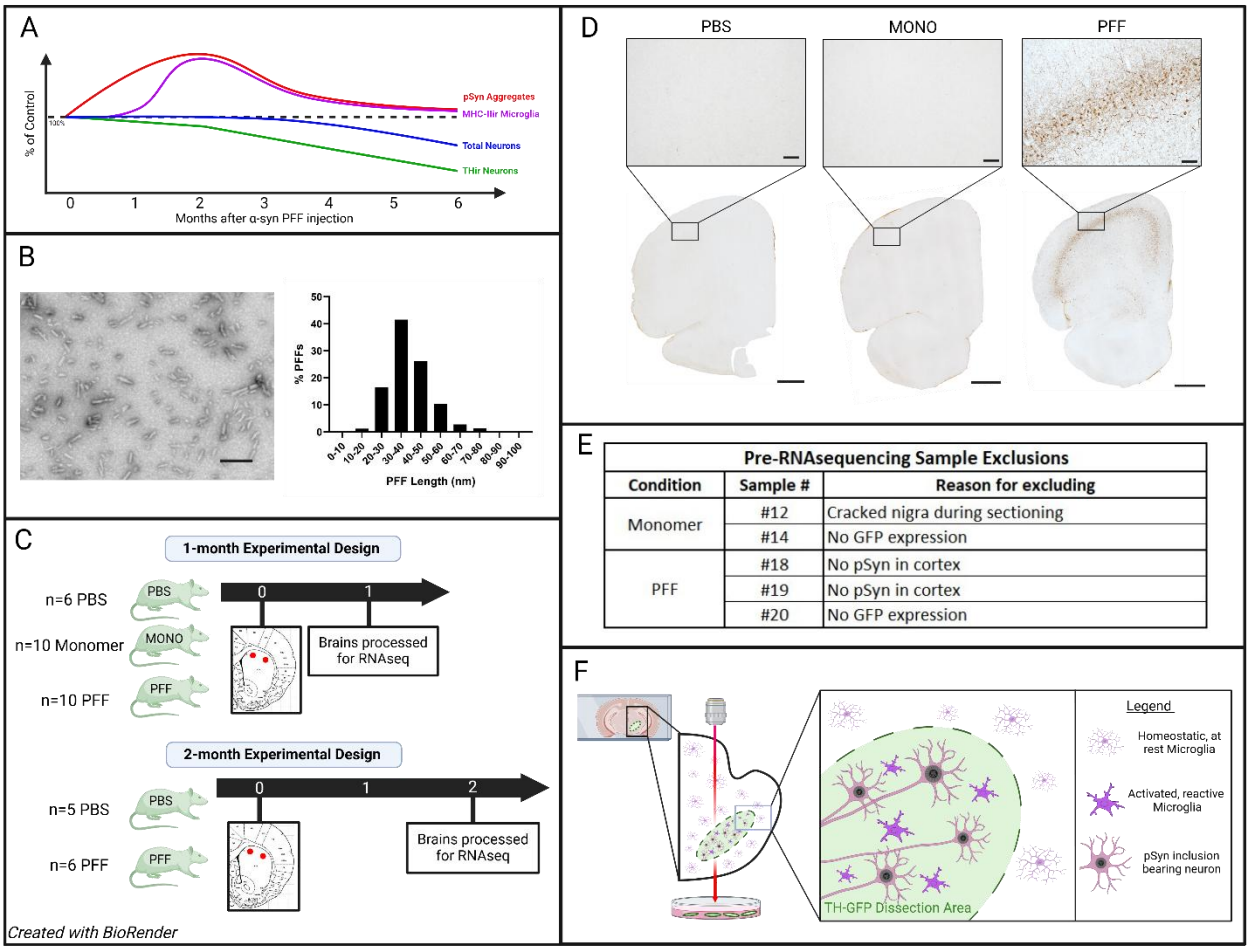

Pre-RNAsequencing Sample Exclusions		
Condition	**Sample #**	**Reason for excluding**
Monomer	#12	Cracked nigra during sectioning
	#14	No GFP expression
PFF	#18	No pSyn in cortex
	#19	No pSyn in cortex
	#20	No GFP expression

Figure 2.1 Experimental design and model validation

(A) Time course and features of the rat preformed fibril (PFF) model in the ipsilateral substantia nigra (SN) following intrastriatal PFF injection based on earlier studies (Duffy et al., 2018; Howe et al., 2021; Miller et al., 2021; J. R. Patterson, Duffy, et al., 2019; Paumier et al., 2015; Stoll, Kemp, Patterson, Howe, et al., 2024). The number of phosphorylated alpha-synuclein (pSyn) inclusion-containing neurons and major histocompatibility complex II immunoreactive (MHC-IIir) microglia peaks two months post intrastriatal injection. The number of pSyn-containing SN neurons and MHC-IIir microglia progressively decreases following this peak. Starting at two months,

Figure 2.1 (cont'd)

progressive loss of SN tyrosine hydroxylase (TH) phenotype is observed, culminating in significant neurodegeneration detectable at five months. **B)** Distribution of mouse α-syn PFF fibril lengths post-sonication. A total of 508 individual fibrils were measured; the average fibril size was 39.10 nm (SEM = 0.47 nm). Transmission electron micrograph of sonicated PFFs, scale bar = 200 nm. **C)** Treatment groups and timeline of the present experiment. Male TH-EGFP rats received unilateral intrastriatal injections of mouse alpha-synuclein (αSyn) PFFs, mouse αSyn monomer or vehicle. Rats were euthanized one or two months following surgery. **D)** Validation of pSyn pathology in the ipsilateral frontal cortex one month following PFF, but not PBS or monomer injection. Scale bar for cortex= 1 mm. Scale bar for insert = 100 μm. **E)** Samples that were removed from the study prior to RNA sequencing and the reason for removal. **F)** Diagram of the laser capture microdissection (LCM) process, showing the SNpc labeled with GFP under the human TH promoter. The SNpc is visualized, traced, cut, and collected in TRIzol for RNA isolation. The captured area includes pSyn containing SNpc neurons, as well as neighboring reactive microglia.

RESULTS

Differentially Expressed Genes (DEGs) at One and Two Months Post PFF Injection

I first examined differential gene expression between PFF, monomer and PBS injected rats at the one-month time point. Principal component analysis (PCA) of the one-month dataset revealed that the monomer group displayed a bimodal distribution of differential expression (Figure 2.2). Except for one sample, all monomer samples clustered with either PBS or PFF groupings. Samples from monomer-injected rats injected at shorter intervals between monomer preparation and surgical injection (approximately < 1 hour) clustered with PBS-injected rat samples, in contrast, samples from monomer-injected rats injected at longer intervals between monomer preparation and surgical injection (approximately > 1 hour) clustered with PFF-injected rat samples. This unexpected finding suggests that there is a time after which α-syn monomer injectate begins to fibrillize and is no longer a suitable control condition for comparisons with PFF injection. This phenomenon deserves further investigation. Due to the unique distribution of the monomer group, we focused solely on differential gene expression between PFF and PBS injected rats within our one- and two- month datasets.

At the one-month timepoint, using a p adjusted (padj) cutoff value of 0.01, 3436 genes were differentially expressed between the PFF group compared to PBS, 1431 differentially expressed genes (DEGs) were upregulated in inclusion-bearing SNpc compared to non-inclusion bearing SNpc and 2005 DEGs were downregulated. At the two-month timepoint a total of 758 genes were differentially expressed between the PBS and PFF group, with 512 upregulated DEGs in inclusion-bearing SN and 246 downregulated DEGs (Figure 2.3A). Comparing across both time points, a total of 340

genes were differentially expressed at both one and two months (Figure 2.3B). Of the 340 DEGs common to both time points, 262 were upregulated in inclusion-bearing SN, 71 were downregulated, and 7 genes were bidirectional, meaning differentially expressed at both time points but in opposite directions (Figure 2.3C). Specifically, *Ciart, Dbp, Nr1d2, Tef*, ENSRNOG00000006939 and ENSRNOG00000058568 were upregulated in the inclusion-bearing SNpc at one month and downregulated at two months. Only one gene, *Bmal1*, was downregulated at 1 month and then upregulated at two months.

We next determined the number of DEGs that were uniquely upregulated or uniquely downregulated at one or two months (Figure 2.3C). We observed 1169 uniquely upregulated genes and 1927 uniquely downregulated genes in the inclusion bearing SNpc at the one-month timepoint. At 2-months, we observed 250 uniquely upregulated genes and 168 uniquely downregulated genes in the inclusion bearing SNpc. Overall, we observed more DEGs associated with the earlier one-month time point, compared to the number of DEGs observed at two months. However, the proportion of directionality of DEGs differed between time points. Specifically, at one month, a greater number of downregulated DEGs were observed than upregulated, whereas at two months a greater number of upregulated DEGs were observed than downregulated. The complete list of DEGs between PFF and PBS injected rats at both the one and two-month time point is available in Excel Sheet #1.

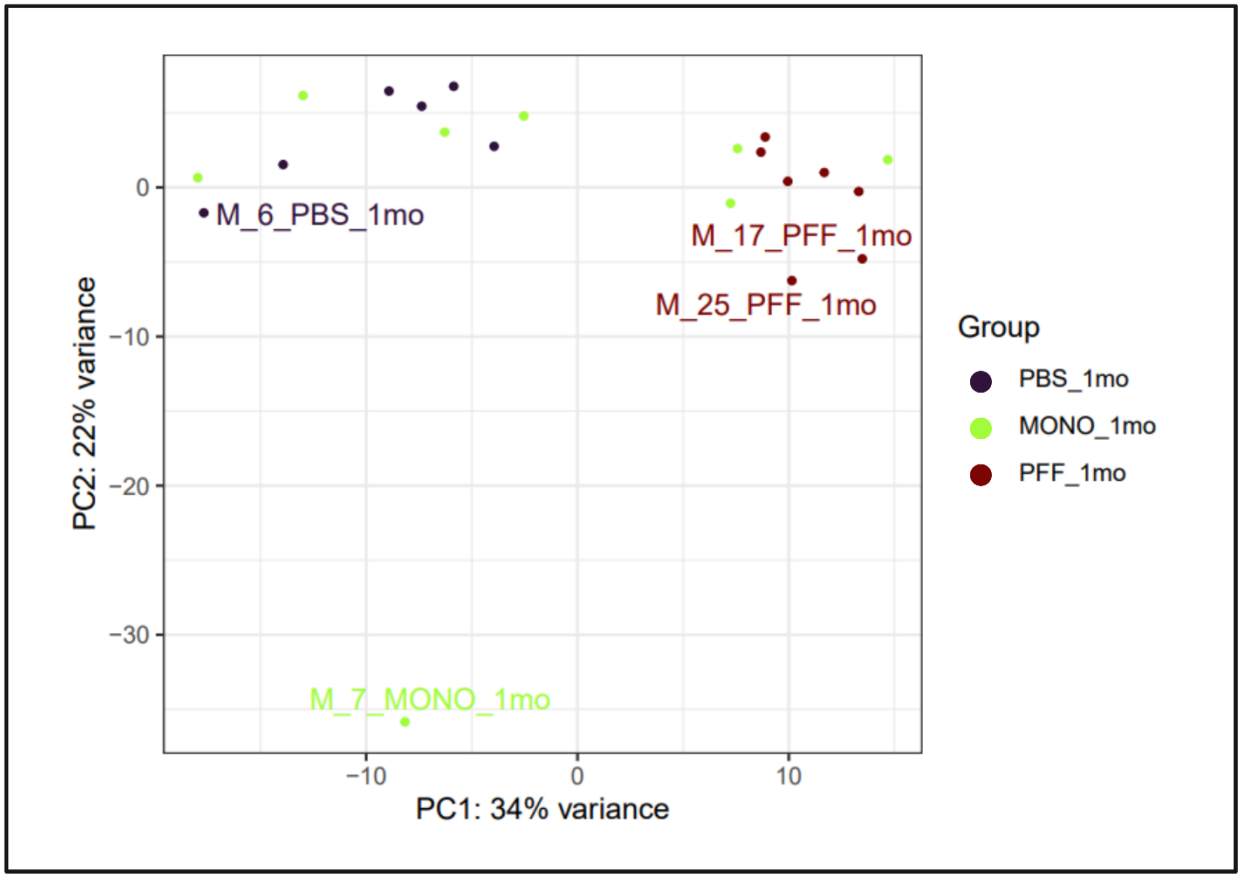

Figure 2.2 Principal component analysis of RNA-Seq results from SNpc samples one month following PFF, monomer or PBS injection

RNAseq results revealed similarities in gene expression patterns between PBS (black) and between PFF (brown) SNpc samples. However, lack of similarity in gene expression patterns were observed between monomer SNpc samples in which a bimodal distribution was observed.

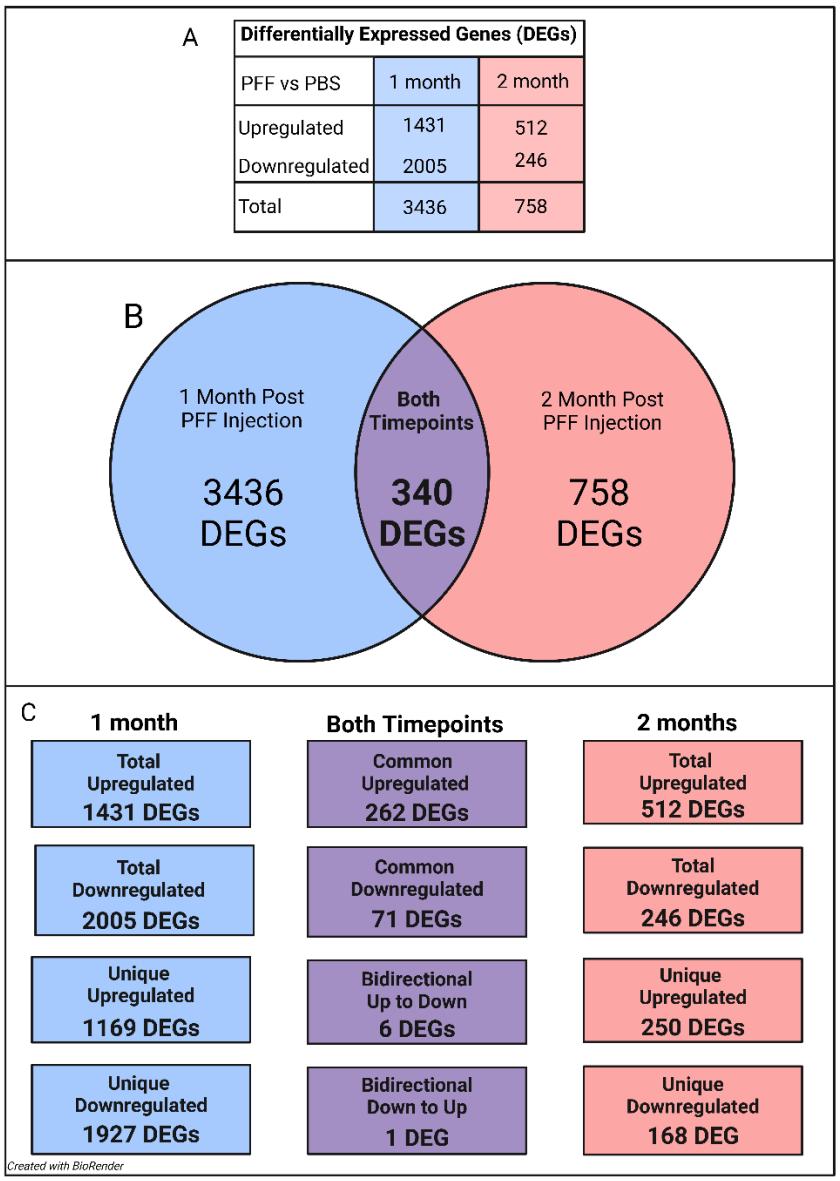

Figure 2.3 Overview of results of differential gene expression analysis

A) Total number of upregulated or downregulated differentially expressed genes (DEGs) in the SNpc of PFF injected rats compared to PBS injected rats at one or two months. Padj <0.01. **B)** Venn diagram demonstrating the number of DEGs common to both the one and two month time points. **C)** Distribution of upregulated and downregulated DEGs unique to, or common between, the one or two month timepoint. An additional small set of DEGs common to both time points demonstrated bidirectionality.

One- and Two-months Analysis: Individual DEGs

Distribution of DEGs in the inclusion-bearing SNpc at the one-month and two-month time points were visualized using volcano plots (Figure 2.4A, D). In general, despite fewer upregulated DEGs observed at two months compared to one month, more DEGs displayed a greater magnitude of upregulation (log2FC > 2.0) at two months (n=47) than at one month after PFF injection (n=15). At the 1-month timepoint, the most upregulated DEGs in inclusion-bearing SNpc included *Fam111a*, *Mmp12, Cxcl13, Cxcl10, Plac8, Mx1, Atf3, Rt1-Da, Cd74,* and *Rt1-Db1* (Figure 2.4B, log2FC range from 1.9 to 4.9). At one month, the upregulated DEG with the lowest padj value was *Cst3* (padj = 1.77 E-15, log2FC = 0.64). At the 2-month time point, the most upregulated DEGs in inclusion-bearing SNpc included *Cxcl13, Mx1, Plac8, Zbp1, Cxcl10, Slamf9, Ccl12, F10, Adgrg5, and Glipr1* (Figure 2.4E, log2FC range from 3.4 to 5.9). At two months, the upregulated DEG with the lowest padj value was *Plek* (padj = 1.26 E-12, log2FC = 1.5).

With regards to the magnitude of downregulated DEGs, we observed that more DEGs displayed a greater magnitude of downregulation (log2FC > -0.5) at the one month time point (n=217) than at two months after PFF injection (n=7). The most downregulated DEGs in the inclusion-bearing SNpc at the one-month time point included *Scube1*, *Tacr3, Foxa2, Cpne7, Slc39a4, Mmp14, Lmx1b, Slc6a3, Chrna5* and *Th* (Figure 2.4C, log2FC range from -0.85 to -1.0). At one month, the downregulated DEG in the inclusion-bearing SNpc with the lowest padj value was *Bcorl1* (padj = 7.8 E-12, log2FC = -0.41). The most downregulated DEGs at the two-month time point in the inclusion-bearing SNpc included *Alox5, Strip2, Syce1l, Ciart, Pmfbp1, Npy5r, Galnt14,*

Lynx1, Fkbp1b, and Dbp (Figure 2.4F, log2FC range from -0.43 to -0.86). At two months, the downregulated DEG with the lowest padj value was *Lynx1* (padj = 1.59 E-8, log2FC = -0.45).

Further One- and Two-months Upregulated DEG Analysis: Focus on Cathepsins

At both the one- and two-month time point, we observed that genes for many members of the cathepsin family were differentially expressed in inclusion-bearing SNpc. Specifically, at the one-month time point, a total of seven cathepsin genes were upregulated: *Ctsb, Ctsc, Ctse, Ctsh, Ctsl, Ctss,* and *Ctsz* (Figure 2.5A) with *Ctse* the most upregulated (log2FC= 0.79), followed by *Ctsz* (log2FC= 0.72), and *Ctsc* (log2CF= 0.69) (Figure 2.5C). At the 2-month timepoint, five cathepsins were significantly upregulated, including *Ctsc, Ctse, Ctsh, Ctss,* and *Ctsz* (Figure 2.5B). The most upregulated cathepsins at the two-month time point were *Ctsz* (log2FC= 1.32), followed by *Ctsc* (log2FC= 1.06), and *Ctsh* (log2FC= 0.89) (Figure 2.5D).

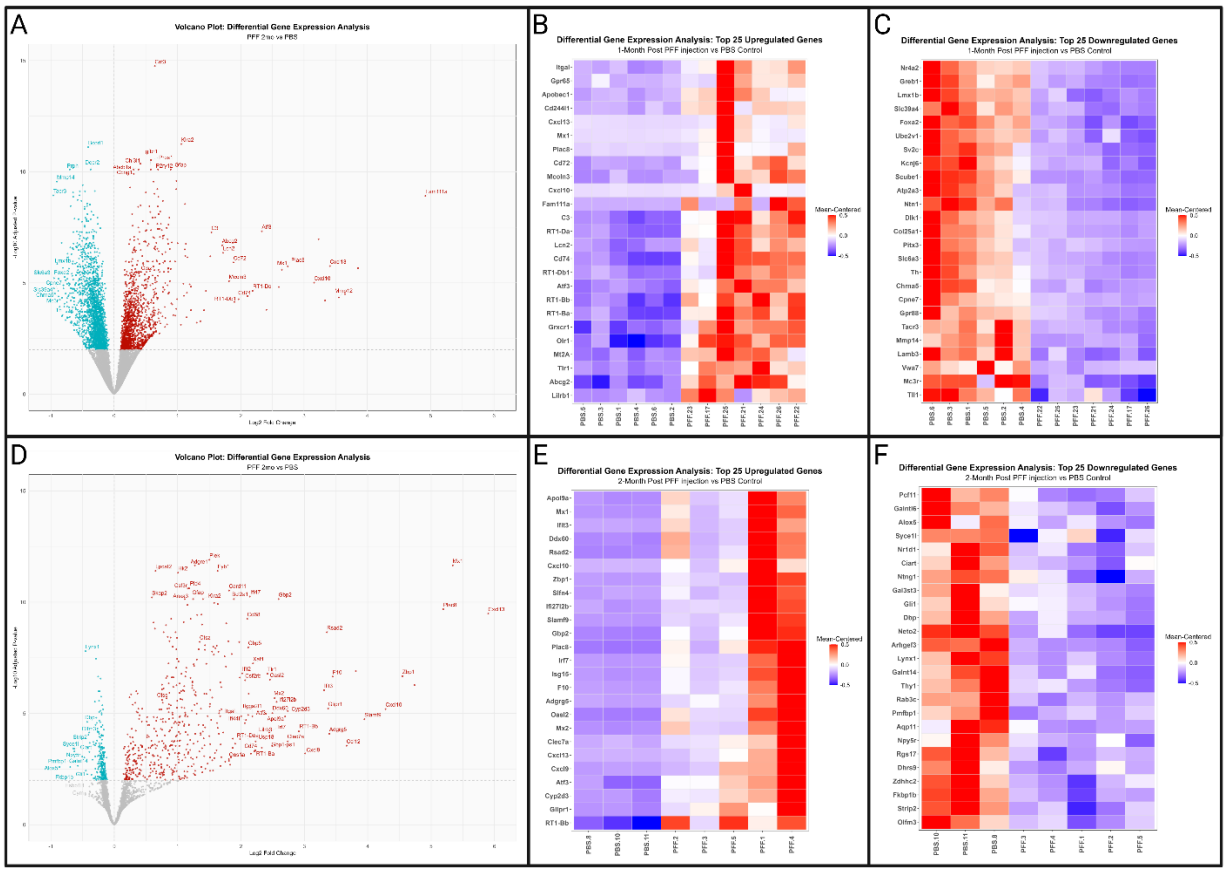

Figure 2.4 Volcano plots and heat maps of PFF induced DEGs at one or two months

(A, D) Volcano plots illustrating the distribution of all DEGs between the PFF and PBS treatment groups at one month **(A)** and two months **(D)**. Y-axis represents padj values with a -Log10 transformation, X-axis represents log fold change. Dashed line represents the padj cutoff value of <0.01. **(B,C)** Heatmaps of the top 25 upregulated **(B)** and downregulated **(C)** DEGs associated with PFF injection at 1 month. **(E,F)** Heatmaps of the top 25 upregulated **(E)** and downregulated **(F)** DEGs associated with PFF injection at 2 months. TPM values from each gene are mean-centered and scaled to fit between -0.5 and 0.5. Hierarchical clustering of genes and samples was performed to plot similar expression patterns.

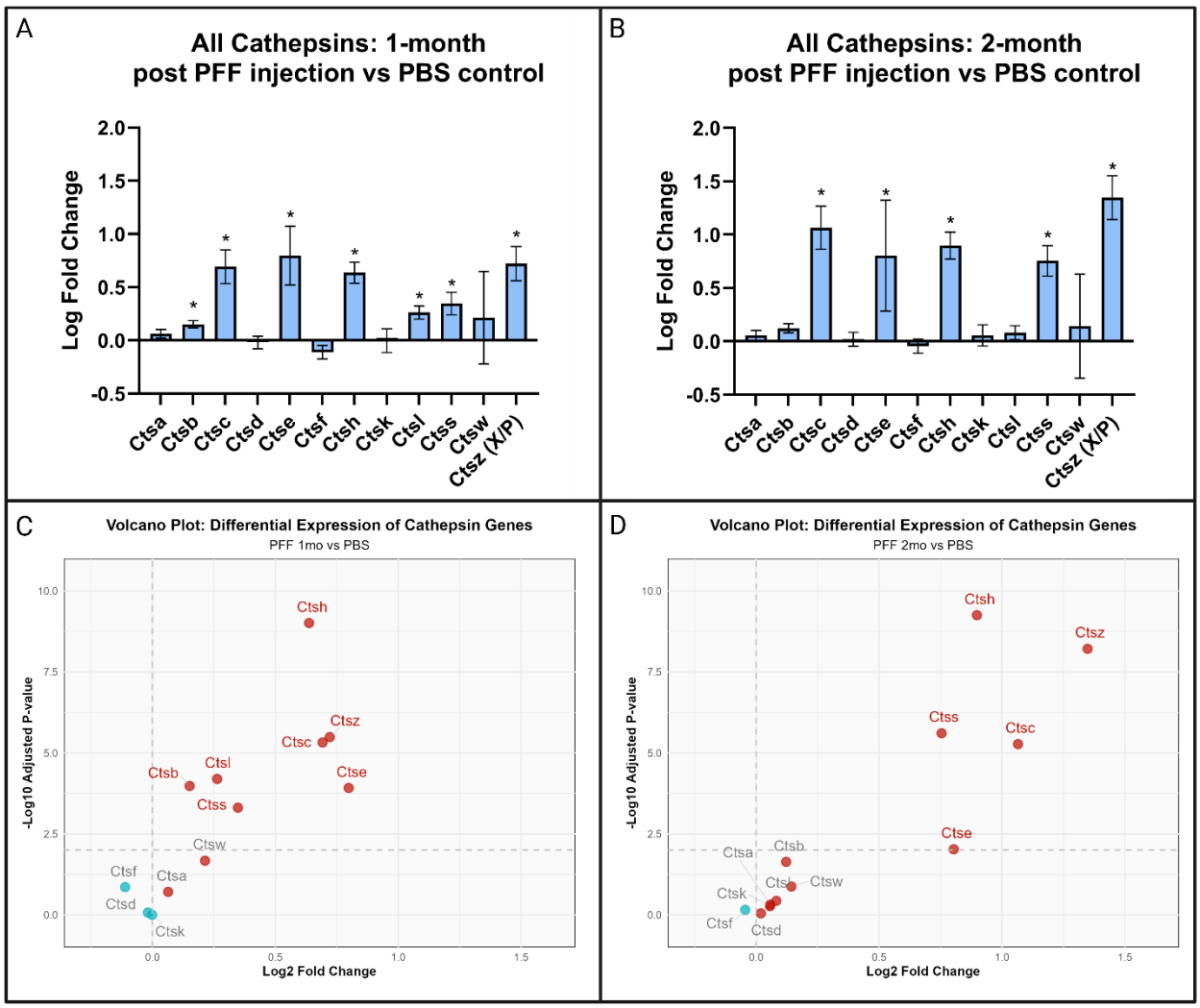

Figure 2.5 One- and two-months analysis of cathepsin gene expression

Expression of all cathepsins plotted by log fold change at 1 month **(A)** and 2 months **(B)**. * Indicates DGE (padj < 0.01). Error bars indicate SEM. (**C, D**) Volcano plots for all cathepsins at 1 month **(C)** and 2 months **(D)**. Dashed line indicates padj <0.01 (-log10(> 2)). Red dots indicate positive log fold change, and blue dots represent negative log fold change. Grey labels indicate a non-significant padj value > 0.01.

DEG Analysis by Time Point: Kyoto Encyclopedia of Genes and Genomes (KEGG) Enrichment Analysis

KEGG, or Kyoto Encyclopedia of Genes and Genomes, is a database that integrates genomic, biochemical and phylogenetic information to provide an understanding of biological systems from genome sequencing data (M Kanehisa & Goto, 2000; Minoru Kanehisa, 2019; Minoru Kanehisa et al., 2023). KEGG enrichment analyses were generated from the upregulated DEGs at the one-month time point (n=1431), downregulated DEGs at one month (n=2005), upregulated DEGs at two months (n=512) and downregulated DEGs at two months (n=246). Using a significance cutoff threshold of FDR enrichment < 0.05, KEGG analysis of upregulated DEGs at one month revealed 91 enriched pathways and analysis of downregulated DEGs at 1 month revealed enrichment of 127 pathways. The top three enriched upregulated KEGG pathways in the inclusion-bearing SNpc at one month were examples of pathways associated with immune response to pathogens, "*Coronavirus disease-COVID-19*", and "*Tuberculosis*" as well as expression of ribosomal subunits, "*Ribosome*" (Figure 2.6A). The most enriched downregulated KEGG pathways at one month were associated with synaptic transmission, including "*Cholinergic synapse*", "*Glutamatergic synapse*", and "*Dopaminergic synapse*" (Figure 2.6C). At two months, KEGG analysis of upregulated DEGs identified 96 enriched pathways, whereas analysis of downregulated DEGs identified 38 enriched pathways. The top three enriched upregulated KEGG pathways in the inclusion-bearing SNpc at two months were, similar to one month, associated with the immune responses, including immune responses associated with "*Osteoclast differentiation*", and the immune responses to pathogens "*Influenza A*" and

"*Tuberculosis*" (Figure 2.6B). The most enriched downregulated KEGG pathways were associated with synaptic transmission, similar to the one-month time point, including "*Synaptic vesicle cycle*" and "*Collecting duct acid secretion*", as well as a pathway associated with coordinating rhythmic gene expression, "*Circadian rhythm*" (Figure 2.6D). The full list of upregulated and downregulated enriched KEGG pathways at each time point is available in Excel sheet 2.

DEG Analysis by Time Point: Gene Ontology (GO) Biological Processes

We also used Gene Ontology (GO): Biological Process enrichment analysis (Ashburner et al., 2000; Gene Ontology Consortium et al., 2023) to provide more insight into the basic functional aspects of the genes differentially expressed at one and two months in the inclusion-bearing SNpc. GO: Biological Process enrichment analyses were generated from the upregulated DEGs at the one-month timepoint (n=1431), downregulated DEGs at one month (n=2005), upregulated genes at two months (n=512) and downregulated genes at two months (n=246) (Figure 2.7). Using an FDR enrichment cutoff value of <0.05, >1,000 GO terms were enriched in the one-month upregulated dataset and 947 GO terms were enriched in the downregulated dataset. At two months, 937 GO terms were enriched in the upregulated dataset and 59 GO terms were enriched in the downregulated dataset. The top enriched GO terms from the one-month upregulated DEGs were "*response to molecule of bacterial origin*", "*positive regulation of cytokine production*", and "*response to lipopolysaccharide*" (Figure 2.7A). Top GO terms for the one-month downregulated DEGs were "*synapse organization*", "*regulation of trans-synaptic signaling*", and "*modulation of chemical synaptic transmission*" (Figure 2.7C). Top GO terms in the two-month upregulated DEGs were

"*response to virus*", "*positive regulation of cytokine production*", and "*leukocyte mediated immunity*" (Figure 2.7B). Top GO terms for the two-month downregulated DEGs were "*tricarboxylic acid cycle*", "*proton transmembrane transport*", and "*vesicle-mediated transport in synapse*" (Figure 2.7D). The full list of GO enriched terms at one and two months is available in Excel sheet 3.

For the GO: Biological Processes analyses, we sought to identify DEGs associated with inclusion-bearing SNpc that were most frequently included within the top ten enrichment terms (sorted by FDR enrichment). We extracted the top 10 DEGs (ranked by log fold change) for each time point and direction (Figure 2.7E-H). At the one-month timepoint, the top three upregulated DEGs in inclusion-bearing SNpc were *Mmp12, RT1-Da,* and *Cd74* (Figure 2.7E), with both *Mmp12* and *Cd74* components of the "*positive regulation of cytokine production*" top three GO term. The top three downregulated DEGs were *Lmx1b, Slc6a3,* and *Col25a1* (Figure 2.7F). For the two-month timepoint, the top three upregulated DEGs in the inclusion-bearing SNpc were *Cxcl13, Zbp1,* and *Cxcl10* (Figure 2.7G), with both *Zbp1* and *Cxcl10* components of the "*response to virus*" top three GO term. The top three downregulated DEGs were *Atp6v1g2, Napb,* and *Dnajc6* (Figure 2.7H), with *Atp6v1g2* associated with the "*proton transmembrane transport*" top three GO term and both *Napb* and *Dnajc6* associated with the "*vesicle-mediated transport in synapse" GO* term. Collectively, our KEGG and GO enrichment analyses at either one or two months suggest that upregulated DEGs at one month are associated with upregulation of the immune responses whereas downregulated DEGs suggest dysfunction of synaptic transmission. At two months upregulation of DEGs continues to implicate immune responses, whereas

downregulated DEGs at two months continue to suggest synaptic transmission deficits as well as deficits in coordination of rhythmic gene expression.

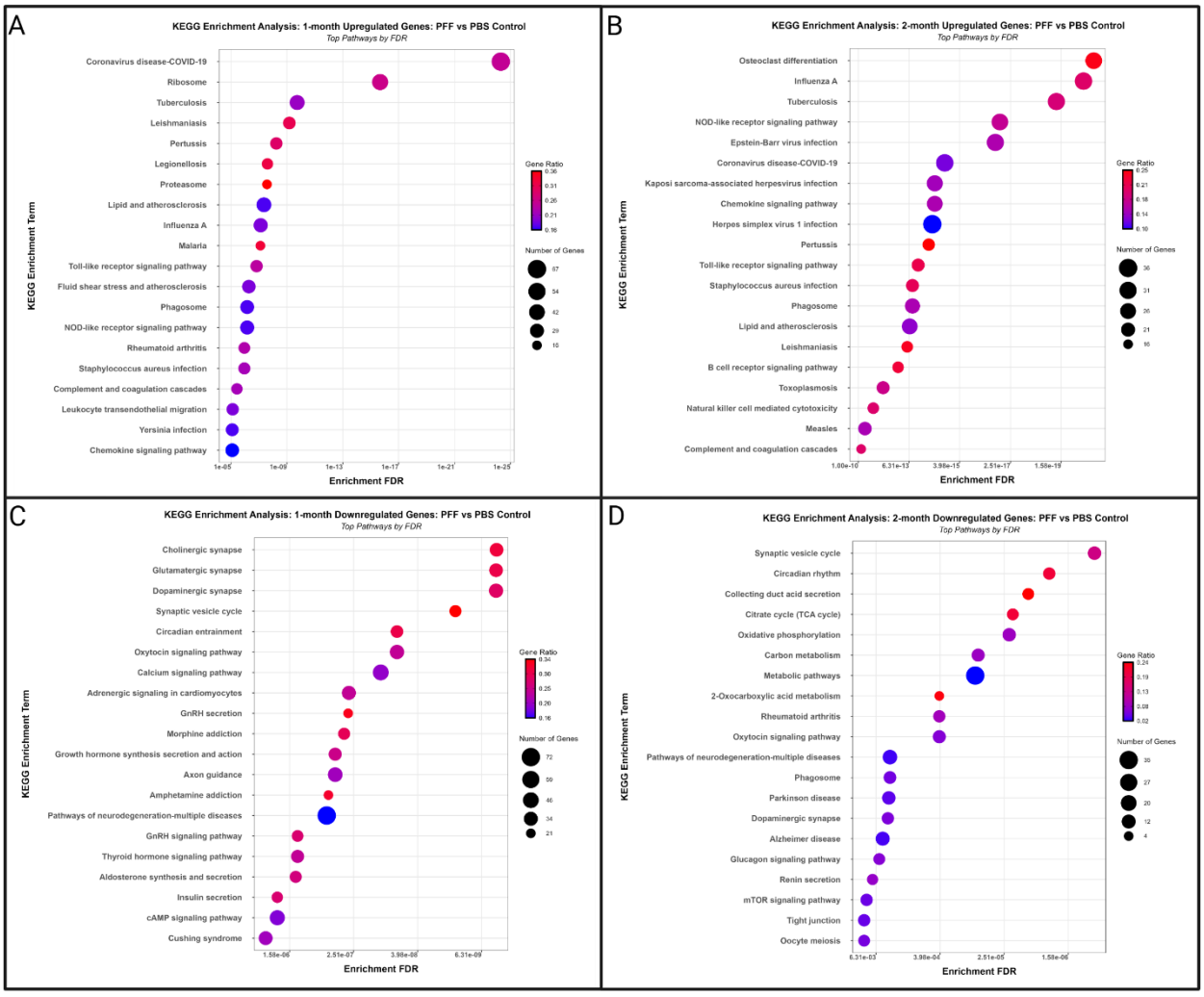

Figure 2.6 KEGG enrichment analysis of PFF induced DEGs at one or two months

(A,C) KEGG enrichment analysis of upregulated **(A)** or downregulated **(C)** DEGs at 1 month. **(B,D)** KEGG enrichment analysis of upregulated **(B)** or downregulated **(D)** DEGs at 2 months.

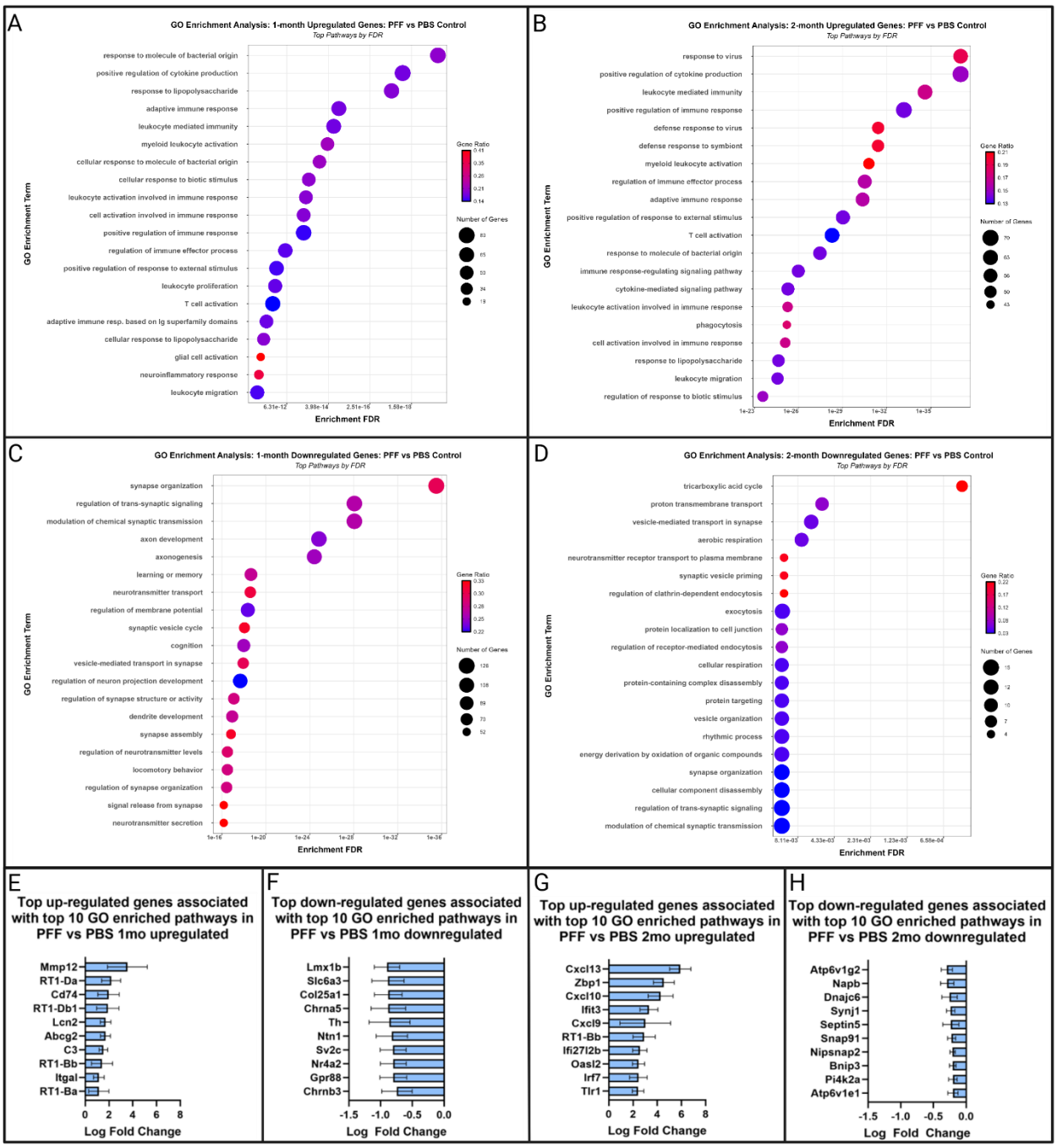

Figure 2.7 Gene Ontology (GO) enrichment analysis of PFF induced DEGs at one or two months

(A,C) GO enrichment analysis of upregulated **(A)** or downregulated **(C)** DEGs at 1 month. **(B,D)** GO enrichment analysis of upregulated **(B)** or downregulated **(D)** DEGs at 2 months. (**E-F**) Top ten upregulated **(E)** and **(F)** downregulated genes at one month.

Figure 2.7 (cont'd)

(**G-H**) Top ten upregulated **(G)** and **(H)** downregulated genes at two months. The top ten genes (log fold change) from the top ten GO enrichment terms (FDR) were used. Error bars represent SEM.

DEGs Common and Unique to Both Time Points: KEGG Enrichment Analysis

To further understand the biological processes that are associated with both early and late pSyn inclusions, we examined DEGs that were commonly upregulated (n=262) or commonly downregulated (n=71) across both the one- and two-month time points using KEGG enrichment analysis. Using an enrichment FDR of <0.05, KEGG analysis of upregulated DEGs common to both the one- and two-month time point revealed 73 enriched pathways in inclusion-bearing SNpc (Figure 2.8A). The top three enriched pathways in the common upregulated dataset were examples of pathways associated with immune response to pathogens, specifically "*Staphylococcus aureus infection*", "*Tuberculosis*", and "*Pertussis*". KEGG analysis of downregulated DEGs common to both the one- and two-month time point revealed 33 enriched pathways in inclusion-bearing SNpc (Figure 2.8C). The most enriched pathways in the common downregulated dataset included intracellular signaling pathways such as "*Oxytocin signaling*", "*Calcium signaling*" and "*Glucagon signaling*", the dopamine synthesis pathway "*Phenylalanine tyrosine and tryptophan biosynthesis*" as well as a pathway associated with deficits in calcium signaling, energy metabolism and energy metabolism, "*Hypertrophic cardiomyopathy*".

Most of the pathways upregulated across both time points were associated with immune responses (Figure 2.8A). To further appreciate whether enrichment of any immune response KEGG pathways was unique to either time point, we identified DEGs that were uniquely upregulated at either one (n=1169) or two months (n=250) and performed KEGG enrichment analyses on these time point-specific DEGs. KEGG enrichment analyses identified 74 pathways that were uniquely upregulated at one

month including pathways related to cellular processes involved in ribosomal biogenesis, "*Ribosome*", response to COVID-19 "*Coronavirus disease-COVID-19*", and protein degradation "*Proteasome*" (Figure 2.8B). KEGG enrichment analyses of DEGs uniquely upregulated at two months identified 29 enriched pathways including immune responses associated with "*Osteoclast differentiation*", and response to the specific pathogens "*Epstein-Barr virus infection*", and "*Measles*" (Figure 2.8D). The full list of KEGG enrichment pathways for these analyses is available in Excel sheet #2.

DEGs Common and Unique to Both Time Points: GO Biological Processes

GO: Biological Process enrichment analyses were also conducted on DEGs commonly upregulated (n=262) or commonly downregulated (n=71) at both time points (Figure 2.9). Using an enrichment FDR cutoff value of <0.05, there were 769 enriched GO terms in the common upregulated DEG dataset and 32 enriched terms in the common downregulated DEG dataset. The top enriched common upregulated GO terms by FDR included "*leukocyte mediated immunity*", "*myeloid leukocyte activation*", and "*positive regulation of cytokine production*" (Figure 2.9A). The top three genes upregulated at both time points, associated with the top ten GO terms, were *Cxcl13*, *Cxcl10*, and *RT1-Da* (Figure 2.9C, D). The top enriched common downregulated GO terms by FDR included "*regulation of neurotransmitter levels*", "*regulation of clathrin-dependent endocytosis*", and "*synaptic vesicle cycle*" (Figure 2.9B). The top three genes downregulated at both time points, associated with the top ten GO terms, were *Fkbp2b*, *Cntnap1* and *Thy1* (Figure 2.9E, F).

Most of the enriched upregulated GO terms common to both time points were associated with immune responses (Figure 2.9A). To further appreciate whether

enrichment of any immune-related GO term was unique to either time point we performed a GO: Biological Processes enrichment analysis for the DEGs uniquely upregulated at one (n=1169) and two months (n=250) (Figure 2.10). The top enriched GO terms from the unique one-month upregulated DEGs included "*ribosome biogenesis*", "*ribonucleoprotein complex biogenesis*" and "*rRNA processing*" (Figure 2.10A). The top three genes uniquely upregulated at one month, associated with the top ten GO terms, were *Lcn2, Apobec1,* and *Ccl2* (Figure 2.10B). The top enriched GO terms from the unique two-month upregulated DEGs included "*response to virus*", "*defense response to symbiont*", and "*defense response to virus*" (Figure 2.10C). The top three genes uniquely upregulated at two months, associated with the top ten GO terms, were *Zbp1, Slamf9,* and Clec7a (Figure 2.10D) with *Zbp1* associated with all top 3 GO terms. Collectively, using both KEGG and GO enrichment analyses, our results reveal upregulation of DEGs associated with cytokine production, microglial activation, ribosomal biogenesis, RNA processing and protein degradation at the one-month time point in the inclusion-bearing SNpc. At the two-month time point, continued upregulation of DEGs associated with cytokine production and microglial activation is observed, however DEGs associated with the activation of specific defense responses to virus also become upregulated. Across both time points our analyses suggest that downregulation of DEGs involved in cell signaling, neurotransmitter synthesis and synaptic transmission.

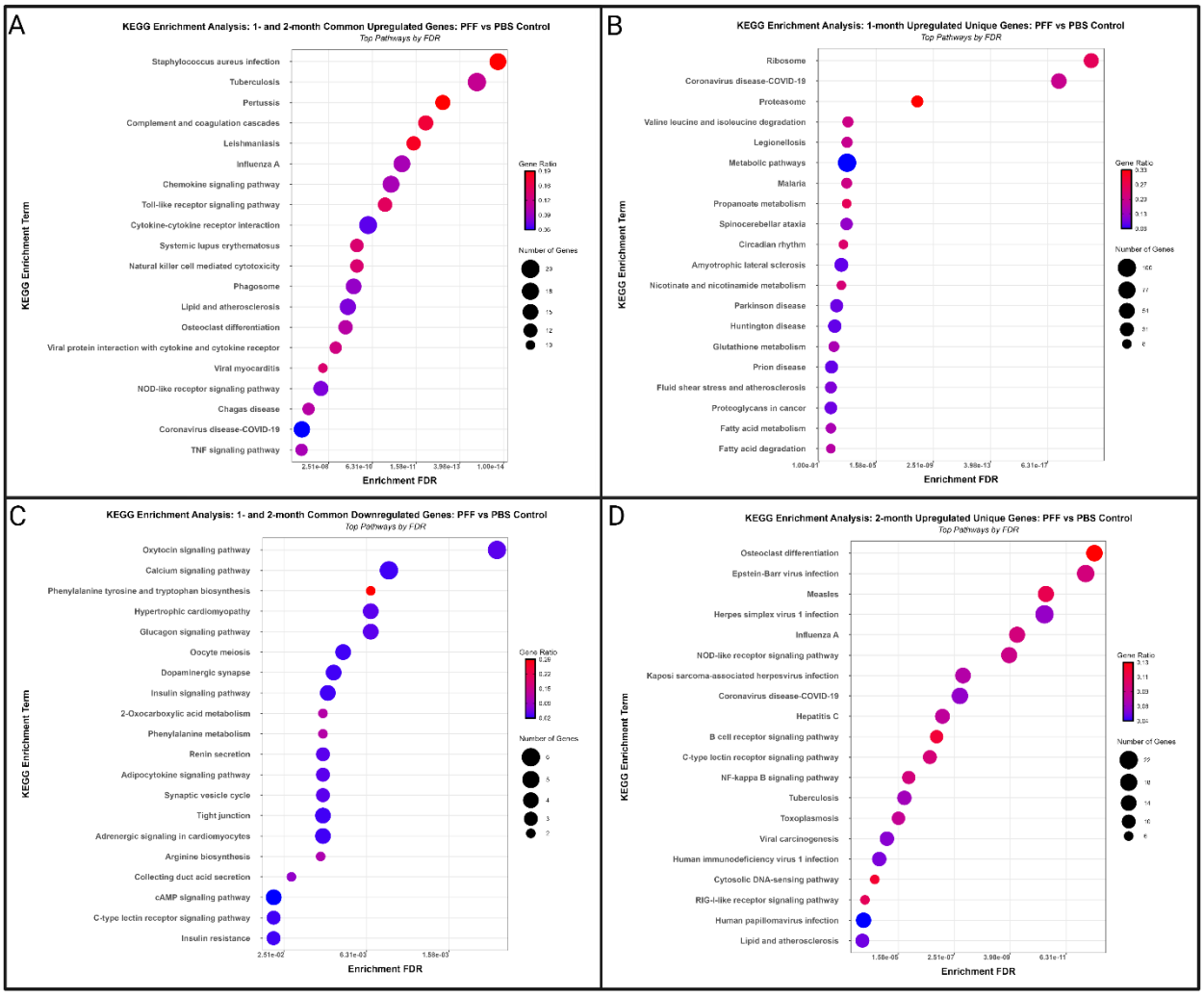

Figure 2.8 KEGG enrichment analysis of PFF induced DEGs common or unique to one and two months

(A,C) KEGG enrichment analysis of upregulated **(A)** or downregulated **(C)** DEGs common to both one and two months. **(B)** KEGG enrichment analysis of DEGs uniquely upregulated at one month. **(D)** KEGG enrichment analysis of DEGs uniquely upregulated at two months.

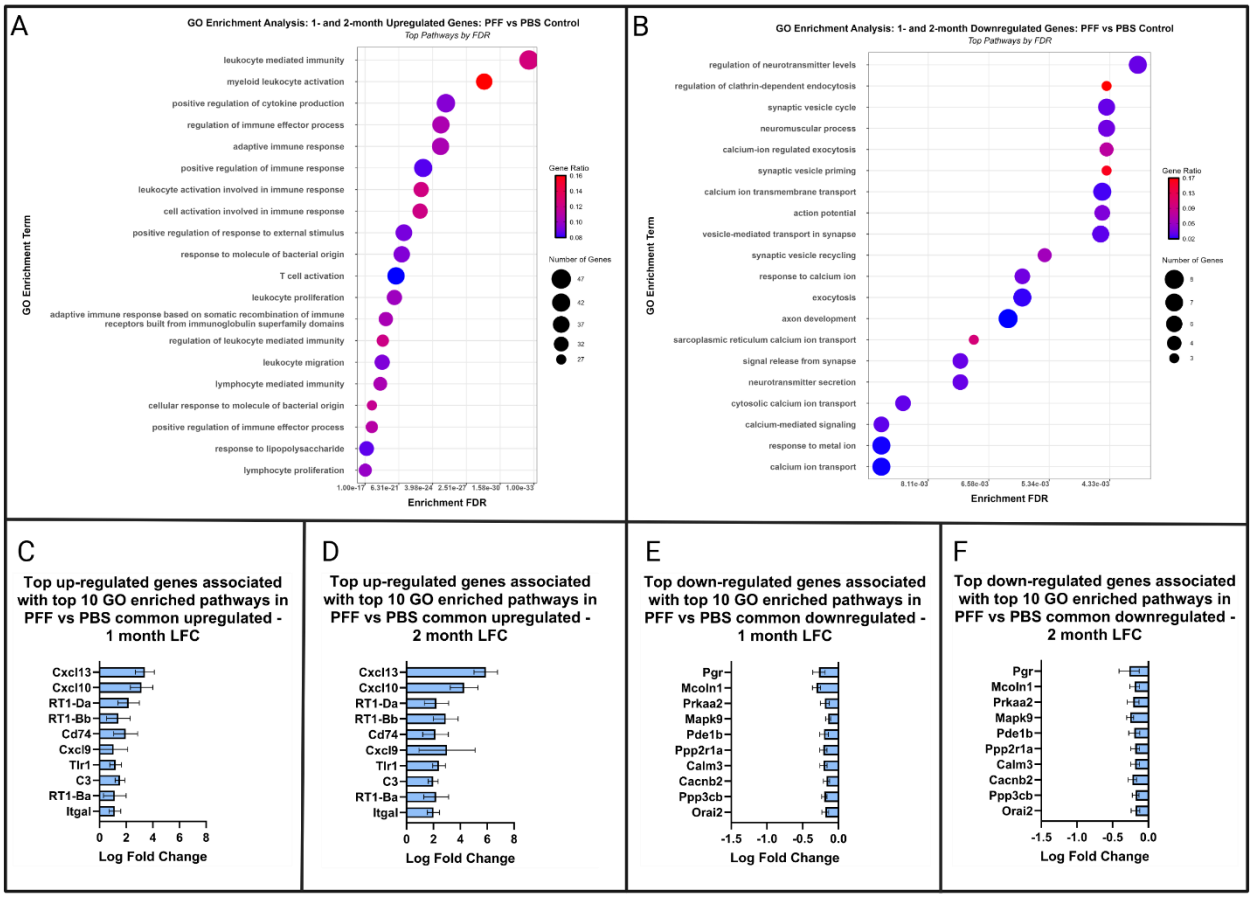

Figure 2.9 Gene Ontology (GO) enrichment analysis of PFF induced DEGs common to both time points

(A) GO enrichment analysis of upregulated DEGs common to both one and two months. **(B)** GO enrichment analysis of upregulated DEGs common to both one and two months. **(C)** Top ten common upregulated genes at one month. **(D)** Top ten common upregulated genes at two months. **(E)** Top ten common downregulated genes at one month. **(F)** Top ten common downregulated genes at two months. The top ten genes (log fold change) from the top ten GO enrichment terms (FDR) were used. Error bars represent SEM.

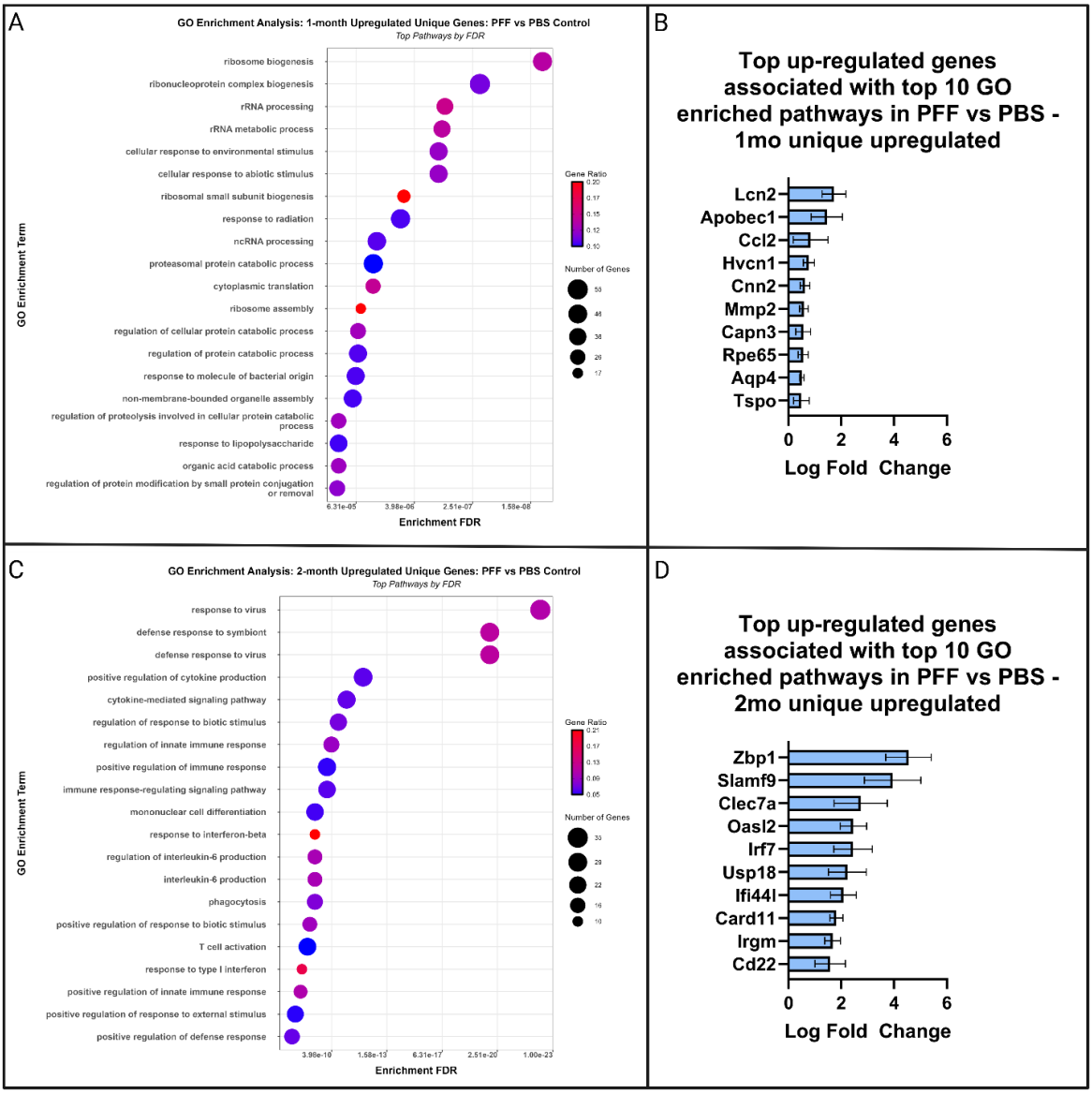

Figure 2.10 Gene Ontology (GO) enrichment analysis of PFF induced DEGs unique to each time point

(A) GO enrichment analysis of upregulated DEGs unique to the one month time point. **(B)** Top ten upregulated genes unique to one month. **(C)** GO enrichment analysis of upregulated DEGs unique to the two month time point. **(D)** Top ten upregulated genes unique to the 2 month time point. The top ten genes (log fold change) from the top ten GO enrichment terms (FDR) were used. Error bars represent SEM.

DISCUSSION

In a previous study we investigated the transcriptomic response in the SNpc at a single time point - two months following intrastriatal PFF injection (J. Patterson et al., 2024). We observed upregulated immune response transcripts at the two-month timepoint, whereas downregulated transcripts were associated with neurotransmission and the dopamine pathway. In the present study we broadened our approach to investigate whether differential gene expression associated with inclusion accumulation in the SNpc is temporally dynamic. At one and two months following PFF injection, rats display an equivalent number of pSyn containing nigral neurons (Duffy et al., 2018; Miller et al., 2021). However, *in vitro* and *in vivo* data suggest that αSyn inclusions at two months should be relatively more mature and LB-like compared to one month (Duffy et al., 2018; Mahul-Mellier et al., 2020; J. R. Patterson, Duffy, et al., 2019). Thus, in the present experiment we leveraged these two time points to compare differential gene expression. Although we initially intended to use two surgical control groups for comparison, PBS, and monomer, our PCA results revealed that DGE of the monomer group had a bimodal distribution, clustering with either PBS or PFF injected rats. Our data suggests that this may be related to the length of time between monomer preparation and surgical injection and will be the focus of further study. Until the optimal time parameters are identified we do not recommend the use of monomer preparations as a control condition. Therefore, in the present study we examined differential gene expression between PFF and PBS injected rats within each time point and as well as differential gene expression common to both time points. Lastly, to investigate whether enrichment of any immune-related process was unique to either time point, we focused

our analysis on DEGs uniquely upregulated at one or two months. Overall, we find that the one-month inclusion bearing SNpc is associated with more differential gene expression compared to two months. At one month, the number of DEGs is mostly downregulated, whereas at the two-month time point the number of DEGs is primarily upregulated. We also observe that the magnitude of upregulation of DEGs is greater at two months compared to one month. Upregulation of DEGs associated with increased cytokine production and microglial activation, and downregulation of DEGs associated with cell signaling, neurotransmitter synthesis, and synaptic transmission was revealed to be common across both time points. The one-month time point is specifically associated with upregulation of DEGs associated with ribosomal biogenesis, RNA processing and protein degradation. In contrast, the later two-month time point is specifically associated with the upregulation of DEGs implicating activation of defense responses to viruses to protect the host.

We observed downregulation of DEGs associated with cell signaling, neurotransmitter synthesis, and synaptic transmission across both time points. KEGG enrichment analysis of DEGs in the inclusion-bearing SNpc at one month implicate downregulation of the pathways associated with cholinergic, glutamatergic, and dopaminergic synapses, suggesting an early and direct detrimental effect of neuronal pSyn inclusions on neurotransmission. Although the SNpc is primarily composed of DA neurons, there are cholinergic and glutamatergic projections that innervate the SNpc. The cholinergic, glutamatergic, and dopaminergic pathways identified by the KEGG enrichment analysis contain genes that are ubiquitously expressed by neurons such as *Gnb2*, *Camk2b*, and *Mapk* genes. Additionally, each pathway contains genes that are

specific to their respective neurotransmitter type, including *Th* and *Slc6a3* (DAT) in the DA pathway, *Chrn* (nicotinic acetylcholine receptor subunits), *Chrm* (muscarinic acetylcholine receptor subunits) genes in the cholinergic pathway, and *Gria* (AMPA receptor subunits), *Grik* (Kainate receptor subunits), and *Grin* (NMDA receptor subunits) genes in the glutamatergic pathway. This suggests there is general synaptic dysfunction specific to neural connections in the SNpc associated with early inclusion formation, and is in agreement with our previous results examining transcriptomic differences at the 2-month time point only (J. Patterson et al., 2024). Interestingly, in the present study we were able to detect downregulation of both *Th,* which encodes tyrosine hydroxylase (rate limiting step in dopamine synthesis) and *Slc6a3,* which encodes the dopamine transporter, at one month but not at two. In our previous study (J. Patterson et al., 2024), significant downregulation of both *Th* and *Slc6a3* was detected in the inclusion-bearing SN at two months using droplet digital PCR in wild type rats. This discrepancy could be due to the rat species used, or sensitivity of methodology, or both. The most downregulated DEG in the inclusion-bearing SNpc at the one-month time point was *Scube1*, which encodes for Signal peptide, CUB domain, and EGF-like domain-containing protein 1, a protein expressed by platelets and endothelial cells (Tu *et al.*, 2008) that is activated by inflammation (Bouter et al., 2014). The most downregulated gene at two months was *Alox5,* which encodes for arachidonate 5-lipoxygenase (5-LOX), a key enzyme in leukotriene biosynthesis that is expressed by both neurons and microglia, that contributes to inflammatory processes (Rådmark et al., 2015). Of note, 5-LOX downregulation has been associated with immunosuppression, impaired innate immune response, reduced phagocytic capability, and reduced production of other

inflammatory mediators such as cytokines and/or chemokines (Peters-Golden et al., 2005). The downregulation of pro-inflammatory genes such as *Scube1* and *Alox5* in association with SNpc inclusions may reflect an attempt to counteract the upregulation of pro-inflammatory responses.

We observed a striking upregulation of DEGs associated with cytokine production and microglial activation in the pSyn inclusion-bearing SNpc across both time points examined. KEGG enrichment analyses identified DEGs associated with bacterial, viral, and parasitic infections, complement and coagulation cascades, cytokine-cytokine receptor interaction, chemokine signaling and toll-like receptor signaling pathways. GO enrichment highlights the upregulation of DGEs involved in the biological processes of leukocyte mediated immunity and activation, cytokine production, and the adaptive immune response at both one and two months. The top upregulated genes associated with the top ten GO enriched pathways across both one and two months were the chemokines *Cxcl13, Cxcl10*, genes involved in antigen processing*, RT1-Da, RT1-Bb (*both encode components of the MHC-II complex*)* and *Cd74*. We have previously observed upregulation of *Cd74* mRNA and MHC-II protein in activated microglia immediately adjacent to pSyn inclusions in the SNpc at two months (Duffy et al., 2018; Stoll, Kemp, Patterson, Howe, et al., 2024). One of the most consistent observations in postmortem PD tissue is an increased expression of MHC-II on microglia adjacent to LB deposition (Croisier et al., 2005; Imamura et al., 2003). Interestingly, upregulation of Rt1-Bb (component of MHC-II) is detectable in the inclusion-bearing SNpc at 1 month using RNA sequencing, whereas we do not observe protein expression of MHC-II via immunohistochemistry (IHC) until 2 months (Duffy et

al., 2018), perhaps suggesting a delay between mRNA and adequate protein expression for IHC labeling.

We observed a unique pattern of upregulated expression when examining DEGs unique to either the one- or two-month time point. At one month the upregulation of DEGs associated with ribosomal biogenesis, RNA processing and protein degradation were uniquely enriched. This suggests that pSyn containing neurons and/or neighboring microglia, astrocytes or other cell types are rapidly increasing mRNA and protein synthesis during the early stages of pSyn inclusion formation. In addition, we found that the later two-month time point is specifically associated with the upregulation of DEGs implicating activation of defense responses to viruses to protect the host. This suggests that microglia may be responding to pSyn inclusion formation by engaging specific antiviral responses. KEGG enrichment analysis conducted on unique two-month upregulated DEGs suggest that microglia may respond to pSyn inclusion-bearing neurons in a similar manner as the response to Epstein-Barr, Measles, Herpes simplex virus 1, Influenza or Coronavirus. Microglial response to virus involves increased expression of the proinflammatory cytokines interleukin-6 (IL-6), tumor necrosis factor-alpha (TNFα), and interleukin-1beta (IL-1ß) (Barrios-González et al., 2024). IL-6, IL-1ß and TNFα are upregulated in the brain, CSF and blood of PD subjects (Stoll & Sortwell, 2022) and TNFα and IL-1ß mRNA are upregulated in inclusion-bearing SNpc in the PFF model (Stoll & Sortwell, 2022). Microglial response to virus also involves phagocytosis of infected cells. The top gene uniquely upregulated at two months, associated with the top ten GO terms, was *Zbp1*. ZBP1 encodes Z-DNA binding protein 1 which activates neighboring microglia & astrocytes via the cyclic GMP-AMP synthase (cGAS)/stimulator

of interferon genes (STING) immune pathway (X.-Y. Chen et al., 2022). Upregulation of STING is detected in the PD SNpc and blockade or genetic deletion of STING prevents neurodegeneration in the mouse αSyn PFF model (Hinkle et al., 2022). ZBP-1 is a master regulator of PANoptosis (W. Chen et al., 2023; Hao et al., 2022), sensing of viral infection by ZBP-1 ultimately leads to the elimination of infected cells (Upton & Kaiser, 2017). The upregulation of viral response pathways combined with the 4.5 log2FC of *Zbp1* in the inclusion-bearing SNpc occurs distinctly at two months. This suggests that the ZBP-1/cGas/STING pathway may play a critical role in the nigral neuron degeneration that begins to take place in the PFF model starting after the two-month peak of pSyn aggregation (Duffy et al., 2018; J. R. Patterson, Duffy, et al., 2019).

In a study conducted by Mathys and colleagues (Mathys et al., 2017) single-cell RNA sequencing was used to examine the transcriptome of microglia at varying stages of Aß accumulation and degeneration in the hippocampus of CK-p25 mice. Distinct stage-specific microglial phenotypes were identified that were associated with either early stages of the pathology progression (Aß accumulation, DNA damage) or late stages (neuronal loss). In our rat αSyn PFF model the one- and two-month time points in the SNpc are most analogous to the early stages of the CK-p25 mouse model. However, comparisons of top GO terms reported by Mathys et al. in the early response microglial phenotype revealed little overlap with our one- or two-month top GO terms. Rather, the GO terms and upregulated microglial late response genes, associated with neuronal death revealed significant overlap in the top GO terms we uncovered, including “*translation*”, “*immune system process*”, “*defense response to virus*”, “*innate immune response*” and “*response to virus*”. Further, many of the most highly

upregulated DEGs in our dataset overlap with the late response microglial DEGs reported by Mathys et al., including *Cd74*, *C3*, *Rt1-Da*, *Rt1-Bb*, *Clec7a*, *Ifit2* and *Oasl2*. The discordance in our findings and the findings of Mathys et al. may be due to the difference in methodologies, perhaps because our LCM RNAseq approach was not sensitive enough to detect the full range of changes in microglial gene expression. It is noted however that using in microglial-specific *in situ* hybridization we can detect upregulation of Cd74, C3, and Rt1-Bb at 2 months in the rat PFF model (Stoll, Kemp, Patterson, Howe, et al., 2024), prior to SNpc degeneration (Duffy et al., 2018; J. R. Patterson, Duffy, et al., 2019). Alternatively, DGEs related to "*translation*", "*DNA replication*", and "*chromosome segregation*" that were defining GO terms in the Mathys et al. early microglial response may be specific to the CK-p25 driven AD mouse model though p25/Cdk5 induced DNA damage. Microglial states are context dependent and what is observed in one disease model is likely dependent on the specific pathogen or insult (Paolicelli et al., 2022).

At both the one- and two-month time point, we observed that genes for many members of the cathepsin family were differentially expressed in inclusion-bearing SNpc. A total of fourteen cathepsins are expressed in rodents (Vizovišek et al., 2019), twelve of which were detected using RNAseq within the rat SNpc. Of the twelve cathepsins, seven are significantly upregulated at the one-month timepoint (*Ctsb, Ctsc, Ctse, Ctsh, Ctsl, Ctss,* and *Ctsz/x/p*), and five are significantly upregulated at the 2-month timepoint (*Ctsc, Ctse, Ctsh, Ctss,* and *Ctsz/x/p*). In addition, both *Ctsc* and *Ctsh* are associated with the Top GO term identified using DEGs upregulated at both one and two months. Cathepsins are of interest in terms of their function as the 'executioners' of

the lysosomal system, and are contained within exosomes, endosomes, lysosomes, and autophagosomes where they participate in functions that include protein degradation, antigen processing, autophagy and apoptosis (Yadati et al., 2020). Further, *Ctsl* has been shown to be efficient in degradation of alpha-synuclein oligomers and fibrils *in-vitro* (McGlinchey & Lee, 2015; McGlinchey et al., 2017). Interestingly, at one month, the upregulated DEG with the lowest padj value was *Cst3,* which encodes for cystatin C. Cystatin C functions as a protease inhibitor that primarily inhibits cathepsin B, H, L, and S, and has been associated with β-amyloid depositions in post-mortem Alzheimer's disease (AD) brains (Stańczykiewicz et al., 2024). Taken together, our dataset suggests a role for cathepsins and regulation of cathepsins in the pSyn inclusion-bearing SNpc.

The limitations of the present study include a lack of validation of mRNA expression changes, lack of validation of protein changes, and a lack of cellular localization of transcriptional changes. While RNAseq is an excellent tool to comprehensively measure differential gene expression, confirmation of these changes with complementary approaches like PCR would strengthen our findings. There are technical limitations with RNAseq (library preparation bias, PCR amplification bias, and/or sequencing errors (Shi et al., 2021), as well as biological limitations. Due to varying rates of mRNA degradation, varying rates of translation, and the complex relationship between mRNA and protein levels regarding post transcriptional modifications, the biological relevance of transcriptional changes may not have a direct relationship to functional protein output (Buccitelli & Selbach, 2020). Lastly, the lack of information related to spatial resolution of transcriptional changes poses a limitation of

the current study. Alternative methodologies like immunofluorescence (IF), *in situ* hybridization and spatial transcriptomics provide the ability to localize changes to specific cell types (e.g., microglia), as well as to visualize gradient dependent effects. In the following chapter I describe studies in which I use both droplet digital PCR (ddPCR), fluorescent *in situ* hybridization (FISH) and IF to follow up on the expression of multiple cathepsins and microglial-specific cathepsin expression patterns in the inclusion-bearing SN.

The present study is the first to reveal a differential gene expression response to LB-like inclusions in the SNpc over time. Results suggest that cytokine production and microglial activation are upregulated in association with both early and more mature pSyn inclusions. The earlier one-month time point is specifically associated with upregulation of DEGs associated with ribosomal biogenesis, RNA processing and protein degradation whereas the later two-month time point is specifically associated with the upregulation of DEGs implicating microglial activation of defense responses to viruses to protect the host. Downregulation of DEGs associated with cell signaling, neurotransmitter synthesis, and synaptic transmission are to be common across both time points. Collectively, these results suggest that the impact of pSyn inclusions in the SNpc is temporally dynamic. Further, my results support a role for multiple cathepsins over the course of both early and more mature pSyn inclusions. In the next chapter I will validate microglial cathepsin expression in the pSyn inclusion-bearing SNpc at one and two months using the complementary approaches of ddPCR, *in situ* hybridization and immunofluorescence.

BIBLIOGRAPHY

Abdelmotilib, H., Maltbie, T., Delic, V., Liu, Z., Hu, X., Fraser, K. B., Moehle, M. S., Stoyka, L., Anabtawi, N., Krendelchtchikova, V., Volpicelli-Daley, L. A., & West, A. (2017). α-Synuclein fibril-induced inclusion spread in rats and mice correlates with dopaminergic Neurodegeneration. *Neurobiology of Disease*, *105*, 84–98. https://doi.org/10.1016/j.nbd.2017.05.014

Ashburner, M., Ball, C. A., Blake, J. A., Botstein, D., Butler, H., Cherry, J. M., Davis, A. P., Dolinski, K., Dwight, S. S., Eppig, J. T., Harris, M. A., Hill, D. P., Issel-Tarver, L., Kasarskis, A., Lewis, S., Matese, J. C., Richardson, J. E., Ringwald, M., Rubin, G. M., & Sherlock, G. (2000). Gene Ontology: Tool for the unification of biology. *Nature Genetics*, *25*(1), 25–29. https://doi.org/10.1038/75556

Barrios-González, D. A., Philibert-Rosas, S., Martínez-Juárez, I. E., Sotelo-Díaz, F., Rivas-Alonso, V., Sotelo, J., & Sebastián-Díaz, M. A. (2024). Frequency and Focus of in Vitro Studies of Microglia-Expressed Cytokines in Response to Viral Infection: A Systematic Review. *Cellular and Molecular Neurobiology*, *44*(1), 21. https://doi.org/10.1007/s10571-024-01454-9

Bouter, Y., Kacprowski, T., Weissmann, R., Dietrich, K., Borgers, H., Brauß, A., Sperling, C., Wirths, O., Albrecht, M., Jensen, L. R., Kuss, A. W., & Bayer, T. A. (2014). Deciphering the molecular profile of plaques, memory decline and neuron loss in two mouse models for Alzheimer's disease by deep sequencing. *Frontiers in Aging Neuroscience*, *6*, 75. https://doi.org/10.3389/fnagi.2014.00075

Buccitelli, C., & Selbach, M. (2020). mRNAs, proteins and the emerging principles of gene expression control. *Nature Reviews. Genetics*, *21*(10), 630–644. https://doi.org/10.1038/s41576-020-0258-4

Chen, W., Gullett, J. M., Tweedell, R. E., & Kanneganti, T.-D. (2023). Innate immune inflammatory cell death: PANoptosis and PANoptosomes in host defense and disease. *European Journal of Immunology*, *53*(11), e2250235. https://doi.org/10.1002/eji.202250235

Chen, X.-Y., Dai, Y.-H., Wan, X.-X., Hu, X.-M., Zhao, W.-J., Ban, X.-X., Wan, H., Huang, K., Zhang, Q., & Xiong, K. (2022). ZBP1-Mediated Necroptosis: Mechanisms and Therapeutic Implications. *Molecules*, *28*(1). https://doi.org/10.3390/molecules28010052

Croisier, E., Moran, L. B., Dexter, D. T., Pearce, R. K. B., & Graeber, M. B. (2005). Microglial inflammation in the parkinsonian substantia nigra: relationship to alpha-synuclein deposition. *Journal of Neuroinflammation*, *2*, 14. https://doi.org/10.1186/1742-2094-2-14

Dobin, A., Davis, C. A., Schlesinger, F., Drenkow, J., Zaleski, C., Jha, S., Batut, P., Chaisson, M., & Gingeras, T. R. (2013). STAR: ultrafast universal RNA-seq aligner. *Bioinformatics*, *29*(1), 15–21. https://doi.org/10.1093/bioinformatics/bts635

Duffy, M. F., Collier, T. J., Patterson, J. R., Kemp, C. J., Luk, K. C., Tansey, M. G., Paumier, K. L., Kanaan, N. M., Fischer, D. L., Polinski, N. K., Barth, O. L., Howe, J. W., Vaikath, N. N., Majbour, N. K., El-Agnaf, O. M. A., & Sortwell, C. E. (2018). Lewy body-like alpha-synuclein inclusions trigger reactive microgliosis prior to nigral degeneration. *Journal of Neuroinflammation*, *15*(1), 129. https://doi.org/10.1186/s12974-018-1171-z

Gene Ontology Consortium, Aleksander, S. A., Balhoff, J., Carbon, S., Cherry, J. M., Drabkin, H. J., Ebert, D., Feuermann, M., Gaudet, P., Harris, N. L., Hill, D. P., Lee, R., Mi, H., Moxon, S., Mungall, C. J., Muruganugan, A., Mushayahama, T., Sternberg, P. W., Thomas, P. D., … Westerfield, M. (2023). The Gene Ontology knowledgebase in 2023. *Genetics*, *224*(1), iyad031. https://doi.org/10.1093/genetics/iyad031

Ge, S. X., Jung, D., & Yao, R. (2020). ShinyGO: a graphical gene-set enrichment tool for animals and plants. *Bioinformatics*, *36*(8), 2628–2629. https://doi.org/10.1093/bioinformatics/btz931

Hao, Y., Yang, B., Yang, J., Shi, X., Yang, X., Zhang, D., Zhao, D., Yan, W., Chen, L., Zheng, H., Zhang, K., & Liu, X. (2022). ZBP1: A Powerful Innate Immune Sensor and Double-Edged Sword in Host Immunity. *International Journal of Molecular Sciences*, *23*(18). https://doi.org/10.3390/ijms231810224

Harrison, P. W., Amode, M. R., Austine-Orimoloye, O., Azov, A. G., Barba, M., Barnes, I., Becker, A., Bennett, R., Berry, A., Bhai, J., Bhurji, S. K., Boddu, S., Branco Lins, P. R., Brooks, L., Ramaraju, S. B., Campbell, L. I., Martinez, M. C., Charkhchi, M., Chougule, K., … Yates, A. D. (2024). Ensembl 2024. *Nucleic Acids Research*, *52*(D1), D891–D899. https://doi.org/10.1093/nar/gkad1049

Hinkle, J. T., Patel, J., Panicker, N., Karuppagounder, S. S., Biswas, D., Belingon, B., Chen, R., Brahmachari, S., Pletnikova, O., Troncoso, J. C., Dawson, V. L., & Dawson, T. M. (2022). STING mediates neurodegeneration and neuroinflammation in nigrostriatal α-synucleinopathy. *Proceedings of the National Academy of Sciences of the United States of America*, *119*(15), e2118819119. https://doi.org/10.1073/pnas.2118819119

Howe, J. W., Sortwell, C. E., Duffy, M. F., Kemp, C. J., Russell, C. P., Kubik, M., Patel, P., Luk, K. C., El-Agnaf, O. M. A., & Patterson, J. R. (2021). Preformed fibrils generated from mouse alpha-synuclein produce more inclusion pathology in rats than fibrils generated from rat alpha-synuclein. *Parkinsonism & Related Disorders*, *89*, 41–47. https://doi.org/10.1016/j.parkreldis.2021.06.010

Imamura, K., Hishikawa, N., Sawada, M., Nagatsu, T., Yoshida, M., & Hashizume, Y. (2003). Distribution of major histocompatibility complex class II-positive microglia and cytokine profile of Parkinson's disease brains. *Acta Neuropathologica*, *106*(6), 518–526. https://doi.org/10.1007/s00401-003-0766-2

Ji, X., Li, P., Fuscoe, J. C., Chen, G., Xiao, W., Shi, L., Ning, B., Liu, Z., Hong, H., Wu, J., Liu, J., Guo, L., Kreil, D. P., Łabaj, P. P., Zhong, L., Bao, W., Huang, Y., He, J., Zhao, Y., … Shi, T. (2020). A comprehensive rat transcriptome built from large scale RNA-seq-based annotation. *Nucleic Acids Research*, *48*(15), 8320–8331. https://doi.org/10.1093/nar/gkaa638

Kanehisa, M, & Goto, S. (2000). KEGG: Kyoto encyclopedia of genes and genomes. *Nucleic Acids Research*, *28*(1), 27–30. https://doi.org/10.1093/nar/28.1.27

Kanehisa, Minoru, Furumichi, M., Sato, Y., Kawashima, M., & Ishiguro-Watanabe, M. (2023). KEGG for taxonomy-based analysis of pathways and genomes. *Nucleic Acids Research*, *51*(D1), D587–D592. https://doi.org/10.1093/nar/gkac963

Kanehisa, Minoru. (2019). Toward understanding the origin and evolution of cellular organisms. *Protein Science*, *28*(11), 1947–1951. https://doi.org/10.1002/pro.3715

Liu, X., Zhao, J., Xue, L., Zhao, T., Ding, W., Han, Y., & Ye, H. (2022). A comparison of transcriptome analysis methods with reference genome. *BMC Genomics*, *23*(1), 232. https://doi.org/10.1186/s12864-022-08465-0

Love, M. I., Huber, W., & Anders, S. (2014). Moderated estimation of fold change and dispersion for RNA-seq data with DESeq2. *Genome Biology*, *15*(12), 550. https://doi.org/10.1186/s13059-014-0550-8

Luk, K. C., Kehm, V. M., Zhang, B., O'Brien, P., Trojanowski, J. Q., & Lee, V. M. Y. (2012). Intracerebral inoculation of pathological α-synuclein initiates a rapidly progressive neurodegenerative α-synucleinopathy in mice. *The Journal of Experimental Medicine*, *209*(5), 975–986. https://doi.org/10.1084/jem.20112457

Mahul-Mellier, A.-L., Burtscher, J., Maharjan, N., Weerens, L., Croisier, M., Kuttler, F., Leleu, M., Knott, G. W., & Lashuel, H. A. (2020). The process of Lewy body formation, rather than simply α-synuclein fibrillization, is one of the major drivers of neurodegeneration. *Proceedings of the National Academy of Sciences of the United States of America*, *117*(9), 4971–4982. https://doi.org/10.1073/pnas.1913904117

Mathys, H., Adaikkan, C., Gao, F., Young, J. Z., Manet, E., Hemberg, M., De Jager, P. L., Ransohoff, R. M., Regev, A., & Tsai, L.-H. (2017). Temporal Tracking of Microglia Activation in Neurodegeneration at Single-Cell Resolution. *Cell Reports*, *21*(2), 366–380. https://doi.org/10.1016/j.celrep.2017.09.039

McGlinchey, R. P., Dominah, G. A., & Lee, J. C. (2017). Taking a Bite Out of Amyloid: Mechanistic Insights into α-Synuclein Degradation by Cathepsin L. *Biochemistry*, *56*(30), 3881–3884. https://doi.org/10.1021/acs.biochem.7b00360

McGlinchey, R. P., & Lee, J. C. (2015). Cysteine cathepsins are essential in lysosomal degradation of α-synuclein. *Proceedings of the National Academy of Sciences of the United States of America*, *112*(30), 9322–9327. https://doi.org/10.1073/pnas.1500937112

Miller, K. M., Patterson, J. R., Kochmanski, J., Kemp, C. J., Stoll, A. C., Onyekpe, C. U., Cole-Strauss, A., Steece-Collier, K., Howe, J. W., Luk, K. C., & Sortwell, C. E. (2021). Striatal afferent BDNF is disrupted by synucleinopathy and partially restored by STN DBS. *The Journal of Neuroscience*, *41*(9), 2039–2052. https://doi.org/10.1523/JNEUROSCI.1952-20.2020

Paolicelli, R. C., Sierra, A., Stevens, B., Tremblay, M.-E., Aguzzi, A., Ajami, B., Amit, I., Audinat, E., Bechmann, I., Bennett, M., Bennett, F., Bessis, A., Biber, K., Bilbo, S., Blurton-Jones, M., Boddeke, E., Brites, D., Brône, B., Brown, G. C., … Wyss-Coray, T. (2022). Microglia states and nomenclature: A field at its crossroads. *Neuron*, *110*(21), 3458–3483. https://doi.org/10.1016/j.neuron.2022.10.020

Patro, R., Duggal, G., Love, M. I., Irizarry, R. A., & Kingsford, C. (2017). Salmon provides fast and bias-aware quantification of transcript expression. *Nature Methods*, *14*(4), 417–419. https://doi.org/10.1038/nmeth.4197

Patterson, J., Kochmanski, J., Stoll, A., Kubik, M., Kemp, C., Duffy, M., Thompson, K., Howe, J., Cole-Strauss, A., Kuhn, N., Miller, K., Nelson, S., Onyekpe, C., Beck, J., Counts, S., Bernstein, A., Steece-Collier, K., Luk, K., & Sortwell, C. (2024). Transcriptomic Profiling of Early Synucleinopathy in Rats Induced with Preformed Fibrils. *Research Square*. https://doi.org/10.21203/rs.3.rs-3253289/v1

Patterson, J. R., Duffy, M. F., Kemp, C. J., Howe, J. W., Collier, T. J., Stoll, A. C., Miller, K. M., Patel, P., Levine, N., Moore, D. J., Luk, K. C., Fleming, S. M., Kanaan, N. M., Paumier, K. L., El-Agnaf, O. M. A., & Sortwell, C. E. (2019). Time course and magnitude of alpha-synuclein inclusion formation and nigrostriatal degeneration in the rat model of synucleinopathy triggered by intrastriatal α-synuclein preformed fibrils. *Neurobiology of Disease*, *130*, 104525. https://doi.org/10.1016/j.nbd.2019.104525

Patterson, J. R., Polinski, N. K., Duffy, M. F., Kemp, C. J., Luk, K. C., Volpicelli-Daley, L. A., Kanaan, N. M., & Sortwell, C. E. (2019). Generation of Alpha-Synuclein Preformed Fibrils from Monomers and Use In Vivo. *Journal of Visualized Experiments*, *148*. https://doi.org/10.3791/59758

Paumier, K. L., Luk, K. C., Manfredsson, F. P., Kanaan, N. M., Lipton, J. W., Collier, T. J., Steece-Collier, K., Kemp, C. J., Celano, S., Schulz, E., Sandoval, I. M., Fleming, S., Dirr, E., Polinski, N. K., Trojanowski, J. Q., Lee, V. M., & Sortwell, C. E. (2015).

Intrastriatal injection of pre-formed mouse α-synuclein fibrils into rats triggers α-synuclein pathology and bilateral nigrostriatal degeneration. *Neurobiology of Disease*, *82*, 185–199. https://doi.org/10.1016/j.nbd.2015.06.003

Peters-Golden, M., Canetti, C., Mancuso, P., & Coffey, M. J. (2005). Leukotrienes: underappreciated mediators of innate immune responses. *Journal of Immunology*, *174*(2), 589–594. https://doi.org/10.4049/jimmunol.174.2.589

Polinski, N. K., Volpicelli-Daley, L. A., Sortwell, C. E., Luk, K. C., Cremades, N., Gottler, L. M., Froula, J., Duffy, M. F., Lee, V. M. Y., Martinez, T. N., & Dave, K. D. (2018). Best Practices for Generating and Using Alpha-Synuclein Pre-Formed Fibrils to Model Parkinson's Disease in Rodents. *Journal of Parkinson's Disease*, *8*(2), 303–322. https://doi.org/10.3233/JPD-171248

Rådmark, O., Werz, O., Steinhilber, D., & Samuelsson, B. (2015). 5-Lipoxygenase, a key enzyme for leukotriene biosynthesis in health and disease. *Biochimica et Biophysica Acta*, *1851*(4), 331–339. https://doi.org/10.1016/j.bbalip.2014.08.012

Reimand, J., Isserlin, R., Voisin, V., Kucera, M., Tannus-Lopes, C., Rostamianfar, A., Wadi, L., Meyer, M., Wong, J., Xu, C., Merico, D., & Bader, G. D. (2019). Pathway enrichment analysis and visualization of omics data using g:Profiler, GSEA, Cytoscape and EnrichmentMap. *Nature Protocols*, *14*(2), 482–517. https://doi.org/10.1038/s41596-018-0103-9

Schaarschmidt, S., Fischer, A., Zuther, E., & Hincha, D. K. (2020). Evaluation of Seven Different RNA-Seq Alignment Tools Based on Experimental Data from the Model Plant Arabidopsis thaliana. *International Journal of Molecular Sciences*, *21*(5). https://doi.org/10.3390/ijms21051720

Schneider, C. A., Rasband, W. S., & Eliceiri, K. W. (2012). NIH Image to ImageJ: 25 years of image analysis. *Nature Methods*, *9*(7), 671–675. https://doi.org/10.1038/nmeth.2089

Shi, H., Zhou, Y., Jia, E., Pan, M., Bai, Y., & Ge, Q. (2021). Bias in RNA-seq Library Preparation: Current Challenges and Solutions. *BioMed Research International*, *2021*, 6647597. https://doi.org/10.1155/2021/6647597

Soneson, C., Love, M. I., & Robinson, M. D. (2015). Differential analyses for RNA-seq: transcript-level estimates improve gene-level inferences. [version 2; peer review: 2 approved]. *F1000Research*, *4*, 1521. https://doi.org/10.12688/f1000research.7563.2

Stańczykiewicz, B., Łuc, M., Banach, M., & Zabłocka, A. (2024). Cystatins: unravelling the biological implications for neuroprotection. *Archives of Medical Science : AMS*, *20*(1), 157–166. https://doi.org/10.5114/aoms/171706

Stoll, A. C., Kemp, C. J., Patterson, J. R., Howe, J. W., Steece-Collier, K., Luk, K. C., Sortwell, C. E., & Benskey, M. J. (2024). Neuroinflammatory gene expression profiles of reactive glia in the substantia nigra suggest a multidimensional immune response to alpha synuclein inclusions. *Neurobiology of Disease*, *191*, 106411. https://doi.org/10.1016/j.nbd.2024.106411

Stoll, A. C., Kemp, C. J., Patterson, J. R., Kubik, M., Kuhn, N., Benskey, M., Duffy, M. F., Luk, K. C., & Sortwell, C. E. (2024). Alpha-synuclein inclusion responsive microglia are resistant to CSF1R inhibition. *Journal of Neuroinflammation*, *21*(1), 108. https://doi.org/10.1186/s12974-024-03108-5

Stoll, A. C., & Sortwell, C. E. (2022). Leveraging the preformed fibril model to distinguish between alpha-synuclein inclusion- and nigrostriatal degeneration-associated immunogenicity. *Neurobiology of Disease*, *171*, 105804. https://doi.org/10.1016/j.nbd.2022.105804

Tarutani, A., Suzuki, G., Shimozawa, A., Nonaka, T., Akiyama, H., Hisanaga, S.-I., & Hasegawa, M. (2016). The Effect of Fragmented Pathogenic α-Synuclein Seeds on Prion-like Propagation. *The Journal of Biological Chemistry*, *291*(36), 18675–18688. https://doi.org/10.1074/jbc.M116.734707

Tyner, C., Barber, G. P., Casper, J., Clawson, H., Diekhans, M., Eisenhart, C., Fischer, C. M., Gibson, D., Gonzalez, J. N., Guruvadoo, L., Haeussler, M., Heitner, S., Hinrichs, A. S., Karolchik, D., Lee, B. T., Lee, C. M., Nejad, P., Raney, B. J., Rosenbloom, K. R., … Kent, W. J. (2017). The UCSC Genome Browser database: 2017 update. *Nucleic Acids Research*, *45*(D1), D626–D634. https://doi.org/10.1093/nar/gkw1134

Upton, J. W., & Kaiser, W. J. (2017). DAI another way: necroptotic control of viral infection. *Cell Host & Microbe*, *21*(3), 290–293. https://doi.org/10.1016/j.chom.2017.01.016

Vizovišek, M., Fonović, M., & Turk, B. (2019). Cysteine cathepsins in extracellular matrix remodeling: Extracellular matrix degradation and beyond. *Matrix Biology*, *75–76*, 141–159. https://doi.org/10.1016/j.matbio.2018.01.024

Volpicelli-Daley, L. A., Luk, K. C., Patel, T. P., Tanik, S. A., Riddle, D. M., Stieber, A., Meaney, D. F., Trojanowski, J. Q., & Lee, V. M.-Y. (2011). Exogenous α-synuclein fibrils induce Lewy body pathology leading to synaptic dysfunction and neuron death. *Neuron*, *72*(1), 57–71. https://doi.org/10.1016/j.neuron.2011.08.033

Yadati, T., Houben, T., Bitorina, A., & Shiri-Sverdlov, R. (2020). The ins and outs of cathepsins: physiological function and role in disease management. *Cells*, *9*(7). https://doi.org/10.3390/cells9071679

CHAPTER 3: VALIDATION AND LOCALIZATION OF THE MICROGLIAL TRANSCRIPTIONAL RESPONSE TO A-SYN INCLUSIONS

INTRODUCTION

Cathepsins are a family of proteases that play crucial roles in multiple physiological and pathological processes (Yadati et al. 2020; Reiser, Adair, and Reinheckel 2010). Cathepsins were originally identified as lysosomal enzymes that participate in intracellular protein degradation, their name derived from the Greek work “kathepsein” which means “to digest”. However, recent advances have suggested a more diverse role for cathepsins in extralysosomal locations, including the nucleus, cytosol and extracellular space (Vizovišek, Fonović, and Turk 2019). Cathepsins are categorized into three groups based on the amino acids expressed at their active site: cysteine cathepsins (B, C, F, H, K, L, O, S, V, W, and X), aspartic cathepsins (D and E), and serine cathepsins (A and G). There are 15 cathepsins expressed in human, and 14 cathepsins expressed in rat, with cathepsin V being absent in rodents (V. Turk et al. 2012). Most cathepsins are expressed ubiquitously (e.g. B, H, L, X), whereas the expression of some cathepsins (e.g. S, W) is limited to immune cells (Brix et al. 2008; Vizovišek et al. 2019; Stoeckle et al. 2009; Honey and Rudensky 2003).

The structural composition of cathepsins determine their specific function and specialty. For example, cathepsins F, K, L, and S are examples of endopeptidases that cleave peptide bonds located internally within protein structures, whereas cathepsins B, H, and X are examples of exopeptidases, that cleave N- or C-terminus regions (V. Turk et al. 2012). Cathepsins can also express loops or mini loops near their active site that determines whether they are capable of cleaving single amino acids or multiple amino acids, called dipeptidases. Cathepsin activity is also heavily dependent on the pH of their environment. Cathepsins primarily exist and are most active in acidic, low pH,

environments. However, there are some cathepsins that are still stable and active outside of the optimal pH of 5.0. For example, cathepsin S has an optimal pH of 6.5, while cathepsin D has an optimal pH of 4.0 but is still stable at pH 7.4 (Yadati et al. 2020). Although most cathepsins require and prefer an acidic environment, there is still a wide range of pH's at which cathepsins can operate. This is related with the wide array of physiological functions that cathepsins perform within and outside of the cell.

Increasing evidence suggests a role for cathepsins in both neurons and microglia in the context of PD. Cathepsins B, K and L are particularly effective in degrading alpha-synuclein (α-Syn), with cathepsin K the most potent in degrading α-Syn fibrils (McGlinchey et al. 2020; McGlinchey and Lee 2015). The C-terminal truncated fibrils that result from cathepsin cleavage are found to be enriched in Lewy bodies (Baba et al. 1998). Of interest, variants in the *Ctsb* gene, which can lead to altered activity of cathepsin B, are considered PD risk factors (Chang et al. 2017). Exposure to a variety insults, including lipopolysaccharide (LPS), interleukin-1ß (IL-1ß), and α-Syn preformed fibrils (PFF) results in increased expression and secretion of cathepsins from microglia that is associated with microglial activation, polarization and chemokine production (Pišlar et al. 2017; Biggs et al. 2025; Fan et al. 2012; Pišlar et al. 2021). Cathepsins secreted from microglia can directly activate multiple proinflammatory and proapoptotic cascades that can result in neuronal death (Nakanishi 2020; Lowry and Klegeris 2018; Kingham and Pocock 2001; Xu et al. 2018). Cathepsin S is a known regulator of major histocompatibility complex class II (MHC-II) antigen presentation, as it is associated with preparing the binding groove for antigen loading prior to extracellular presentation (Bird, Trapani, and Villadangos 2009). These findings suggest that cathepsins may play a key

role in the response of both neurons and microglia to α-Syn aggregation, a role that may contribute to the neurodegenerative process in PD.

Results from our RNAseq study described in Chapter 2 demonstrate alterations in the expression of many cathepsin genes in inclusion-bearing substantia nigra pars compacts (SNpc) at both the one- and two-month time point. Specifically, we observed that *Ctsb, Ctsc, Ctse, Ctsh, Ctsl, Ctss,* and *Ctsx* are significantly upregulated at the one-month timepoint and *Ctsc, Ctse, Ctsh, Ctss,* and *Ctsx* are significantly upregulated at the 2-month timepoint. These results suggest that the presence of pSyn inclusions within nigral neurons triggers cathepsin upregulation. Validation of these findings using alternate methodologies, in additional rat cohorts, would 1) provide additional evidence of the relationship of pSyn inclusions to cathepsin expression and 2) identify the cellular source of the pSyn inclusion-associated cathepsin response.

In the experiments described in this chapter I first used droplet digital PCR (ddPCR) to measure mRNA in the SN of the twelve cathepsins that were detected in our previous RNAseq study. In a separate cohort of rats, mRNA of *Ctsa, Ctsb*, *Ctsc*, *Ctsd*, *Ctse*, *Ctsf*, *Ctsh*, *Ctsk*, *Ctsl*, *Ctss, Ctsw* and *Ctsz* was measured one and two months following intrastriatal injections of control phosphate buffered saline (PBS), alpha-synuclein (α-Syn) monomer, or α-Syn preformed fibrils (PFFs). We also leveraged fluorescent in-situ hybridization (FISH) combined with immunofluorescence (IF) to localize microglial-specific cathepsin expression patterns in the SNpc of specific cathepsins implicated in our RNAseq and/or ddPCR results. Overall, my results provide evidence that microglia in the pSyn inclusion-bearing SNpc markedly increase expression of *Ctsh, Ctss* and Ctsx.

METHODS

Experimental Subjects

All rats used were housed 2-3 to a cage in a room with a 12h light/dark cycle and were provided food and water ad libitum. All animal work was performed inside the Michigan State Research Center vivarium in Grand Rapids, MI, an Association for Assessment and Accreditation of Laboratory Animal Care (AAALAC) accredited facility. All procedures were conducted with approval from the Institute for Animal Care and Use Committee (IACUC) at Michigan State University. Male two-month-old Fischer 344 rats were purchased from Charles River Laboratories. Fischer 344 rats were used in this set of experiments instead of Sprague Daley rats that were used in the LCM-RNAseq experiments to control for differences in genetic background, or transgenic contributions, that may have influenced results in the LCM-RNAseq experiment. A total of 48 rats were used (n=8 per group/timepoint) (Figure 3.1A).

α-Syn Preformed Fibrils (PFFs) preparation and size validation

PFFs were generated from wild-type, full length, recombinant mouse α-Syn monomers as previously described (Patterson, Duffy, et al. 2019; Polinski et al. 2018; Volpicelli-Daley et al. 2011; Luk et al. 2012). Prior to use, quality control assessments were performed *in vitro* to assess amyloid structure (Thioflavin T assay), pelletability (sedimentation assay), structure (electron microscopy), and endotoxin levels (Limulus amebocyte lysate assay; <0.5 endotoxin units/mg of total protein); and *in vivo* to confirm seeding efficiency. For surgery, monomers were diluted to 4 μg/μL with phosphate-buffered saline (PBS) and centrifuged at 15,000 x g for 30 min. at 4°C. During surgery monomers were kept on wet ice. Centrifugation and storage on ice limits the

presence/formation of oligomers. To prepare PFFs for surgeries, PFFs were diluted to 4 µg/µL in PBS and sonicated at room temperature using an ultrasonic homogenizer (Q125 Sonicator; Qsonica, newtown, CT); amplitude 30%, 60, 1s pulses with 1s between pulses(Patterson, Polinski, et al. 2019). Aliquots of sonicated PFFs were imaged via transmission electron microscopy, and fibril lengths were measured using ImageJ (Schneider, Rasband, and Eliceiri 2012). Fibril length had an average size of 42.5 ± 0.7 nm and 89.4% of sonicated PFFs measured were ≤60 nm (Figure 3.1B). Notably, the average size is <50 nm, which previously has been determined to be the optimal size for fibril uptake (Tarutani et al. 2016; Abdelmotilib et al. 2017).

Stereotaxic Surgeries

Rats received bilateral injections of 16 ug of PFFs or an equal quantity of α-Syn monomer (4 µg/µl, 2x2 µl injections, both hemispheres), or Dulbecco's phosphate buffered saline (dPBS) vehicle as previously described (Patterson, Duffy, et al. 2019). Rats were anesthetized with isoflurane and received intrastriatal injections (bilateral injections; AP + 1.0, ML ± 2.0, DV - 4.0; AP + 0.1, ML ± 4.2, DV - 5.0). AP and ML coordinates were measured from bregma, and DV coordinates were measured from dura. These PFF coordinates result in > 90% of α-Syn inclusions forming in the SNpc, with minimal inclusions forming in the VTA (Polinski et al. 2018). Injections were delivered using a pulled glass needle attached to a 10 µl Hamilton syringe with a flow rate of 0.5 µl min^{-1}. Needles remained in place for 1 minute following injection, retracted 0.5 µl and remained in place for an additional 2 minutes to prevent possible backflow. Following surgeries, rats received an injection of buprenorphine (1.2 mg / kg^{-1}) and

monitored until day 30 (one month post injection) or day 60 (two months post injection). Surgeries for each treatment group were completed within three hours.

Tissue Collection

Rats were euthanized with an overdose of pentobarbital (Beuthanasia-D Special, Merck Animal Health; 30 mg/kg) and perfused intracardially with ~150mL of cold heparinized saline (0.9%, 10,000 units per liter). Brains were removed and transferred to a chilled brain matrix, the frontal cortex, rostral to the corpus callosum, was collected, as well as the left and right mesencephalon (Figure 3.1C). The left mesencephalic hemisphere designated for ddPCR experiments were flash frozen in 2-methylbutane on dry ice and stored at -80°C. The cortex, as well as right mesencephalic hemisphere designated for immunohistochemistry (IHC), immunofluorescence (IF) and fluorescent *in situ* hybridization (FISH) was immersed in 4% paraformaldehyde in 0.1 M phosphate buffer (pH 7.3) for 48 h at 4°C and transferred to a 30% sucrose solution.

RNA Isolation - ddPCR

Phasemaker tubes (Invitrogen, A33248) were labeled and centrifuged for 30s at 16,000 x g. Samples in TRIzol were thawed on ice and briefly vortexed and centrifuged. Samples were transferred to a phasemaker tube and incubated at RT for 5mins. 200 µL of 100% chloroform was added to each sample and shaken by hand in the phasemaker tube before incubating at RT for 10 mins. Tubes were centrifuged at 4°C at 16,000 x g for 5 min. Following, the aqueous phase (clear liquid) was removed and transferred to an RNase-free 1.5mL tube and an equal volume of 100% ethanol was added. Samples were vortexed for 3s and ran through a column-based nucleic acid purification kit using a method modified from manufacturer's instructions (Zymo Research, R1016). Samples

were transferred to the columns 600 µL at a time and centrifuged for 1m at 12,000 x g until the entire sample was transferred. All RNA wash & prep buffers were added to the column and centrifuged for 1m at 4°C at 12,000 x g. First, samples were washed with 400 µL of RNA wash buffer, then incubated in a 1X concentration of a DNase I cocktail (DNase I from Thermo Scientific, FEREN0521, with a reaction buffer containing $MgCl_2$ from Thermo Scientific, FERB43) for 15m at RT. After incubation, DNase I cocktail was centrifuged through the column, then 400 µL of RNA prep buffer was washed through the column, followed by 700 µL of RNA wash buffer, and lastly 400 µL of RNA wash buffer. Columns were then dried by centrifuging for 2m at 12,000 x g. 15 µL of DNase/RNase free molecular grade water was added to the column, incubated for 1m at RT, and then centrifuged for 1m at 10,0000 x g. 10 µL of the flow-through (containing the RNA) was re-run through the column to increase RNA yield. Quality and quantity of RNA was assessed with an Agilent RNA 6000 Pico (5067-1513) on an Agilent 2100 Bioanalyzer. Samples were stored at -80°C until further processing. Samples #22 (PFF 1 month) and #28 (PBS 2 month) were removed due to low RIN values (Figure 3.1D).

Droplet Digital PCR (ddPCR)

ddPCR preparation and analysis was performed as previously published (Patterson et al. 2022). Briefly, microdissection was performed using a cryostat and precision micro punches of the SN were collected. RNA was cleaned and isolated as described in the previous section. RNA was removed from the -80°C and thawed on ice and 2-3 ng was used with iScripts Reverse Transcription Supermix for cDNA synthesis (Bio-Rad, 1708841). cDNA synthesis was performed in a thermocycler with the following settings: constant lid temperature at 105°C, 5 min. at 25°C, 20 min. at 46°C, 1 min. at

95°C, hold at 4°C. cDNA was diluted with 2X cDNA storage buffer (equal parts 10mM Tris HCl (pH: 7.5) and 0.1mM EDTA (pH: 8.0)). To prepare samples for ddPCR, samples were thawed on ice and added to a master mix containing 2X ddPCR Supermix for Probes (Bio-Rad, 186-3026) and the 20X TaqMan primer probe. Probes for rats used were: *Ctsa* (Applied Biosystems, Rn01424035_g1, Lot# P240826-008 D04, FAM-MGB), *Ctsb* (Applied Biosystems, Rn00575030_m1, Lot# P240826-008 D05, FAM-MGB), *Ctsc* (Applied Biosystems, Rn00567311_m1, Lot# P240826-008 D06, FAM-MGB), *Ctsd* (Applied Biosystems, Rn00592528_m1, Lot# P240826-008 D07, FAM-MGB), *Ctse* (Applied Biosystems, Rn01483642_m1, Lot# P240826-008 D08, FAM-MGB), *Ctsf* (Applied Biosystems, Rn01450703_m1, Lot# P240826-008 D09, FAM-MGB), *Ctsh* (Applied Biosystems, Rn00564052_m1, Lot# P240826-008 D10, FAM-MGB), *Ctsk* (Applied Biosystems, Rn00580723_m1, Lot# P240826-008 D11, FAM-MGB), *Ctsl* (Applied Biosystems, Rn04341361_m1, Lot# P240826-008 D12, FAM-MGB), *Ctss* (Applied Biosystems, Rn00569036_m1, Lot# P240826-008 E01, FAM-MGB), *Ctsw* (Applied Biosystems, Rn01759878_m1, Lot# P240826-008 E02, FAM-MGB), *Ctsz* (Applied Biosystems, Rn00788336_m1, Lot# P240826-008 E03, FAM-MGB), *Th* (Applied Biosystems, Rn00562500_m1, Lot# 2013779, FAM-MGB) and the reference probe used was *Rpl13a* (Applied Biosystems, Rn00821946_g1, Lot# P231024-004 E09, VIC-MGB). TaqMan primer probes selected were exon-exon junction spanning whenever possible. Equal parts cDNA and master mix were added to tubes and briefly centrifuged before 20µL was added to sample wells of D8 droplet generator cartridges (Bio-Rad, 1864008). 70µL of droplet generator oil (Bio-Rad, 1863005) was added to each well before being covered with a rubber gasket (Bio-Rad, 1863009) and a QX

droplet generator (Bio-Rad, 186-4002) was used to generate droplets. 40µL of droplets were added to a 96-well plate (Bio-Rad, 12001925) before being sealed with pierceable foil (Bio-Rad, 181-4040) using a plate sealer (Bio-Rad, 181-4000). Plates were transferred to a thermocycler (Bio-Rad, C1000) with the following settings: constant lid temperature at 105°C, 10 min. at 95°C, 39 cycles (30 s at 94°C, 1 min. at 60°C), 10 min. at 98°C, hold at 12°C. Plates were then transferred to a QX200 droplet reader (Bio-Rad, 1864003) and results were analyzed with QuantaSoft software. All samples were normalized to reference gene *Rpl13a*. Sample #14 (MONO 1 month) was removed due to low *Th* mRNA values, indicating inaccurate SN microdissection (Figure 3.1D).

Immunohistochemistry

As previously shown in this model, intrastriatal injection of PFFs results in the accumulation of pSyn pathology within the cortex and SNpc, and thus, the presence of cortical pSyn can be used as a surrogate-marker for PFF injection accuracy and seeding efficiency (Polinski et al. 2018; Duffy et al. 2018; Patterson, Duffy, et al. 2019; Howe et al. 2021). Therefore, cortical pSyn pathology was used as an inclusion criteria for PFF injected rats designated for ddPCR experiments, as well as to confirm lack of pSyn pathology following monomer or PBS injection. Rostral portions were sectioned at 40 µm on a freezing microtome and transferred into cryoprotectant solution. The right hemisphere (containing the SNpc) was similarly sectioned for IHC, IF, and FISH procedures. Free-floating sections (1:6 series) were transferred to 0.1M tris-buffered saline containing 0.5% triton-X100 (TBS-Tx) and washed 4 times for 5 minutes each. Tissue was quenched in 0.3% hydrogen peroxide for 1h followed by TBS-Tx washes. Tissue was blocked with 10% normal goat serum (NGS) for 1h and washed with TBS-Tx

before being transferred to primary antibody solution overnight at 4°C (TBS-Tx, 1% NGS, 1:10,000 mouse anti-phosphorylated α-Syn at serine 129; Abcam, AB184674). Sections were washed in TBS-Tx and transferred to secondary antibody solution for 2.5h at RT (TBS-Tx, 1% NGS, 1:500 goat anti-mouse; Millipore, AP124B). Sections were washed in TBS-Tx and incubated for 2h at RT in standard avidin-biotin complex detection kit (Vector Laboratories, PK-6100). Following TBS-Tx washes, tissue was developed using nickel ammonium enhanced DAB solution (2.5mg mL^{-1} nickel ammonium sulfate hexahydrate (Fisher, N48-500) / 0.5 mg/mL^{-1} diaminobenzidine (DAB, Sigma-Aldrich, D5637) and 0.03% hydrogen peroxide in TBS-Tx). Sections were mounted onto subbed microscope slides and dehydrated in a graded ethanol series before incubating in two 100% xylene solutions and cover slipped with Cytoseal (Thermo-Fisher, 22-050-262). All PFF injected rats displayed cortical pSyn pathology (Figure 3.1E).

Total Enumeration - Phosphorylated α-Syn Inclusion in SNpc

Total enumeration of pSyn inclusions was performed using Microbrightfield Stereoinvestigator (MBF Bioscience). 1:6 series of sections containing SNpc was used for counts with an investigator blinded to treatment groups. Contours were drawn around the SNpc using a 4X objective and a 20X objective was used to quantify pSyn containing cells. pSyn inclusions were defined as dark staining either throughout the cell soma or as distinct puncta. Non-specific staining within blood vessels was excluded. Total counts for each animal were multiplied by 6 to estimate the total inclusions (Figure 3.1F).

Fluorescent In Situ Hybridization (FISH) and Immunofluorescence (IF)

Cathepsins that displayed significant upregulation in either our RNAseq data set and/or our ddPCR results, with TPMs > 10 in PBS rats (RNAseq results) were selected for FISH (*Ctsh, Ctsl, Ctss*) or IF (Ctsx). Tissue sections immediately adjacent to sections displaying robust pSyn pathology in PFF injected rats in both the one- and two-month groups were selected. Sections from the PBS control were selected to match the caudal-rostral plane of the sections selected from the PFF groups. FISH and IF was used to examine colocalization of individual cathepsins within microglia in one nigral section per rat using the following combinations: *Ctsh* and *Ctss* FISH/TH plus Iba1 IF, *Ctsl* FISH/TH plus Iba1IF and Ctsx/TH/Iba1 IF.

For FISH, 40 µm thick coronal rat brain sections were washed in TBS-Tx and quenched in hydrogen peroxide for 1 hour from the RNAscope Pretreatment Kit (Advanced Cell Diagnostics; ACD, Hayward, CA, 322335). Sections were washed in a 4:1 ddH_20:TBS-Tx mixture and mounted on VistaVision HistoBond slides (VWR, Randor, PA, 16004-406) before being placed on a slide warmer set to 60°C overnight. Slides were incubated for 10 mins. in 99°C target retrieval buffer (1:10 dilution, ACD, 322001) and washed twice in water. A Pap Pen (Abcam, Cambridge, UK, ab2601) was used to outline the tissue and protease III (ACD, 322337) was applied for 30 mins. in a hybridization oven set to 40°C. Tissue was washed twice in water and incubated with the rat probe for *Ctsh* (ACD, Cat#: 1591591-C1), *Ctsl* (ACD, Cat#: 466281-C2), *Ctss* (ACD, Cat#:1042021-C3), for 2 hours in the hybridization oven. Probes were diluted 1:50 in TSA buffer (ACD, 322809) if they were not already prediluted. Probe incubation was followed with washes in ACD wash buffer (1:500 dilution, ACD, 310091) followed by

amplification steps. Amplicon 1 (ACD, 323101) and amplicon 2 (ACD, 323102) were applied for 30 minutes each, with washes in wash buffer in between, followed by amplicon 3 (ACD, 323103) incubation for 15 minutes. Tissue was washed twice in wash buffer before adding HRP-C1 (ACD, 323104), HRP-C2 (ACD, 323105), or HRP-C3 (ACD, 323106) for 15 mins. in the hybridization chamber set at 40°C. Tissue was washed twice in wash buffer followed by fluorophore incubation for 30 mins. in the hybridization oven at 40°C; opal fluorophore 570 (1:1000 dilution in TSA buffer, Akoya Biosciences, Marlborough, MA, OP-001003), or opal fluorophore 650 (1:1000 dilution in TSA buffer, Akoya Biosciences, OP-001005). Tissue was washed twice in wash buffer before HRP blocker was added (RNAscope™ Multiplex FL v2 HRP Blocker, ACD, 323107) and incubated for 15 mins. in the hybridization oven.

For IF, mounted tissue or free-floating sections were washed twice with wash buffer followed by blocking in either 10% normal goat serum or 10% normal donkey serum diluted in TBS-Tx for 1 hour at RT before incubating with primary antibody in 1% serum diluted in TBS-Tx overnight at RT. Primaries used included: Rabbit anti-Iba1 (1:200-1:2000, Fujifilm Wako, Richmond, VA, Cat# 019-19741), chicken anti-tyrosine hydroxylase (1:400, Thermo Fisher Scientific, Waltham, MA, Cat# PA5-143583) and goat anti-cathepsin X/Z/P (1:50, R&D Systems, Minneapolis, MN, Cat# AF934). For cathepsin X/Z/P IF free-floating sections were used. Tissue was washed n TBS-Tx and incubated in appropriate secondaries for 2 hours at RT (1:250 goat anti rabbit 488, Thermo Fisher Scientific, Cat# A11034; 1:250 goat anti chicken 750, Abcam, Cambridge, UK, Cat# AB175755, 1:500 donkey anti-goat 647, Thermo Fisher, A-21447, 1:500 goat anti rabbit 488, Thermo Fisher Scientific, Cat# A11034). After additional

washes in TBS-Tx, FISH slides were cover slipped with ProLong™ Gold antifade reagent (Thermo Fisher, P36930). Free-floating dual IF sections were washed, mounted on HistoBond+ slides (VWR VistaVision, 16004-406) and cover slipped with VECTASHIELD Vibrance antifade mounting medium (Vector Laboratories, H-1700). Slides were kept in the dark until imaging. Figure images were taken using the Nikon Eclipse Ni-U microscope with CFI60 infinity optical system (Nikon Instruments Inc.) using the 10X and 40X objectives.

Image Acquisition and Fluorescence Quantification

FISH/IF or IF nigral tissue sections were scanned using a Zeiss Axioscan.Z1 scanning microscope at 20X magnification. TH immunofluorescence was used to validate the SNpc boundary, and sections with fewer than 10 TH immunoreactive neurons were considered to be outside the boundaries of the SNpc and removed from analyses. Mean immunofluorescence intensity of TH, Iba1 and cathepsin X/Z/P as well as *Ctsh*, *Ctsl*, *Ctss* FISH signal was generated using Zen 2 Blue edition software (Carl Zeiss Microscopy, Germany, version 3.10.103.03000). Fixed area contours were sized to 0.38 mm^2 for mean fluorescence intensity analyses and 0.27 mm^2 for HALO® analyses and consistently placed within the SNpc across all tissue sections. Background fluorescence (from a fixed area contour dorsolateral to the SNpc) was subtracted from the mean fluorescence intensity values of the SNpc to calculate final values, which were grouped by treatment/timepoint and normalized to % PBS control for their respective timepoints. Enumeration and colocalization were quantified used HALO® (Indica Labs, Albuquerque, NM) image analysis module “Object Colocalization FL v2.1.4” and total fluorescent area was determined using the HALO® module “Area

Quantification FL v2.3.3". Fluorescent thresholds were set based on PBS controls and kept consistent between treatment groups. Values were normalized to % PBS control of their respective timepoint.

Statistical Analysis

All statistical analysis was performed on raw data. Statistical analysis was performed using GraphPad Prism Version 10.4.0. Comparisons between PBS, monomer and PFF ddPCR results were made within each timepoint using one-way analysis of variance ANOVA with a *post-hoc* Tukey's test. Comparisons between PBS and PFF FISH and IF results were made within each timepoint using unpaired two-tailed t-tests. Statistical significance was set to $\alpha \leq 0.05$. Outliers were assessed via the absolute deviation from the median method (Leys et al. 2013) utilizing the very conservative difference of 2.5X median absolute deviation as the exclusion criterion. All group means, standard errors, and statistical test information can be found in Excel File #4.

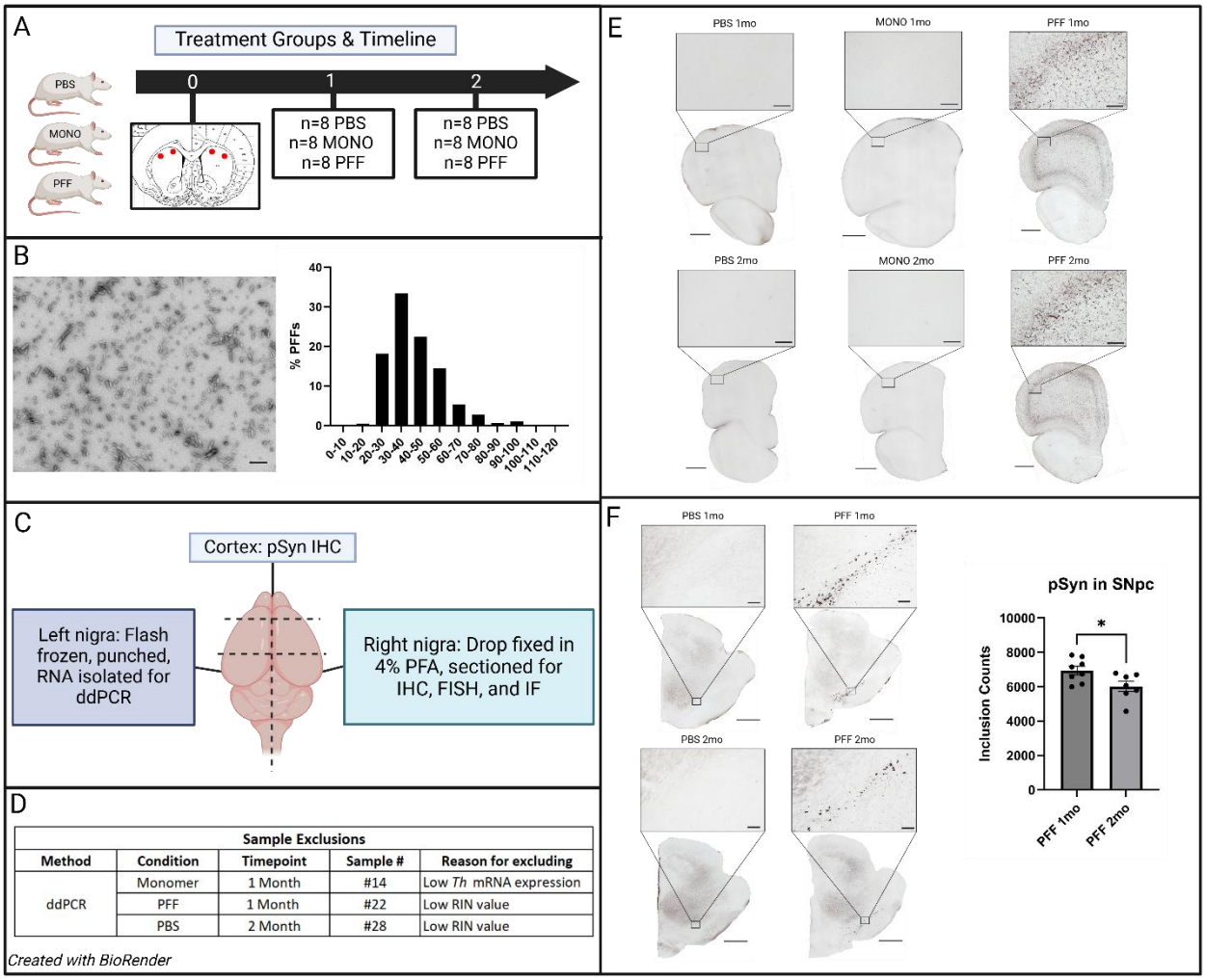

Figure 3.1 Experimental design and approach

(A) Treatment groups and timeline of present experiment. Male Fischer 344 rats received bilateral intrastriatal injections of mouse alpha-synuclein (α-Syn) preformed fibrils (PFFs), mouse α-Syn monomer (MONO) or phosphate buffered saline (PBS). Rats were euthanized one or two months following surgery. **(B)** Transmission electron micrograph of sonicated PFFs, scalebar = 200 nm. Distribution of mouse α-Syn PFF fibril lengths post sonication. Average fibril size was 42.54 nm (SD = 15.67 nm). **(C)** Overview of brain processing. The prefrontal cortex was isolated and sectioned for immunohistochemistry (IHC) for phosphorylated α-Syn (ser129, pSyn). Left SN was

Figure 3.1 (cont'd)

flash frozen and microdissected for droplet digital PCR experiments. Right SN was sectioned for IHC and fluorescent *in situ* hybridization (FISH). **(D)** List and rationale for individual sample exclusion. **(E)** Validation of successful pSyn inclusion seeding in the ipsilateral frontal cortex of rats designated for ddPCR of the SN at one or two months following PFF, but not monomer or PBS injection. **(F)** Left: Validation of pSyn pathology in the ipsilateral SNpc of rats designated for IHC/FISH one or two months following PFF but not PBS injection. Right: Quantification of pSyn-containing SN pars compacta (SNpc) neurons at one month and two months post PFF injection. Values represent the mean ± SEM. * $p \leq 0.05$.

RESULTS

Robust pSyn pathology in the SNpc at one and two months post PFF injection

Intrastriatal injections of α-Syn PFFs resulted in the accumulation of pSyn aggregates in the SNpc at both the one and two month timepoints, while no pSyn pathology was observed in PBS or monomer treated animals (Figure 3.1F). Total enumeration revealed a slight reduction in individual pSyn aggregates at two months compared to the one-month timepoint (one month = 6,944 ± 243.9 inclusions; two months = 6,018 ± 295.6 inclusions; $p < 0.05$).

pSyn accumulation in the SNpc is associated with alterations in cathepsin mRNA

Using ddPCR, the expression of 12 cathepsin transcripts were measured within the SN of α-Syn PFF, monomer, or PBS vehicle control treated animals at one and two months post injection. In four of the cathepsins, cathepsin C (*Ctsc*), cathepsin L (*Ctsl*), cathepsin K (*Ctsk*), and cathepsin S (*Ctss*) no significant differences were observed between the PFF and PBS groups ($p > 0.05$, Figure 3.2). Indeed, no differences in *Ctsc*, *Ctsl*, *Ctsk*, and *Ctss* expression were observed between any treatment groups, at any timepoint, except that *Ctsc* mRNA was significantly higher in the SN of PFF-injected rats than monomer-injected rats at two months ($p < 0.05$, Figure 3.2). Four cathepsins were observed to be decreased in the SN of PFF-injected rats compared to PBS injected rats, *Ctsa* ($p < 0.01$), *Ctsb* ($p < 0.05$), *Ctsd* ($p < 0.05$), and *Ctsf* ($p < 0.001$), however this decrease was only at the one month timepoint (Figure 3.3). Levels of *Ctsb* ($p < 0.05$) and *Ctsf* ($p < 0.001$) in PFF-injected rats also were significantly decreased compared to monomer-injected rats at the one-month timepoint (Figure 3.3). Finally, four cathepsins displayed increased expression in the SN of PFF-injected rats compared to PBS-

injected rats at either one and/or two months, *Ctse*, *Ctsh*, *Ctsw*, and *Ctsx* (Figure 3.4). At the one-month timepoint, *Ctsw* expression was increased in the PFF group compared to the PBS group (Figure 3.4, $p < 0.001$). At the two-month timepoint, expression of both *Ctse* ($p < 0.01$) and *Ctsh* ($p < 0.05$) mRNA was increased in the SN of PFF-injected rats (Figure 3.4). *Ctsx* was the only cathepsin that was increased in the SN at both timepoints in PFF-injected rats compared to both PBS- and monomer-injected rats. (Figure 3.4, $p < 0.001$). Collectively these results demonstrate that the presence of pSyn inclusions in the SN is associated with a heterogeneous cathepsin response. Decreased *Ctsa*, *Ctsb*, *Ctsd* and *Ctsf* mRNA and increased *Ctsw* and *Ctsx* mRNA is observed at one month ($p < 0.05$, Figure 3.5). At two months, increased *Ctse*, *Ctsh*, and *Ctsx* mRNA is observed ($p < 0.05$, Figure 3.5).

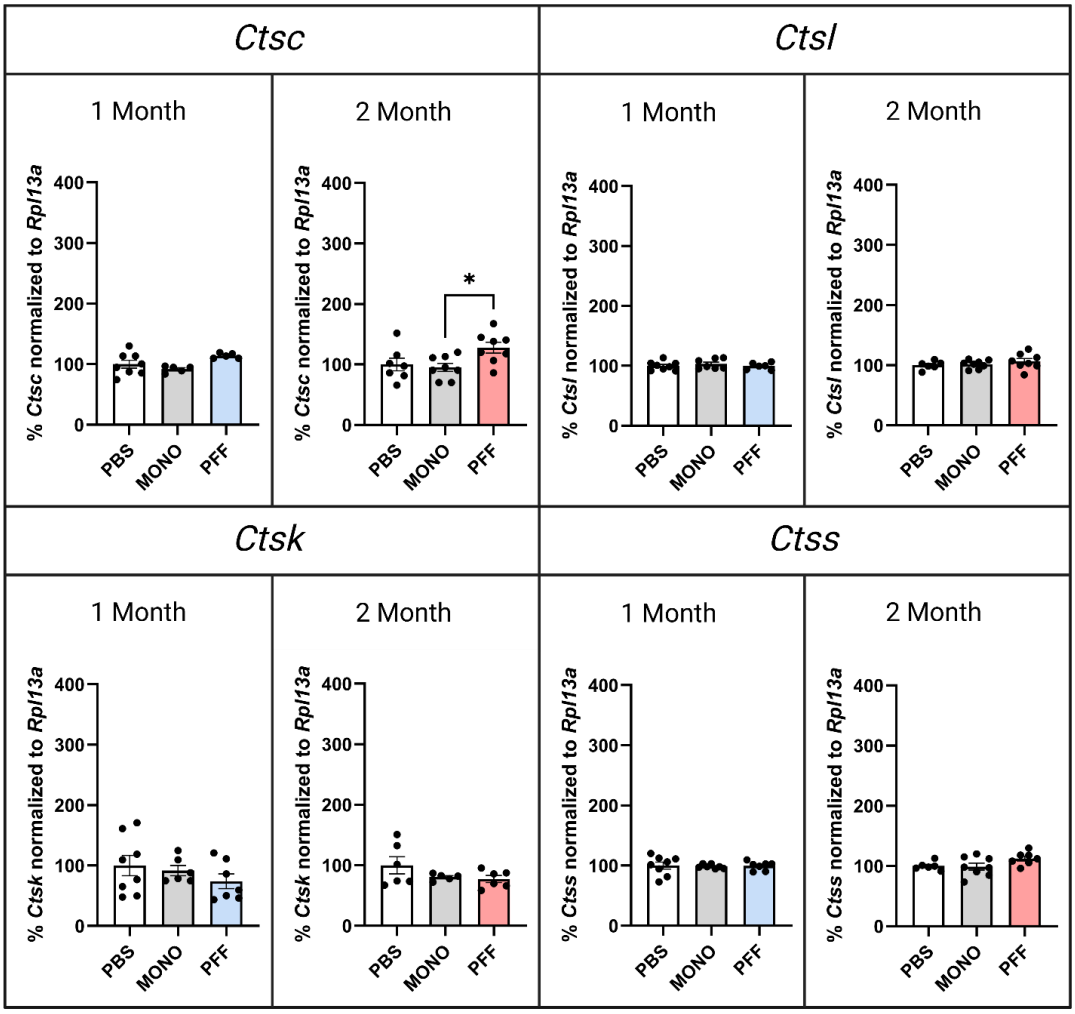

Figure 3.2 Expression of *Ctsc, Ctsl, Ctsk*, and *Ctss* in the substantia nigra is not impacted by accumulation of phosphorylated alpha-synuclein inclusions

Rats received bilateral intrastriatal injections of alpha-synuclein preformed fibrils (α-Syn PFFs), α-Syn monomer (MONO) or phosphate buffered saline (PBS). mRNA expression of individual cathepsins was measured in the substantia nigra (SN) one or two months post injection. No significant differences in *Ctsc, Ctsl, Ctsk*, and *Ctss* between PFF and vehicle-injected rats were observed. mRNA of individual cathepsins was normalized to *Rpl13a* and expressed as percent of PBS control. Values represent the mean ± SEM. *p ≤ 0.05.

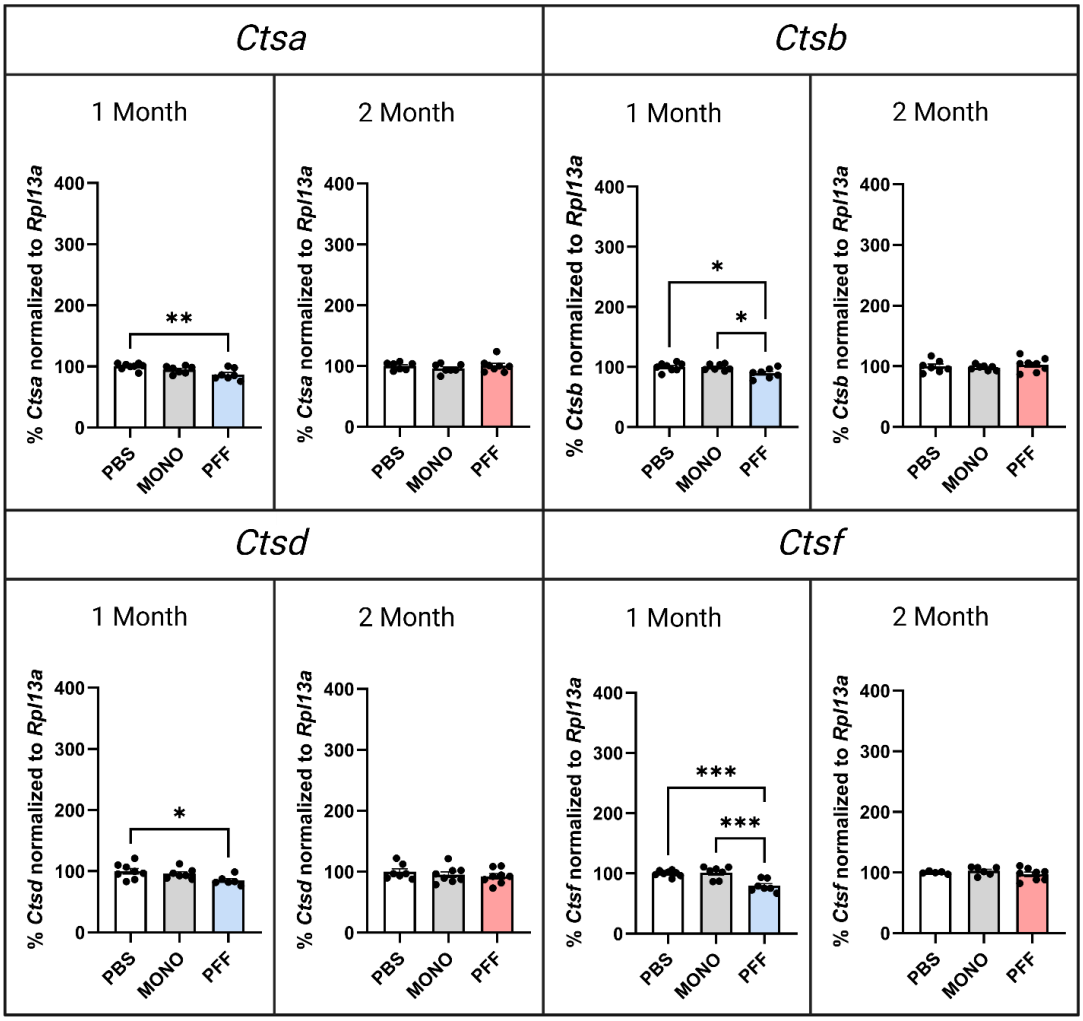

Figure 3.3 Expression of *Ctsa, Ctsb, Ctsd*, and *Ctsf* is decreased in the substantia nigra in association with phosphorylated alpha-synuclein inclusions

Rats received bilateral intrastriatal injections of alpha-synuclein preformed fibrils (α-Syn PFFs), α-Syn monomer (MONO) or phosphate buffered saline (PBS). mRNA expression of individual cathepsins was measured in the substantia nigra (SN) one or two months post injection. Decreased expression of *Ctsa, Ctsb, Ctsd*, and *Ctsf* was observed one month following PFF injection. mRNA of individual cathepsins was normalized to *Rpl13a* and expressed as percent of PBS control. Values represent the mean ± SEM. *p ≤ 0.05**, p ≤ 0.01, ***p ≤ 0.001.

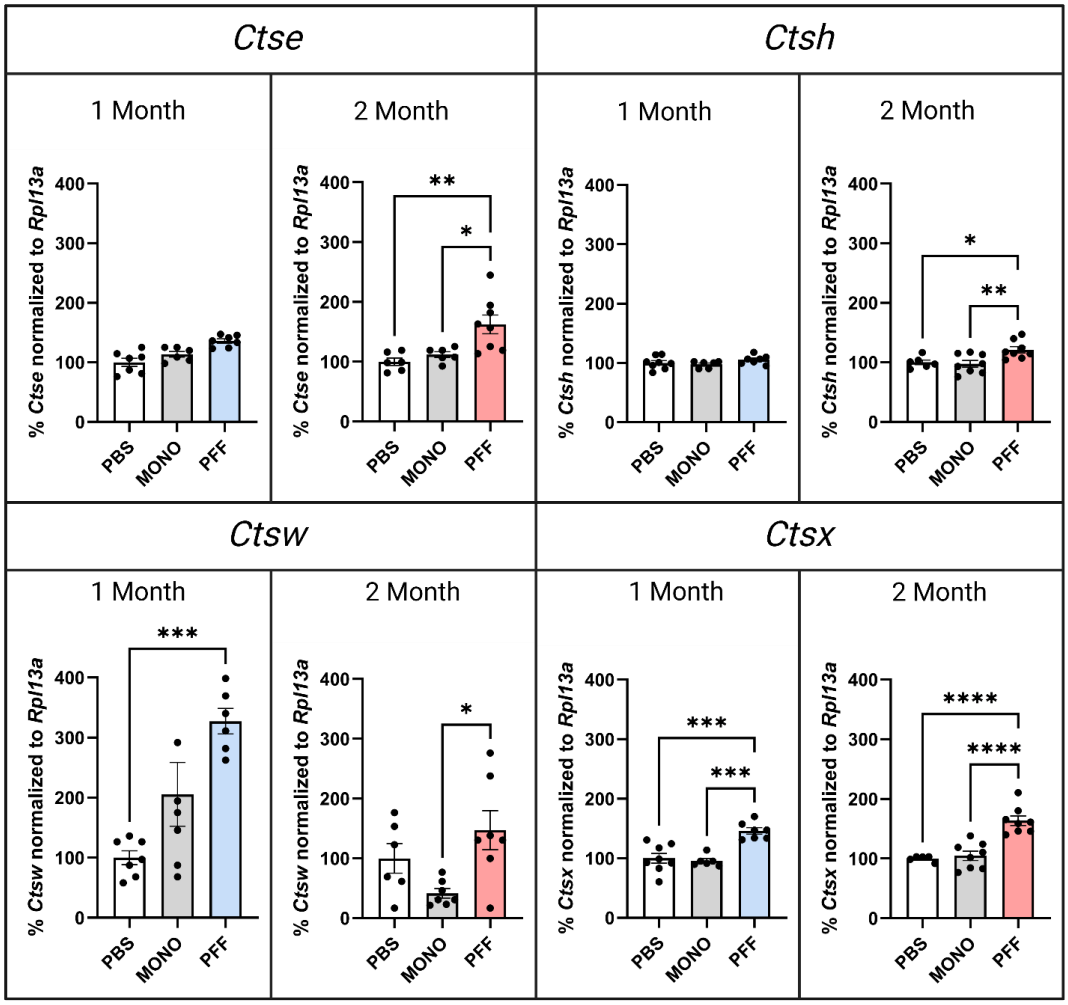

Figure 3.4 Phosphorylated α-Synuclein inclusions are associated with increased expression of *Ctse, Ctsh, Ctsw*, and *Ctsx* in the substantia nigra

Rats received bilateral intrastriatal injections of alpha-synuclein preformed fibrils (α-Syn PFFs), α-Syn monomer (MONO) or phosphate buffered saline (PBS). mRNA expression of individual cathepsins was measured in the substantia nigra (SN) one or two months post injection. Increased expression of Ctsw was observed at one month following PFF injection. *Ctse* and *Ctsh* was observed at two months following PFF injection. Increased expression of *Ctsx* was observed at both one and two months following PFF injection. mRNA of individual cathepsins was normalized to *Rpl13a* and expressed as percent of

Figure 3.4 (cont'd)

PBS control. Values represent the mean ± SEM. One data point outside the y axis is not visible on the *Ctsw* graph (476.4) in the 1 month monomer group. *p ≤ 0.05, **p ≤ 0.01, ***p ≤ 0.001, ****p ≤ 0.0001.

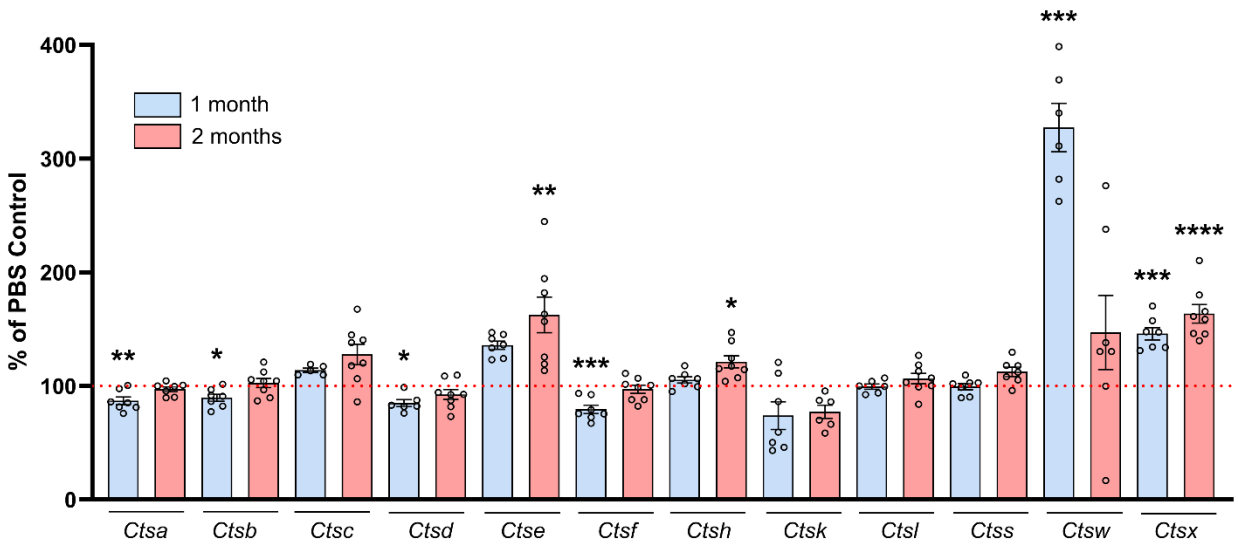

Figure 3.5 Impact of phosphorylated α-Synuclein inclusions on cathepsin expression in the substantia nigra

Rats received bilateral intrastriatal injections of alpha-synuclein preformed fibrils (α-Syn PFFs) or phosphate buffered saline (PBS). mRNA expression of individual cathepsins was measured in the substantia nigra (SN) one or two months post injection. One month: Decreased expression of *Ctsa, Ctsb, Ctsd*, and *Ctsf* and increased expression of *Ctsw* and *Ctsx* was observed in PFF injected rats. Two months: Increased expression of *Ctse, Ctsh*, and *Ctsx* was observed in PFF injected rats. mRNA of individual cathepsins was normalized to *Rpl13a* and expressed as percent of PBS control. Values represent the mean ± SEM. *p ≤ 0.05, **p ≤ 0.01, ***p ≤ 0.001, ****p ≤ 0.0001.

Downregulation of Tyrosine Hydroxylase in the SNpc at One and Two Months Following PFF Injection

We also examined the impact of pSyn accumulation on expression of *Th* mRNA and protein. We observed a decrease in *Th* mRNA in PFF-injected rats at both one ($p < 0.01$) and two months ($p < 0.001$) compared to PBS controls (Figure 3.6). Whereas the total number of TH immunofluorescent neurons was not impacted by PFF injection at either time point ($p > 0.05$), we observed a significant reduction in the mean fluorescence intensity at both one ($p < 0.05$) and two months ($p < 0.001$) in rats with nigral pSyn inclusions (Figure 3.6). Further, we also observed that the total TH fluorescent area decreased in PFF-injected rats at one month ($p<0.05$) but not at two months ($p > 0.05$, Figure 3.6). These results suggest that pSyn accumulation does not result in overt loss of nigral dopamine neurons at these early time points but rather is associated with downregulation of *Th* mRNA and protein, and perhaps decreased size of TH neurons, as we have previously observed (Patterson et al. 2024; Miller et al. 2021).

Robust Increases in Microglia size and intensity in the SNpc Following PFF Injection

Previously we have observed that nigral pSyn inclusions two months following PFF injection are associated with an increase in the number and size of Iba1 immunoreactive microglia (Stoll et al. 2024; Duffy et al. 2018). To determine the impact of pSyn inclusions on microglial number and size in the present cohort, as well as to investigate effects at the earlier one-month time point, we examined Iba1 immunoreactive microglia number, mean Iba1 immunofluorescent intensity and total

Iba1 fluorescent area in PFF and PBS-injected rats at both time points. We observed increases in microglia number, and larger increases in Iba1 fluorescence and Iba1 fluorescent area at both one and two months in PFF-injected rats compared to PBS controls ($p < 0.001$, Figure 3.7). These data suggest that nigral pSyn inclusions are associated with a modest recruitment of microglia and more pronounced increases in microglial Iba1 and size.

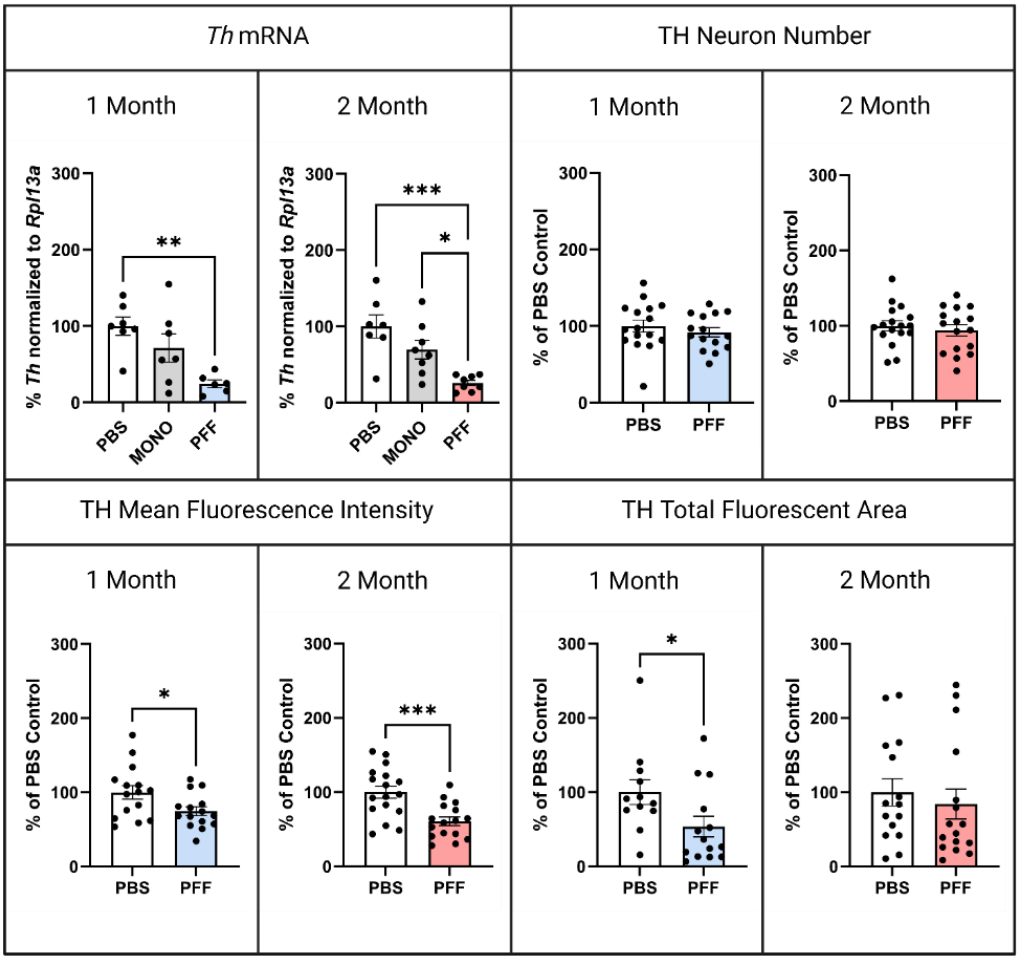

Figure 3.6 Phosphorylated α-Synuclein inclusions are associated with decreased *Th* mRNA and tyrosine hydroxylase immunoreactivity in the substantia nigra

Rats received bilateral injection of alpha-synuclein preformed fibrils (α-Syn PFFs), or phosphate buffered saline (PBS). Top left: mRNA expression of *Th* was measured in the substantia nigra (SN) one or two months post injection. Decreased *Th* expression was observed at both one and two months following PFF injection. mRNA was normalized to *Rpl13a* and expressed as percent of PBS control. In the opposite nigral hemisphere, tyrosine hydroxylase (TH) immunofluorescence was used to quantify number of TH neurons (top right), mean TH fluorescence intensity (bottom left), and total area of TH fluorescence (bottom right) at one and two months post α-Syn PFFs. TH fluorescence

Figure 3.6 (cont'd)

intensity and total TH fluorescent area were decreased in PFF-injected rats at both 1 and 2 months, TH number was not decreased at either time point. TH immunofluorescence was normalized to percent of PBS control. Values represent the mean ± SEM.*p ≤ 0.05, **p ≤ 0.01, ***p ≤ 0.001.

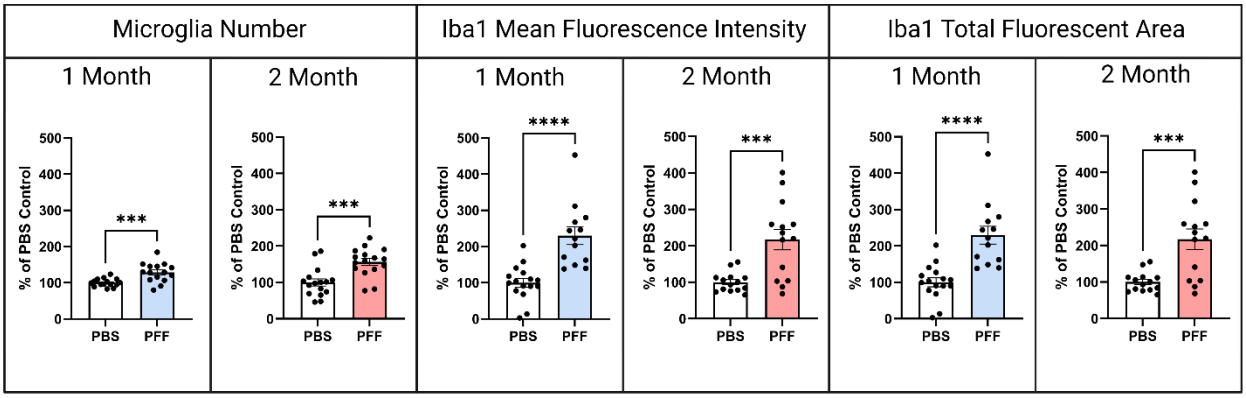

Figure 3.7 Phosphorylated α-Synuclein inclusions are associated with increased microglial number, size, and ionized calcium binding adapter molecule 1 (Iba1) immunoreactivity

Rats received bilateral injection of alpha-synuclein preformed fibrils (α-Syn PFFs) or phosphate buffered saline (PBS). Immunofluorescence of ionized calcium binding adaptor molecule 1 (Iba1) was used to quantify number of microglia (top left), mean Iba1 fluorescence intensity (middle), and total Iba1 fluorescent area (right) at one and two months post α-Syn PFF. Number of microglia, Iba1 fluorescence intensity and Iba1 fluorescent area were increased in PFF-injected rats at both 1 and 2 months. Iba1 immunofluorescence was normalized to percent of PBS control. Values represent the mean ± SEM. ***p ≤ 0.001, **** = p ≤ 0.0001.

Increased microglial cathepsin transcripts Ctsh, Ctss and Ctsx are associated with nigral pSyn inclusions

We next used FISH combined with IF to investigate the cellular source of two cathepsins in which increased mRNA was detected via ddPCR (*Ctsh* and *Ctsx*, Figure 3.5) as well as two additional cathepsins in which increases were detected in our previous RNAseq study (*Ctsl* and *Ctss*, Figure 2.5). As previously presented (Figure 3.7), Iba1 immunoreactive microglia in rats with nigral pSyn inclusions displayed increased size and immunofluorescence intensity. Qualitative examination of *Ctsh* mRNA expression revealed a robust increase in expression at both one and two months in the SNpc of PFF injected rats (Supplemental Figure 3.1, Figure 3.8). In the SNpc of PBS-injected rats, at both time points, *Ctsh* puncta colocalized with Iba1 immunoreactive microglia, yet appeared more abundant in non-Iba1 immunoreactive regions. In contrast, in PFF-injected rats at both timepoints, there appeared to be an increase in *Ctsh* mRNA puncta specifically within Iba1 immunoreactive microglia. We quantified the number of *Ctsh* mRNA puncta, the mean fluorescence *Ctsh* intensity, the total *Ctsh* fluorescent area and colocalization of *Ctsh* puncta with Iba1 immunoreactivity in PFF- and PBS-injected rats at both time points (Figure 3.8). At both one and two months, the inclusion-bearing SNpc was associated with an increase in *Ctsh* puncta ($p < 0.05$), area of *Ctsh* fluorescence ($p < 0.01$) and colocalization of *Ctsh* mRNA with Iba1 ($p < 0.01$). In addition, at two months the SNpc of PFF-injected rats displayed increased *Ctsh* immunofluorescent intensity ($p < 0.001$). These findings suggest that pSyn inclusions in the SNpc are associated with an increase in *Ctsh* within microglia.

We next examined *Ctsl* expression (Supplemental Figure 3.2, Figure 3.9). As previously observed, Iba1 immunoreactive microglia in rats with nigral pSyn inclusions displayed increased size and immunofluorescent intensity. Qualitatively, *Ctsl* mRNA expression appeared to be slightly increased in *Ctsl* mRNA expression at both one and two months in the SNpc of PFF injected rats (Supplemental Figure 3.2, Figure 3.9). In the SNpc of PBS-injected rats, at both time points, very few *Ctsl* puncta were observed and *Ctsl* puncta appeared to be expressed ubiquitously. In PFF-injected rats at both timepoints, *Ctsl* mRNA puncta appeared to be increased in both Iba1 positive and Iba1 negative areas, with more pronounced increases visible at one month. Quantification revealed a significant difference in only one metric. Specifically, the number of *Ctsl* mRNA puncta was significantly increased at one month only in the inclusion-bearing SNpc (Figure 3.9, $p < 0.05$). No significant differences were observed between PBS- and PFF-injected rats in mean fluorescence *Ctsl* intensity, the total *Ctsl* fluorescent area and colocalization of *Ctsl* puncta with Iba1 immunoreactivity at either timepoint (Figure 3.9, $p > 0.05$). These findings suggest that pSyn inclusions in the SNpc are associated with a modest, transient increase in *Ctsl* within both microglia as well as other cellular profiles.

We also examined *Ctss* expression (Supplemental Figure 3.3, Figure 3.10). As with previous analyses, Iba1 immunoreactive microglia in rats with nigral pSyn inclusions displayed increased size and immunofluorescence intensity. In both PBS- and PFF-injected rats *Ctss* mRNA expression was strictly colocalized with Iba1-immunoreactive microglia. Qualitative examination of *Ctss* mRNA expression revealed an appreciable increase in expression at both one and two months in the SNpc of PFF

injected rats (Supplemental Figure 3.3, Figure 3.10). Quantification revealed increased *Ctss* puncta ($p < 0.001$), increased mean *Ctss* fluorescence intensity ($p < 0.01$), increased area of *Ctss* fluorescence ($p < 0.001$) and increased colocalization of *Ctss* mRNA with Iba1 ($p < 0.001$) at both timepoints in the inclusion-bearing SNpc (Figure 3.10). These findings suggest that pSyn inclusions in the SNpc are associated with an increase in *Ctss,* specifically within microglia.

Lastly, we investigated the cellular source of Ctsx and the impact of nigral pSyn inclusions using dual label IF (Supplemental Figure 3.4, Figure 3.11). As with previous analyses, Iba1 immunoreactive microglia in PFF injected rats displayed increased in size and IF intensity. In both PBS- and PFF-injected rats, Ctsx IF was restricted to microglia. A marked increase in Ctsx IF was observed in the SNpc of PFF injected rats at both one and two months, the most pronounced increase of the cathepsins examined (Supplemental Figure 3.4, Figure 3.11). Quantification revealed a greater number of Ctsx immunoreactive profiles ($p < 0.05$), increased mean Ctsx fluorescence intensity ($p < 0.01$), increased total area of Ctsx fluorescence ($p < 0.05$) and increased colocalization of Ctsx IF with Iba1 ($p < 0.001$) at both timepoints in the inclusion-bearing SNpc (Figure 3.10). Overall, our results suggest that pSyn inclusions in the SNpc are associated with a marked increase in Ctsx protein, specifically within microglia.

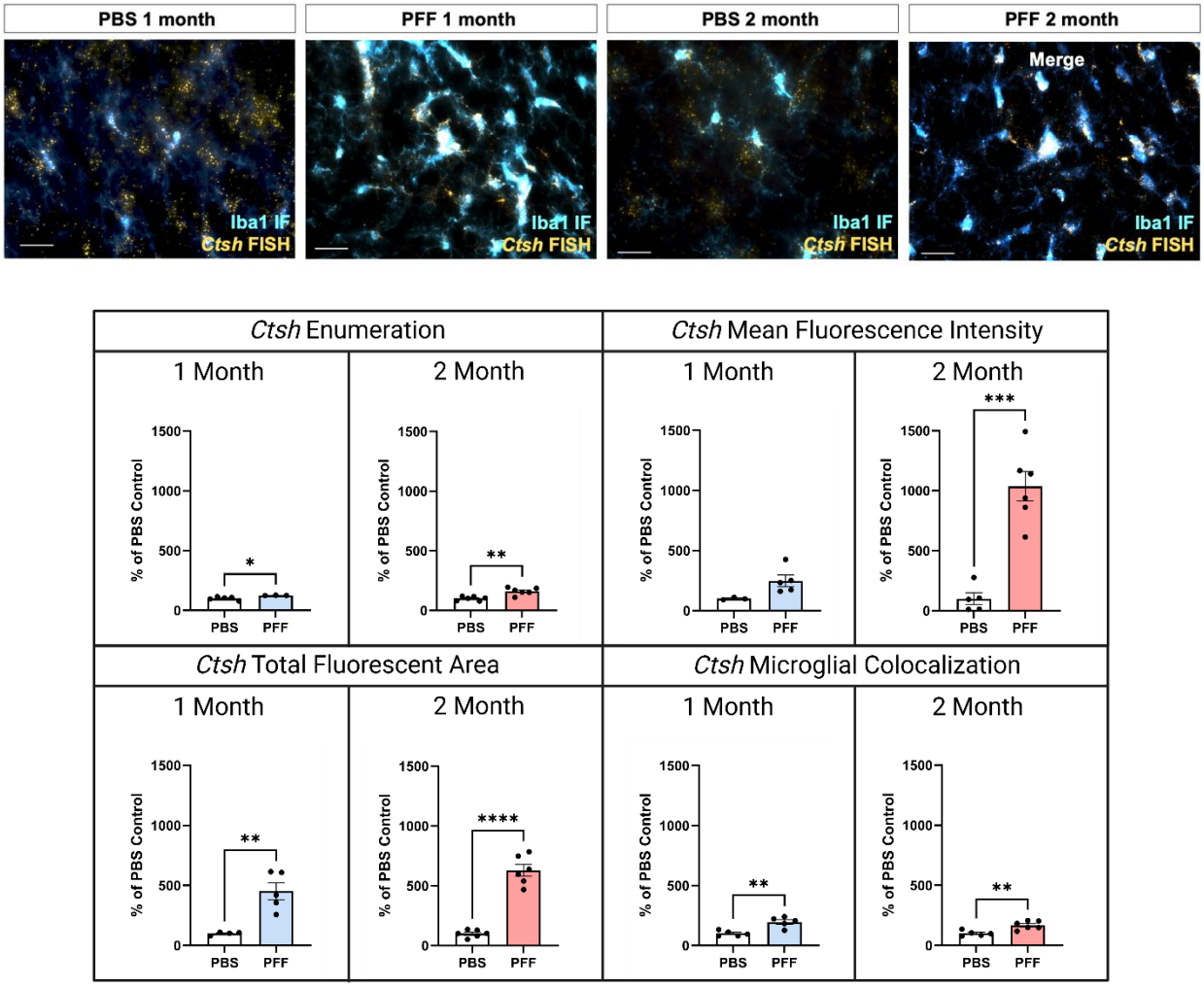

Figure 3.8 Accumulation of phosphorylated α-Synuclein in the substantia nigra is associated with increased *Ctsh* mRNA in microglia

Rats received bilateral intrastriatal injections of alpha-synuclein preformed fibrils (α-Syn PFFs) or phosphate buffered saline (PBS). Immunofluorescence (IF) of ionized calcium binding adaptor molecule 1 (Iba1) was combined with fluorescent *in-situ* hybridization (FISH) to quantify *Ctsh* expression in microglia. Top: Representative images illustrate Iba1 IF (blue) and *Ctsh* FISH (yellow) in PBS and PFF injected rats at either one or two months. *Ctsh* expression overlapped with both Iba1 IF as well as areas without Iba1 immunoreactivity. Scale bar = 100μM. Bottom: Quantification of cellular profiles

Figure 3.8 (cont'd)

expressing *Ctsh*, mean *Ctsh* fluorescence intensity, total *Ctsh* fluorescent area and Iba1/*Ctsh* colocalization was conducted. An increase in *Ctsh* profiles, *Ctsh* fluorescent area and *Ctsh*/Iba1 colocalization was observed in PFF-injected rats at both 1 and 2 months. In addition, the mean *Ctsh* fluorescence intensity was increased in PFF-injected rats at 2 months. *Ctsh* immunofluorescence was normalized to percent of PBS control. Values represent the mean ± SEM. *p ≤ 0.05, **p ≤ 0.01, ***p ≤ 0.001, **** = p ≤ 0.0001.

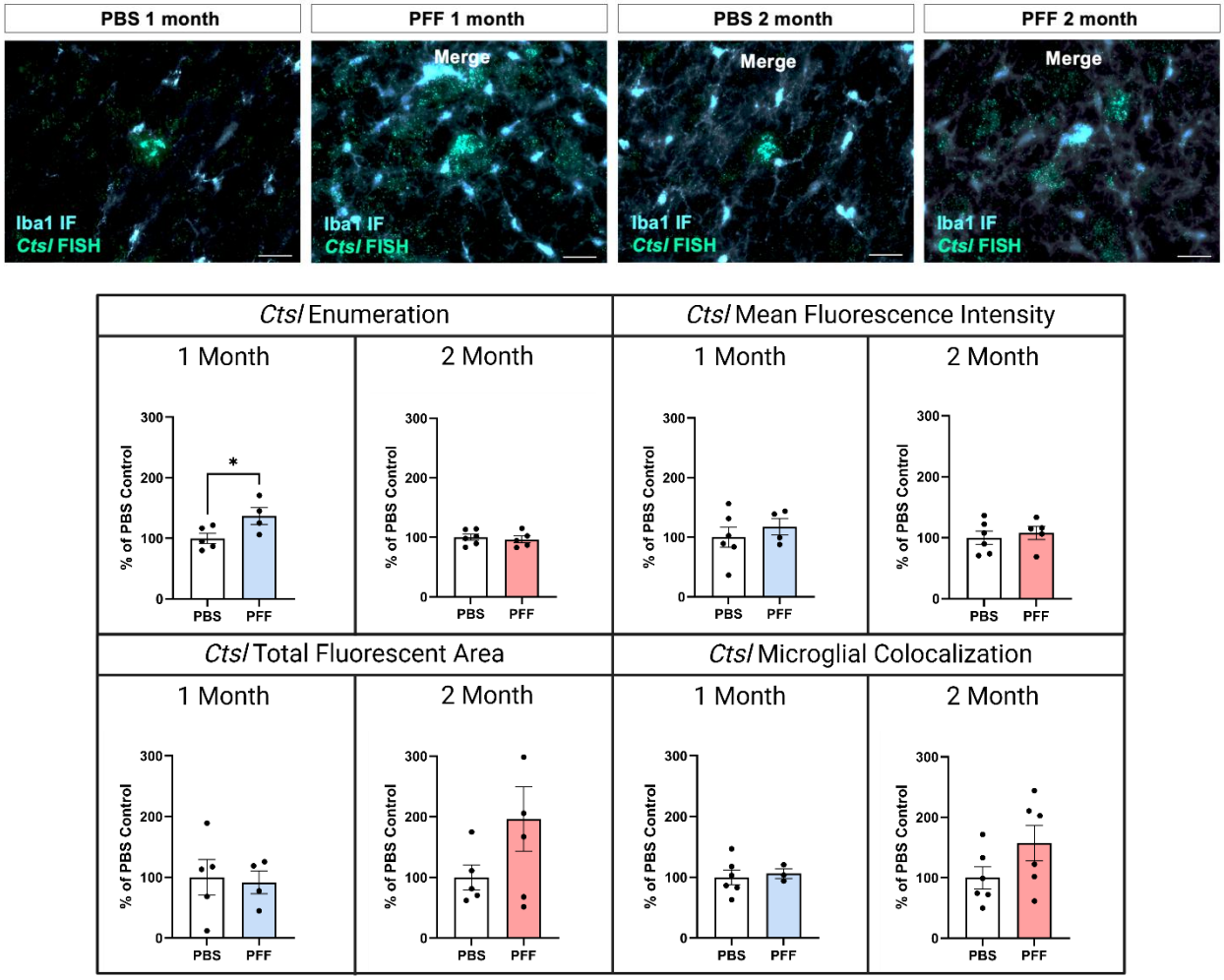

Figure 3.9 Minimal impact of phosphorylated α-Synuclein accumulation on *Ctsl* mRNA in the substantia nigra

Rats received bilateral intrastriatal injections of alpha-synuclein preformed fibrils (α-Syn PFFs) or phosphate buffered saline (PBS). Immunofluorescence (IF) of ionized calcium binding adaptor molecule 1 (Iba1) was combined with fluorescent *in situ* hybridization (FISH) to quantify *Ctsl* expression in microglia. Top: Representative images illustrate Iba1 IF (blue) and *Ctsh* FISH (green) in PBS and PFF injected rats at either one or two months. *Ctsl* expression overlapped with both Iba1 IF as well as areas without Iba1 immunoreactivity. Scale bar = 100μM. Bottom: Quantification of cellular profiles

Figure 3.9 (cont'd)

expressing *Ctsl*, mean *Ctsl* fluorescence intensity, total *Ctsl* fluorescent area and Iba1/*Ctsl* colocalization was conducted. An increase in *Ctsl* profiles was observed in PFF-injected rats at 1 month only. No detectable differences in *Ctsl* fluorescence intensity, *Ctsl* fluorescent area or *Ctsl*/Iba1 colocalization was observed in PFF-injected rats at either time point. One data point (386.9) outside the y axis is not visible on the total fluorescent area two month PFF graph. *Ctsl* immunofluorescence was normalized to percent of PBS control. Values represent the mean ± SEM. *$p \leq 0.05$.

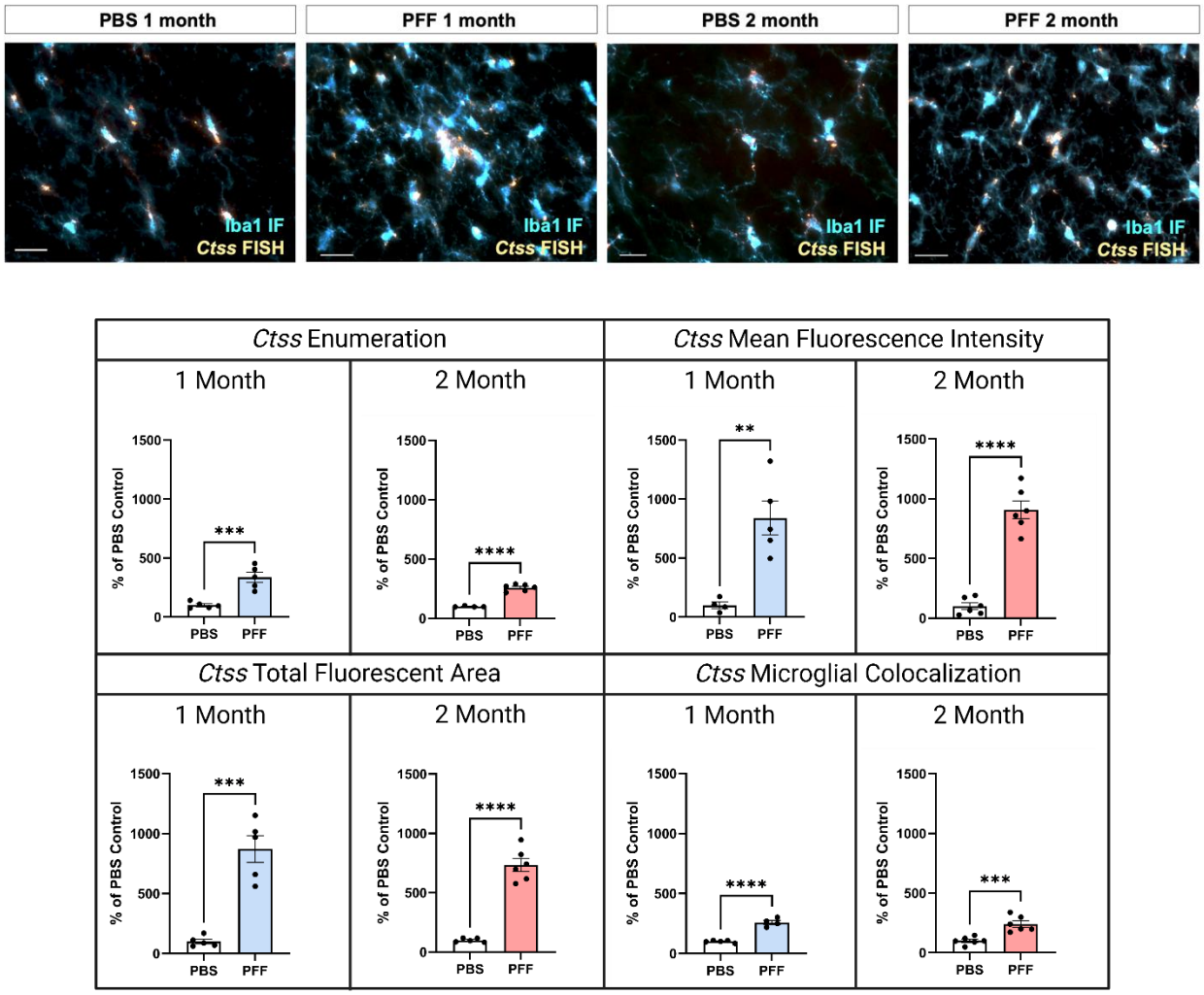

Figure 3.10 Accumulation of phosphorylated α-Synuclein in the substantia nigra is associated with increased Ctss mRNA in microglia

Rats received bilateral intrastriatal injections of alpha-synuclein preformed fibrils (α-Syn PFFs) or phosphate buffered saline (PBS). Immunofluorescence (IF) of ionized calcium binding adaptor molecule 1 (Iba1) was combined with fluorescent *in situ* hybridization (FISH) to quantify *Ctss* expression in microglia. Top: Representative images illustrate Iba1 IF (blue) and *Ctss* FISH (yellow) in PBS and PFF injected rats at either one or two months. *Ctss* expression appeared to exclusively overlap with Iba1 IF. Scale bar = 100μM. Bottom: Quantification of cellular profiles expressing *Ctss*, mean *Ctss*

Figure 3.10 (cont'd)

fluorescence intensity, total *Ctss* fluorescent area and Iba1/*Ctss* colocalization was conducted. An increase in *Ctss* profiles, *Ctss* fluorescence intensity, *Ctss* fluorescent area and *Ctss*/Iba1 colocalization was observed in PFF-injected rats at both 1 and 2 months. *Ctss* immunofluorescence was normalized to percent of PBS control. Values represent the mean ± SEM. **p ≤ 0.01, ***p ≤ 0.001, **** = p ≤ 0.0001.

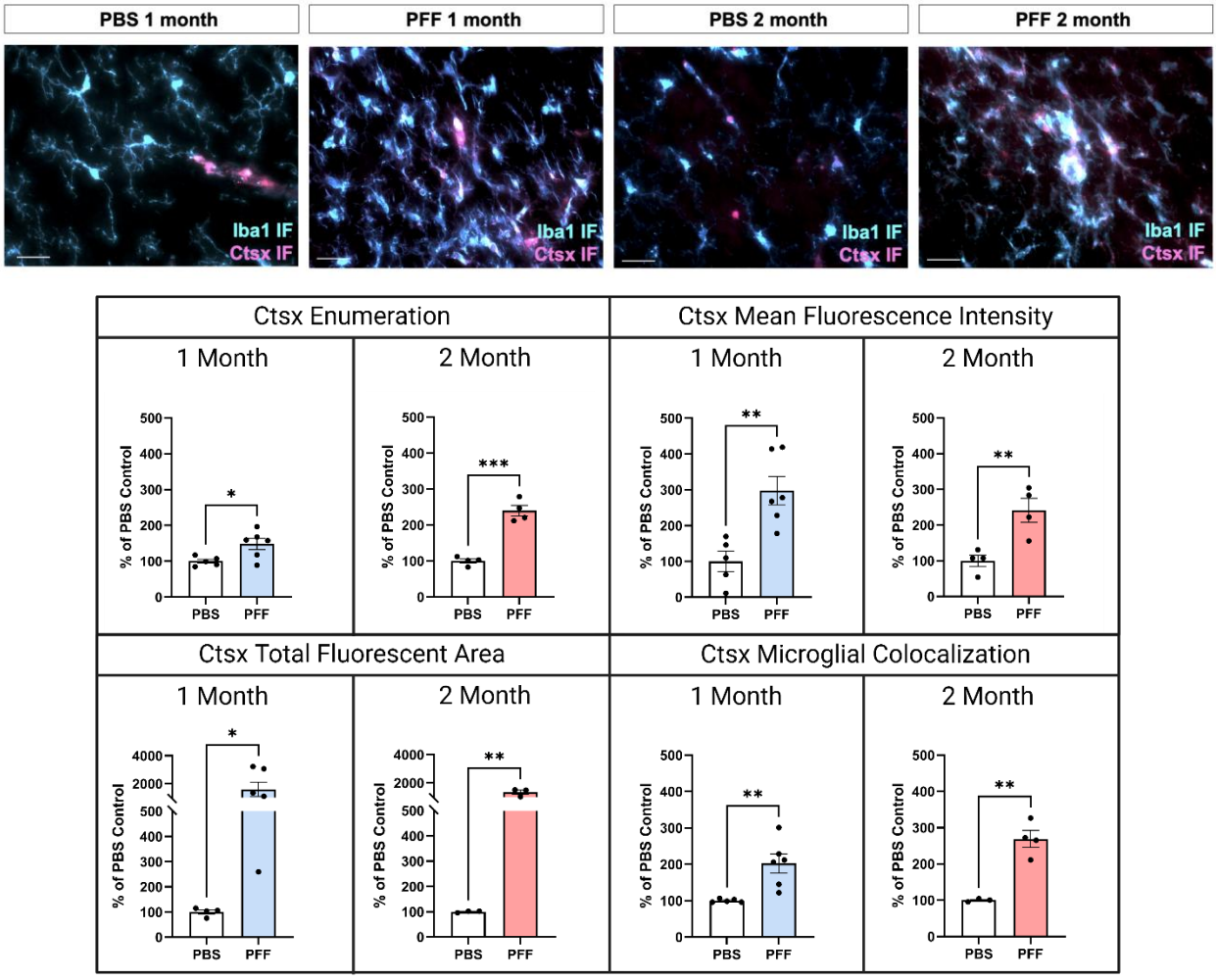

Figure 3.11 Accumulation of phosphorylated α-Synuclein in the substantia nigra is associated with increased cathepsin X in microglia

Rats received bilateral intrastriatal injections of alpha-synuclein preformed fibrils (α-Syn PFFs) or phosphate buffered saline (PBS). Dual immunofluorescence (IF) of ionized calcium binding adaptor molecule 1 (Iba1) and cathepsin X (Ctsx) were combined to quantify cathepsin X expression in microglia. Top: Representative images illustrate Iba1 IF (blue) and Ctsx (pink) in PBS and PFF injected rats at either one or two months. Ctsx IF appeared to exclusively overlap with Iba1 IF. Scale bar = 100μM. Bottom: Quantification of cellular profiles expressing Ctsx, mean Ctsx fluorescence intensity,

Figure 3.11 (cont'd)

total Ctsx fluorescent area and Iba1/ Ctsx colocalization was conducted. An increase in Ctsx profiles, Ctsx fluorescence intensity, Ctsx fluorescent area and Ctsx/Iba1 colocalization was observed in PFF-injected rats at both 1 and 2 months. One data point (624.8) is not visible due to the break in Y axis on the total fluorescent area one month PFF graph. Ctsx immunofluorescence was normalized to percent of PBS control. Values represent the mean ± SEM. **p ≤ 0.01, ***p ≤ 0.001.

DISCUSSION

In the present study we used intrastriatal α-Syn PFF injections in rats to induce the formation of pSyn inclusions in the SNpc and examined the expression of multiple cathepsins and *Th* using ddPCR. In the SN of PFF injected rats, the one-month timepoint featured decreased expression of *Th, Ctsa*, *Ctsb*, *Ctsd* and *Ctsf* and increased expression of *Ctsw* and *Ctsx* compared to control PBS-injected rats. At two months, decreased *Th* expression in the SN was again observed in PFF-injected rats, along with increased *Ctse*, *Ctsh*, and *Ctsx.* We next investigated the cellular source of specific cathepsins (*Ctsh*, *Ctsl, Ctss, Ctsx*) by leveraging various combinations of FISH combined with IF. We observed that microglia in the pSyn inclusion-bearing SNpc increase expression of *Ctsh, Ctss* and Ctsx at both timepoints after PFF injection suggesting that these specific cathepsins play a role in the microglial response to α-Syn inclusions.

These experiments were performed to validate our previous RNAseq findings using complementary methodology, as well as to identify the cellular source of some altered cathepsins. In general, we did not observe disagreement between our RNAseq and ddPCR findings (Table 3.1), however there were many examples in which one technique detected alterations when the other did not, at either one or both timepoints (*Ctsa, Ctsc, Ctsd, Ctse, Ctsf, Ctsh, Ctsl, Ctss, Ctsw*). The sole cathepsin in which the directionality of change was opposite between the RNAseq and ddPCR results was *Ctsb.* In our RNAseq results *Ctsb* was increased at one month following PFF injection, whereas *Ctsb* was decreased when measured using ddPCR. These discrepancies may be due to the different nigral dissection areas and/or differing rat strains between the

two studies and deserve further investigation. The most consistent change we observed across all methodological approaches was an increase in *Ctsx* at both timepoints in PFF-injected rats.

Table 1: Overview of cathepsin alterations in the inclusion-bearing substantia nigra

	RNAseq		ddPCR		FISH/IF		Cellular source
Cathepsin	*1 mo*	*2 mo*	*1 mo*	*2 mo*	*1 mo*	*2 mo*	
A	nc	nc	down	nc			
B	up	nc	down	nc			
C	up	up	nc	nc			
D	nc	nc	down	nc			
E	up	up	nc	up			
F	nc	nc	down	nc			
H	up	up	nc	up	up	up	microglia only
K	nc	nc	nc	nc			
L	up	nc	nc	nc	up	nc	microglia/non-microglia
S	up	up	nc	nc	up	up	microglia only
W	nc	nc	up	nc			
X	up	up	up	up	up	up	microglia only

nc = no change, up = significantly increased vs. PBS, down = significantly decreased vs. PBS

We observed that Cathepsin X (Ctsx) is almost exclusively expressed in Iba1 immunoreactive microglia and is markedly upregulated in the SNpc of PFF-injected rats. Ctsx is a carboxypeptidase, cleaving single amino acids or dipeptides from the C-terminus of protein peptides (Kos, Jevnikar, and Obermajer 2009; Kos et al. 2005; A. Pišlar et al. 2020). Ctsx expression has been shown to be induced by cytokines and TLR3/TLR4 activation, amplify cytokine release via the nuclear factor-kappa B (NF- κB) pathway and facilitate the migration and invasion of T-lymphocytes (Jevnikar et al. 2008; Zhao and Herrington 2016). In the brain, Ctsx has typically been localized to microglia but expression has also been observed in by astrocytes, oligodendrocytes and neurons, particularly aged neurons (Kos, Jevnikar, and Obermajer 2009; Wendt et al. 2007; A. Pišlar, Bolčina, and Kos 2021). Most relevant, increased microglial Ctsx expression has been reported in *in vitro* and *in vivo* models of neurodegeneration, as well as in association with plaques in postmortem AD brains (Wendt et al. 2007; Wendt et al. 2009; Pišlar et al. 2020; Pišlar and Kos 2014; Pišlar et al. 2022; Pišlar et al. 2017). Specifically, exposure of microglial cultures to LPS results in upregulation and release of Ctsx and leads to death of neurons, which can be blocked by a Ctsx inhibitor (Pišlar et al. 2017). LPS injection similarly leads to microglial Ctsx upregulation in multiple brain regions (Pišlar et al. 2020). Following 6-OHDA injections to rats, Ctsx is increased first within nigral neurons and later in nigral microglia during the neurodegenerative phase of the model (Pišlar et al. 2018). Within a transgenic AD mouse model, increased Ctsx is associated with plaque depositions (Wendt et al. 2007). Ctsx is known to cleave γ-enolase, which is known to mitigate Aß-associated toxicity, suggesting a possible neuroprotective role for Ctsx (Wendt et al. 2007; Hafner et al. 2013; A. H. Pišlar and Kos

2013; A. Pišlar et al. 2020). Our results are the first to identify increased Ctsx in response to pSyn inclusions. Collectively, whereas most evidence suggests that Ctsx promotes a damaging, proinflammatory response further investigation will be required to determine functional impact of increased microglial Ctsx in the inclusion-bearing SN.

We also observed that pSyn inclusions in the SNpc are associated with an increase in *Ctsh* within microglia. This upregulation was observed via ddPCR at two months and via IF/FISH at both time points. Interestingly, under homeostatic conditions, most *Ctsh* expression appeared to not be expressed within microglia whereas in the SN with pSyn inclusions most *Ctsh* expression shifted to microglia and was upregulated. Cathepsin H (Ctsh) is generally associated with neurotoxicity induced by inflammatory signaling, however the mechanisms remain unclear. It has been shown that LPS injections induce upregulation of microglial *Ctsh* and protein throughout the brain (Fan et al. 2015). In vitro, addition of Ctsh to microglia leads to the release of nitric oxide (NO), IL-1β, IL-6, and IFN-γ, and addition of Ctsh to cultured neurons result in higher rates of LPS induced cell death (Fan et al. 2015). This indicates that Ctsh is upregulated in response to inflammation and may have a neurotoxic influence on neurons. An increase in Ctsh has been observed in Huntington's disease brains (Mantle et al. 1995), but not in AD or PD brains. The specific mechanisms underlying these relationships is not completely understood, and it has been proposed that Ctsh may be binding to an unidentified receptor on neurons resulting in neurotoxic effects (Fan et al. 2015).

Our investigation into *Ctsl* expression revealed no changes in the inclusion-seeded SNpc using ddPCR, and only a modest transient increase in *Ctsl* within microglia and other cellular profiles. Cathepsin L (Ctsl) is normally expressed in

neurons, astrocytes and microglial (Funkelstein et al. 2008; Gu et al. 2015). Secretion of Ctsl from microglia is observed following LPS exposure, occurring prior to upregulation of inflammatory cytokines, suggesting it may play a role in amplifying inflammatory responses (Liu et al. 2008; Li et al. 2016). In further support of this role, inhibition of Ctsl in vivo lessens microglia-mediated neuroinflammation (Xu et al. 2018). Ctsl, along with Ctsb, Ctsh and Ctsk, can activate apoptotic cascades via cleavage of the pro-apoptotic Bid protein (Guicciardi et al. 2000). Similar to Ctsx, increased Ctsl is associated Aß plaques in the AD brain (Cataldo et al. 1991). Further, Ctsl expression has been shown to be increased in the SN and blood of PD patients (Li et al. 2011; Xu et al. 2018). Ctsl also has been shown to be involved in the response of both microglia and neurons to α-Syn. Exposure of microglial cultures to α-Syn oligomers results in Ctsl release, activation of microglial P2XY receptors and release of proinflammatory cytokines that are ultimately associated with neuronal damage and death (Jiang et al. 2022). Ctsl in neurons can digest both soluble and fibrillar α-Syn and may attenuate α-Syn aggregation (Matsuki et al. 2024; McGlinchey and Lee 2015; McGlinchey et al. 2017; McGlinchey et al. 2020). Our present results cannot confirm any of these roles for Ctsl in response to pSyn inclusions. We cannot rule out a role for secreted Ctsl, which would not be detectable in our examination of mRNA expression only.

We observed that *Ctss* expression was exclusively expressed by microglia and upregulated in microglia in the inclusion bearing SNpc, however ddPCR results revealed no overall changes. The restriction of Cathepsin S (Ctss) expression to microglia and other antigen presenting immune cells is well-documented (Yadati et al. 2020; A. Pišlar, Bolčina, and Kos 2021; Honey and Rudensky 2003). Ctss is a unique

cathepsin due to its ability to retain activity at a neutral pH, thereby increasing its possible involvement in extracellular processes (Petanceska et al. 1996; Kirschke et al. 1989; Jordans et al. 2009). Like Ctsx, Ctsh and Ctsl, Ctss can be released by microglia following stimulation with inflammatory cytokines and LPS (Nakanishi 2020). In the extracellular matrix (ECM), Ctss is associated with degradation of ECM components such as collagen, elastin, laminin, and tenascin (Vizovišek, Fonović, and Turk 2019). Ctss expression in the brain is normally low, but has been shown to be induced during inflammation, aging and associated with plaques in AD (Schechter and Ziv 2011; Wendt et al. 2008). Within microglia, it is well understood that Ctss plays a key role in maturation of MHC-II antigen processing. Ctss interacts with the CD74 invariant chain component of the MHC-II complex that normally sits in the antigen binding groove to prevent premature loading of antigens, Ctss cleaves CD74 upon activation, allowing for proper loading of antigens (Smyth et al. 2022; Hsing and Rudensky 2005). Notably, in the inclusion-bearing SNpc, we observe upregulation of MHC-II and *Cd74* expression in microglia (Duffy et al. 2018; Miller et al. 2021; Stoll, Kemp, Patterson, Howe, et al. 2024; Stoll, Kemp, Patterson, Kubik, et al. 2024). It is tempting to assume that the same microglial subpopulation co-express Ctss and MHC-II, however this deserves to be specifically examined. Paradoxically, Ctss can also exert anti-inflammatory effects. Ctss secreted from microglia in exosomes can cleave Cx3cl1 (fractalkine) on neurons, cleaved fractalkine can then activate Cx3cr1 receptors on microglia which is known to inhibit release of pro-inflammatory cytokines and return microglia to a quiescent state (Clark and Malcangio 2012). Whether the increase in microglial *Ctss* expression we

observe in the SNpc with pSyn inclusions represents a pro- or anti-inflammatory response remains to be determined.

Overall, this set of experiments aimed to validate and follow up on the findings from our RNA sequencing dataset in a separate cohort of rats using complementary approaches. Our results provide evidence that microglia in the pSyn inclusion-bearing SNpc markedly increase expression of *Ctsh, Ctss* and Ctsx. Whereas previous studies have documented increases in all three of these cathepsins in relationship to AD or HD, to our knowledge this has not been reported in the PD brain. Our findings are the first to connect increased *Ctsh, Ctss* and Ctsx to LB-like pathology. Ctsx, in particular, was revealed to be consistently upregulated in the inclusion-bearing SNpc across both timepoints regardless of the methodological approach used. This suggests that further studies investigating the role of Ctsx in the microglial response to pSyn inclusions should be conducted to explore whether targeting Ctsx may be a useful therapeutic strategy for neuroprotection in PD.

FIGURES

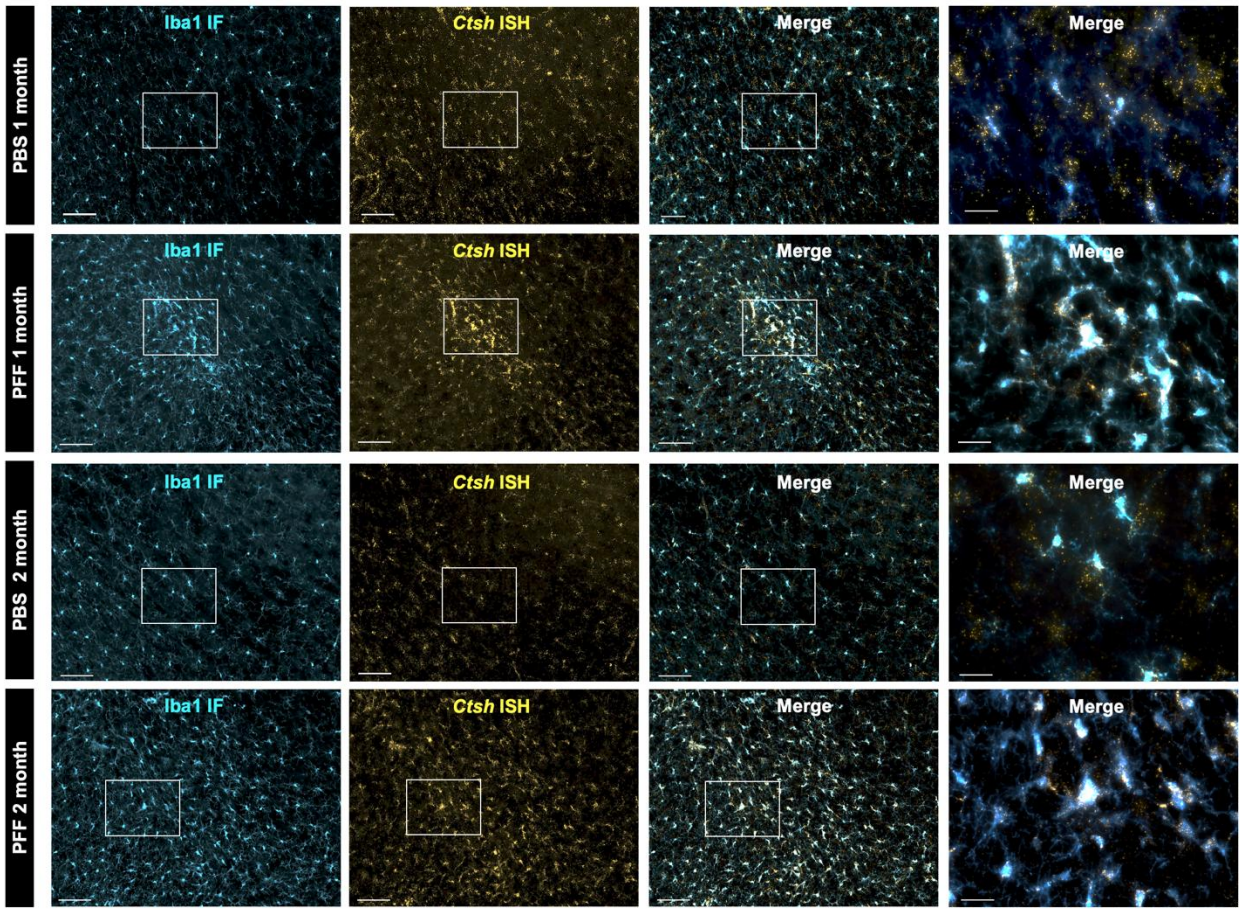

Figure S3.1: *Ctsh* expression

Rats received bilateral intrastriatal injections of alpha-synuclein preformed fibrils (α-Syn PFFs) or phosphate buffered saline (PBS). Immunofluorescence (IF) of ionized calcium binding adaptor molecule 1 (Iba1) was combined with fluorescent *in situ* hybridization (FISH) to quantify *Ctsh* expression in microglia. Representative images illustrate Iba1 IF (blue) and *Ctsh* FISH (yellow) in PBS and PFF injected rats at either one or two months. *Ctsh* expression overlapped with both Iba1 IF as well as areas without Iba1 immunoreactivity. Scale bars in columns 1-3 = 1000μM, scale bars in column 4 = 100 μM.

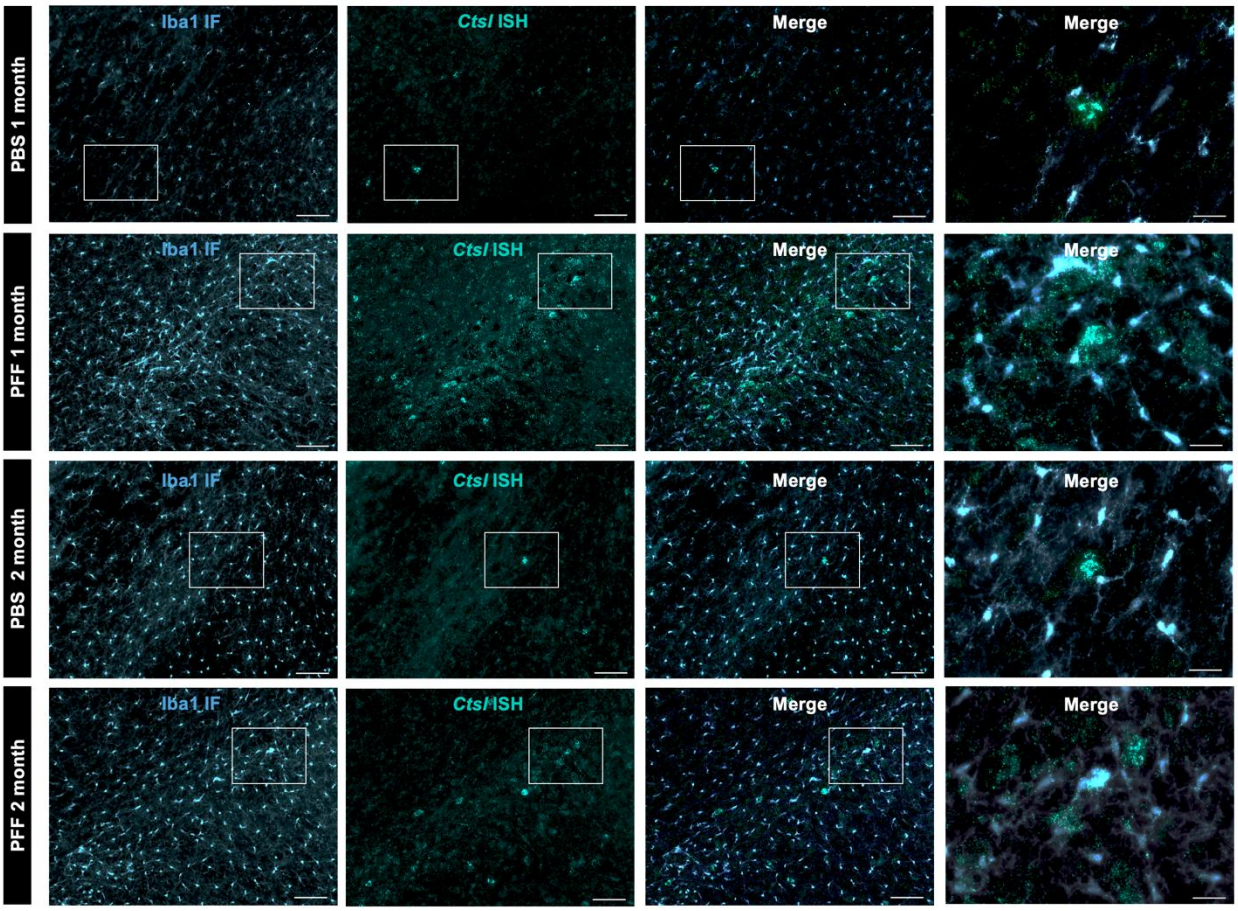

Figure S3.2: *Ctsl* expression

Rats received bilateral intrastriatal injections of alpha-synuclein preformed fibrils (α-Syn PFFs) or phosphate buffered saline (PBS). Immunofluorescence (IF) of ionized calcium binding adaptor molecule 1 (Iba1) was combined with fluorescent *in situ* hybridization (FISH) to quantify *Ctsl* expression in microglia. Representative images illustrate Iba1 IF (blue) and *Ctsh* FISH (green) in PBS and PFF injected rats at either one or two months. *Ctsl* expression overlapped with both Iba1 IF as well as areas without Iba1 immunoreactivity. Scale bars in columns 1-3 = 1000μM, scale bars in column 4 = 100 μM.

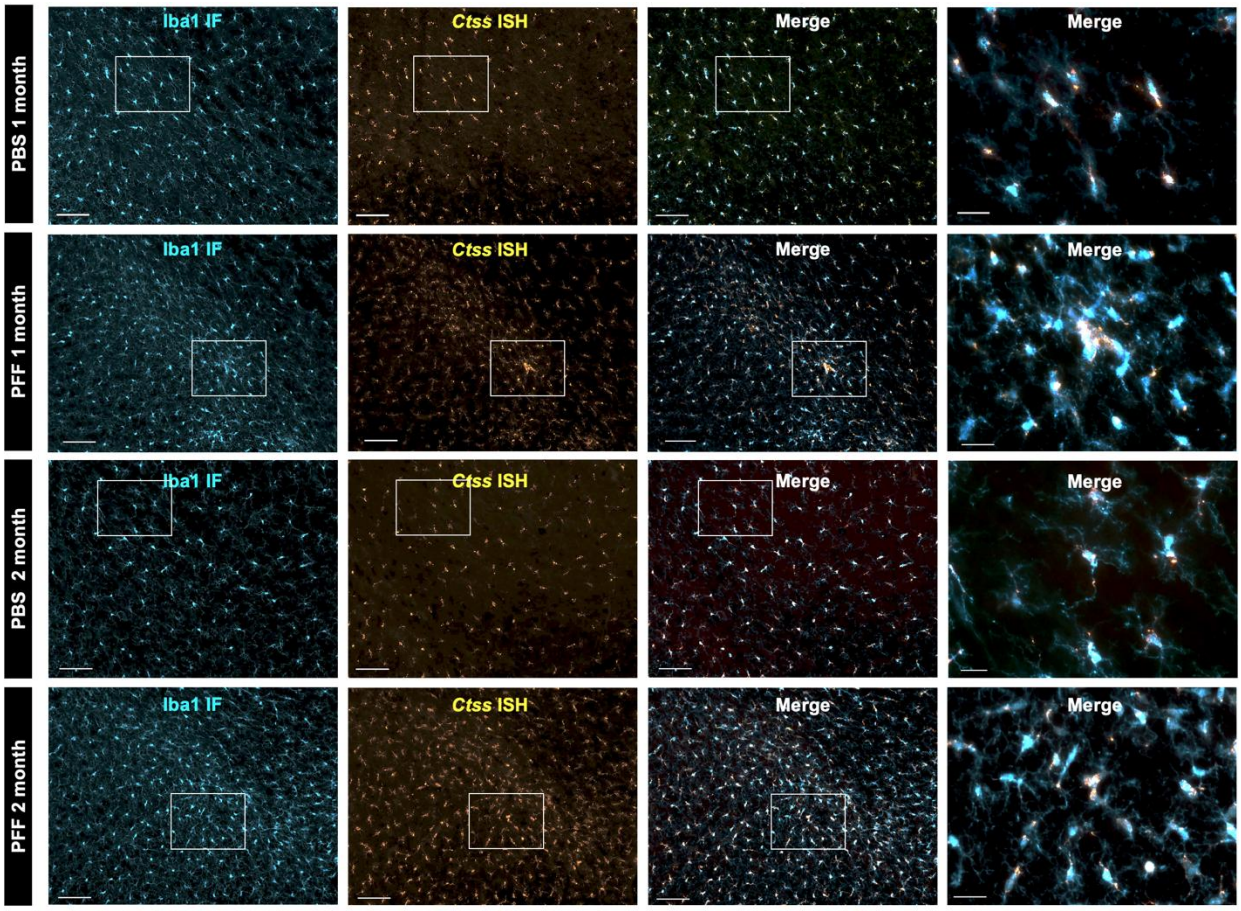

Figure S3.3: *Ctss* expression

Rats received bilateral intrastriatal injections of alpha-synuclein preformed fibrils (α-Syn PFFs) or phosphate buffered saline (PBS). Immunofluorescence (IF) of ionized calcium binding adaptor molecule 1 (Iba1) was combined with fluorescent *in situ* hybridization (FISH) to quantify *Ctss* expression in microglia. Representative images illustrate Iba1 IF (blue) and *Ctss* FISH (yellow) in PBS and PFF injected rats at either one or two months. *Ctss* expression appeared to exclusively overlap with Iba1 IF. Scale bars in columns 1-3 = 1000μM, scale bars in column 4 = 100 μM.

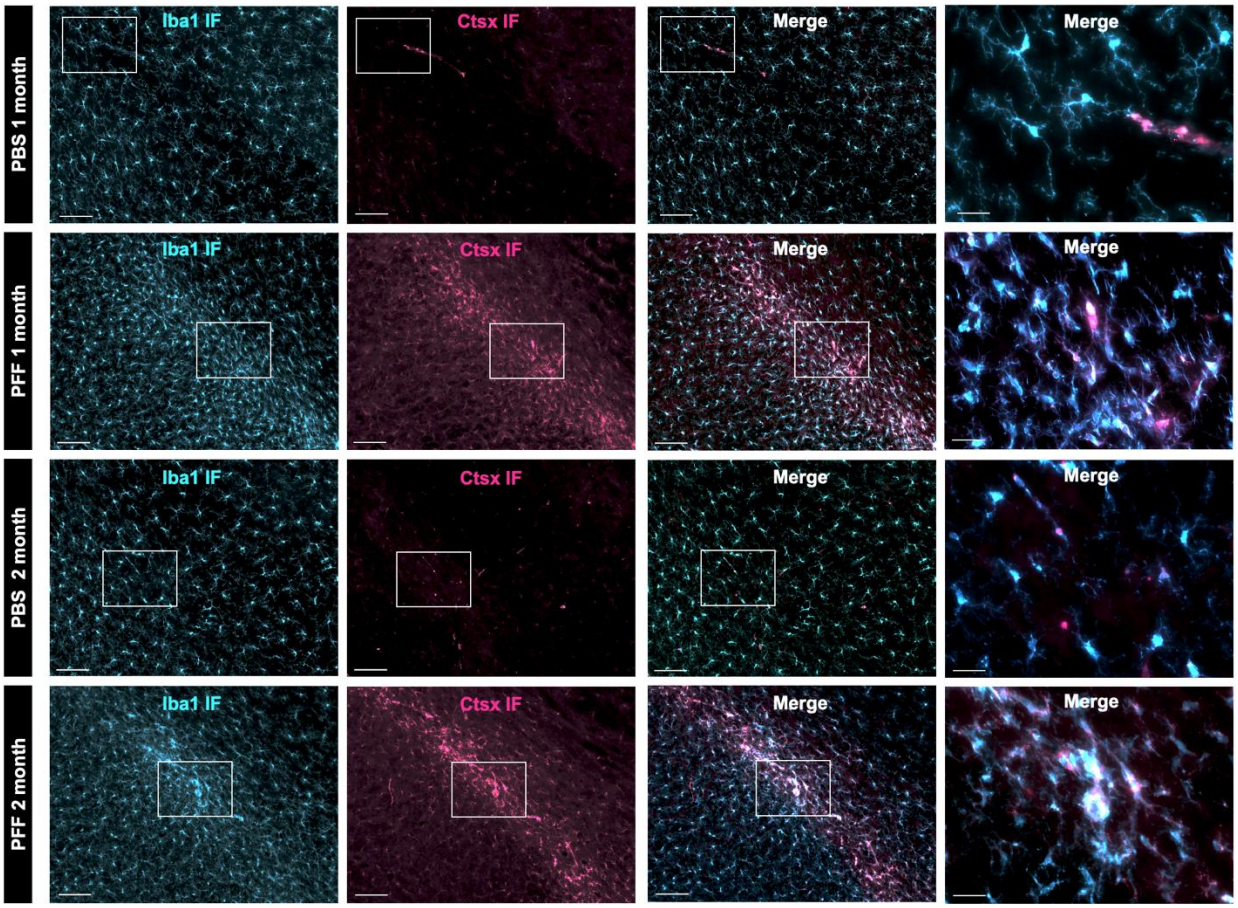

Figure S3.4: Cathepsin X expression

Rats received bilateral intrastriatal injections of alpha-synuclein preformed fibrils (α-Syn PFFs) or phosphate buffered saline (PBS). Dual immunofluorescence (IF) of ionized calcium binding adaptor molecule 1 (Iba1) and cathepsin X (Ctsx) were combined to quantify cathepsin X expression in microglia. Representative images illustrate Iba1 IF (blue) and Ctsx (pink) in PBS and PFF injected rats at either one or two months. Ctsx IF appeared to exclusively overlap with Iba1 IF. Scale bars in columns 1-3 = 1000μM, scale bars in column 4 = 100 μM.

BIBLIOGRAPHY

Abdelmotilib, Hisham, Tyler Maltbie, Vedad Delic, Zhiyong Liu, Xianzhen Hu, Kyle B Fraser, Mark S Moehle, et al. 2017. “α-Synuclein Fibril-Induced Inclusion Spread in Rats and Mice Correlates with Dopaminergic Neurodegeneration.” Neurobiology of Disease 105 (September): 84–98. https://doi.org/10.1016/j.nbd.2017.05.014.

Bird, Phillip I, Joseph A Trapani, and José A Villadangos. 2009. “Endolysosomal Proteases and Their Inhibitors in Immunity.” Nature Reviews. Immunology 9 (12): 871–82. https://doi.org/10.1038/nri2671.

Brix, Klaudia, Anna Dunkhorst, Kristina Mayer, and Silvia Jordans. 2008. “Cysteine Cathepsins: Cellular Roadmap to Different Functions.” Biochimie 90 (2): 194–207. https://doi.org/10.1016/j.biochi.2007.07.024.

Dijk, Karin D van, Emanuele Persichetti, Davide Chiasserini, Paolo Eusebi, Tommaso Beccari, Paolo Calabresi, Henk W Berendse, Lucilla Parnetti, and Wilma D J van de Berg. 2013. “Changes in Endolysosomal Enzyme Activities in Cerebrospinal Fluid of Patients with Parkinson’s Disease.” Movement Disorders 28 (6): 747–54. https://doi.org/10.1002/mds.25495.

Duffy, Megan F, Timothy J Collier, Joseph R Patterson, Christopher J Kemp, Kelvin C Luk, Malú G Tansey, Katrina L Paumier, et al. 2018. “Lewy Body-like Alpha-Synuclein Inclusions Trigger Reactive Microgliosis Prior to Nigral Degeneration.” Journal of Neuroinflammation 15 (1): 129. https://doi.org/10.1186/s12974-018-1171-z.

Fan, Kai, Daobo Li, Yanli Zhang, Chao Han, Junjie Liang, Changyi Hou, Hongliang Xiao, Kazuhiro Ikenaka, and Jianmei Ma. 2015. “The Induction of Neuronal Death by Up-Regulated Microglial Cathepsin H in LPS-Induced Neuroinflammation.” Journal of Neuroinflammation 12 (March): 54. https://doi.org/10.1186/s12974-015-0268-x.

Funkelstein, Lydiane, Thomas Toneff, Shin-Rong Hwang, Thomas Reinheckel, Christoph Peters, and Vivian Hook. 2008. “Cathepsin L Participates in the Production of Neuropeptide Y in Secretory Vesicles, Demonstrated by Protease Gene Knockout and Expression.” Journal of Neurochemistry 106 (1): 384–91. https://doi.org/10.1111/j.1471-4159.2008.05408.x.

Hafner, Anja, Gordana Glavan, Nataša Obermajer, Marko Živin, Reinhard Schliebs, and Janko Kos. 2013. “Neuroprotective Role of γ-Enolase in Microglia in a Mouse Model of Alzheimer’s Disease Is Regulated by Cathepsin X.” Aging Cell 12 (4): 604–14. https://doi.org/10.1111/acel.12093.

Honey, Karen, and Alexander Y Rudensky. 2003. “Lysosomal Cysteine Proteases Regulate Antigen Presentation.” Nature Reviews. Immunology 3 (6): 472–82. https://doi.org/10.1038/nri1110.

Hook, Vivian, Lydiane Funkelstein, Jill Wegrzyn, Steven Bark, Mark Kindy, and Gregory Hook. 2012. “Cysteine Cathepsins in the Secretory Vesicle Produce Active Peptides: Cathepsin L Generates Peptide Neurotransmitters and Cathepsin B Produces Beta-Amyloid of Alzheimer’s Disease.” Biochimica et Biophysica Acta 1824 (1): 89–104. https://doi.org/10.1016/j.bbapap.2011.08.015.

Horvat, Selena, Janko Kos, and Anja Pišlar. 2024. “Multifunctional Roles of γ-Enolase in the Central Nervous System: More than a Neuronal Marker.” Cell & Bioscience 14 (1): 61. https://doi.org/10.1186/s13578-024-01240-6.

Howe, Jacob W, Caryl E Sortwell, Megan F Duffy, Christopher J Kemp, Christopher P Russell, Michael Kubik, Pooja Patel, Kelvin C Luk, Omar M A El-Agnaf, and Joseph R Patterson. 2021. “Preformed Fibrils Generated from Mouse Alpha-Synuclein Produce More Inclusion Pathology in Rats than Fibrils Generated from Rat Alpha-Synuclein.” Parkinsonism & Related Disorders 89 (August): 41–47. https://doi.org/10.1016/j.parkreldis.2021.06.010.

Hsing, Lianne C, and Alexander Y Rudensky. 2005. “The Lysosomal Cysteine Proteases in MHC Class II Antigen Presentation.” Immunological Reviews 207 (October): 229–41. https://doi.org/10.1111/j.0105-2896.2005.00310.x.

Jevnikar, Zala, Natasa Obermajer, Matthew Bogyo, and Janko Kos. 2008. “The Role of Cathepsin X in the Migration and Invasiveness of T Lymphocytes.” Journal of Cell Science 121 (Pt 16): 2652–61. https://doi.org/10.1242/jcs.023721.

Jiang, Tianfang, Chuanying Xu, Shane Gao, Jia Zhang, Jia Zheng, Xiaolin Wu, Qiuyun Lu, et al. 2022. “Cathepsin L-Containing Exosomes from α-Synuclein-Activated Microglia Induce Neurotoxicity through the P2X7 Receptor.” Npj Parkinson’s Disease 8 (1): 127. https://doi.org/10.1038/s41531-022-00394-9.

Kamath, Tushar, Abdulraouf Abdulraouf, S J Burris, Jonah Langlieb, Vahid Gazestani, Naeem M Nadaf, Karol Balderrama, Charles Vanderburg, and Evan Z Macosko. 2022. “Single-Cell Genomic Profiling of Human Dopamine Neurons Identifies a Population That Selectively Degenerates in Parkinson’s Disease.” Nature Neuroscience 25 (5): 588–95. https://doi.org/10.1038/s41593-022-01061-1.

Kirschke, H, B Wiederanders, D Brömme, and A Rinne. 1989. “Cathepsin S from Bovine Spleen. Purification, Distribution, Intracellular Localization and Action on Proteins.” The Biochemical Journal 264 (2): 467–73. https://doi.org/10.1042/bj2640467.

Kos, Janko, Zala Jevnikar, and Natasa Obermajer. 2009. “The Role of Cathepsin X in Cell Signaling.” Cell Adhesion & Migration 3 (2): 164–66. https://doi.org/10.4161/cam.3.2.7403.

Kos, Janko, Andreja Sekirnik, Ales Premzl, Valentina Zavasnik Bergant, Tomaz Langerholc, Boris Turk, Bernd Werle, et al. 2005. “Carboxypeptidases Cathepsins X

and B Display Distinct Protein Profile in Human Cells and Tissues." Experimental Cell Research 306 (1): 103–13. https://doi.org/10.1016/j.yexcr.2004.12.006.

Leys, Christophe, Christophe Ley, Olivier Klein, Philippe Bernard, and Laurent Licata. 2013. "Detecting Outliers: Do Not Use Standard Deviation around the Mean, Use Absolute Deviation around the Median." Journal of Experimental Social Psychology 49 (4): 764–66. https://doi.org/10.1016/j.jesp.2013.03.013.

Lin, Liyu, Zilun Wu, Haocheng Luo, and Yunxuan Huang. 2024. "Cathepsin-Mediated Regulation of Alpha-Synuclein in Parkinson's Disease: A Mendelian Randomization Study." Frontiers in Aging Neuroscience 16 (May): 1394807. https://doi.org/10.3389/fnagi.2024.1394807.

Luk, Kelvin C, Victoria M Kehm, Bin Zhang, Patrick O'Brien, John Q Trojanowski, and Virginia M Y Lee. 2012. "Intracerebral Inoculation of Pathological α-Synuclein Initiates a Rapidly Progressive Neurodegenerative α-Synucleinopathy in Mice." The Journal of Experimental Medicine 209 (5): 975–86. https://doi.org/10.1084/jem.20112457.

Matsuki, Ayumi, Yoshihisa Watanabe, Sho Hashimoto, Atsushi Hoshino, and Satoaki Matoba. 2024. "Cathepsin L Prevents the Accumulation of Alpha-Synuclein Fibrils in the Cell." Genes To Cells 29 (4): 328–36. https://doi.org/10.1111/gtc.13099.

McGlinchey, Ryan P, Gifty A Dominah, and Jennifer C Lee. 2017. "Taking a Bite Out of Amyloid: Mechanistic Insights into α-Synuclein Degradation by Cathepsin L." Biochemistry 56 (30): 3881–84. https://doi.org/10.1021/acs.biochem.7b00360.

McGlinchey, Ryan P, and Jennifer C Lee. 2015. "Cysteine Cathepsins Are Essential in Lysosomal Degradation of α-Synuclein." Proceedings of the National Academy of Sciences of the United States of America 112 (30): 9322–27. https://doi.org/10.1073/pnas.1500937112.

Miller, Kathryn M, Joseph R Patterson, Joseph Kochmanski, Christopher J Kemp, Anna C Stoll, Christopher U Onyekpe, Allyson Cole-Strauss, et al. 2021. "Striatal Afferent BDNF Is Disrupted by Synucleinopathy and Partially Restored by STN DBS." The Journal of Neuroscience 41 (9): 2039–52. https://doi.org/10.1523/JNEUROSCI.1952-20.2020.

Ni, Junjun, Zhou Wu, Christoph Peterts, Kenji Yamamoto, Hong Qing, and Hiroshi Nakanishi. 2015. "The Critical Role of Proteolytic Relay through Cathepsins B and E in the Phenotypic Change of Microglia/Macrophage." The Journal of Neuroscience 35 (36): 12488–501. https://doi.org/10.1523/JNEUROSCI.1599-15.2015.

Patterson, Joseph R, Megan F Duffy, Christopher J Kemp, Jacob W Howe, Timothy J Collier, Anna C Stoll, Kathryn M Miller, et al. 2019. "Time Course and Magnitude of Alpha-Synuclein Inclusion Formation and Nigrostriatal Degeneration in the Rat Model of Synucleinopathy Triggered by Intrastriatal α-Synuclein Preformed Fibrils."

Neurobiology of Disease 130 (October): 104525. https://doi.org/10.1016/j.nbd.2019.104525.

Patterson, Joseph R, Warren D Hirst, Jacob W Howe, Christopher P Russell, Allyson Cole-Strauss, Christopher J Kemp, Megan F Duffy, et al. 2022. “Beta2-Adrenoreceptor Agonist Clenbuterol Produces Transient Decreases in Alpha-Synuclein MRNA but No Long-Term Reduction in Protein.” Npj Parkinson’s Disease 8 (1): 61. https://doi.org/10.1038/s41531-022-00322-x.

Patterson, Joseph R, Nicole K Polinski, Megan F Duffy, Christopher J Kemp, Kelvin C Luk, Laura A Volpicelli-Daley, Nicholas M Kanaan, and Caryl E Sortwell. 2019. “Generation of Alpha-Synuclein Preformed Fibrils from Monomers and Use In Vivo.” Journal of Visualized Experiments, no. 148 (June). https://doi.org/10.3791/59758.

Petanceska, S, P Canoll, and L A Devi. 1996. “Expression of Rat Cathepsin S in Phagocytic Cells.” The Journal of Biological Chemistry 271 (8): 4403–9. https://doi.org/10.1074/jbc.271.8.4403.

Pišlar, Anja, Lara Bolčina, and Janko Kos. 2021. “New Insights into the Role of Cysteine Cathepsins in Neuroinflammation.” Biomolecules 11 (12). https://doi.org/10.3390/biom11121796.

Pišlar, Anja, Biljana Božić, Nace Zidar, and Janko Kos. 2017. “Inhibition of Cathepsin X Reduces the Strength of Microglial-Mediated Neuroinflammation.” Neuropharmacology 114 (March): 88–100. https://doi.org/10.1016/j.neuropharm.2016.11.019.

Pišlar, Anja, Biljana Božić Nedeljković, Mina Perić, Tanja Jakoš, Nace Zidar, and Janko Kos. 2022. “Cysteine Peptidase Cathepsin X as a Therapeutic Target for Simultaneous TLR3/4-Mediated Microglia Activation.” Molecular Neurobiology 59 (4): 2258–76. https://doi.org/10.1007/s12035-021-02694-2.

Pišlar, Anja, Larisa Tratnjek, Gordana Glavan, Nace Zidar, Marko Živin, and Janko Kos. 2019. “Therapeutic Potential of Inhibition of the Neuroinflammation Induced Cathepsin X: In Vivo Evidence.” BioRxiv, January. https://doi.org/10.1101/513671.

Pišlar, Anja, Larisa Tratnjek, Gordana Glavan, Nace Zidar, Marko Živin, and Janko Kos. 2020. “Neuroinflammation-Induced Upregulation of Glial Cathepsin X Expression and Activity in Vivo.” Frontiers in Molecular Neuroscience 13 (November): 575453. https://doi.org/10.3389/fnmol.2020.575453.

Pišlar, Anja, Larisa Tratnjek, Gordana Glavan, Marko Živin, and Janko Kos. 2018. “Upregulation of Cysteine Protease Cathepsin X in the 6-Hydroxydopamine Model of Parkinson’s Disease.” Frontiers in Molecular Neuroscience 11 (November): 412. https://doi.org/10.3389/fnmol.2018.00412.

Pišlar, Anja Hafner, and Janko Kos. 2013. “C-Terminal Peptide of γ-Enolase Impairs Amyloid-β-Induced Apoptosis through P75(NTR) Signaling.” Neuromolecular Medicine 15 (3): 623–35. https://doi.org/10.1007/s12017-013-8247-9.

Polinski, Nicole K, Laura A Volpicelli-Daley, Caryl E Sortwell, Kelvin C Luk, Nunilo Cremades, Lindsey M Gottler, Jessica Froula, et al. 2018. “Best Practices for Generating and Using Alpha-Synuclein Pre-Formed Fibrils to Model Parkinson’s Disease in Rodents.” Journal of Parkinson’s Disease 8 (2): 303–22. https://doi.org/10.3233/JPD-171248.

Reiser, Jochen, Brian Adair, and Thomas Reinheckel. 2010. “Specialized Roles for Cysteine Cathepsins in Health and Disease.” The Journal of Clinical Investigation 120 (10): 3421–31. https://doi.org/10.1172/JCI42918.

Schneider, Caroline A, Wayne S Rasband, and Kevin W Eliceiri. 2012. “NIH Image to ImageJ: 25 Years of Image Analysis.” Nature Methods 9 (7): 671–75. https://doi.org/10.1038/nmeth.2089.

Smyth, Peter, Jutharat Sasiwachirangkul, Rich Williams, and Christopher J Scott. 2022. “Cathepsin S (CTSS) Activity in Health and Disease - A Treasure Trove of Untapped Clinical Potential.” Molecular Aspects of Medicine 88 (December): 101106. https://doi.org/10.1016/j.mam.2022.101106.

Stoll, Anna C, Christopher J Kemp, Joseph R Patterson, Michael Kubik, Nathan Kuhn, Matthew Benskey, Megan F Duffy, Kelvin C Luk, and Caryl E Sortwell. 2024. “Alpha-Synuclein Inclusion Responsive Microglia Are Resistant to CSF1R Inhibition.” Journal of Neuroinflammation 21 (1): 108. https://doi.org/10.1186/s12974-024-03108-5.

Tarutani, Airi, Genjiro Suzuki, Aki Shimozawa, Takashi Nonaka, Haruhiko Akiyama, Shin-Ichi Hisanaga, and Masato Hasegawa. 2016. “The Effect of Fragmented Pathogenic α-Synuclein Seeds on Prion-like Propagation.” The Journal of Biological Chemistry 291 (36): 18675–88. https://doi.org/10.1074/jbc.M116.734707.

Turk, B, I Dolenc, B Lenarcic, I Krizaj, V Turk, J G Bieth, and I Björk. 1999. “Acidic PH as a Physiological Regulator of Human Cathepsin L Activity.” European Journal of Biochemistry / FEBS 259 (3): 926–32. https://doi.org/10.1046/j.1432-1327.1999.00145.x.

Turk, Vito, Veronika Stoka, Olga Vasiljeva, Miha Renko, Tao Sun, Boris Turk, and Dušan Turk. 2012. “Cysteine Cathepsins: From Structure, Function and Regulation to New Frontiers.” Biochimica et Biophysica Acta 1824 (1): 68–88. https://doi.org/10.1016/j.bbapap.2011.10.002.

Vizin, Tjasa, and Janko Kos. 2015. “Gamma-Enolase: A Well-Known Tumour Marker, with a Less-Known Role in Cancer.” Radiology and Oncology 49 (3): 217–26. https://doi.org/10.1515/raon-2015-0035.

Vizovišek, Matej, Marko Fonović, and Boris Turk. 2019. “Cysteine Cathepsins in Extracellular Matrix Remodeling: Extracellular Matrix Degradation and Beyond.” Matrix Biology 75–76 (January): 141–59. https://doi.org/10.1016/j.matbio.2018.01.024.

Volpicelli-Daley, Laura A, Kelvin C Luk, Tapan P Patel, Selcuk A Tanik, Dawn M Riddle, Anna Stieber, David F Meaney, John Q Trojanowski, and Virginia M-Y Lee. 2011. “Exogenous α-Synuclein Fibrils Induce Lewy Body Pathology Leading to Synaptic Dysfunction and Neuron Death.” Neuron 72 (1): 57–71. https://doi.org/10.1016/j.neuron.2011.08.033.

Wang, Hao, Jingjing Li, Han Zhang, Mengyao Wang, Lifang Xiao, Yitong Wang, and Qiong Cheng. 2023. “Regulation of Microglia Polarization after Cerebral Ischemia.” Frontiers in Cellular Neuroscience 17 (June): 1182621. https://doi.org/10.3389/fncel.2023.1182621.

Wendt, Wiebke, Xin-Ran Zhu, Hermann Lübbert, and Christine C Stichel. 2007. “Differential Expression of Cathepsin X in Aging and Pathological Central Nervous System of Mice.” Experimental Neurology 204 (2): 525–40. https://doi.org/10.1016/j.expneurol.2007.01.007.

Yadati, Tulasi, Tom Houben, Albert Bitorina, and Ronit Shiri-Sverdlov. 2020. “The Ins and Outs of Cathepsins: Physiological Function and Role in Disease Management.” Cells 9 (7). https://doi.org/10.3390/cells9071679.

Yusufujiang, Aishanjiang, Shan Zeng, and Hongyan Li. 2024. “Cathepsins and Parkinson’s Disease: Insights from Mendelian Randomization Analyses.” Frontiers in Aging Neuroscience 16 (June): 1380483. https://doi.org/10.3389/fnagi.2024.1380483.

Zhao, Caroline F, and David M Herrington. 2016. “The Function of Cathepsins B, D, and X in Atherosclerosis.” American Journal of Cardiovascular Disease 6 (4): 163–70.

CHAPTER 4: CONCLUSION AND FUTURE DIRECTIONS

OVERVIEW

Parkinson's Disease (PD) is progressive neurodegenerative disorder with no cure or disease modifying therapies available to patients. Significant neurodegeneration of dopamine (DA) neurons within the substantia nigra pars compacta (SNpc) has already occurred prior to onset of symptoms. There are no available strategies to revive DA neurons after they have died, and thus, understanding the early pathogenic mechanisms of PD may provide an intervention window to slow or halt disease progression. It is appreciated that the earliest pathology in PD is the aggregation of alpha-synuclein (α-Syn) into aggregates called Lewy bodies (LBs) or Lewy neurites (LNs) that are primarily composed of phosphorylated α-Syn (pSyn). Concurrently, there is a neuroinflammatory response from reactive microglia that may be contributing to disease progression and neurodegeneration. The specific mechanisms and contributions of reactive microglia responding to early α-Syn aggregates is not well understood and is the current focus of this research.

To study this, we leveraged the rat preformed fibril (PFF) model, which has two distinct phases of synucleinopathy, the aggregation phase, characterized by the formation of pSyn inclusions, and the degeneration phase, characterized by the loss of tyrosine hydroxylase (TH; rate limiting enzyme of DA synthesis) phenotype in DA neurons, followed by overt neurodegeneration. This two-phase model allows us to dissect mechanisms associated with the distinct stages of disease progression. Our work is focused on the early aggregation phase, where pSyn inclusions are considered immature (one-month post PFF injection) and more mature (two-months post PFF injection), but prior to TH phenotype loss or overt neurodegeneration. Importantly, pSyn

aggregation is associated with microglial expression of major histocompatibility complex II (MHC-II) within the pSyn bearing SNpc. Using laser capture microdissection (LCM) and bulk RNA sequencing (RNAseq), we were able to selectively dissect nigral pSyn bearing neurons and immediately adjacent reactive microglia at one and two months following PFF injection and identify differentially expressed genes (DEGs) in the PFF treated SNpc compared to the PBS treated SNpc.

Our results from the LCM-RNAseq experiment suggest that cytokine production and microglial activation are upregulated in association with both early and more mature pSyn inclusions. The earlier one-month time point is specifically associated with upregulation of DEGs associated with ribosomal biogenesis, RNA processing and protein degradation whereas the later, two-month, time point is specifically associated with the upregulation of DEGs implicating microglial activation of defense responses to viruses to protect the host. Downregulation of DEGs associated with cell signaling, neurotransmitter synthesis, and synaptic transmission are also common across both time points. Collectively, these results suggest that the response to pSyn inclusions in the SNpc is temporally dynamic. Further, the results support a role for multiple cathepsins over the course of both early and more mature pSyn inclusions.

We then followed up on cathepsins, a family of proteases associated with the lysosomal system, using droplet digital PCR (ddPCR), fluorescent *in situ* hybridization (FISH), and immunofluorescence (IF). In the SN of PFF injected rats, the one-month timepoint featured decreased expression of *Th, Ctsa, Ctsb, Ctsd* and *Ctsf* and increased expression of *Ctsw* and *Ctsx* compared to control PBS-injected rats. At two months, decreased *Th* expression in the SN was again observed in PFF-injected rats,

along with increased *Ctse, Ctsh*, and *Ctsx*. We next investigated the cellular source of specific cathepsins (*Ctsh, Ctsl, Ctss*, Ctsx) by leveraging various combinations of FISH combined with IF. We observed that microglia in the pSyn inclusion-bearing SNpc increases expression of *Ctsh, Ctss* and Ctsx at both timepoints after PFF injection suggesting that these specific cathepsins play a role in the microglial response to α-syn inclusions.

TECHNICAL LIMITATIONS OF THE CURRENT METHODS

The methods used in this set of experiments – LCM / RNA sequencing, ddPCR, and fluorescent *in situ* hybridization – each present their own technical limitations that can impact data interpretation. RNA sequencing, while a powerful tool for transcriptome analysis, is susceptible to RNA degradation during sampling handling and preparation, and potential amplification bias during library preparation. To mitigate these issues, we implemented a 60-minute time limit when collecting the tissue during LCM and dropped the isolated tissue directly into TRIzol to prevent RNase degradation. For the RNA sequencing, we used 50 base pair read depth, which has been shown to be accurate for differential gene expression analysis (Shetty et al., 2020), as well as a paired-ends reads, to further ensure results were as accurate as possible.

As powerful as it is, RNA sequencing as a technique is not attempting to detect a specific gene, but rather reading raw cDNA generated from mRNA, and aligning the reads to a genome. The results from these analyses are dependent on how accurate the alignment was to the genome, and how well the annotated the genome is, which pose limitations for the technique. Additionally, we performed bulk RNA sequencing, as opposed to single cell RNA sequencing, where information about cell-type specific RNA

changes is lost. To understand biological implications of the DEGs identified, we used Kyoto Encyclopedia of Genes and Genomes (KEGG) and Gene Ontology (GO) enrichment analyses (Ashburner et al., 2000; Kanehisa & Goto, 2000). The pathway enrichment analyses also demonstrate technical limitations. For example, the pathways do not differentiate from a specific cell-type or tissue location, I.E the pathways are not specific to neurons, microglia, astrocytes, etc. Genes and genetic changes could be shared between multiple cell types in and out of the CNS, which could bias the pathway results to lean towards more generic inflammatory pathways, rather than CNS specific pathways.

To validate our findings and overcome some of the aforementioned limitations, we used ddPCR, a more accurate technique to determine differential gene expression. What makes ddPCR more accurate is that a primer/probe set is specific to the target, rather than reading anything and everything, like from RNAseq. This technique is much more sensitive, accurate, and dependable, when looking for a known gene, especially since it is not dependent on genome alignment and annotation. With that, we appreciated some discrepancies between our RNAseq and ddPCR results. This could be attributed to a few factors. As discussed, ddPCR is much more sensitive and accurate when the gene of interest is already known, in addition, there were differences between the experiments that could have contributed to the mismatch. Namely, the strain of rat used and the sampling technique. Because our LCM-RNAseq was performed in a transgenic rat, we wanted to validate biological differences and used a different strain of rat for our ddPCR results. This would ensure that differences were not due to the use of a transgenic animal, but a biological response to pSyn inclusions.

Additionally, the sampling method of LCM is incredibly precise – with the ability to selectively isolate the SNpc. In contrast, with ddPCR we implemented a microdissection punching strategy that collects a broader region, including the whole SN. This broader sampling may have diluted the signal from the reactive microglia specifically responding to pSyn inclusions, potentially explaining some of the observed differences in cathepsin expression profiles between the two techniques (Figure 4.1).

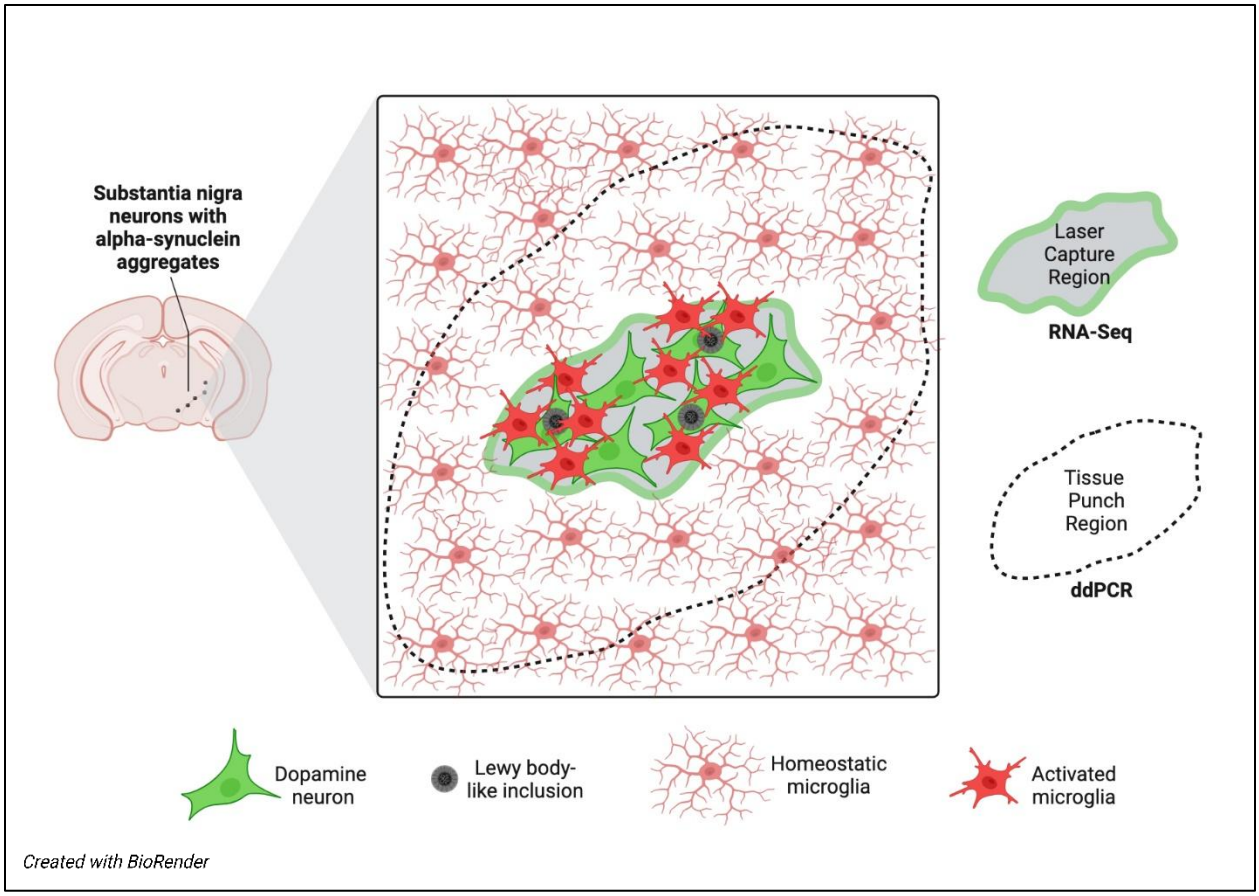

Figure 4.1 Tissue collection strategies that may have impacted transcriptional analysis

BIOLOGICAL LIMITATIONS OF THE CURRENT METHODS

A significant limitation in studying mRNA expression is the non-linear relationship between mRNA and protein levels. Each gene is influenced by several factors that affect protein synthesis, including post transcriptional and translational modifications, varying rates of mRNA decay, as well as differing protein half-lives. For instance, stable proteins with long half-lives will require low mRNA levels, whereas proteins with short half-lives and high turnover can result in inflated mRNA levels. Therefore, it is important to validate protein levels when drawing conclusions from mRNA data. Future studies should investigate the relationship between mRNA and protein levels, either via immunohistochemistry, immunofluorescence, or Western blots, for example.

Specifically regarding cathepsins, post-translational modifications are a key aspect of the regulation and function of the end product. Of the cathepsins that have been investigated, they share a similar pattern of post-translational modification. Cathepsins B, L, and H have shown that cathepsins are synthesized as pre-pro-mature complexes that undergo cleavage and glycosylation to remove the pre- and pro-components resulting in the mature protease (Katunuma, 2010). The mature protease can undergo further processing, depending on the organ or organelle, tailored for where the cathepsin is being expressed (Petushkova & Zamyatnin, 2020). Cathepsin L was one of the cathepsins that we investigated using fluorescent *in situ* hybridization and found little to no increases in mRNA expression. The half-life of cathepsin L is 24h, which is particularly long when compared to cathepsin H, which has a half-life of 12h (Katunuma, 2010). This could explain why we saw such differences in cathepsin H, compared to the modest differences in cathepsin L mRNA expression.

FUTURE DIRECTIONS WITH THE PFF MODEL

A key finding from this study highlights an unexpected consideration for the use of α-Syn monomers as a control condition in the PFF model. Monomer use has become a widely used control group for α-syn PFF injections to account for the introduction of exogenous α-Syn protein into the brain. However, our RNA sequencing analysis revealed unexpected results that may jeopardize the use of α-Syn monomers *in vivo*. Although the differential gene expression analysis resulted in 6 DEGs between PBS and monomer groups one month following injection (padj < 0.01; Excel Sheet #1), principal component analysis (PCA) demonstrated monomer samples clustered with either PBS or PFF treated samples (Figure 2.2). Briefly, PCA analysis is a dimension reduction analysis, which is a way to visualize complex RNA sequencing datasets. Dimension reduction (where each sample is represented by a single datapoint on an X-Y axis) allows for the identification of major sources of variation between samples and is usually a quality control step in RNA sequencing workflows. Our results showed that the bimodal distribution of the monomer group correlated with surgical order of samples, where samples that received monomer soonest after monomer preparation correlated with PBS, and at longer intervals, with the PFF group.

We hypothesize that that α-Syn monomers in solution can rapidly oligomerize, and that introduction of oligomers can induce a transcriptomic response with some similarities to that of PFF, without the full formation of pSyn inclusions. This spontaneous oligomerization is time-dependent and could explain the bimodal distribution we observed in our dataset and is further validated by our ddPCR follow up that showed a similar bi-modal distribution in some instances, for example, in our *Th*

ddPCR results (Figure 3.6; *Top left*). The unintended oligomerization, or hypothesis of oligomerization, requires further validation prior to using monomer as a control in the PFF model. To evaluate this hypothesis, I would propose a series of time-dependent experiments, where monomer is prepped as if for surgery and held on ice for multiple durations of time (1, 2, 4h, for example) and then evaluated for oligomerization properties. Specifically, I would run the samples on a native gel to visualize different molecular weights and directly observe the formation of oligomeric species. Also, a ThioT experiment would be useful to validate the formation of amyloid structure, and electron microscopy could be used to visualize oligomerization. These experiments could potentially provide optimal monomer handling parameters for use in future studies in which monomer injections are used as a control condition.

FUTURE RESEARCH DIRECTIONS

Our ddPCR analysis revealed a striking 327% increase in cathepsin W (*Ctsw*) mRNA levels at one month following PFF injection compared to PBS controls ($p = 0.0008$), this is in contrast with the modest 21% log-fold change (LFC) increase observed in the RNAseq dataset (padj = 0.021) at the same time point. This discrepancy may reflect differences in tissue collection (LCM vs tissue punches), or methodological differences, as ddPCR is more sensitive and accurate in quantification of low-abundance transcripts such as *Ctsw*. Notably, Ctsw was no longer upregulated at the 2-month time point. Cathepsin W is exclusively expressed in natural killer (NK) cells and CD8+ T cells, and this pronounced upregulation suggests peripheral immune cell infiltration during the early stages of pSyn inclusion formation (Stoeckle et al., 2009). Peripheral immune cell infiltration is well documented in clinical PD, as well as Lewy

body dementia, in addition to preclinical PD models (mainly direct toxin models) (Gate et al., 2021; Guan et al., 2022; Kannarkat et al., 2013). Peripheral cell infiltration, including CD8+ T cells and natural killer cells, has previously been reported during the pSyn aggregation phase following intrastriatal human PFF (hPFF) injections into wildtype mice (Earls et al., 2019). In α-Syn overexpressing mice, intrastriatal injection of PFFs, pSyn accumulation in the SNpc is accompanied by a 5-fold increase in infiltration of natural killer (NK) cells (Earls & Lee, 2020). These results suggest that NK cells participate in the earliest innate response to pSyn inclusions, but that this response is not sustained. Future experiments could examine this possibility by characterizing infiltrating immune cells at the one- and two-month time point following PFF injection. Enumeration of infiltrating immune cells could be performed using IHC, as there are commercially available antibodies that stain NK cells, as well as CD4+ and CD8+ cells.

Fluorescent *in situ* hybridization analysis revealed significant increases in cathepsin S (*Ctss*) mRNA expression within ionized calcium-binding adaptor 1 (Iba1) reactive microglia. Qualitatively, there was a heterogeneity of *Ctss* expression within adjacent Iba1 immunoreactive microglia, suggestive of differential expression within microglia subtypes. It is known that microglia display a wide range of phenotypes depending on activation sate (Paolicelli et al., 2022). Additionally, cathepsin S is a multifunctional cathepsin expressed by microglia – as a regulator of MHC-II antigen processing, as well also released extracellularly to effect extracellular matrix (ECM) degradation (Hao et al., 2007; Lively & Schlichter, 2013; Nakagawa et al., 1999; Pišlar et al., 2021; Vizovišek et al., 2019). The functional role of cathepsin S in response to pSyn inclusions in the PFF model will be difficult to discern, however, if cathepsin S is

enriched specifically within MHC-II immunoreactive microglia, which may suggest a primary role in regulation of antigen presentation. Follow up experiments could be conducted that explore the expression of cathepsin S in MHC-IIir microglia, relative to expression in Iba1ir microglia using immunohistological analysis and quantification or enumeration.

Cathepsin X has a unique relationship with gamma enolase (γ-enolase; *ENO2;* also known as neuron-specific-enolase; NSE) that has recently gained momentum as a potential therapeutic target in neurodegenerative disorders. NSE has been regarded as neuronal specific marker, but contrary to the nomenclature, is understood to be expressed in neurons, astrocytes, as well as microglia (Hafner et al., 2013; Haque et al., 2016). The primary function of NSE is twofold, it is involved in glycolysis, catalyzing the conversion of 2-phosphoglycerate (2-PG) to phosphoenolpyruvate (PEP), as well as intracellular neurotrophic signaling via activating PI3K/Akt and MAPK/ERK pathways (Horvat et al., 2024). Cathepsin X has been shown to regulate NSE activity, cleaving 2 amino acids from the C-terminal domain (residues 433-434), inhibiting NSE intracellular trafficking and signaling (Hafner et al., 2010). Inhibition of NSE via cathepsin X results in impaired neurotrophic activity and cell survival *in vitro*, further, cathepsin X inhibition has shown neuroprotective properties (Hafner et al., 2012; Obermajer et al., 2009). *In vivo* cathepsin X has been shown to colocalize with NSE in multiple cell types. For example, in an amyloid beta (Aβ) transgenic mouse model, cathepsin X and NSE are shown to colocalize within microglia surrounding Aβ plaques (Hafner et al., 2013). Interestingly, in non-plaque areas, NSE was expressed in neurons with minimal cathepsin X expression, suggesting a cell-type specific disease response. *In vitro* and *in vivo* models of spinal

cord injury have shown that cathepsin X / NSE mechanism may be a promising therapeutic target. Specifically, the use of ENOblock, which prevents cathepsin X cleavage of NSE, has shown to reduce metabolic neuroinflammatory markers (cytokines and chemokines), reduced glial activation and pro-inflammatory phenotypes, as well as ROCK activity attenuation within microglia in response to spinal cord injury associated with neurodegeneration (McCoy et al., 2023). ROCK (rho kinase) has previously been implicated in α-syn aggregation, and has been investigated as a therapeutic target in PD using a pharmacological inhibitor (Lage et al., 2025). NSE and cathepsin X inhibition may provide a therapeutic target that indirectly inhibits ROCK activity, as well. Collectively, these studies suggest that NSE can be a neuroprotective intracellular mechanism that is being inhibited by cathepsin X.

Future directions with cathepsin X and NSE should focus on the cell-type specific localization of NSE expression and colocalization with cathepsin X in the PFF model. There are commercially available antibodies that bind to the N terminal of NSE, the middle amino-acid sequences of NSE, and the C terminus cleavage site of NSE. Importantly, antibodies that target the C terminus region do not bind following cathepsin X cleavage, thus allowing for ratios of intact-active NSE to total NSE to be generated from IHC or IF quantification (Majc et al., 2022). My prediction is that total NSE will be unchanged in the SNpc following PFF injection, aligning with our RNA sequencing data, but that the amount of intact-active enolase will be significantly decreased, associated with cathepsin X increases. I would expect that NSE expression will be mainly neuronal in PBS conditions, and that in PFF conditions the expression of NSE will shift to microglia, colocalizing with cathepsin X, surrounding pSyn inclusions. Following, I would

be interested in testing a cathepsin X inhibitor, such as ENOblock or other commercially available cathepsin X inhibitors, in the PFF model, and would predict an attenuation of microglial reactivity and neuroinflammatory markers.

Lastly, RNA sequencing pathway enrichment analysis revealed pathways associated with “response to virus” unique to the two-month timepoint, which was an unexpected finding. *Zbp1,* Z-DNA binding protein 1, was identified as a key gene in the enriched pathways with a 454% log foldchange increase at 2 months. *Zbp1* is a master regulator of PANoptosis, a recently discovered form of programmed cell death (PCD) that integrates multiple components of apoptosis, pyroptosis, and necroptosis (Chen et al., 2022; Christgen et al., 2020). The protein, Zbp1, interacts with Z form DNA (zDNA), a structural variant of DNA that has a left-handed double helical structure recognized as a damage-associated molecular pattern (DAMP) (Herbert, 2019; Szczesny et al., 2018). zDNA could result from damaged nuclear or mitochondrial DNA. Previous work in the PFF model has shown that α-Syn inclusions can disrupt mitochondrial function, resulting in oxidative stress related DNA damage (Geibl et al., 2024). Additionally, it has been shown that PFF induced inclusions can lead to nuclear DNA damage, which could also be activating Zbp1 (Schaser et al., 2019). Interestingly, our RNA sequencing dataset suggests mitochondrial protein coding genes are significantly altered at one month post PFF injection, further suggesting that α-syn inclusions are disrupting mitochondrial function that could result in mtDNA being released from damaged cells and binding with Zbp1. However, the type of DNA that is directly activating Zbp1 is not known. Future studies should focus on localizing Zbp1 to a specific cell type, in addition to localizing Zbp1 expression in relationship to pSyn inclusions. Additional studies could validate the

activation of PANoptosis via using IHC or Western blotting to quantify phosphorylated mixed lineage kinase domain-like (MLKL) the terminal protein of the necroptosis. To better understand the type of DNA (mitochondrial vs. nuclear) that binds to Zbp1 and activates PANoptosis pathways, a CHIPseq experiment could determine if specific sequences are more susceptible to interacting with Zbp1. For an intervention strategy to mitigate Zbp1 activity, thus preventing PANoptosis activation, a virus such as an AAV or ASO (adeno-associated virus; antisense oligonucleotide) could be used to knock down Zbp1, or a pharmacological inhibitor could be used. If the spatiotemporal relationship is connected between Ctsx, NSE, and Zbp1, using ENOblock may prevent mitochondrial dysfunction, thus prevent the release of mtDNA, and prevent Zbp1 activation as a neuroprotective strategy.

In conclusion, these studies have provided novel insights into the early pathogenic mechanisms of PD through the use of the PFF model and leveraging LCM-RNAseq with FISH/IF follow-up analyses. Our findings suggest a temporally dynamic microglial response to pSyn inclusions within the SN and highlighted the involvement of various microglial cathepsins and discussed their potential roles in disease progression. Additionally, we encountered unexpected results with the use of α-Syn monomer as a control group *in vivo,* suggesting the need to reevaluate its' use in future PD research. Exploring the role of cathepsin X's interaction with NSE, as well as Zbp1's role in PANoptosis, may offer promising directions for the development of therapeutic interventions. The future studies proposed in this chapter would not only deepen our understanding of PD's molecular pathology but could also pave the way for innovative treatments aimed at slowing or halting the neurodegenerative process.

BIBLIOGRAPHY

Ashburner, M., Ball, C. A., Blake, J. A., Botstein, D., Butler, H., Cherry, J. M., Davis, A. P., Dolinski, K., Dwight, S. S., Eppig, J. T., Harris, M. A., Hill, D. P., Issel-Tarver, L., Kasarskis, A., Lewis, S., Matese, J. C., Richardson, J. E., Ringwald, M., Rubin, G. M., & Sherlock, G. (2000). Gene Ontology: Tool for the unification of biology. *Nature Genetics*, *25*(1), 25–29. https://doi.org/10.1038/75556

Chen, X.-Y., Dai, Y.-H., Wan, X.-X., Hu, X.-M., Zhao, W.-J., Ban, X.-X., Wan, H., Huang, K., Zhang, Q., & Xiong, K. (2022). ZBP1-Mediated Necroptosis: Mechanisms and Therapeutic Implications. *Molecules*, *28*(1). https://doi.org/10.3390/molecules28010052

Christgen, S., Zheng, M., Kesavardhana, S., Karki, R., Malireddi, R. K. S., Banoth, B., Place, D. E., Briard, B., Sharma, B. R., Tuladhar, S., Samir, P., Burton, A., & Kanneganti, T.-D. (2020). Identification of the panoptosome: A molecular platform triggering pyroptosis, apoptosis, and necroptosis (panoptosis). *Frontiers in Cellular and Infection Microbiology*, *10*, 237. https://doi.org/10.3389/fcimb.2020.00237

Earls, R. H., & Lee, J.-K. (2020). The role of natural killer cells in Parkinson's disease. *Experimental & Molecular Medicine*, *52*(9), 1517–1525. https://doi.org/10.1038/s12276-020-00505-7

Earls, R. H., Menees, K. B., Chung, J., Barber, J., Gutekunst, C.-A., Hazim, M. G., & Lee, J.-K. (2019). Intrastriatal injection of preformed alpha-synuclein fibrils alters central and peripheral immune cell profiles in non-transgenic mice. *Journal of Neuroinflammation*, *16*(1), 250. https://doi.org/10.1186/s12974-019-1636-8

Gate, D., Tapp, E., Leventhal, O., Shahid, M., Nonninger, T. J., Yang, A. C., Strempfl, K., Unger, M. S., Fehlmann, T., Oh, H., Channappa, D., Henderson, V. W., Keller, A., Aigner, L., Galasko, D. R., Davis, M. M., Poston, K. L., & Wyss-Coray, T. (2021). CD4+ T cells contribute to neurodegeneration in Lewy body dementia. *Science*, *374*(6569), 868–874. https://doi.org/10.1126/science.abf7266

Geibl, F. F., Henrich, M. T., Xie, Z., Zampese, E., Ueda, J., Tkatch, T., Wokosin, D. L., Nasiri, E., Grotmann, C. A., Dawson, V. L., Dawson, T. M., Chandel, N. S., Oertel, W. H., & Surmeier, D. J. (2024). α-Synuclein pathology disrupts mitochondrial function in dopaminergic and cholinergic neurons at-risk in Parkinson's disease. *Molecular Neurodegeneration*, *19*(1), 69. https://doi.org/10.1186/s13024-024-00756-2

Guan, Q., Liu, W., Mu, K., Hu, Q., Xie, J., Cheng, L., & Wang, X. (2022). Single-cell RNA sequencing of CSF reveals neuroprotective RAC1+ NK cells in Parkinson's disease. *Frontiers in Immunology*, *13*, 992505. https://doi.org/10.3389/fimmu.2022.992505

Hafner, A., Glavan, G., Obermajer, N., Živin, M., Schliebs, R., & Kos, J. (2013). Neuroprotective role of γ-enolase in microglia in a mouse model of Alzheimer's disease is regulated by cathepsin X. *Aging Cell*, *12*(4), 604–614. https://doi.org/10.1111/acel.12093

Hafner, A., Obermajer, N., & Kos, J. (2010). γ-1-syntrophin mediates trafficking of γ-enolase towards the plasma membrane and enhances its neurotrophic activity. *Neuro-Signals*, *18*(4), 246–258. https://doi.org/10.1159/000324292

Hafner, A., Obermajer, N., & Kos, J. (2012). γ-Enolase C-terminal peptide promotes cell survival and neurite outgrowth by activation of the PI3K/Akt and MAPK/ERK signalling pathways. *The Biochemical Journal*, *443*(2), 439–450. https://doi.org/10.1042/BJ20111351

Hao, H. P., Doh-Ura, K., & Nakanishi, H. (2007). Impairment of microglial responses to facial nerve axotomy in cathepsin S-deficient mice. *Journal of Neuroscience Research*, *85*(10), 2196–2206. https://doi.org/10.1002/jnr.21357

Haque, A., Ray, S. K., Cox, A., & Banik, N. L. (2016). Neuron specific enolase: a promising therapeutic target in acute spinal cord injury. *Metabolic Brain Disease*, *31*(3), 487–495. https://doi.org/10.1007/s11011-016-9801-6

Herbert, A. (2019). Z-DNA and Z-RNA in human disease. *Communications Biology*, *2*, 7. https://doi.org/10.1038/s42003-018-0237-x

Horvat, S., Kos, J., & Pišlar, A. (2024). Multifunctional roles of γ-enolase in the central nervous system: more than a neuronal marker. *Cell & Bioscience*, *14*(1), 61. https://doi.org/10.1186/s13578-024-01240-6

Kanehisa, M., & Goto, S. (2000). KEGG: Kyoto encyclopedia of genes and genomes. *Nucleic Acids Research*, *28*(1), 27–30. https://doi.org/10.1093/nar/28.1.27

Kannarkat, G. T., Boss, J. M., & Tansey, M. G. (2013). The role of innate and adaptive immunity in Parkinson's disease. *Journal of Parkinson's Disease*, *3*(4), 493–514. https://doi.org/10.3233/JPD-130250

Katunuma, N. (2010). Posttranslational processing and modification of cathepsins and cystatins. *Journal of Signal Transduction*, *2010*, 375345. https://doi.org/10.1155/2010/375345

Lage, L., Rodriguez-Perez, A. I., Labandeira-Garcia, J. L., & Dominguez-Meijide, A. (2025). Fasudil inhibits α-synuclein aggregation through ROCK-inhibition-mediated mechanisms. *Neurotherapeutics*, e00544. https://doi.org/10.1016/j.neurot.2025.e00544

Lively, S., & Schlichter, L. C. (2013). The microglial activation state regulates migration and roles of matrix-dissolving enzymes for invasion. *Journal of Neuroinflammation*, *10*, 75. https://doi.org/10.1186/1742-2094-10-75

Majc, B., Habič, A., Novak, M., Rotter, A., Porčnik, A., Mlakar, J., Župunski, V., Pečar Fonović, U., Knez, D., Zidar, N., Gobec, S., Kos, J., Lah Turnšek, T., Pišlar, A., & Breznik, B. (2022). Upregulation of Cathepsin X in Glioblastoma: Interplay with γ-Enolase and the Effects of Selective Cathepsin X Inhibitors. *International Journal of Molecular Sciences*, *23*(3). https://doi.org/10.3390/ijms23031784

McCoy, H. M., Polcyn, R., Banik, N. L., & Haque, A. (2023). Regulation of enolase activation to promote neural protection and regeneration in spinal cord injury. *Neural Regeneration Research*, *18*(7), 1457–1462. https://doi.org/10.4103/1673-5374.361539

Nakagawa, T. Y., Brissette, W. H., Lira, P. D., Griffiths, R. J., Petrushova, N., Stock, J., McNeish, J. D., Eastman, S. E., Howard, E. D., Clarke, S. R., Rosloniec, E. F., Elliott, E. A., & Rudensky, A. Y. (1999). Impaired invariant chain degradation and antigen presentation and diminished collagen-induced arthritis in cathepsin S null mice. *Immunity*, *10*(2), 207–217. https://doi.org/10.1016/s1074-7613(00)80021-7

Obermajer, N., Doljak, B., Jamnik, P., Fonović, U. P., & Kos, J. (2009). Cathepsin X cleaves the C-terminal dipeptide of alpha- and gamma-enolase and impairs survival and neuritogenesis of neuronal cells. *The International Journal of Biochemistry & Cell Biology*, *41*(8–9), 1685–1696. https://doi.org/10.1016/j.biocel.2009.02.019

Paolicelli, R. C., Sierra, A., Stevens, B., Tremblay, M.-E., Aguzzi, A., Ajami, B., Amit, I., Audinat, E., Bechmann, I., Bennett, M., Bennett, F., Bessis, A., Biber, K., Bilbo, S., Blurton-Jones, M., Boddeke, E., Brites, D., Brône, B., Brown, G. C., … Wyss-Coray, T. (2022). Microglia states and nomenclature: A field at its crossroads. *Neuron*, *110*(21), 3458–3483. https://doi.org/10.1016/j.neuron.2022.10.020

Petushkova, A. I., & Zamyatnin, A. A. (2020). Redox-Mediated Post-Translational Modifications of Proteolytic Enzymes and Their Role in Protease Functioning. *Biomolecules*, *10*(4). https://doi.org/10.3390/biom10040650

Pišlar, A., Bolčina, L., & Kos, J. (2021). New Insights into the Role of Cysteine Cathepsins in Neuroinflammation. *Biomolecules*, *11*(12). https://doi.org/10.3390/biom11121796

Schaser, A. J., Osterberg, V. R., Dent, S. E., Stackhouse, T. L., Wakeham, C. M., Boutros, S. W., Weston, L. J., Owen, N., Weissman, T. A., Luna, E., Raber, J., Luk, K. C., McCullough, A. K., Woltjer, R. L., & Unni, V. K. (2019). Alpha-synuclein is a DNA binding protein that modulates DNA repair with implications for Lewy body disorders. *Scientific Reports*, *9*(1), 10919. https://doi.org/10.1038/s41598-019-47227-z

Shetty, A. C., Mattick, J., Chung, M., McCracken, C., Mahurkar, A., Filler, S. G., Fraser, C. M., Rasko, D. A., Bruno, V. M., & Dunning Hotopp, J. C. (2020). Cost effective, experimentally robust differential-expression analysis for human/mammalian, pathogen and dual-species transcriptomics. *Microbial Genomics*, *6*(1). https://doi.org/10.1099/mgen.0.000320

Stoeckle, C., Gouttefangeas, C., Hammer, M., Weber, E., Melms, A., & Tolosa, E. (2009). Cathepsin W expressed exclusively in CD8+ T cells and NK cells, is secreted during target cell killing but is not essential for cytotoxicity in human CTLs. *Experimental Hematology*, *37*(2), 266–275. https://doi.org/10.1016/j.exphem.2008.10.011

Szczesny, B., Marcatti, M., Ahmad, A., Montalbano, M., Brunyánszki, A., Bibli, S.-I., Papapetropoulos, A., & Szabo, C. (2018). Mitochondrial DNA damage and subsequent activation of Z-DNA binding protein 1 links oxidative stress to inflammation in epithelial cells. *Scientific Reports*, *8*(1), 914. https://doi.org/10.1038/s41598-018-19216-1

Vizovišek, M., Fonović, M., & Turk, B. (2019). Cysteine cathepsins in extracellular matrix remodeling: Extracellular matrix degradation and beyond. *Matrix Biology*, *75–76*, 141–159. https://doi.org/10.1016/j.matbio.2018.01.024